

# **Biotechnological Production of Carotenoids by Aquatic Microorganisms**

## **Dissertation**

in fulfilment of the requirements for the degree of Dr. rer. nat.  
of the Faculty of Mathematics and Natural Sciences  
at Kiel University

submitted by  
Inga Klara Koopmann

Flensburg, 2023







First examiner: Prof. Dr. Antje Labes

Second examiner: Prof. Dr. Rüdiger Schulz

Date of the oral examination: 28.11.2023







The present work was conducted at Flensburg University of Applied Sciences under the supervision of Prof. Dr. Antje Labes.







## Table of Contents

<b>Summary .....</b>	<b>1</b>
<b>Zusammenfassung .....</b>	<b>2</b>
<b>General Introduction .....</b>	<b>3</b>
Carotenoids.....	3
Biosynthesis of Carotenoids .....	4
Carotenoids in Photosynthesis.....	5
Further Functions of Carotenoids .....	5
Functions of Carotenoids in Animals .....	6
Health Related Effects of Carotenoids in Humans .....	6
Applications of Carotenoids .....	7
Production of Carotenoids.....	8
Qualification and Quantification of Carotenoids .....	12
Aim of this Thesis .....	13
<b>Chapter I Development and Validation of Reliable Astaxanthin Quantification from Natural Sources .....</b>	<b>16</b>
<b>Chapter II Optimization of Astaxanthin Recovery in the Downstream Process of <i>Haematococcus pluvialis</i> .....</b>	<b>52</b>
<b>Chapter III Screening of a Thraustochytrid Strain Collection for Carotenoid and Squalene Production Characterized by Cluster Analysis, Comparison of 18S rRNA Gene Sequences, Growth Behavior, and Morphology .....</b>	<b>80</b>
<b>Synthesis and General Discussion .....</b>	<b>123</b>
Quantification of Astaxanthin from Natural Sources .....	124
Optimization of Downstream Processing for Astaxanthin Production .....	126
Production of Carotenoids Using Novel Groups of Microorganisms .....	128
<b>Perspectives.....</b>	<b>130</b>
<b>References .....</b>	<b>133</b>
<b>Appendix .....</b>	<b>153</b>
<b>Danksagung.....</b>	<b>176</b>
<b>Eidesstattliche Erklärung.....</b>	<b>178</b>



### Summary

Population growth, higher expectations for a long and healthy life, and climate change are currently major drivers for the development and production of health-promoting, sustainable, and climate-friendly substances. A particular focus is on the food and pharmaceutical sectors, as these directly impact human health. This progress led to an increase in demand for additives improving the properties of food and feed. In this context, carotenoids play an important role. They comprise a group of natural pigments, which are used to color food and feed. Some carotenoids such as  $\beta$ -carotene also have health-maintaining effects due to their provitamin A activity. Other carotenoids like astaxanthin are still the subject of scientific investigations with regard to their antioxidant effects on the human body. The biotechnological production enables a sustainable supply of natural carotenoids, but there is still room for improvements in manufacturing processes.

The aim of this work was to support the further development of the biotechnological production of carotenoids by optimizing methods and processes and by searching for new, promising production organisms:

1. The development of a method for the determination of astaxanthin from *Haematococcus pluvialis* helped to find a good compromise between simple and fast but also accurate measurement procedures. The method allowed the cleavage of carotenoid esters, which are the natural occurrence of many carotenoids. Different isomers could be individually detected.
2. The application of the developed method in the optimization of the downstream process of astaxanthin from *H. pluvialis* aimed to maximize astaxanthin yield while minimizing process costs and energy consumption. The evaluation revealed that potentially astaxanthin-damaging process steps had a less detrimental effect on yield than expected. These findings offer further opportunities for developments in climate-friendly downstream processing.
3. The screening of a Thraustochytriaceae strain collection indicated that some strains are potentially suitable for a sustainable production of carotenoids. The thraustochytrids studied revealed a wide variability in their carotenoid profiles, which varied further depending on the media composition. Parameter optimization increased growth and metabolite yield.

The knowledge gained contributes to the further development of biotechnological processes. In this context, it is important that future studies take particular account of the therapeutic effect, mechanisms of action, and the applicability of carotenoids in addition to production optimization. The gained comprehensive understanding is essential to improve the necessary production through optimized synthesis and processing, to enable targeted and economical use, and thus to make a lasting contribution to public health and climate protection.



## Zusammenfassung

Bevölkerungswachstum, höhere Erwartungen an ein langes und gesundes Leben und nicht zuletzt auch der Klimawandel sind wichtige Treiber für die Entwicklung und Produktion von gesundheitsfördernden, nachhaltigen und klimafreundlichen Substanzen. Ein besonderer Fokus liegt dabei auf den Bereichen der Nahrungsmittel und Pharmazeutika, da diese einen direkten Einfluss auf die menschliche Gesundheit haben. Dabei ist die Nachfrage nach Zusatzstoffen, die die Eigenschaften von Nahrungsmitteln verbessern, stark gestiegen. Hierbei spielen Carotinoide eine wichtige Rolle. Sie umfassen eine Gruppe von natürlichen Pigmenten, die zur Färbung in Lebens- und Futtermitteln eingesetzt werden. Einige Carotinoide, wie  $\beta$ -Carotin, haben durch ihre Provitamin-A-Aktivität auch gesundheitserhaltende Wirkungen. Andere, wie Astaxanthin, sind aktuell noch Gegenstand wissenschaftlicher Untersuchungen hinsichtlich ihrer antioxidativen Wirkungen auf den menschlichen Körper. Die biotechnologische Produktion ermöglicht die nachhaltige Versorgung mit natürlichen Carotinoiden. Hier gibt es noch Spielraum hinsichtlich der Verbesserung der Herstellungsverfahren.

Ziel dieser Arbeit war es, die Weiterentwicklung der biotechnologischen Produktion von Carotinoiden durch die Optimierung von Methoden, Prozessen und durch die Suche nach neuen, potentiellen Produktionsorganismen zu unterstützen:

1. Durch die Entwicklung einer Methode zur Bestimmung von Astaxanthin aus *Haematococcus pluvialis* ist ein guter Kompromiss zwischen einem einfachen und schnellen, aber auch genauen Messverfahren gefunden worden. Diese ermöglicht die Spaltung von Carotinoidestern, wie sie in natürlichen Quellen vorkommen sowie die einzelne Erfassung von verschiedenen Isomeren.
2. Die Anwendung der entwickelten Methode bei der Optimierung des Downstream Prozesses von Astaxanthin aus *H. pluvialis* ermöglichte, die Astaxanthinausbeute bei gleichzeitiger Minimierung von Prozesskosten und Energieaufwand zu maximieren. Die Untersuchung hat ergeben, dass potentiell Astaxanthin schädigende Prozesse einen weniger nachteiligen Effekt auf die Ausbeute hatten als erwartet. Daraus ergeben sich weitere Möglichkeiten für Entwicklungen klimafreundlicher Aufarbeitungsmethoden.
3. Das Screening einer Stammsammlung von Thraustochytriaceae ließ erkennen, dass auch andere Stämme potentiell für eine nachhaltige Produktion von Carotinoiden geeignet sind. Die untersuchten Thraustochytriden ließen eine große Variabilität in ihren Carotinoidprofilen erkennen, die in Abhängigkeit der Medienzusammensetzung weiter variierte. Durch Parameteroptimierung konnten Wachstum und Metabolitenausbeute gesteigert werden.

Die gewonnenen Erkenntnisse tragen dazu bei, biotechnologische Prozesse weiterzuentwickeln. Zukünftige Studien sollten neben der Produktionsoptimierung insbesondere die Wirksamkeit, Wirkmechanismen und Anwendbarkeit von Carotinoiden berücksichtigen. Das daraus gewonnene umfassende Verständnis ist essentiell, um die notwendige Produktion durch optimierte Synthese und Aufarbeitung zu verbessern, einen zielgerichteten und ökonomischen Einsatz zu ermöglichen und somit dauerhaft zur Gesundheit der Bevölkerung und dem Klimaschutz beizutragen.



### General Introduction

#### Carotenoids

Carotenoids comprise a class of pigments widespread in nature. They are produced by a variety of organisms [1–3]: mainly plants [4] and (micro)algae [5–9], but also bacteria [3,10–13], archaea [14,15], fungi [16,17], and protists [18–22]. The majority of carotenoids is produced by plants, but they also occur exogenously in higher quantities in terrestrial animals, such as arthropods [23–25], birds [26], reptiles [27,28], amphibians [29,30], and in aquatic animals like fish and invertebrates [31], such as crustaceans [32], echinoderms [33,34], mussels, sea snails, and corals [35]. They all rely on carotenoid uptake by their diet but may be able to modify the ingested molecules by metabolic conversions. An exception are some arthropods like aphids, spider mites, and gall midges, which obtained carotenoid biosynthetic genes by lateral gene transfer from fungi [36–38]. Carotenoids are also present in mammals, but unlike the previously mentioned animals, most of them do not absorb and display carotenoids to any great extent, with very few exceptions [39].

#### Chemical Structure

The structures of well above 500 carotenoids are known, and more are still being discovered [40,41]. Carotenoids belong to the tetra- or polyterpenes and are composed of isoprene subunits. The basic structure of carotenoids is a linear polyene chain with conjugated double bonds and various end groups (Figure 1). These are often cyclic structures at one or both ends. Their large delocalized  $\pi$ -electron system is responsible for many of their characteristic attributes, like their yellow to red color and the physio-chemical properties described below. Carotenoids can be structurally classified into xanthophylls and carotenes depending on whether oxygenated functional groups are or are not part of the molecular structure, respectively. These include hydroxy, epoxy, keto, formyl, and methoxy groups. They determine the polarity of the molecule and whether derivatives such as esters can be formed. Carotenoids occur in the form of various stereoisomers. Different diastereomers result from the *E/Z*-configurations of the conjugated double bonds within the polyene chain [42]. The all-*E*-configuration is the most abundant in nature, but sterically unhindered forms like 9-*Z*, 13-*Z*, 15-*Z*, and the corresponding di-*Z*-isomers also occur [42–46]. Xanthophylls may also have different enantiomers depending on stereogenic carbon atoms in their structure. E.g., if two stereocenters are present in a carotenoid molecule, three to four enantiomers can be formed when a symmetric or asymmetric diastereomer is considered, respectively ([S,S], [R,R], [S,R]/[R,S]).



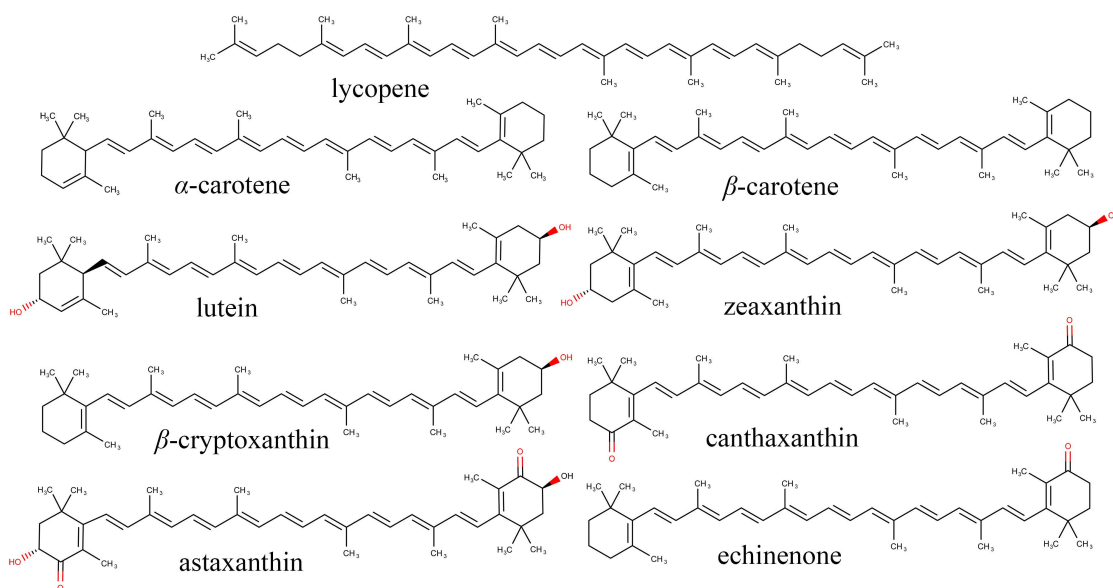


**Figure 1:** Different carotenoids abundant in plants and microorganisms.

### Biosynthesis of Carotenoids

The synthesis of carotenoids is a rather complex process involving various enzymes and molecules. The general mechanism for their synthesis in plants is as follows: In the first step, isoprenoid precursors are formed via two different routes, either the mevalonate (MVA) pathway or the non-mevalonate pathway, also called the methylerythritol phosphate (MEP) pathway. The MVA pathway takes place in the cytoplasm. Its precursor is acetyl-CoA. The MEP pathway takes place in plant plastids, and its reactants are pyruvate and glyceraldehyde 3-phosphate (GAP). The MEP pathway is the main route for the synthesis of carotenoid precursors in plants [47]. The starting molecules are converted to isopentenyl diphosphate (IPP) in seven steps, whereas the MEP pathway can also directly form dimethylallyl diphosphate (DMAPP) in the last step. IPP and DMAPP can be converted into each other by IPP/DMAPP isomerase. These molecules are, in turn, the precursors for the synthesis of isoprenoids and carotenoids, as well as other molecular groups, such as chlorophylls, plastoquinones, and tocopherols [48].

The second part of carotenoid synthesis begins with the condensation of three molecules of IPP and one molecule of DMAPP to form geranylgeranyl diphosphate (GGPP), two molecules of which are in turn converted by phytoene synthase to phytoene, the first carotene in the series. Phytoene is transformed into lycopene by desaturases. From here, cyclases form the ring structures in the previously linear carotenoids, leading to the formation of  $\alpha$ - and  $\beta$ -carotene. Hydroxylation mediated by different enzymes produces xanthophylls, initially lutein and zeaxanthin, but these can cascade to form a variety of carotenoids [48,49].



## General Introduction

Carotenoid synthesis is similar in a variety of different organisms, but in detail, the transformation steps, transcriptional regulators, enzymes, cascades, and the ability to produce specific carotenoids differ [50–53].

### Carotenoids in Photosynthesis

In photosynthetic organisms, carotenoids act as photoreceptors in the light-harvesting pigment-protein complexes and transfer absorbed light energy to the reaction centers, where the excitation energy is transformed and finally chemically bound [54,55]. By absorbing visible light in the blue-green spectrum (450–500 nm), carotenoids extend the total light absorption spectrum of these complexes beyond the capacity of chlorophylls and increase the light collection efficiency. Simultaneously, carotenoids protect the photosynthetic apparatus from photoinhibition and oxidative damage through different mechanisms. In short, carotenoids take over the excited state energy of a chlorophyll molecule by non-photochemical quenching and dissipate it by releasing heat energy [56,57]. This reaction is possible in singlet and triplet quenching of chlorophyll [58,59]. If an excited triplet state of a chlorophyll is not quenched, it is likely to react with other molecules. Hereby, and in other parts of the photosynthetic machinery, reactive oxygen species (ROS) can be generated [60]. Many carotenoids are capable of quenching ROS and reactive nitrogen species by chemical quenching [61–67], leading to the formation of carotenoid epoxides, endoperoxides, and different volatile derivatives [67–70]. In turn, some of these derivatives may act as signaling molecules and induce responses to oxidative stress [70].

### Further Functions of Carotenoids

In plants, carotenoid derivatives play an important role in growth, stress response, and herbivore resistance. They can act as phytohormones and internal and external interspecific communication signals. Strigolactones and apocarotenoids, such as abscisic acid and  $\beta$ -cyclocitral, have been well described [71–74]. Other apocarotenoids with similar functions have been recently discovered, like zaxinone [75,76], anchorene [77,78], and others [73,79–81], suggesting that this group will be further expanded. Along with other pigments, carotenoids are responsible for the coloration of petals [82–85] and fruits [86,87] of many plants. They attract pollinators [88–90] and seed dispersers [91] by coloration and odor, forming aromatic cleavage products, such as ionones and other apocarotenoids [85,92–94]. The potent quenching ability of carotenoids is not only used in photosynthetic organisms. Non-photosynthetic organisms use them as a countermeasure against oxidative stress from external sources like UV radiation [12,95] and chemicals [96] and internal sources like respiratory bursts [97]. Carotenoids incorporated in membranes can prevent lipid peroxidation [98,99]. They help regulate membrane fluidity and order with different purposes and effects [100,101], e.g., membrane folding [102], oxygen exclusion [103], hydrophobicity regulation [104], temperature adaptation, cryoprotection, and thermostabilization [95,105,106].



### Functions of Carotenoids in Animals

Carotenoids are also important for signaling in animals and can change the appearance of species that ingest carotenoids. Birds use (modified) carotenoids as ornamentation in their plumage to signal fitness to increase sexual attractiveness [26,107,108] and as an agonistic signal for male dominance and fighting ability [109,110]. Carotenoid-based ornaments with a similar goal have been found in several fishes [111–114] and a reptile species [28]. In birds, carotenoids have been reported to play an important role in communication between parents and offspring by enhancing mouth pigmentation [115,116]. Signaling research has mainly focused on vertebrates, especially birds and fish [117]. Similar functions of carotenoids have also been observed in certain terrestrial arthropods, where carotenoids support camouflage [118,119] or are used as aposematic signals [120,121]. The situation is similar in marine invertebrates [31,122]. In crustaceans, carotenoid-protein complexes ( $\beta$ -crustacyanin) cause a bathochromic color shift and better crypsis in the marine environment [123,124].

In addition to these morphology-based purposes, carotenoids serve animals in various ways through their antioxidative properties. They have been shown to support immunoprotective functions [34,107,125–130] and to be important for reproduction [34,127,131,132]. They are deposited in eggs, possibly to inhibit peroxidative reactions, protect embryonic development [25,133–137], and support growth and survival [128,130,138,139]. However, divergent results in avian immune response [140,141] or fish survival [142] show that this complex issue needs further clarification to define the exact role of carotenoids. Some carotenoids, particularly  $\beta$ -carotene, are essential for vision, cell and tissue development, and immune function in animals through their provitamin A activity (see below) [143,144]. Some carotenoids occur in the ocular structures of humans and are suspected to protect the eye from light and oxidative damage [145–147]. They are also found in the eyes of birds and tune the spectral sensitivity of photoreceptors [148].

### Health Related Effects of Carotenoids in Humans

About 20 carotenoids are the basis for derivatives in fruits and vegetables [149]. Most abundant are  $\beta$ -carotene,  $\alpha$ -carotene, lycopene, lutein, and zeaxanthin [87]. Carotenoids most frequently occurring in human blood plasma of Europeans are lycopene and  $\beta$ -carotene, but also  $\beta$ -cryptoxanthin, lutein, zeaxanthin, and  $\alpha$ -carotene were observed. Their content varied according to region, gender, and lifestyle [150,151].

Probably the best-studied function of carotenoids in the human body, and the only one considered essential to date, is their provitamin A activity, with  $\beta$ -carotene,  $\alpha$ -carotene, and  $\beta$ -cryptoxanthin being major vitamin A precursors [152–155].  $\beta$ -Carotene is considered the most important of the aforementioned vitamin A precursor carotenoids [156]. Vitamin A is essential for vision, immune system function, development, and growth [157–159]. It has been shown that intake of  $\beta$ -carotene increases serum vitamin A levels [160] and improves ocular cytology and vision in individuals with vitamin A deficiency [158,161]. It is abundant in foods and the only carotenoid that can form two retinal



## General Introduction

molecules by symmetric oxidative cleavage [152,162]. It was supposed to have the highest retinol activity [163], although the conversion ratios vary depending on the food source [164]. Higher bioavailability of  $\beta$ -cryptoxanthin might reinforce its importance as a vitamin A precursor [165–167].

Lutein and zeaxanthin are pigments of the human macula [146]. Carotenoids have been associated with the amelioration of ocular diseases. Supplementation with lutein and zeaxanthin has been linked to the prevention of age-related cataract and the increase of macular pigment optical density, but the results obtained varied, and no definite conclusions can be drawn [168–171]. Similarly, positive effects of astaxanthin on cataract were observed in chicken embryos and rats [172,173].

In recent studies, a positive influence of blood carotenoid levels and carotenoid intake on the risk of breast [174] and prostate cancer [175,176] was observed. The significance of the positive effect of carotenoids on lung cancer risk varied [177,178]. Some studies also showed an inverse correlation between  $\beta$ -carotene intake and lung cancer risk in smokers, suggesting that the causative reactions may need further elucidation [179–181].

There is evidence that fucoxanthin supplementation may help reduce body and liver fat in obese individuals, and it shows antidiabetic effects [182–185]. These have been observed in humans and mice, but adverse findings indicate that the underlying mechanism is still unclear [186,187].

In general, carotenoids contribute to the maintenance of human health through their antioxidant and anti-inflammatory effects and support of immune functions [188,189]. Astaxanthin has especially become the focus of research. In the context of its antioxidant function, astaxanthin has been reported to exert neuroprotective properties, improve cognitive deficits [190–193], and positively affect depressive behavior [194,195] in mice and rats.

Overall, carotenoids have potential for pharmaceutical applications in addition to their well-studied functions, but there is a need for further clinical trials with a higher number of participants.

## Applications of Carotenoids

Carotenoids are mainly applied in feed and food, dietary supplements, pharmaceuticals, and cosmetics [196]. The European Union (EU) and the United States Food and Drug Administration (US FDA) have approved some carotenoids and apocarotenoids as colorants for food, feed and cosmetics [197–200]. Some of them have also been authorized by the EU as novel food ingredients [201], have been granted “generally recognized as safe” (GRAS) status by the US FDA [202], or have been positively evaluated by the European Food and Safety Authority (EFSA) for food and feed, e.g., astaxanthin [203–205] (GRN No. 580), lycopene (GRN No. 185), zeaxanthin [206] (GRN No. 639), and lutein [207].

In addition to their use as colorants in food and feed, some carotenoids are gaining popularity due to their putative health benefits. The potent antioxidant effects of carotenoids were also observed in mammalian cells *in vitro* and *in vivo* [208–212]. Together with the aforementioned beneficial effects on various health conditions, this activity led to the application of carotenoids as nutritional supplements and in cosmetics. An increasing number of clinical trials has been performed on the effects of



carotenoids [213]. Although not approved as pharmaceuticals, they can be added to them. An example is lutein in the context of eye health. Carotenoids can also be sold as nutraceuticals, such as astaxanthin or  $\beta$ -carotene, which is used in connection with its provitamin A activity. Although health claims are not allowed, customers are already aware of the supposed positive effects. Astaxanthin especially is often marketed as “the strongest antioxidant”, with studies by Nishida et al. [214] and Shimidzu et al. [65] referenced. However, some other studies vary [62,63] and none were conducted *in vivo*. Astaxanthin from natural sources is approved for human consumption in many countries worldwide, with few adverse effects reported [215] and a low likelihood of allergic reactions to the total product [204]. Its synthetic counterpart has been reported to be inferior [216] and is only approved for feed supplementation [217]. Carotenoids like lycopene,  $\beta$ -carotene, and astaxanthin are also used in cosmetics. In addition to their dyeing properties, described positive effects on wrinkle reduction, skin moisture content [218,219], and irradiation damage [220] make them attractive supplements. However, oral administration has been regarded as more effective than topical [218]. They also play a role in technological developments being investigated for their use in solar panels [221].

Due to their coloring properties and their expected beneficial influence on fitness, reproduction, and survival, carotenoids are used in feeds. In particular, astaxanthin is used in aquaculture, where it has been reported to improve fish color, growth, and immunity and sometimes to affect mortality [222–226]. Similar effects on growth, coloration, and survival were also observed in other marine animals [227–230]. Likewise, carotenoids are incorporated in poultry feed, where they lead to enhanced coloration of egg yolk [231,232] and carcass [233]. Study results have been reported on other positive influences, such as weight gain of eggs and chicken, immunity, or reduction of oxidative stress [234–236], but they diverge [237,238], probably because of multiple influencing factors [235]. Few adverse effects have been reported in case of overdose [239].

The carotenoid market was valued at USD 1.3 bio in 2018 and is expected to reach USD 1.7 bio by 2025. Although the market continues to be dominated by synthetic carotenoids, carotenoids from natural sources are forecasted to grow in value. Within the carotenoids,  $\beta$ -carotene dominates, but the share of astaxanthin is predicted to increase due to its use in feed and nutraceuticals [196]. Especially in the latter case, legislation and growing consumer awareness of healthy, sustainable, organic, fossil-free, and environmentally friendly products have led to a higher demand for traceable biotechnological production.

### **Production of Carotenoids**

In order to use carotenoids in the applications mentioned above, they must be provided either as pure substances, which is mainly done by chemical synthesis, or extracts from organisms that produce carotenoids in sufficient quantities. Chemical processes result in mixtures of carotenoid enantiomers. Some of such mixtures, like in the case of astaxanthin, are not approved for direct human consumption. Carotenoids from natural sources do not occur individually but are mixtures of several carotenoids,



## General Introduction

which occur in different stereoisomeric forms (Figure 2). For example, astaxanthin produced from chemical synthesis is a racemic mixture of the enantiomers (~1:2:1 of 3S,3'S, 3R,3'S, and 3R,3'R). Reported ratios of astaxanthin synthesized by *Haematococcus lacustris*, often and here referred to as *H. pluvialis* [240], were 87.6:10.1:2.3 and 99:1:0. *Phaffia rhodozyma* contained a mixture of 0:1.5:98.5 of 3S,3'S, 3R,3'S, and 3R,3'R [241,242]. Different bioavailabilities and antioxidant activities have been demonstrated for different diastereomers of astaxanthin [243,244]. Carotenoids from natural systems are often also linked to other molecules such as fatty acids. This connection results in the formation of esters (see below), which may exhibit differences in micellization and bioaccessibility [245–248].

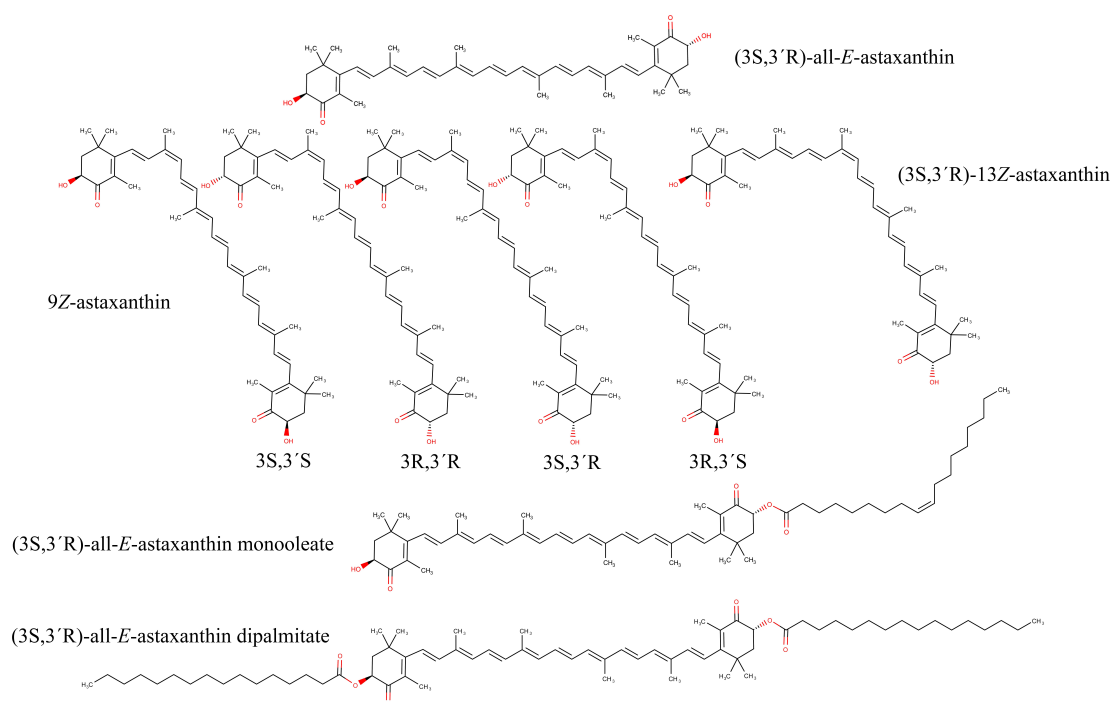


**Figure 2:** Exemplary selection of various diastereomers, enantiomers, and esters of naturally produced astaxanthin.

## Chemical Synthesis

The chemical synthesis of carotenoids is a well-established process. Since the early 20<sup>th</sup> century, various methods have been developed for the chemical synthesis of vitamin A and carotenoids. The Wittig reaction has been a central step in carotenoid synthesis. Isophorones or vitamin A and its building block  $\beta$ -ionone can be used as starting materials [249–253]. Isophorones and  $\beta$ -ionone can be synthesized from acetone and citral. Today, DSM and BASF are among the main producers of carotenoids since F. Hoffmann-La Roche sold its vitamin A and carotenoid production to DSM in 2002. The majority of commercial carotenoids (astaxanthin, canthaxanthin, lycopene,  $\beta$ -carotene, and some derivatives) is produced synthetically on an industrial scale [252,253]. The chemical production to date is



comparatively inexpensive and has a low environmental impact in terms of greenhouse gasses [254]. However, not all carotenoids can be produced efficiently or at all this way, so some carotenoids like lutein are produced naturally to date. Still, chemical processes for lutein synthesis have been developed [255], which may open up the possibility for other chemically synthesized carotenoids.

### Biological and Biotechnological Production Organisms

As described above, many organisms are capable of producing and accumulating carotenoids. Those that deposit higher quantities of them are likely to be used for the production of carotenoid extracts. The most obvious possibility is to use plants.  $\beta$ -Carotene is often still extracted from carrots (*Daucus carota*) [256]. Marigold (*Tagetes erecta*) [257] and sometimes also kale (*Brassica* spp.) [258] are used for the extraction of lutein and zeaxanthin. Lycopene can be extracted from tomatoes and tomato waste [259,260]. Fucoxanthin is produced using brown seaweed (*Undaria pinnatifida*) [182,261].

Microalgae have been established as a further source of carotenoids. The green microalga *Dunaliella salina* has been used for some time for the production of  $\beta$ -carotene. Up to 4% of its cell dry weight is composed of carotenoids, with mainly  $\beta$ -carotene and minor proportions of lutein [262]. Astaxanthin is produced using *H. pluvialis*, which can contain between 0.6 and 7.0% astaxanthin of its cell dry weight under stress conditions [263–267]. And these are likely to be only the first microalgae used for commercial carotenoid production, as also others are already known for their carotenoid synthesis [268], like fucoxanthin from the diatom *Phaeodactylum tricornutum* [269] or lutein and astaxanthin from *Chromochloris zofingiensis* [270].

An industrial source of  $\beta$ -carotene and lycopene is the yeast *Blakeslea trispora* [271,272]. A promising production organism for astaxanthin might be *Xanthophyllomyces dendrorhous* [273] when optimized. It was recently investigated for its use in feed additives [274].

A potentially interesting group of organisms, the thraustochytrids, is capable of synthesizing various carotenoids, particularly astaxanthin,  $\beta$ -carotene, canthaxanthin, echinenone, and phoenicoxanthin [18–20,22,275–280]. They are a family of unicellular microorganisms that is ubiquitous in the marine ecosystem and play an important role in the microbial loop as nutrient recyclers and partners in various relationships with algae and other marine organisms [281,282]. Thraustochytrids are non-photosynthetic organisms and, like yeasts, have the advantage over microalgae production in that they can be grown heterotrophically. Another potential for a low-cost and resource-efficient production of carotenoids from these organisms is their ability to grow on waste streams from food and other industries [283–286]. Some strains produce high amounts of  $\omega$ -3-fatty acids like docosahexaenoic acid (DHA) [22,283–285,287–289] and are already used for their synthesis on an industrial scale [21]. Their oil has GRAS status (e.g., GRN No 860, 777, 1008) and is approved as novel food in the EU [290,291].

It is also possible to insert genes for carotenoid production into already established strains by genetic modification, as it has been done in *Saccharomyces cerevisiae* [292], *Escherichia coli* [293], and some other strains [294].



### Biological and Biotechnological Production Processes

Biotechnological processes used to produce carotenoids can vary greatly depending on the production organism. For plants, classical agricultural processes are applied. Developments toward new aquaponic processes [295] are conceivable. For microalgae, cultivation must supply light for photosynthetic processes in most cases. This is one of the major challenges in microalgae cultivation, as reactors need to provide a high surface area for light transmission. These surfaces are usually achieved by open ponds or tubular and flat-panel systems made of glass or plastic [296–299]. All these systems have certain advantages and disadvantages and may be more or less suitable for certain microalgae. The main advantages are the possible use of atmospheric CO<sub>2</sub> and sunlight for growth. General disadvantages of large-scale phototrophic microalgal cultivation include the difficulty of establishing sufficient gas-liquid mass transfer, adequate mixing [299,300] and temperature regulation [301,302], low cell densities [303], light transfer, biofilm formation, and high cleaning requirements [304], as well as high capital and operational costs [305]. There is also a comparatively higher risk of contamination than using conventional fermenters because even many “closed” systems cannot be operated in a completely closed manner [299]. To induce carotenoid synthesis, microalgae cultivation must include a stress phase after the growth phase. E.g., *H. pluvialis* and *D. salina* accumulate carotenoids only under stress conditions, such as high light irradiation, high salinity, or nutrient (nitrogen) deficiency [306–309]. Therefore, two-stage processes are often used [263–265].

For certain microalgae, heterotrophic processes can also be applied. Still, growth may benefit from a phototrophic phase in addition to cultivation under dark heterotroph conditions, as reported for *C. zoofingensis* [310].

The production of heterotrophic organisms like yeasts or thraustochytrids offers the advantage of using well-established fermentation systems. Heterotrophic cultivation can lead to higher cell densities [311–313], which could help to overcome lower carotenoid yields achieved in phototrophic cultivation of microalgae. Another advantage is that waste streams from food and other industries can be used for cultivation, further reducing the environmental impact and allowing more efficient recycling.

### Downstream Processing

In addition to cultivation, downstream processing is a major component of carotenoid production from microalgae and other microorganisms. Microalgae processing especially requires a cascade of steps to harvest the product, which is often costly, labor intensive, and time consuming [314–317]. Care must be taken to avoid destroying or losing high-value compounds like carotenoids. The process of extracting astaxanthin from *H. pluvialis* is a good example. In general, the biomass must first be harvested and dehydrated to reduce the volume for further processing. Then, disruption is necessary to break the rigid cell wall of the alga, which would otherwise limit extractability [318–320]. Cell disruption might not be necessary for all organisms since, e.g., thraustochytrids and some microalgae such as *D. salina* have unusual cell walls [321–323]. Nevertheless, these also exhibit equivalent structures that may hamper



extraction. Disruption can be performed by mechanical methods like (bead) milling or high-pressure homogenization [317,324–326], classical chemical solvent based extraction [320,327–329], or physical and biological treatments with ultrasound, microwaves, or enzymes [330–332]. Mechanical disruption is a popular method because it is easy to scale up, produces little waste, has good efficiency, and is comparably inexpensive. Caution is required because once the cells are broken, the carotenoids are exposed to the environment and are more prone to oxidation. In a subsequent step, the broken biomass is usually dried to increase shelf life and prepare for extraction. Drying can be accomplished by freeze-drying, spray-drying, or belt-drying [317,333–335]. Drying generally is a very energy consuming step. Due to the large surface area and high temperatures often required for an efficient process, there is a risk of carotenoid degradation [333,334]. Finally, the extraction of astaxanthin can be performed with different solvents. Here, supercritical CO<sub>2</sub> (SC-CO<sub>2</sub>) allows a gentle and selective extraction without the use of toxic or harmful solvents [336–339].

### Qualification and Quantification of Carotenoids

In ecological studies, carotenoids are often measured only indirectly by determining the color of the research object using photographs and color comparison or by non-invasive spectrophotometric methods [340]. Such approaches can only estimate carotenoid content because not all components of coloration are well correlated with carotenoid content [340], and complex mixtures of carotenoids are difficult to distinguish [341]. Similarly, carotenoid measurements in microorganisms are often performed using estimative photometric quantification methods, which measure the absorbance of extracts at different wavelengths [16,263,342]. Photometry does not require sophisticated equipment and is fast and simple. Although the characteristic absorption spectra of carotenoids are useful for their identification, a detailed and reliable quantification of different carotenoids is often hindered by similar or overlapping absorption spectra. Furthermore, carotenoids produced by biological systems do not necessarily occur only in their free all-*E*-form. E.g., in *H. pluvialis*, predominantly all-*E*-astaxanthin is present, along with reported occurrences of 9*Z* and 13*Z*-isomers [343–348]. 15*Z*-astaxanthin and di-*Z*-isomers have been observed in isomerized astaxanthin solutions [44,45]. They have similar absorption spectra and maxima but different absorption coefficients [44,45,244], making quantification by photometric methods inaccurate. Determination of carotenoids by chromatographic methods is possible but also requires some precaution. Natural carotenoids are often esterified with a variety of different fatty acids. Using *H. pluvialis* as an example, it has been shown that 76-94% of astaxanthin occurred in the form of monoesters and 2-23% in the form of diesters. Among others, oleic acid (C18:1) and linoleic acid (C18:2) are the most abundantly linked fatty acids [343,349–351]. The esters have different retention times on chromatographic systems and must either be determined and quantified individually or the carotenoids must be deesterified prior to chromatographic analysis. This might be an issue not only in microorganisms but also in plants [352].



## General Introduction

With the focus on the health-promoting characteristics of carotenoids and in the context of differences in bioavailability and antioxidant properties, and the possible variation of these traits in diastereomers [243,244,353–355], enantiomers, esters, and natural extract compositions [216], detailed and correct quantification of carotenoid mixtures extracted from biological systems is crucial.

### Aim of this Thesis

Carotenoids are ubiquitous molecules with a multitude of applications. Their sustainable and environmentally friendly production is a major goal to ensure a robust supply of healthy supplements or even pharmaceuticals, should they be approved. The biotechnological production of carotenoids is a comparatively young discipline and not yet competitive in terms of energy efficiency, but it offers some advantages over chemical synthesis, such as the theoretical elimination of fossil raw materials and the direct production of natural isomeric mixtures of carotenoids. To optimize biotechnological production, several approaches can be addressed. One of them is minimizing energy consumption, which can be achieved by using solar energy for lighting and drying, developing more efficient photobioreactors, and powering processes with renewable energy. Another approach might be to use heterotrophic production organisms and reduce the amount of energy and fossil raw materials used to produce fertilizers by using waste streams from the food industry to supply nutrients.

The aim of this work was to support the development of biotechnological production processes of carotenoids by different means and at different locations along the process chain. The two main aspects were the downstream processing of the astaxanthin production from a microalgae species and the screening and evaluation of potentially new carotenoid-producing organisms. To assess and compare processing methods and ascertain their efficacy, a precise, robust, and reliable measurement of parameters and results is crucial. The measurement of carotenoids plays a pivotal role in this context. Accurate qualification and quantification of carotenoids allow the evaluation and optimization of process parameters. Different cultivation, processing, and storage methods can be compared, and shelf life can be predicted. Even assertions about the bioaccessibility, bioavailability, and activity of the final product are conceivable if data on the individual compounds are available. Ideally, such determination methods should be comparably simple, fast, and robust, so that they can be carried out by the manufacturers themselves and enable rapid development and optimization of production processes. Therefore, a method for the extraction, deesterification, and chromatographic measurement of astaxanthin esters or their free form from differently processed biomass of *H. phuvialis* was developed (Chapter 1).

One approach to improve the efficacy of biotechnological carotenoid production is to analyze its processes. Downstream processing is an important but energy-consuming [314–317] and delicate part. Carotenoids degrade by reaction with oxygen [356,357], which generally needs to be addressed by processing methods that are fast and in a dark, cool, and oxygen-free environment. The process costs,



energy expenditure, and astaxanthin yield can be compared to find the sweet spot for production. There are various ways to improve processes. Different devices and operational methods can be compared and optimized. The effects that different processes within a process cascade have on each other should also be considered in order to make a holistic statement. Therefore, various downstream process steps of astaxanthin production from *H. pluvialis* were optimized by measuring astaxanthin yield, labor input, and costs. In each process step, different process methods, such as different disruption and drying techniques, were compared. Finally, differently coupled cascades of the investigated processes were evaluated to find their optimal combination in terms of overall efficiency (Chapter 2).

As described, there is a plethora of carotenoid-producing organisms, but few of them have been studied for their potential to be used in biotechnological processes. Worse, often neither the portfolio of carotenoids that can be synthesized by these organisms nor their optimal growth conditions or triggers for the induction of carotenoid synthesis are known. This limits the ability to evaluate and compare them with already established organisms. Thraustochytrids, which are already recognized for their ability to produce carotenoids, were examined to gain a more precise understanding of this little-researched group of marine microorganisms [18,19,22,277,278]. A strain collection of members of the Thraustochytriaceae was classified using 18S rRNA gene sequencing. Their growth behavior and carotenoid synthesis were optimized using experimental design, growth models, and cluster analysis (Chapter 3).







# **Chapter I**

**Development and Validation of Reliable Astaxanthin Quantification from Natural Sources**



RESEARCH ARTICLE

# Development and validation of reliable astaxanthin quantification from natural sources

Inga K. Koopmann , Annemarie Kramer, Antje Labes \*

ZAiT, Center for Analytics in Technology Transfer of Bio and Food Technology Innovations, Flensburg University of Applied Sciences, Flensburg, Schleswig-Holstein, Germany

\* [antje.labes@hs-flensburg.de](mailto:antje.labes@hs-flensburg.de)



## Abstract

Astaxanthin derived from natural sources occurs in the form of various esters and stereoisomers, which complicates its quantitative and qualitative analysis. To simplify and standardize astaxanthin measurement with high precision, an enzymolysis-based astaxanthin quantification method was developed to hydrolyze astaxanthin esters and determine free astaxanthin in all its diastereomeric forms. Astaxanthin standards and differently processed *Haematococcus pluvialis* biomass were investigated. Linear correlation of standards of all-*E*-astaxanthin was observed in a measurement range between extract concentrations of 1.0 µg/mL and 11.2 µg/mL with a coefficient of variation below 5%. The diastereomers 9*Z*-, and 13*Z*-astaxanthin, and two di-*Z*-forms were detected. In contrast to the measurement of standards, the observed measurement range was extended to 30 µg/mL in extracts from *H. pluvialis*. The nature of the sample had to be taken into account for measurement, as cell, respectively, sample composition altered the optimal concentration for astaxanthin determination. The measurement precision of all-*E*-astaxanthin quantification in dried *H. pluvialis* biomass (1.2–1.8 mg dried biomass per sample) was calculated with a coefficient of variation of maximum 1.1%, whereas it was below 10% regarding the diastereomers. Complete enzymolysis was performed with 1.0 to 2.0 units of cholesterol esterase in the presence of various solvents with up to 2.0 mg biomass (dry weight). The method was compared with other astaxanthin determination approaches in which astaxanthin is converted to acetone in a further step before measurement. The developed method resulted in a higher total astaxanthin recovery but lower selectivity of the diastereomers. The reliability of photometric astaxanthin estimations was assessed by comparing them with the developed chromatographic method. At later stages in the cell cycle of *H. pluvialis*, all methods yielded similar results (down to 0.1% deviation), but photometry lost precision at earlier stages (up to 31.5% deviation). To optimize sample storage, the shelf life of astaxanthin-containing samples was investigated. Temperatures below -20°C, excluding oxygen, and storing intact *H. pluvialis* cells instead of dried or disrupted biomass reduced astaxanthin degradation.

## OPEN ACCESS

**Citation:** Koopmann IK, Kramer A, Labes A (2022) Development and validation of reliable astaxanthin quantification from natural sources. PLoS ONE 17(12): e0278504. <https://doi.org/10.1371/journal.pone.0278504>

**Editor:** Vandana Vinayak, Doctor Harisingh Gour Vishwavidyalaya: Dr Hari Singh Gour University, INDIA

**Received:** March 10, 2022

**Accepted:** November 9, 2022

**Published:** December 2, 2022

**Peer Review History:** PLOS recognizes the benefits of transparency in the peer review process; therefore, we enable the publication of all of the content of peer review and author responses alongside final, published articles. The editorial history of this article is available here: <https://doi.org/10.1371/journal.pone.0278504>

**Copyright:** © 2022 Koopmann et al. This is an open access article distributed under the terms of the [Creative Commons Attribution License](https://creativecommons.org/licenses/by/4.0/), which permits unrestricted use, distribution, and reproduction in any medium, provided the original author and source are credited.

**Data Availability Statement:** All relevant data are within the paper and its [Supporting information](#) files.



**Funding:** IKK, AK, AL: The ZAIT is part of the project Grenzland INNOVATIV Schleswig-Holstein [innovative border region Schleswig-Holstein] funded by the German Federal Ministry of Education and Research (BMBF) in context of "Inno-vative Hochschule" [innovative university], [https://www.bmbf.de/bmbf/en/home/home\\_node.html](https://www.bmbf.de/bmbf/en/home/home_node.html). We acknowledge financial support by Land Schleswig-Holstein (federal state Schleswig-Holstein) within the funding program Open Access-Publikationsfonds. The funders had no role in study design, data collection and analysis, decision to publish, or preparation of the manuscript.

**Competing interests:** IK has worked for Sea and Sun Technology, a provider of *H. pluvialis* biomass for the study. All authors have declared that no other competing interests exist. This does not alter our adherence to PLOS ONE policies on sharing data and materials.

## Introduction

Astaxanthin (3,3'-dihydroxy- $\beta,\beta'$ -carotene-4,4'-dione) is a secondary ketocarotenoid. It has a hydrocarbon backbone that comprises a central, delocalized  $\pi$ -electron system.  $\beta$ -ionone rings terminate the hydrocarbon chain at both ends [1, 2]. The presence of one hydroxy- and one oxo-group at each of these terminal rings further classifies it as xanthophyll. Its biosynthesis has been observed mainly in microalgae [3–12] but also in a few protists [13–15], bacteria [16–20], archaea [21] as well as yeasts [22, 23], and very few plant species [24, 25]. Astaxanthin exhibits properties against photooxidative stress by scavenging free radicals [26–31]. These antioxidative effects were also observed in mammalian cells *in vitro* and *in vivo* [32–37] and led to its application as a nutritional supplement, food and feed additive, and in cosmetics. Astaxanthin from natural sources has been authorized for human consumption in many countries worldwide [38]. Few minor adverse effects of dosed astaxanthin consumption were observed [38]. Allergic reactions to the consumption of *H. pluvialis* proteins cannot be excluded, but their likelihood has been considered low in tested astaxanthin-rich novel food ingredients by the European Food Safety Authority (EFSA) [39]. It can also be produced synthetically, but its natural form has gained interest with respect to consumer demands [40, 41]. A major source for the biotechnological production of astaxanthin is the green alga *Haematococcus pluvialis* [11, 42]. It contains 1.9 to 7.0% astaxanthin of its dry weight in certain life cycle stages and under stress conditions [43–48]. As in other producing organisms, astaxanthin in *H. pluvialis* is derivatized at one or both hydroxyl groups with various fatty acids, mainly leading to the formation of monoesters (76–94%), besides diesters (2–23%) and free astaxanthin (0.3–4%) [49–53]. The most common fatty acids occurring in these combinations are C18:1 and C18:2, amongst many others [49–52]. The conjugated double-bound system can theoretically form a variety of diastereomers [54]. The most abundant form in *H. pluvialis* is the all-*E* configuration followed by the sterically unhindered 9*Z*-, 13*Z*- and 15*Z*-forms [55–59] as well as corresponding di-*Z*-forms [50, 58, 60]. Due to the two stereogenic carbon atoms C-3 and C-3', three or four enantiomers are possible when a symmetrical or asymmetrical *Z*-form is considered, respectively (3*S*,3'*S*, 3*R*,3'*R*, 3*S*,3'*R* / 3*R*,3'*S*). In *H. pluvialis*, the ratio of the astaxanthin enantiomers was reported to be 88:10:2 and 99:0:1 (3*S*,3'*S*, 3*R*,3'*R* and 3*S*,3'*R*) [57, 61, 62].

Determining total astaxanthin in biological samples is crucial on the analytical and production scale. Most studies use estimating, photometric quantification methods instead of precise determination of total astaxanthin including its isomers for the means of hyphenated chromatography. Photometry enables simple and fast determination without the need for sophisticated equipment [23, 43, 63–65]. The biological variability of astaxanthin with all its different isomeric forms and esters [49, 51] complicates the exact quantification of astaxanthin. Moreover, astaxanthin is sensitive to treatment with solvents [54, 66, 67]. Access to sophisticated hyphenated chromatography protocols is limited. Here we demonstrate a fast, robust, and reliable method to get reproducible and comparable results of an overall astaxanthin content.

Many available methods to determine the astaxanthin content in *H. pluvialis* have been described. The most sophisticated ones extract, identify, and quantify a variety of esters and isomers with liquid chromatographic and spectrophotometric/mass spectrometric methods [46, 49–51, 64, 68–74]. However, this is time-consuming, as liquid chromatographic methods that differentiate the varying esters require much time for separation. Correct evaluation is elaborate because absorption spectra of carotenoids are similar. Moreover, correct quantification is difficult due to the different absorption coefficients of the geometric isomers.



A faster and more general approach is to extract all carotenoids and determine astaxanthin photometrically by estimating its proportion of total carotenoids [23, 43, 63]. The methods optionally include or destroy residual chlorophylls with a chemical treatment before measurement [45, 64, 65, 75, 76]. Recent approaches suggested the use of a higher wavelength (530 nm) than the absorbance maximum of astaxanthin for quantification to avoid overlapping absorption by chlorophylls and other carotenoids [48, 59, 77]. These photometric methods are cost-extensive, though the estimation may lead to unpredictable deviations, and the chlorophyll destruction may also impact the carotenoids. The geometrical isomers of astaxanthin have similar absorption spectra [50, 58–60, 66, 78], though different extinction coefficients [79], which impedes their individual quantification. To refine those photometric methods, astaxanthin can be fractionated by chromatographic methods (thin layer or column chromatography) beforehand and the corresponding fractions can be measured photometrically, applying the respective absorption coefficients [80–82]. However, the correct merging of the many esters and isomers is still difficult, leading to inaccuracy and deviation.

An option is to saponify the esters and isolate and quantify the resulting free astaxanthin with a shorter chromatographic method. Here, different methods for deesterification have been applied. Alkaline treatments with NaOH [55, 70, 83–88] or KOH [86, 89] are possible but can cause changes in the structural conformation and/or degradation of carotenoids [77, 85, 86, 90]. Thus, another approach is enzymolysis with esterases [61, 83, 85, 91, 92], lipases [93–95] or whole-cell catalysts [96].

The enzymolysis of astaxanthin is a promising compromise to quantify astaxanthin precisely while minimizing time consumption. Based on the enzymolysis of carotenoid esters, developed by Jacobs et al. [91], methods for quantification of astaxanthin were adapted by various studies and protocols [61, 83, 87, 92, 97–99]. However, to our knowledge, an in-depth evaluation of the process boundaries, detection limits, accuracy, and applicability of various astaxanthin-containing natural sources has not yet been performed. Therefore, a method for robust and reliable determination of astaxanthin from *H. pluvialis* was developed and validated, which was still faster than methods determining the various esters of astaxanthin. The five step-method comprises the preparation of biological samples and astaxanthin extraction, enzymolysis, liquid-liquid extraction of astaxanthin, processing of the resulting extract, and measurement with ultra-high performance liquid chromatography (UHPLC) and UV/VIS spectrometry. Particular emphasis was set to relevant factors: Enzyme and biomass amount, shelf life, incubation time, quantification limits, linearity, precision, systematic errors, robustness, and isomerization effects were tested. The final method was compared to photometric astaxanthin determination approaches. We aimed to develop a method that is applicable at all different stages of astaxanthin production and works with different formulations of astaxanthin. Therefore, it was tested with commercially available *H. pluvialis* and astaxanthin samples.

## Materials and methods

### Chemicals and reagents

Analytical grade acetone (SupraSolv), petroleum ether, and acetonitrile (hypergrade) were obtained from Merck (Darmstadt, Germany). Ethanol and Tris(hydroxymethyl)aminomethane (TRIS) ( $\geq 99.9\%$ ) were provided by Carl Roth (Karlsruhe, Germany) and formic acid (99% ULC/MS) by Biosolve (Valkenswaard, Netherlands). Hydrochloric acid for pH value adjustment was purchased from Merck (Darmstadt, Germany). Cholesterol esterase from *Pseudomonas* sp. for enzymolysis was obtained from MP Biomedicals (Eschwege, Germany). All-*E*-astaxanthin standard in its free form (SML0982,  $\geq 97\%$ , 3S,3'S, from *Blakeslea trispora*) was



provided by Sigma-Aldrich (Taufkirchen, Germany) and astaxanthin monopalmitate (1017, 3RS,3'RS) by CaroteNature (Münsingen, Swiss).

### ***H. pluvialis* biomass and astaxanthin containing extracts**

Various commercially available sources of *Haematococcus pluvialis* biomass containing astaxanthin were used: Dried and disrupted cysts were obtained from Golden Peanut (Garstedt, Germany). Sea & Sun Technology GmbH (Trappenkamp, Germany) provided concentrated *H. pluvialis* aplanospores from seven different batches in nutrient depleted media. Sea & Sun Technology also provided oleoresins of *H. pluvialis* obtained from supercritical CO<sub>2</sub> (SC-CO<sub>2</sub>) extraction either pure or diluted in ethanol. Cultivation and harvest parameters are not available on those samples, but for two batches of concentrated, fresh biomass obtained from Sea & Sun Technology. Those were taken from day 22 to 28 of a light and nutrient-induced stress phase. All had been cultivated in BG11 medium (Culture Collection of Algae at the University of Göttingen): 17.6 mM NaNO<sub>3</sub>, 0.18 mM K<sub>2</sub>HPO<sub>4</sub> x 3H<sub>2</sub>O, 0.3 mM MgSO<sub>4</sub> x 7H<sub>2</sub>O, 0.25 mM CaCl<sub>2</sub> x 2H<sub>2</sub>O, 0.031 mM citric acid, 0.023 mM ferric ammonium citrate, 0.003 mM Na<sub>2</sub>EDTA x H<sub>2</sub>O, 0.19 mM NaCO<sub>3</sub> and 1 mL/L trace metal solution made of 1.0 mM H<sub>3</sub>BO<sub>3</sub>, 1.0 mM MnSO<sub>4</sub> x H<sub>2</sub>O, 1.00 mM ZnSO<sub>4</sub> x 7H<sub>2</sub>O, 0.01 mM (NH<sub>4</sub>)<sub>6</sub>Mo<sub>7</sub>O<sub>24</sub> x 4H<sub>2</sub>O and 0.1 mM CuSO<sub>4</sub> x 5H<sub>2</sub>O. These were used exclusively for the experiments in which the developed method was to be compared with photometric methods.

### **Disruption of *H. pluvialis* and astaxanthin extraction**

Undisrupted biomass was bead-milled to ensure astaxanthin accessibility during further processing. Therefore, 0.2–4.0 mg cell dry mass were weighed into lysis tubes type C (ceramic beads, diameter 0.4–0.6 mm) by Analytik Jena (Jena, Germany). 500 µL acetone were added for astaxanthin extraction. When analyzing aplanospores in liquid medium, volumes of equal to or less than 300 µL of well-homogenized samples were filled into the same lysis tubes and matched to a final amount of 0.5–2.0 mg of biomass. The tubes were filled up to 500 µL with acetone accordingly. The cysts were broken mechanically in a swing mill (MM 2000, Retsch, Haan, Germany) at 27 Hz for 3 minutes without cooling and centrifuged at 10,000 x g. The supernatant of both sample types was transferred to a centrifuge tube, and 500 µL of fresh acetone were added to the lysis tube. This procedure was repeated twice until the supernatant and the residual biomass were colorless.

### **Astaxanthin deesterification by enzymolysis**

The preparation for enzymolysis varied with the sample type. Using concentrated fresh or dried biomass, the combined supernatants obtained from astaxanthin extraction were filled up to 3 mL with acetone (Δ 90–100% v/v). Highly viscous oleoresins were weighed directly into centrifuge tubes with 0.4 to 15.8 mg and diluted in 3 mL acetone. Oleoresins dissolved in ethanol were used at 0.1 to 3 mL and filled up with acetone to 3 mL. 2 mL of 50 mM TRIS buffer (pH 7 at 21°C) and 600 µL cholesterol esterase solution at a concentration of 3.3 U/mL suspended in the same buffer were added. Accordingly, final cholesterol esterase concentration in the sample was 2.0 units or 0.36 units per mL. The tubes were incubated at 37°C in a water bath and mixed gently every 10 minutes. Astaxanthin was recovered by liquid-liquid extraction with 2 mL (Δ 26% v/v) of petroleum ether. The mixture was shaken vigorously for 10 s to ameliorate astaxanthin transfer into the petroleum ether. Subsequent phase separation was enhanced by centrifugation at 3,000 x g for 1 minute. The upper, astaxanthin-containing phase



was filtered (0.45  $\mu\text{m}$ , PET) into amber vials. It was either measured directly or stored at  $-21^{\circ}\text{C}$  for one night before analysis.

### Analysis and quantification of free astaxanthin and lutein by UHPLC-PDA-MS

Extracts were vortexed (Vortex 3, IKA-Werke GmbH und Co. KG, Staufen, Germany) and ultrasonicated for 20–30 s (Sonorex Super RK 103 H, Bandelin electronic GmbH und Co. KG, Berlin, Germany) before analysis if they had been stored overnight. Qualification and quantification of astaxanthin were performed by UHPLC using an ACQUITY Arc system by Waters (Milford, MA, USA) equipped with a sample manager (FTN-R), a quaternary solvent manager (R), an UV/Vis detector (2998 PDA Detector), and a mass spectrometer (Acquity QDa Detector). A C18-column (Cortecs C18 2.7  $\mu\text{m}$ , 90  $\text{\AA}$ , 3.0 x 100 mm) was operated at  $40^{\circ}\text{C}$ . The injection volume was 5  $\mu\text{L}$ . Starting conditions were 70% millipore water and 30% acetonitrile, both containing 0.1% formic acid. Over four minutes, the gradient increased linearly to 90% acetonitrile and 10% millipore water. This ratio was kept isocratic for five minutes. A rinsing step on 100% acetonitrile was attached for a further 2.5 minutes. 3.5 minutes were used for regeneration of the starting conditions. Flow velocity was 0.5 mL/min. Optical spectra were measured in a range of 200 to 800 nm, and astaxanthin data were analyzed and quantified at its determined absorbance maximum of 474 nm. The absorption maximum of lutein was shown to be at 448 nm. This wavelength was used for quantification. The mass spectrometer with electrospray ionization (ESI) was operated in positive mode with a cone voltage of 15 V and a probe temperature of  $600^{\circ}\text{C}$ , measuring in a range of  $m/z$  150 to 1250. For further accuracy, the mass of astaxanthin was observed by selected ion recording (SIR) at  $m/z$  598  $[\text{M}+\text{H}]^{+}$  and lutein at  $m/z$  570  $[\text{M}+\text{H}]^{+}$ . Besides the major all-*E*-astaxanthin peak, peaks with UV/Vis absorption spectra corresponding to *Z*-astaxanthin isomers [50, 58–60, 66, 78] that were additionally accompanied by peaks with the mass of astaxanthin in SIR were assigned to 9*Z*- and 13*Z*-astaxanthin and several di-*Z*-isomers. However, as the latter are difficult to differentiate without further validation, they were summed and are consecutively termed di-*Z*-isomers. Quantities of all diastereomers were estimated by using the quantification of all-*E*-astaxanthin, corrected by factors adjusting the different extinction coefficients published by Bjerkeng et al. [79], namely 1.20 for 9*Z*-astaxanthin, 1.56 for 13*Z*-astaxanthin, and 1.11 for the di-*Z*-isomers.

### Calibration curve—Astaxanthin

For identification and quantification, free all-*E*-astaxanthin was used at concentrations of 0.5–45.0  $\mu\text{g/mL}$  in acetone. Blank acetone was applied for zero value determination. Samples of 0.5 to 54.8  $\mu\text{g}$  free astaxanthin and 1.0 to 62.6  $\mu\text{g}$  astaxanthin monopalmitate were subjected to the deesterification process to determine their recoveries. Both were diluted in acetone and treated as described above. In the processing of free astaxanthin, the cholesterol esterase solution was replaced with the same amount of TRIS buffer. For quantification of monopalmitate-ester derived free astaxanthin, a proportion of 69.4% w/w astaxanthin was assumed by molecular weight calculation.

### Calibration curve—Lutein

To identify and quantify lutein from *H. pluvialis*, free lutein standard in concentrations of 1.0 to 61.5  $\mu\text{g/mL}$  dissolved in acetone was used for calibration. Linear regression was performed by ordinary least squares and forced through zero for optimal approximation to standards recovered in petroleum ether.



### Optimization of enzymolysis and liquid-liquid extraction

**Enzyme amount and duration of enzymolysis.** The amount of cholesterol esterase was varied between 0.05 to 2.0 units per reaction for equal amounts of astaxanthin esters in 0.4 mg *H. pluvialis* powder (Golden Peanut) to pinpoint optimal enzyme concentration for astaxanthin conversion during 0.75 hours of incubation. In addition, the incubation time of enzymolysis was doubled to 1.5 hours using 0.5 units and 2.0 units of cholesterol esterase.

**Influence of ethanol on astaxanthin enzymolysis.** The recovery of astaxanthin in samples processed in the presence and absence of ethanol was compared. Therefore, two different ethanolic SC-CO<sub>2</sub> extracts (n = 7 and n = 5) of *H. pluvialis* with volumes between 150 and 1000 µL were used. They were either fed directly to the deesterification process (n = 5 and n = 3) or ethanol was evaporated at 40°C under nitrogen, and the sample was subsequently resuspended in acetone and TRIS buffer containing 2.0 units of cholesterol esterase for deesterification (n = 2 and n = 2). All samples were enzymolyzed, extracted, and astaxanthin content was quantified based on UHPLC-PDA measurements as described above.

**Influence of solvents used in liquid-liquid extraction on astaxanthin quantification.** The volume of the upper petroleum ether layer was determined after liquid-liquid extraction to determine extract concentrations. Therefore, blank samples (n = 8) consisting of 3 mL acetone and 2.6 mL TRIS buffer were heated to 37°C for 20 minutes in a water bath. Afterward, the samples were shaken vigorously with 2 mL petroleum ether, centrifuged at 3,000 x g for 1 minute, and cooled to 21°C in a water bath. The complete upper layer was transferred into reaction tubes and weighed (n = 4). Its density was determined by measuring the upper layer of the remaining samples with a pycnometer (n = 4). The corresponding volume was calculated.

To quantify the influence of ethanol on the volume of the upper extraction phase, various volumes of ethanol (0 to 2010 µL) were filled up to 3 mL with acetone and treated similarly to the previous experiment.

### Extract processing

After liquid-liquid extraction, various processing procedures of the petroleum ether fraction were compared to reach the maximum recovery of astaxanthin. Therefore, 20 µg of free astaxanthin standard were deesterified and extracted with petroleum ether as described above. The upper layer was treated in three ways: (1) The extraction phase was not treated. (2) An aliquot of the extraction phase was dried under nitrogen and redissolved in the same volume of acetone. (3) Most of the extraction phase was transferred to another tube, and fresh petroleum ether was added to the original sample. The extraction and transfer steps were repeated twice until the upper layer was colorless. The combined fractions were dried at 40°C under nitrogen and redissolved in 2 mL of acetone. The samples were filtered, and astaxanthin was measured by the UHPLC-PDA-MS method. All experiments were performed in triplets or quartets.

### Evaluation of detection limits and linearity of astaxanthin determination

Detection limits and linearity of astaxanthin measurement were determined by varying the amount of *H. pluvialis* powder (Golden Peanut) from 0.04 mg to 2.0 mg in triplets. 3.3 and 4.0 mg were tested without replicates. They were enzymolyzed with a constant concentration of 2.0 units cholesterol esterase in 3 mL of acetone and 2.6 mL of TRIS buffer and 0.75 hours of incubation.



## Determination of measurement precision

The astaxanthin content of two samples from different packages of dried *H. pluvialis* biomass (Golden Peanut) was measured using the standard enzymolytic UHPLC-PDA procedure described above. Measurements were performed once on three and four different days to determine the variation between experiments carried out independently. Between 1.2 and 1.8 mg of sample were applied.

## Method adjustment

**Liquid cultures and oleoresins.** Various liquid culture batches of *H. pluvialis* biomass (Sea & Sun Technology) concentrated at 7.1, 39.5, 182, and 262 g/L were examined. For disruption, volumes of 1 to 45  $\mu$ L of these samples were transferred to lysis tubes to get final amounts of 0.1 to 2.0 mg of biomass. Further processing was accomplished as described above.

Additionally, four oleoresins of *H. pluvialis* extracted with SC-CO<sub>2</sub> were investigated. Therefore, 0.15 to 1.8 mg of oleoresin were directly added to the deesterification solution. Enzymolysis was carried out with 2.0 units and 4.0 units of cholesterol esterase per reaction. Extraction and quantification were performed as described above.

**Sample mixtures.** Various astaxanthin-containing samples were deesterified individually and merged to examine cross-interactions. The individual samples contained either 240  $\mu$ g of *H. pluvialis* powder (Golden Peanut), 16  $\mu$ g of astaxanthin monopalmitate, or 12  $\mu$ g of free astaxanthin. Maximum 4.5% w/w of the *H. pluvialis* powder were considered to be free astaxanthin by measurements. Astaxanthin monopalmitate consists of about 69.4% w/w of free astaxanthin. Thus, the final extracts of the samples contained 4.2 to 4.7  $\mu$ g/mL of free astaxanthin. Moreover, three samples were prepared, two containing mixtures of two of the single solutions, and one sample containing all three. In these, the individual samples were represented at identical amounts as in the samples containing only one of the analytes.

After enzymolysis and recovery in petroleum ether, three aliquots of 600  $\mu$ L were taken from each sample. They were prepared either with 63  $\mu$ L pure acetone, 31.5  $\mu$ L pure acetone and 31.5  $\mu$ L of astaxanthin standard solution containing 3.6  $\mu$ g free astaxanthin, or with 63  $\mu$ L of astaxanthin standard solution containing 7.2  $\mu$ g free astaxanthin. Furthermore, 600  $\mu$ L pure petroleum ether were enriched with acetone and astaxanthin like the samples. The experiment was performed once.

## Method comparison to photometric astaxanthin estimation

To compare the developed method to simpler photometric approaches, the astaxanthin content of several *H. pluvialis* samples (Sea & Sun Technology) taken towards the end of a cultivation phase were measured with UHPLC-PDA-MS and photometrically. From two individual culture batches, samples were taken on days 22–24 and 27–28 of the cultivation. For each UHPLC measurement, 1.0 mg of *H. pluvialis* biomass was used. Extraction, enzymolysis, and quantification were carried out as described above. All samples were measured once. For photometric measurements, samples were extracted similarly. The extracts were measured at  $\lambda = 470$  nm and with a wavelength scan from 300 to 700 nm in steps of 2 nm. Astaxanthin content was calculated using two different approaches: (1) Lambert-Beer was applied with the concentration of astaxanthin ( $C_{ax}$ ) in g/mL, the optical path length  $d$  in cm, the absorption at the wavelength represented with the subscript number and the 1%-absorption coefficient  $A_{1\%}^{1\text{cm}} \epsilon_{ax} = 1980$  [100mL/(g\*cm)] of a carotenoid mixture in 80% acetone and 20% water [100]. A factor of 0.8 for the astaxanthin proportion of total carotenoids was assumed based on various literature data [45, 53, 59, 101]. This (Eq 1) will be termed “general equation” hereafter. (2)



The calculations of Lichtenthaler [100] for chlorophylls and total carotenoids were used to determine the carotenoid fraction. See Eqs 2.1–2.3 with the concentration of chlorophyll *a* ( $C_a$ ), chlorophyll *b* ( $C_b$ ), and of total carotenoids ( $C_{x+c}$ ) in  $\mu\text{g/mL}$  in acetone with 20% water, and the absorptions at corresponding wavelengths represented with the subscript numbers. Again, the astaxanthin proportion was calculated by multiplying the total carotenoid content with a factor of 0.8 (Eq 2.4).

$$C_{ax} = \frac{0.8 A_{470}}{\epsilon_{ax} d} \quad (1)$$

$$C_a = 12.2 A_{663.2} - 2.79 A_{646.8} \quad (2.1)$$

$$C_b = 21.50 A_{646.8} - 25.10 A_{663.2} \quad (2.2)$$

$$C_{x+c} = \frac{(1000 A_{470} - 1.82 C_a - 85.02 C_b)}{198} \quad (2.3)$$

$$C_{ax} = 0.8 C_{x+c} \quad (2.4)$$

### Shelf life experiments

Different samples were prepared to determine the shelf life of astaxanthin in various matrices and environmental conditions. (1) Free all-*E*-astaxanthin at a concentration of 1  $\mu\text{g/mL}$  in acetone was stored in amber vials at  $-80^\circ\text{C}$ ,  $-20^\circ\text{C}$ ,  $4^\circ\text{C}$ , and room temperature for 833 days. Optical density was measured initially, after 11, 42, and 833 days by UV/Vis photometry at  $\lambda = 474$  nm. (2) Astaxanthin concentration of a concentrated *H. pluvialis* culture (40 g/L) (Sea & Sun Technology) was determined directly and after storage at  $4^\circ\text{C}$  in the dark for 104 and 489 days. (3) The same sample was freeze-dried. Therefore, aliquots were poured into small glass vessels with a filling height of approximately 0.5 cm. They were placed into a freeze drier (Alpha 1–4, Christ, Osterode, Germany) for 24 hours at  $\leq 37$  Pa. After the lyophilization was finished, the vessels were sealed under vacuum and stored at  $4^\circ\text{C}$  in the dark. However, one sample was measured directly using the described enzymolytic UHPLC-PDA standard method. The other samples were exposed to ambient air after 7, 108, and 489 days and measured. Afterward, the samples were closed without vacuum sealing and stored under the same conditions until 489 days after lyophilization. Hereafter, all samples were measured again. (4) Two sealed packages of *H. pluvialis* biomass (Golden Peanut) were stored as purchased at  $-21^\circ\text{C}$  in the dark over the whole experiment. One was opened and closed again tightly at the beginning of the experiment. Both packages were opened after two and a half years and measured using the UHPLC-PDA standard method.

### Statistics

Linear regression was performed by ordinary least squares method, and the significance of the deviation of the  $y$ -intercepts from zero was evaluated by *t*-tests. To determine the device-related measurement deviation, free all-*E*-astaxanthin standards dissolved in acetone were measured regularly prior to or after sample measurements. A total of 45 samples with astaxanthin concentrations between 0 and 45.0  $\mu\text{g/mL}$  were taken into account. Tests on significant deviations were calculated using mean difference tests with a level of significance of  $\sigma = 0.05$ .



## Results and discussion

An enzymolysis-based process for astaxanthin deesterification from natural samples was established to quantify astaxanthin easily without having to identify its various esters. Interactions of sample amount and enzyme quantity were evaluated to find optimal conditions for maximum astaxanthin recovery. These were verified with different astaxanthin-containing samples. Moreover, the shelf life was evaluated to minimize losses prior to analysis. Finally, the method was compared to simple photometric approaches for astaxanthin determination to assess their applicability in process monitoring (Fig 1).

### Calibration curve

**Detection limits and linearity of astaxanthin standards.** For astaxanthin quantification, a calibration was established with free all-*E*-astaxanthin standard dissolved in acetone, filtered, and injected directly into the UHPLC-PDA-MS system in various concentrations. The resulting peak areas were integrated for calibration curve determination. The retention time of the all-*E*-astaxanthin peak was 7.50 minutes. Linear regression resulted in the correlation  $f(x) = 1693.4x - 990.57$  with a coefficient of determination of 0.9985. The coefficient of variation was below 4% for all data points, except for the zero value. The calculated y-intercept was significantly different from zero (Table 1). Measurement of all-*E*-astaxanthin dissolved in acetone has a greater number of replicates than the following measurements because it was also used as a parallel check on the stability of the instrument.

As the process should be applied for natural samples that have to be deesterified, the calibration was repeated with free all-*E*-astaxanthin and astaxanthin monopalmitate. Standards of both substances were subjected to enzymolysis conditions to verify the behavior and linearity of the calibration (Fig 1, a1). The retention time of all-*E*-astaxanthin was 6.43 minutes.

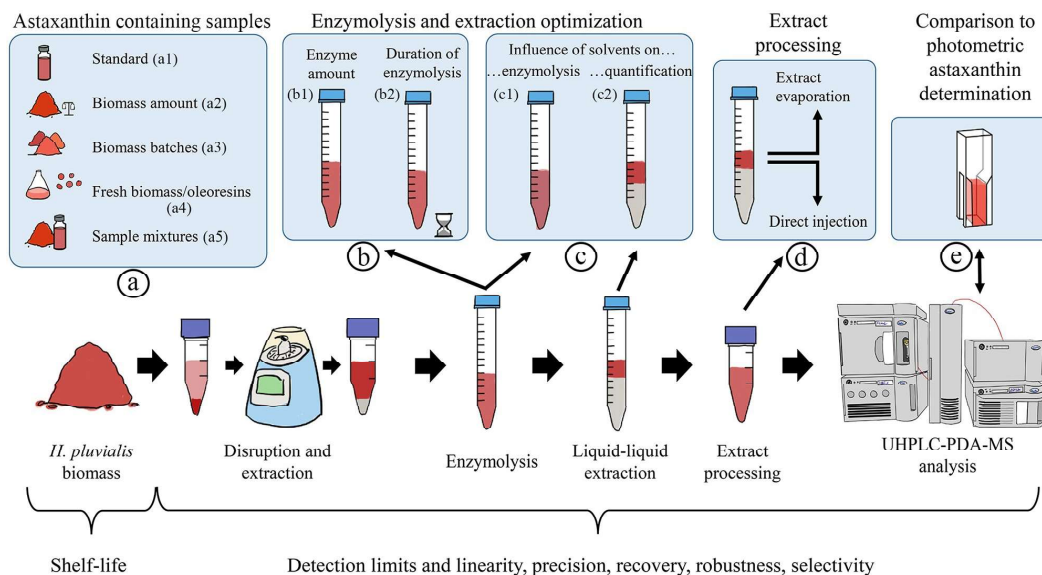


**Fig 1. Schematic overview of the method development for astaxanthin quantification.**

<https://doi.org/10.1371/journal.pone.0278504.g001>



Table 1. Calibration curves of astaxanthin standards.

Sample				Concentration limits ( $\mu\text{g/mL}$ )	Number of measurements	Linear regression		Linear regression through zero	
Standard	Solvent	Processing	Integrated isomers			Equation	$R^2$	Equation	$R^2$
All- <i>E</i> -Ax <sup>a</sup>	acetone	direct	all- <i>E</i> -Ax	0–32.3	112	$1693.4x - 990.57^*$	0.9985	$1643.0x$	0.9966
All- <i>E</i> -Ax	acetone	direct	all- <i>E</i> , 9Z, 13Z, diZ-Ax	0–32.3	27	$1718.2x - 676.84^*$	0.9993	$1724.4x$	0.9982
All- <i>E</i> -Ax	acetone	direct	all- <i>E</i> -Ax	0–11.2	78	$1580.9x - 548.95$	0.9964	$1493.7x$	0.9917
All- <i>E</i> -Ax	acetone	direct	all- <i>E</i> , 9Z, 13Z, diZ-Ax	0–11.2	21	$1626.2x - 429.73$	0.9962	<b><math>1566.1x</math></b>	0.9933
All- <i>E</i> -Ax	PE <sup>c</sup> + acetone	like in enzymolysis	all- <i>E</i> -Ax	0–11.2	10	$1624.4x - 65.64$	0.9996	$1615.3x$	0.9995
Ax-Mp <sup>b</sup>	PE + acetone	like in enzymolysis	all- <i>E</i> -Ax	0–7.5	9	$1700.8x + 5.50$	0.9994	$1702.0x$	0.9994
All- <i>E</i> -Ax & Ax-Mp	PE + acetone	like in enzymolysis	all- <i>E</i> -Ax	0–11.2	18	$1633.6x + 33.13$	0.9982	$1638.9x$	0.9982
All- <i>E</i> -Ax & Ax-Mp	PE + acetone	like in enzymolysis	all- <i>E</i> , 9Z, 13Z, diZ-Ax	0–11.2	18	$1753.3x + 40.56$	0.9985	<b><math>1759.9x</math></b>	0.9985

Regressions used for quantification are highlighted bold.

\*y-intercept significantly different from zero.

<sup>a</sup>Ax = Astaxanthin.

<sup>b</sup>Ax-Mp = Astaxanthin monopalmitate.

<sup>c</sup>PE = Petroleum ether.

<https://doi.org/10.1371/journal.pone.0278504.t001>

Subsequently, calibration was repeated for the obtained astaxanthin UHPLC-PDA peaks and compared to the previous based on the standard dissolved in acetone. Calculations with the previously examined line of best fit did not properly depict the lower concentrations of enzymolyzed astaxanthin in a concentration range between 0.0 to 13.6  $\mu\text{g/mL}$  and resulted in an overestimation of all-*E*-astaxanthin content of a maximum of 131% at a concentration of 0.4  $\mu\text{g/mL}$  and 57% at 1.0  $\mu\text{g/mL}$  astaxanthin. Thus, linear regressions were calculated from the newly obtained values. Regressions resulted in similar linear correlations below 11.2  $\mu\text{g/mL}$  astaxanthin in the liquid-liquid extraction phase, which was the upper detection limit. It was  $f(x) = 1624.4x - 65.639$  ( $R^2 = 0.9996$ ,  $n = 10$ ) for free all-*E*-astaxanthin from free all-*E*-astaxanthin standard and  $f(x) = 1700.8x + 5.500$  ( $R^2 = 0.9994$ ,  $n = 9$ ) for free all-*E*-astaxanthin from astaxanthin monopalmitate (Fig 2). The y-intercept was not significantly different from zero for both. As the aim was to quantify astaxanthin derived from natural samples that have to be prepared by enzymolysis, quantification should be performed by using an appropriate calibration curve. The calibration using astaxanthin and astaxanthin monopalmitate subjected to the standard deesterification procedure was the most trustworthy. For higher accuracy, a calibration curve combining the previous two, including the later described isomers and forced through zero, was used. It was  $f(x) = 1759.9x$  ( $R^2 = 0.9985$ ,  $n = 18$ ). This curve represented astaxanthin concentrations between 1.0  $\mu\text{g/mL}$  and 11.2  $\mu\text{g/mL}$  with less than 5% error in both directions.

At 0.5  $\mu\text{g/mL}$  the calculated recovery decreased by 11%. Thus, a concentration between 0.5 and 1.0  $\mu\text{g/mL}$  should be recognized as the lower detection limit. Moreover, the linear correlation ended when the astaxanthin concentration exceeded 11.2  $\mu\text{g/mL}$ . Higher concentrations resulted in reduced recoveries down to 55% at 27  $\mu\text{g/mL}$ . This behavior was correlated to the



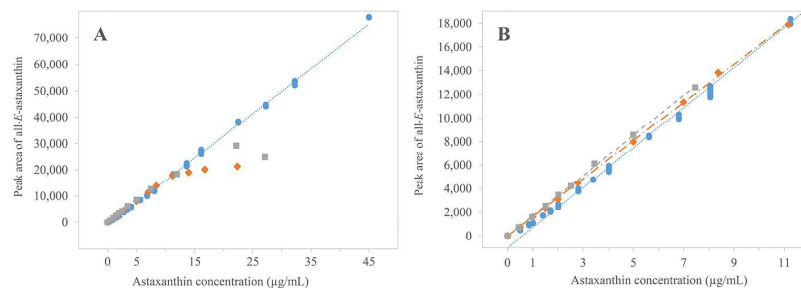


**Fig 2. Calibration curves of differently processed astaxanthin standards.** B close-up from A including the linear regressions through zero of the standards in petroleum ether and acetone mixture. ● all-*E*-astaxanthin standard in acetone, linear  $f(x) = 1693.4x - 990.57$ ,  $R^2 = 0.9985$ , ◆ all-*E*-astaxanthin standard in petroleum ether-acetone mixture, linear  $f(x) = 1615.3x$ ,  $R^2 = 0.9995$ , ■ deesterified astaxanthin monopalmitate in petroleum ether-acetone mixture, linear  $f(x) = 1702.0x$ ,  $R^2 = 0.9994$ .

<https://doi.org/10.1371/journal.pone.0278504.g002>

precipitation of astaxanthin, which was observed at the phase boundary and glass wall when more than 11.2 µg/mL of astaxanthin were present during the liquid-liquid extraction step. The liquid-liquid extraction of astaxanthin into petroleum ether is a delicate step as pure astaxanthin is poorly soluble in pure petroleum ether. During liquid-liquid extraction, acetone is absorbed into the petroleum ether, shifting the equilibrium and accumulating astaxanthin in the upper phase. The solubility of astaxanthin in the petroleum ether-acetone mixture is still limited at an upper boundary of approximately 11.2 µg/mL. This phenomenon was more pronounced for the processed free astaxanthin than processed astaxanthin monopalmitate. E.g., astaxanthin derived from the free standard resulted in a 58% recovery at 22.2 µg/mL, whereas astaxanthin derived from astaxanthin monopalmitate resulted in an 80% recovery at 22.3 µg/mL. This difference indicates an alteration of astaxanthin solubility in the upper layer by the presence of cleaved palmitic acid. Further testing of the type of solvent and ratio might increase astaxanthin solubility, but the functionality of the deesterification process has to be ensured. In the current experimental setup, a concentration of 11.2 µg/mL astaxanthin in the liquid-liquid extraction phase can be considered as the upper detection limit by restricting the amount of biomass for optimal astaxanthin recovery.

The observed shifts in retention time can be attributed to the different solvents. The astaxanthin peak was more than one minute later in pure acetone than in petroleum ether-acetone. This may be due to altered binding behavior on the column at starting conditions and/or miscibility with the mobile phase, which started at a high water content (70% v/v). However, decreasing the water content at the beginning affected peak shape negatively.

**Selectivity.** Considering free all-*E*-astaxanthin standard dissolved in acetone and injected directly, diastereomers were detected besides the main all-*E*-astaxanthin peak (S1 Table). 9*Z*-astaxanthin, 13*Z*-astaxanthin and one di-*Z*-isomer were observed with a medium proportion of total astaxanthin of  $2.4 \pm 0.2\%$  ( $n = 29$ ) at 7.90 minutes,  $0.4 \pm 0.1\%$  ( $n = 26$ ) at 8.84 minutes, and  $0.2 \pm 0.03\%$  ( $n = 26$ ) at 8.56 minutes, respectively. The proportion of 9*Z*- and di-*Z*-astaxanthin remained constant, whereas 13*Z*-astaxanthin rose with prolonged storage and multiple measurements of the same sample up to 2.2%, indicating isomerization reactions during storage in acetone. Organic solvents have been reported to cause the isomerization of carotenoids [54, 66, 67, 102]. These were described to favor the 13*Z*-isomer [67], which can be confirmed here.

In standards processed similarly to enzymolyzed samples, all-*E*-astaxanthin was detected, and two minor peaks were assigned to 9*Z*- (7.51 minutes) and 13*Z*-astaxanthin (8.50 minutes).



The medium proportions of 9Z-astaxanthin, relative to total astaxanthin, were  $5.9 \pm 0.5\%$  ( $n = 9$ ) and  $4.9 \pm 0.3\%$  ( $n = 8$ ), obtained from free astaxanthin and astaxanthin monopalmitate, respectively. The peak areas of 13Z-astaxanthin were  $1.3 \pm 0.5\%$  ( $n = 9$ ) and  $2.1 \pm 0.9\%$  ( $n = 8$ ) obtained from free astaxanthin and astaxanthin monopalmitate, respectively. Thus, 9Z- and 13Z-astaxanthin were detected at significantly higher quantities in processed free astaxanthin and astaxanthin monopalmitate than in free astaxanthin dissolved in acetone. Again, this indicates isomerization reactions of the standards during storage and processing. However, 13Z-astaxanthin was not the most abundant diastereomer observed in these experiments, indicating that stereolability is dependent on the specific isomer and conditions [103]. Enzymolysis was performed at  $37^\circ\text{C}$ ; elevated temperatures have been reported to enforce isomerization in carotenoids [58, 67, 102, 104–107]. Therefore, the enzymolytic reaction itself bears the potential for further isomerization. These significant differences between the abundance of various isomers under different conditions, especially the solvents used, indicate that a proper calculation of the isomers is complicated. Most astaxanthin determination methods require its solution in one or more solvents and multiple reaction steps, which might shift the proportion of the isomers. Consequently, isomer ratios can be compared within one method to estimate variabilities, but statements beyond cannot be made without additional tests. Changes in the proportions of stereoisomers might be interesting for various applications as diastereomers have been described to exhibit different antioxidant activity *in vitro* [108] and variable bioavailability [79]. Therefore, their exact determination should be studied further.

For astaxanthin quantification, in the following experiments, the linear regression of the combined results of the enzymolyzed free-astaxanthin and astaxanthin monopalmitate was used as described above. To account also for the isomers, their peak areas were included. Therefore, their peak areas were multiplied by correction factors to integrate their different extinction properties. These were 1.20 for 9Z-astaxanthin, 1.56 for 13Z-astaxanthin, and 1.11 for the di-Z-astaxanthin isomers based on the extinction coefficients of Bjerkeng et al. [79]. All obtained areas were summed and the resulting calibration curve was  $f(x) = 1759.9x$  ( $R^2 = 0.9983$ ,  $n = 18$ ). All different diastereomers were also found in extracts from *H. pluvialis* (Fig 3).

It can be concluded that the amount of astaxanthin is the limiting factor for enzymolysis or liquid-liquid extraction. A sensible measurement range is 1.0 to 11.2  $\mu\text{g/mL}$  of total astaxanthin concentration in the extraction phase. Moreover, applying the respective calibration curve is essential to keep the quantification error below 5%.

## Method development

Method development was based on dried *H. pluvialis* powder. All relevant process steps, i.e., disruption and extraction, enzymolysis, liquid-liquid extraction, and the processing of the liquid-liquid extracts, were investigated and adapted if needed. Subsequently, detection limits, linearity, and precision of the obtained method were determined (Fig 1).

**Disruption of *H. pluvialis* and astaxanthin extraction.** Astaxanthin was extracted from *H. pluvialis* biomass by disrupting the cells with a bead mill in the presence of acetone. This process was superior to grinding and ultrasonication under various conditions. A complete decolorization of the cell pellet, as an indicator for complete astaxanthin extraction, was only achieved by bead milling.

**Enzymolysis.** The enzymolysis is the core of the established method. Proper enzyme function and turnover must be ensured for complete deesterification of the various astaxanthin esters and free astaxanthin recovery. To find an optimal enzyme concentration, its amount and incubation time were varied, and free astaxanthin was measured (Fig 1b).



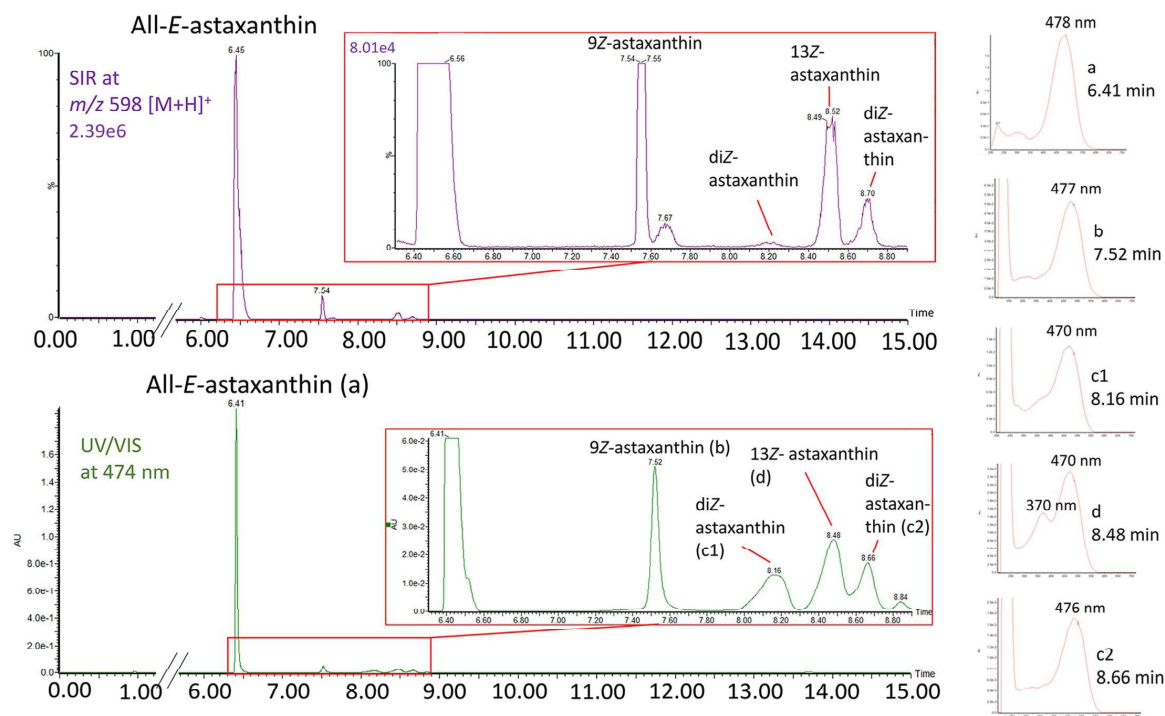
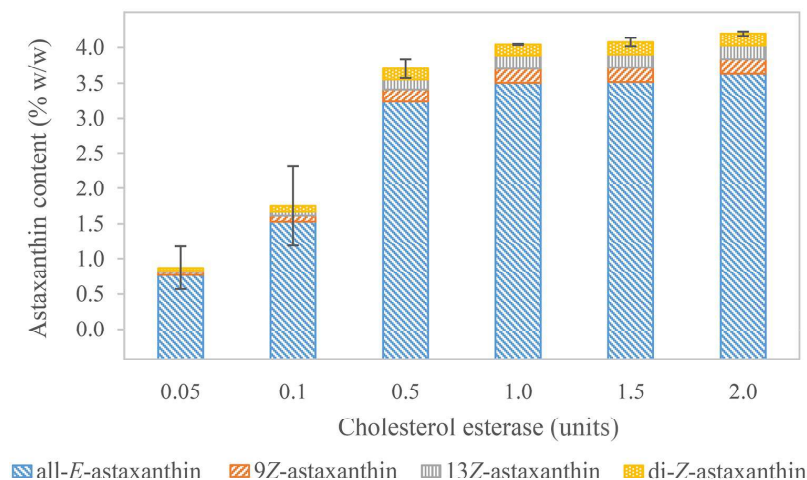


Fig 3. UV/Vis and SIR chromatograms of an enzymolyzed *H. pluvialis* extract and corresponding absorption spectra of astaxanthin diastereomers.

<https://doi.org/10.1371/journal.pone.0278504.g003>

The variation of cholesterol esterase (Fig 1, b1) from 0.05 to 2.00 units added to a constant quantity of 0.4 mg *H. pluvialis* biomass per sample resulted in calculated total astaxanthin proportions between  $0.87 \pm 0.30\%$  w/w ( $n = 3$ ) and  $4.20 \pm 0.03\%$  w/w ( $n = 3$ ) (Fig 4 and S1 Table). Respectively, 0.003 units to 0.12 units had been present per  $\mu\text{g}$  total free astaxanthin. The resulting all-*E*-astaxanthin concentrations in the petroleum ether-acetone phase were between 1.33 and 6.29  $\mu\text{g/mL}$ , thus in the linear calibration range. The increasing astaxanthin content with a higher enzyme concentration indicates substrate conversion by cholesterol esterase in the presence of acetone. Cholesterol esterase has been shown to work in a wide pH- and temperature range and to maintain its activity in the presence of solvents [109]. Furthermore, an activity increase was reported when minor proportions of up to 10% v/v of organic solvents were added [110]. Thus, the enzyme seems appropriate for astaxanthin deesterification in the described solvent-rich environment. The lowest astaxanthin values, accompanied by a distinct increase in the calculated astaxanthin concentration and comparatively high standard deviations (0.13–0.57% w/w), were observed between 0.05 and 0.50 units of cholesterol esterase. Here, enzymolysis was incomplete. Astaxanthin content recovered from treatment with 1.0 unit cholesterol esterase did not differ significantly from 1.5 units. Still, 2.0 units resulted in significantly more total astaxanthin, however, with a small effect size compared to 1.5 units (0.16 percentage points). Therefore, 1.0 to 2.0 units hydrolyzed the majority of astaxanthin esters. Su et al. reported good deesterification results with 4.0 units of cholesterol esterase per reaction. However, they did not specify the used biomass amount [85]. For lipases, slower





**Fig 4. Astaxanthin content in 0.4 mg *H. pluvialis* biomass, enzymolyzed with varying amounts of cholesterol esterase.** Standard deviation is indicated for total astaxanthin in triplicates; 1.0 unit was a duplicate. Standard deviations for the individual isomers can be found in [S1 Table](#).

<https://doi.org/10.1371/journal.pone.0278504.g004>

conversion rates and smaller efficiencies have been reported. 4.6 U/ $\mu$ g carotenoids have resulted in 63.2% free astaxanthin recovery after 7 hours of incubation. Moreover, the recovery even decreased when more enzyme was applied [93]. Huang et al. showed the highest free astaxanthin yields of 80% with 80 units per  $\mu$ g of astaxanthin esters with a recombinant lipase after one hour of incubation [94]. Working with higher enzyme amounts may secure complete conversion, especially at higher astaxanthin concentrations. Nevertheless, astaxanthin solubility in subsequent liquid-liquid extraction is limited, and higher enzyme application is not necessarily more beneficial. Consequently, 0.06 to 0.12 units per  $\mu$ g of total free astaxanthin were considered sufficient for most samples. This corresponded to 1.0 to 2.0 units of cholesterol esterase per sample or 2.5 to 5.0 units per mg of *H. pluvialis* biomass in these experiments. A further optimization might be achieved by using a higher enzyme concentration and simultaneously repeating the liquid-liquid extraction process as performed by Moretti et al. [61].

9*Z*-, 13*Z*- and two di-*Z*-isomers of astaxanthin were observed in all samples. Their biomass proportions were  $0.21 \pm 0.01\%$  w/w ( $n = 3$ ),  $0.19 \pm 0.02\%$  w/w ( $n = 3$ ), and  $0.18 \pm 0.01\%$  w/w ( $n = 3$ ), respectively, at 2.0 units. Regarding their proportions to total astaxanthin, no significant difference was observed in the di-*Z*-isomers when cholesterol esterase concentration was varied. Increasing cholesterol esterase from 0.05 to 2.0 units caused the proportions of 9*Z*- and 13*Z*- to total astaxanthin to rise from 4.35 to 4.89% and from 3.56 to 4.47%, respectively. 9*Z*-astaxanthin was equally or less abundant than in the enzymolyzed standards, whereas 13*Z*-astaxanthin and the di-*Z*-isomers were detected in higher proportions. Higher or equal diastereomer concentrations should be assumed in natural samples than in pure all-*E*-astaxanthin standards. The lack of 9*Z*-astaxanthin in this natural sample might indicate that sample composition influences the isomer equilibria, as it is more complex than the standards. Further isomerization to other isomers or even reverse isomerization to all-*E*-astaxanthin [103, 111] during enzymolysis and extraction is possible. Compared to the standards, a higher proportion of 13*Z*-astaxanthin and its di-*Z*-isomers might be assumed in this sample. However, their abundance might partially also arise from isomerization reactions. Besides the already



mentioned effects of temperature and solvents on isomerization, the sample matrix is more complex due to other cell components from *H. pluvialis*. NaCl and iodine have also been described to catalyze the isomerization behavior of carotenoids [67, 79, 103]. Therefore, reliable quantification of their total amounts is not possible. These results can only be seen as an estimate for the calculation of total astaxanthin.

The duration of enzymolysis was extended from 0.75 to 1.5 hours. 0.5 and 2.0 units of cholesterol esterase were applied to constant biomass of 0.4 mg dried *H. pluvialis* (Fig 1, b2). No significant difference in the measured all-*E*-astaxanthin amount was observed compared to the shorter incubation time at both enzyme concentrations. This indicates that increasing enzyme concentration is more efficient than elongating incubation time. Additionally, studies showed a tendency of free astaxanthin to decrease when enzymolysis was prolonged [85], which further encourages shorter incubation at higher enzyme concentrations. With longer incubation time, the proportion of 9*Z*-astaxanthin and the di-*Z*-isomers decreased by 9–18%, whereas 13*Z*-astaxanthin remained constant. Degradation and/or isomerization of astaxanthin isomers during and after deesterification is possible but seems less severe compared to alkaline saponification [85]. Although longer enzymolysis duration may still result in good all-*E*-astaxanthin recoveries, as also shown by Su et al. [85], relatively higher cholesterol esterase levels at shorter incubation time can result in sufficient total astaxanthin yields without the risk of further isomerization reactions. 2.0 units of cholesterol esterase and 0.75 hours of incubation time can be used as an initial approach toward the astaxanthin measurement of an unknown sample, which can be adapted if necessary. Further improvement of enzymolysis might be achieved by surface-active detergents or bile acids, as indicated by Uwajima et al. [109], but might be limited due to interaction with the used solvents.

**Liquid-liquid extraction.** After enzymolysis, free astaxanthin had to be recovered from the buffer solution. Therefore, liquid-liquid extraction with 2 mL of petroleum ether was performed. After phase separation, the upper layer increased in volume (Fig 1, c2). This volume was determined at  $2.31 \pm 0.03$  mL ( $n = 4$ ). Acetone was dissolved in petroleum ether during phase mixing, resulting in an excess volume [112]. Various studies encountered similar problems by drying and resolving the combined extracts in solvent [61, 83]. This procedure is more laborious and prone to astaxanthin losses. As the volume of the petroleum ether phase is crucial for the exact quantification of astaxanthin, the increased volume was used to calculate astaxanthin content in all samples processed likewise. Moreover, sodium sulfate has been used [61, 83] to remove residual water from the petroleum ether phase and enhance solvent strength. However, this is unnecessary when the described boundaries for astaxanthin solubility are observed and dry or highly concentrated samples are used.

**Processing of liquid-liquid extracts.** The extract obtained from liquid-liquid extraction can be injected directly into UHPLC-PDA-MS or further processed (Fig 1d). Various authors evaporated the upper extraction phase and redissolved the extracts in organic solvents prior to measurement [61, 83]. These methods were compared to evaluate recoveries and find the most cost and time extensive procedure. Direct analysis of this phase resulted in a recovery of  $98.24 \pm 1.43\%$  ( $n = 4$ ) total astaxanthin. Further processing resulted in a decrease in recovery. An aliquot was evaporated and redissolved in the same volume of acetone. Its astaxanthin content was quantified with the respective calibration for astaxanthin in acetone. Total astaxanthin recovery was significantly lower with  $91.68 \pm 1.32\%$  ( $n = 4$ ). A repeated extraction, evaporation, and resumption in acetone resulted in  $96.34 \pm 0.68\%$  ( $n = 3$ ) total astaxanthin recovery. The generally lower recovery might be due to losses during processing. The proportion of 9*Z*-astaxanthin was lower, whereas 13*Z*-astaxanthin and the di-*Z*-isomers were more abundant when the samples were redissolved in acetone (S1 Table). This direct comparison and comparison to the standards for calibration curve determination demonstrate changing isomer recoveries in



different solvents, indicating once more that a valid determination is not possible due to changes during processing. Altogether, these experiments point to direct processing as the most correct and time and cost-reducing procedure. Still, the quantification of the diastereomers in natural samples of *H. pluvialis*, especially in the presence of other carotenoids, is more precise when the samples are dissolved in acetone, as the chromatographic resolution of the diastereomers and lutein was higher.

**Detection limits and linearity of astaxanthin determination.** The complex composition of *H. pluvialis* biomass was assumed to influence enzymolysis. Moreover, the previously determined detection limits should be verified when applying natural samples. Therefore, the biomass quantity of *H. pluvialis* was varied from 0.04 to 3.98 mg at constant saponification time (0.75 hours) and cholesterol esterase concentration (2.0 units) [99] to find an optimal astaxanthin transformation range (Fig 1, a2). A maximum yield of  $3.74 \pm 0.01\%$  w/w ( $n = 3$ ) all-*E*-astaxanthin was observed at 0.8 mg of *H. pluvialis* powder ( $\pm 13.0 \mu\text{g/mL}$  all-*E*-astaxanthin concentration in liquid-liquid extract) (Fig 5 and S1 Table). Between 0.2 and 2.0 mg ( $\pm 3.18$  and  $32.4 \mu\text{g/mL}$  all-*E*-astaxanthin concentration in liquid-liquid extract),  $\geq 97\%$  of the maximum recovery were still reached. This implies an extended measurement range compared to the standards, whose recovery decreased significantly, starting at approximately  $11.2 \mu\text{g/mL}$  astaxanthin concentration. The sample matrix of whole-cell biomass is much more complex than the standards. Lipophilic cellular components such as fatty acids or other carotenoids are dissolved in the hydrophobic solvent, altering its composition and enhancing solubility for other constituents like astaxanthin. *Z*-isomers of many carotenoids, including astaxanthin, have a higher solubility in various solvents than the all-*E*-isomer [104, 113, 114]. Thus, the calibration curve might be applied at astaxanthin concentrations above  $11.2 \mu\text{g/mL}$ . However, a definite range cannot be specified because biomass composition, especially in terms of fatty acids and pigments, is variable, particularly when *H. pluvialis* is exposed to stress conditions [88, 115–117]. The measured all-*E*-astaxanthin content decreased significantly, applying either more or less biomass. It was  $3.33 \pm 0.05$  ( $n = 3$ ), 3.24, and 2.86% w/w for 0.04, 3.26, and 3.98 mg of biomass, respectively ( $\pm 0.64$ , 51.81, and  $63.25 \mu\text{g/mL}$  all-*E*-astaxanthin concentration in

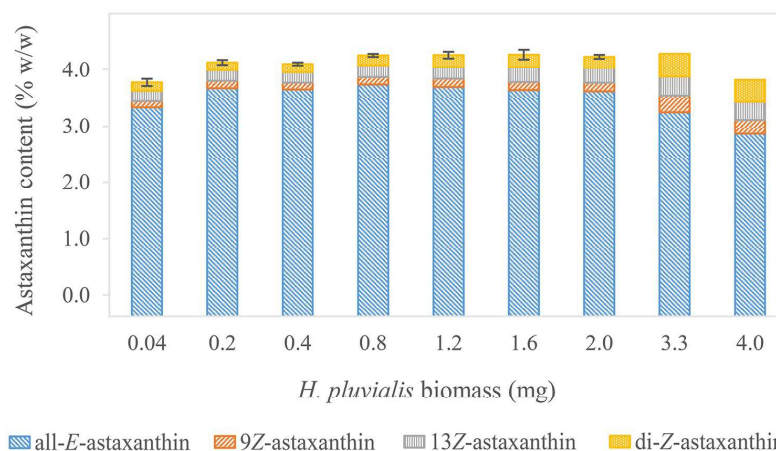


**Fig 5. Astaxanthin content in *H. pluvialis* biomass, deesterified with 2.0 units of cholesterol esterase.** Standard deviation is indicated for total astaxanthin in triplicates. Standard deviations for the individual isomers can be found in S1 Table. The figure demonstrates that the method gets similar results for a broad range of biomass inputs.

<https://doi.org/10.1371/journal.pone.0278504.g005>



liquid-liquid extract). The decrease at 0.04 mg is likely due to measuring inaccuracy at the lower border of the measurement range, which was also determined in the standards. The significant decrease in recovery when using more than 2.0 mg of biomass might be explained by a relatively too low enzyme concentration. Moreover, other carotenoid and cholesterol esters and phospho- and triacylglycerides are in direct competition with the deesterification of astaxanthin-esters and may decelerate the process [118–121]. Jacobs et al. reported higher conversion for carotenoid esters that contain a cyclopentenyl terminal ring rather than a cyclohexenyl terminal ring, implying other carotenoid esters might be hydrolyzed preferably [91]. Moreover, on the fatty acid side, a higher hydrolysis rate has been shown for longer chain and polyunsaturated fatty acids esterified with cholesterol [109]. This might further favor reactions of the enzyme with other molecules. Additionally, proteins might inhibit proper enzyme function [122–124]. Another reason might be insufficient solubility of astaxanthin in the extraction phase. However, for none of the samples, precipitation was visible. The proportion of 9Z- and 13Z-astaxanthin increased significantly only when relating the samples with the lowest and highest biomass (0.04 and 2.0 mg). However, it did not vary significantly when samples with similar concentrations were compared. Moreover, the proportion of all diastereomers increased when the biomass amount was raised to 3.3 and 4.0 mg. These corresponded to all-*E*-astaxanthin concentrations of 51.81 and 63.25  $\mu\text{g/mL}$ , which are well above the upper detection limit. Thus, the higher solubility of the *Z*-isomers [104, 113, 114] might change the equilibrium in their favor.

This experiment expanded the outlined upper detection limit of 11.2  $\mu\text{g/mL}$  of all-*E*-astaxanthin in the extraction phase to approximately 30  $\mu\text{g/mL}$ . The lower detection limit was approved at approximately 1.0  $\mu\text{g/mL}$ .

**Precision of astaxanthin determination.** In order to demonstrate measuring precision and repeatability, astaxanthin content was measured multiple times in two different samples. Each measurement was performed on a different day to prove the similarity of the independent experiments. The samples had an all-*E*-astaxanthin content of  $3.46 \pm 0.04\%$  w/w ( $n = 5$ ) and  $3.98 \pm 0.04\%$  w/w ( $n = 4$ ) (Fig 6 and S1 Table). This equaled coefficients of variation of

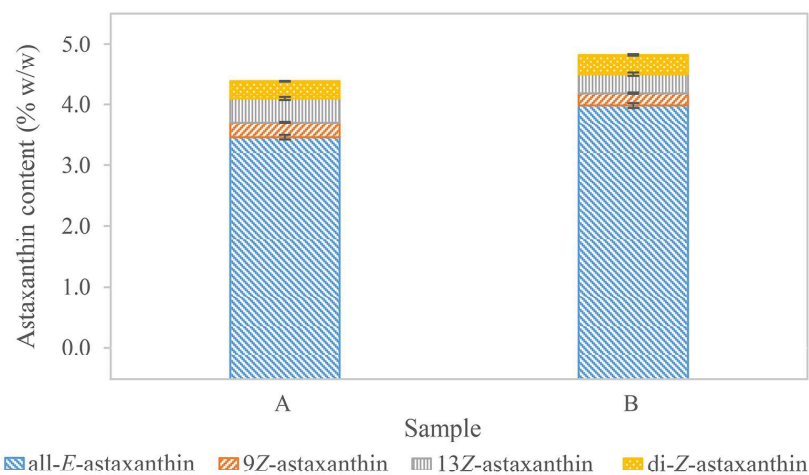


**Fig 6. Astaxanthin content in two *H. pluvialis* powders.** Standard deviation is indicated for each astaxanthin diastereomer. Sample A:  $n = 5$ , sample B:  $n = 4$ .

<https://doi.org/10.1371/journal.pone.0278504.g006>



1.1% and 1.0%, respectively. The isomers 9Z-, 13Z-astaxanthin, and two di-Z-isomers were observed in both samples with coefficients of variation between 1.9 and 9.0%. Thus, the precision of all-*E*-astaxanthin measurement was high, whereas it fluctuated for the diastereomers. It might be improved by evaporating and resolving the extracts in acetone prior to analysis. However, such treatment would be most likely at the expense of total astaxanthin recovery.

### Method adjustment

The resulting method was further validated regarding linearity, detection limits, precision, and robustness when various samples of astaxanthin containing biomass or extracts were used. Therefore, fresh *H. pluvialis* cultures and either pure oleoresins or oleoresins diluted in ethanol were applied at various concentrations. The sample type specific method adjustments and validations are explained in the following.

**Sample type: *H. pluvialis* liquid cultures.** *H. pluvialis* cells concentrated in nutrient-depleted medium were disrupted in the presence of acetone. The first passage in the bead mill had only little effect on the extraction of carotenoids, as hardly any color change of the medium-acetone phase was observed. Major cell disruption and extraction were achieved only in the second and third passage. This might be due to an increased acetone proportion during the passages, which has a stronger dewatering effect on membranes and cell walls.

Biomass of four batches of *H. pluvialis* was processed according to the standard method (Fig 1, a4). All-*E*-astaxanthin content was determined ranging from  $0.73 \pm 0.04\%$  w/w ( $n = 3$ ) to  $3.82 \pm 0.15\%$  w/w ( $n = 3$ ) (Fig 7 and S1 Table). Independently from the actual astaxanthin concentration, the obtained all-*E*-astaxanthin recovery in three of the four batches was above 90% of the maximum achieved concentration when using 0.2 to 1.5 mg of biomass, respectively 2.5 to  $15.0 \mu\text{g/mL}$  of all-*E*-astaxanthin extract concentration. These results confirm the applicability of the linear calibration correlation of all-*E*-astaxanthin at concentrations above  $11.2 \mu\text{g/mL}$  for natural samples. However, the maximum all-*E*-astaxanthin recovery was observed at different extract concentrations in each sample. These extended over the whole measurement

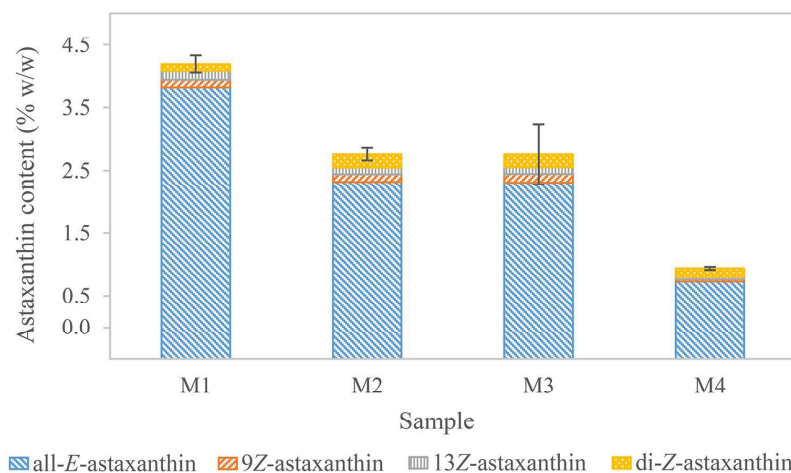


**Fig 7. Astaxanthin content of four batches of *H. pluvialis* suspended in residual medium.** M1 to M4 derive from different batches. Standard deviations are indicated for total astaxanthin. Replicates of M1 to M4 vary between three and five. Standard deviations for the individual isomers and replicates can be found in S1 Table.

<https://doi.org/10.1371/journal.pone.0278504.g007>



range and were found at 2.5, 8.2, 11.3, and 19.7  $\mu\text{g/mL}$ . Thus, the previously determined measurement range should be condensed to an optimal measurement range, which is highly dependent on the sample. Throughout its life cycle, *H. pluvialis* exhibits different characteristics, e.g., highly stressed cells with a high astaxanthin level also indicate an altered composition regarding fatty acids, carotenoids, and other cell compounds [44, 68, 88, 115–117, 125], which might further change enzyme activity, solvent equilibria, and astaxanthin solubility.

In most samples, the measured isomers essentially showed the same proportion when between 0.75 and 1.75 mg of *H. pluvialis* biomass (dry weight) were used. Applying less than 0.75 mg biomass resulted in higher deviations of the measurements. This reinforces the assumption that the proportion of isomers measured is largely stable within a constant experimental setup. In relation to the total astaxanthin content, 2.65 to 14.54% di-*Z*-astaxanthin, 2.96 to 5.03% 9*Z*-astaxanthin, and 3.38 to 4.17% 13*Z*-astaxanthin were observed. Yuan and Chen, who compared the different isomers in extracts of *H. pluvialis* during and after saponification under alkaline conditions, observed a higher peak area ratio of 9*Z*- to 13*Z*-astaxanthin [55–57]. Gong et al. also observed higher 9*Z*- than 13*Z*-astaxanthin proportions after enzymolysis [125], indicating a higher abundance of 9*Z*-astaxanthin in general. However, changes in the composition of isomers have been observed during *H. pluvialis* cultivation [125], leading to the suggestion that strain, cultivation, and stress conditions influence the abundance of the different isomers, as evidenced by the high variance of di-*Z*-isomers in these experiments. As already discussed, storage and processing conditions might also have an influence, and the comparison to other methods is presumably biased.

Compared to the share of geometrical isomers observed in the deesterified all-*E*-astaxanthin standards, 9*Z*-astaxanthin was less or equally abundant, and 13*Z*- as well as the di-*Z*-astaxanthin isomers were more abundant in samples of *H. pluvialis* suspended in medium. Thus, the same principle that biomass, temperature, and solvents affect isomerization behavior applies as already described previously for dried *H. pluvialis* samples.

**Sample type: Oleoresins.** Oleoresins from *H. pluvialis* are mostly obtained by SC-CO<sub>2</sub> extraction. Here, modifiers are often used for enhanced extractability [89, 126–128] and due to system requirements. Ethanol, as a solvent, is very common and can be found in the resulting extracts. For astaxanthin determination, it can be evaporated prior to enzymolysis. For cost and time reduction, direct measurement of ethanolic extracts was investigated using the method developed here. Its robustness and effects on further processing and astaxanthin recovery were examined.

The proper function of the enzymolysis in the presence of ethanol had to be ensured (Fig 1, c1). No significant difference was observed between the samples processed with ethanol and those processed without ethanol with respect to all-*E*-astaxanthin. An extract with a high astaxanthin concentration resulted in  $52.9 \pm 0.4 \mu\text{g/mL}$  ( $n = 5$ ) of all-*E*-astaxanthin when equal or less than 18% v/v ethanol were present during enzymolysis and extraction.  $53.1 \pm 0.5 \mu\text{g/mL}$  ( $n = 2$ ) of all-*E*-astaxanthin were detected when ethanol was evaporated prior to processing (S2 Table). Another extract with a lower astaxanthin concentration resulted in  $8.6 \pm 0.2 \mu\text{g/mL}$  ( $n = 3$ ) of all-*E*-astaxanthin when equal or less than 18% v/v ethanol was present during deesterification. Comparably  $8.8 \pm 0.2 \mu\text{g/mL}$  ( $n = 2$ ) of all-*E*-astaxanthin were obtained when ethanol was evaporated prior to processing. As already described, cholesterol esterase has been shown to maintain its activity in the presence of solvents and, more specifically, ethanol [109]. It might even work better if small amounts of up to 10% v/v of organic solvents are added [110]. Ethanol concentrations above 18% v/v resulted in a sharp decline of the measured all-*E*-astaxanthin content. It decreased to 50% and 16% of the previously calculated astaxanthin quantities for 36% v/v and 54% v/v of ethanol, respectively. A decrease in activity and stability with  $\geq 10\%$  v/v ethanol concentrations has been observed [110]. A



similar effect has been shown for a lipase from *P. aeruginosa* [95]. It can be explained by stabilization and destabilization of hydrophobic interactions depending on ethanol concentration [129–131], suggesting an inhibition of the enzyme with ethanol concentrations  $\geq 18\%$  v/v in these experiments. There was no significant difference in the proportion of 13Z-astaxanthin comparing the deesterification in the presence and without ethanol. However, without ethanol, the proportion of 9Z-astaxanthin was 18 and 40% higher in the samples with a higher or lower total astaxanthin content, respectively. In the sample with less astaxanthin, the proportion of the di-Z-astaxanthin isomers was 60% higher in the absence of ethanol. Solvent-related isomerization might account for this. Overall, the all-*E*-astaxanthin amount did not change significantly. Thus, minor ethanol proportions in the enzymolytic process can be regarded as unproblematic.

After enzymolysis, in the liquid-liquid extraction, the upper phase expansion was studied in the presence of various quantities of ethanol (Fig 1, c2). After processing and extracting with petroleum ether, the upper-phase volume decreased to 2.24, 2.17, 2.11, 2.04, and 2.00 mL when 3, 7, 11, 14, and 18% v/v ethanol were used, respectively. Linear regression resulted in a line of best fit with  $f(x) = -0.0003x + 2.3052$  ( $R^2 = 0.9943$ ,  $n = 6$ ). Binary mixtures of hexane and ethanol cause a volume dilatation [132], whereas mixtures of acetone and ethanol result in volume contraction [133, 134]. This second phenomenon might also impact the ternary mixture of petroleum ether, acetone, and ethanol, resulting in a smaller excess volume than in the absence of ethanol [135]. When 36% v/v ethanol were initially added to the sample, this linear correlation no longer applied as the volume of the upper phase decreased to 1.95 mL. Here the influence of a higher ethanol proportion resulted in a volume contraction.

It can be concluded from both experiments that the presence of ethanol generally does not influence the total astaxanthin recovery as long as its effect on the volumetric change in liquid-liquid extraction is taken into account during quantification and the volumetric maximum of 18% v/v is considered.

To study the optimal concentration range, detection limits, and linearity of astaxanthin determination in oleoresins (Fig 1, a4), three different samples were deesterified with 2.0 units to 4.0 units of cholesterol esterase at quantities between 0.15 and 15.8 mg. Above 90% of the maximum measured astaxanthin content were recovered when using 0.3 to 1.2 mg of oleoresin. This corresponded to 1.8  $\mu\text{g/mL}$  to 20.4  $\mu\text{g/mL}$  of all-*E*-astaxanthin in the respective extract. There was a sample-specific optimal measuring range. Exceeding or falling below it resulted in reduced recoveries.

In oleoresin O1, the highest all-*E*-astaxanthin value of 5.8% w/w was observed at 0.4 mg oleoresin ( $\pm 10.0 \mu\text{g/mL}$  all-*E*-astaxanthin in the liquid-liquid extract) enzymolyzed with 4.0 units of cholesterol esterase. Stepwise increase of oleoresin to 1.6 mg ( $\pm 41.2 \mu\text{g/mL}$  all-*E*-astaxanthin) and reducing the enzyme to 2.0 units resulted in a steady 17% decrease of overall all-*E*-astaxanthin recovery. This indicates an excess of enzyme capacity and/or solubility at higher oleoresin amounts. Oleoresins mainly contain fatty acids and other lipophilic compounds such as carotenoids and their esters [39, 101, 136], which can act as competitive substrates.

In oleoresin O2, which was oleoresin O1 diluted in sunflower oil, the highest all-*E*-astaxanthin levels were observed between 0.75 and 1.00 mg of oleoresin ( $\pm 4.4$  to 5.9  $\mu\text{g/mL}$  all-*E*-astaxanthin in the liquid-liquid extract). Less astaxanthin was detected when applying more or less oleoresin. A doubling of enzyme concentration in sample O2 resulted in a minor increase of maximum 5.5% all-*E*-astaxanthin or 3.9% total astaxanthin when directly comparing samples with equal or less than 1.0 mg ( $\pm 5.9 \mu\text{g/mL}$  in the liquid-liquid extract) oleoresin. Therefore, the enzyme capacity was sufficient to deesterify astaxanthin in the range below 5.9  $\mu\text{g/mL}$ .

Conversely, in sample O3, the highest all-*E*-astaxanthin value of 3.6% w/w was observed at the highest applied oleoresin per sample, which was 1.65 mg ( $\pm 25.9 \mu\text{g/mL}$  all-*E*-astaxanthin



in the liquid-liquid extract) and decreased to 3.0% w/w at 0.78 mg oleoresin ( $\pm 12.3 \mu\text{g/mL}$  all-*E*-astaxanthin in the liquid-liquid extract). This supports the hypothesis that complex lipophilic samples can be used at concentrations exceeding the previously determined measurement range. Possibly the higher abundance of lipophilic substances results in enhanced solubility of astaxanthin. For proper enzymatic activity, the previously outlined maximum astaxanthin concentration of approximately  $30 \mu\text{g/mL}$  should still be considered, or enzyme quantity has to be increased.

No severe influence of the amount of oleoresin used on the proportion of the isomers was observed in the range below 1.8 mg of sample. 7.51 to 19.69% of the total astaxanthin were the di-*Z*-forms, 5.14 to 13.01% 9*Z*-astaxanthin, and 3.99 to 7.24% 13*Z*-astaxanthin. Their abundance was higher than in the alga cultures suspended in medium or dried cells. Two effects might account for this. First, elevated temperatures and high pressures, also present during SC-CO<sub>2</sub> extraction, lead to a higher isomerization rate and altered isomer profiles [58, 102, 104–107]. However, SC-CO<sub>2</sub> extraction is a process that is considered mild. Álvarez et al. did not find significant differences in isomer proportions between different extraction conditions [137]. Second, *Z*-isomers might have higher extraction rates in SC-CO<sub>2</sub> extraction a priori due to their higher solubility in solvents [104, 113, 114]. This might be the reason for the selective accumulation of *Z*-isomers [138, 139].

In this study, significant higher proportions of 9*Z*- than 13*Z*-astaxanthin were detected in all oleoresins (Fig 8 and S1 Table). Various authors have also reported this in enzyme deesterified supercritical fluid extracts of *H. pluvialis* [85, 137]. All-*E*-astaxanthin and all-*E*-astaxanthin diacetate exposed to isomerization inducing conditions showed higher levels of 9*Z*- and 13*Z*-astaxanthin than other di-*Z*-isomers in the resulting mixtures [58, 60].

**Sample mixtures.** To further quantify the observed effects of natural samples on the solubility and thus linear measurement range of astaxanthin in liquid-liquid extracts, different standards and a natural sample with equal astaxanthin amount were examined independently and in mixtures (Fig 1, a5). The all-*E*-astaxanthin recoveries of the independent samples were

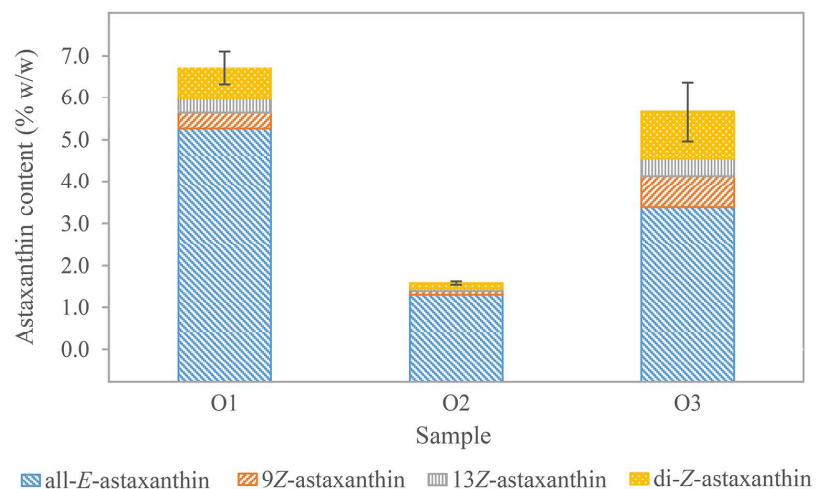


**Fig 8. Astaxanthin content of three different oleoresins of *H. pluvialis*.** Standard deviations are indicated for total astaxanthin. O1 ( $n = 3$ ) and O3 ( $n = 3$ ) derive from different batches. O2 ( $n = 7$ ) is a dilution of O1. Standard deviations for the individual isomers can be found in S1 Table.

<https://doi.org/10.1371/journal.pone.0278504.g008>



88% from astaxanthin monopalmitate, 83% from free astaxanthin, and 98% from *H. pluvialis*. The calculated astaxanthin concentration in the final extraction phase was between 4 and 5 µg/mL. The addition of acetone after liquid-liquid extraction might have caused the unexpected reduced recovery of the standards. Mixtures of those samples yielded recoveries of 95% to 109%, even at a total all-*E*-astaxanthin concentration of 13.3 µg/mL, indicating that the presence of biomass components or acetone facilitates the solution of astaxanthin in the extraction phase. Evaluating all these samples, a proportional increase of the measured astaxanthin concentration to the prepared astaxanthin concentration was observed: a linear regression forced through zero resulted in a proportion of 1.0205 of measured to prepared total astaxanthin concentration with a coefficient of determination of 0.9654. However, the recovery decreased when free all-*E*-astaxanthin standard dissolved in acetone was added after the enzymolysis. The same samples prepared with 3.6 µg and 7.2 µg free all-*E*-astaxanthin standard resulted in a correlation of 0.9408 ( $R^2 = 0.9690$ ) and 0.8836 ( $R^2 = 0.9441$ ), respectively. The addition of astaxanthin and acetone after extraction might change the phase equilibria, density, and astaxanthin solubility, resulting in the observed measurement inaccuracy. Apart from these relations, all-*E*-astaxanthin extract concentrations up to 23.6 µg/mL were detected linearly without precipitation effects. Moreover, those samples containing the whole-cell biomass or mixtures resulted in higher recoveries in all experiments. Thus, fatty acids and other cellular components are the only other differing factors in these experiments that might influence astaxanthin solubility. It is difficult to discriminate between the two observed effects of reduced and enhanced recovery due to acetone/standard addition and the presence of cellular components, respectively, due to the experimental setup. To understand the circumstances affecting all-*E*-astaxanthin solubility, recovery, and thus measurement boundaries for its quantification, a broader concentration range without further astaxanthin addition after processing needs to be considered, as all previous tests showed that the applicable measurement concentration of all-*E*-astaxanthin in *H. pluvialis* biomass is higher than in measurements of standards.

### Method comparison to photometric astaxanthin estimation

Many methods for fast and easy astaxanthin determination are based on a simple photometric measurement of *H. pluvialis* extracts. Two such approaches using different mathematical models were compared to the developed UHPLC-PDA method to evaluate the discrepancy between them and conclude whether photometric techniques can still lead to a reasonable estimate of astaxanthin (Fig 1e). For an even broader impression of the possible validity of those methods, two *H. pluvialis* cultures were tested at different times towards the end of a cultivation period to account for possible changes in the carotenoid and chlorophyll composition. Astaxanthin production had been induced by exposure to high light intensities and nitrogen starvation. Besides astaxanthin, the lutein content was determined by UHPLC-PDA measurements, and spectra of the extracts were compared. UHPLC data revealed steadily increasing all-*E*-astaxanthin content from 0.99 to 2.47% w/w and 1.31 to 2.70% w/w in batch A and B, respectively (Fig 9 and S1 Table). Total astaxanthin concentration rose from 1.13 to 2.79% w/w and from 1.50 to 3.07% w/w in batch A and B, respectively. Photometric data evaluated with the general equation (Eq 1) resulted in total astaxanthin contents between 1.34 and 2.85% w/w and between 1.97 and 2.95% w/w in batch A and B, respectively. Astaxanthin content calculated from the same photometric data but with the equations of Lichtenthaler et al. [100] increased from 1.31 to 2.78% w/w in batch A and from 1.91 to 2.93% w/w in batch B. Astaxanthin amounts obtained from the photometric methods were generally similar. Though, here a higher astaxanthin content was estimated compared to UHPLC-PDA measurements in the first half of both experiments. On the 27th and 28th day, photometric and UHPLC-PDA



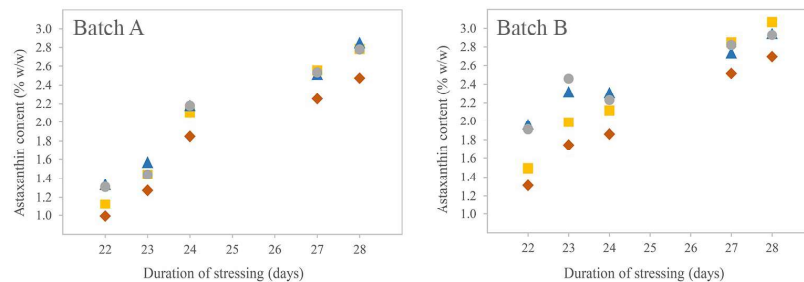


**Fig 9. Astaxanthin content in two different batches of *H. pluvialis* cultures towards the end of a cultivation period.** Left batch A, right batch B. All-*E*-astaxanthin calculated from UHPLC-PDA measurements (◆), total astaxanthin calculated from UHPLC-PDA measurements (■), total astaxanthin calculated from a photometric approach using Eq 1 (▲) and Eq 2 (●).

<https://doi.org/10.1371/journal.pone.0278504.g009>

approaches resulted in similar or slightly smaller astaxanthin concentrations calculated from photometric data.

The initial deviation may be due to a misestimation of other carotenoids and chlorophylls by the photometric approach. It has been shown that carotenoid composition changes during cultivation; astaxanthin increases faster than other carotenoids, and lutein and chlorophylls even decrease [44, 68, 125]. This was confirmed for lutein, as concentration fell from 0.09 to 0.06% w/w and 0.13 to 0.08% w/w in batch A and B, respectively, during the trial period. In addition, the wavelength scans of the whole extracts revealed the presence of chlorophyll *a* by maxima at 661 and 662 nm as well as a shoulder in the carotenoid peak at 434 nm [100], which decreased over the measurement period. The extract spectra also revealed a shifting absorption maximum from 466 to 472 nm and 468 to 478 nm in batch A and B, respectively. This  $\lambda_{\max}$  shift was probably also due to a reduction of chlorophylls and possibly other carotenoids that absorb at shorter wavelengths while astaxanthin levels increased. This experiment was made towards the end of two cultivation periods and is in accordance with measurements of Bous-siba et al. They measured absorbance spectra of extracts of *H. pluvialis* at different cell cycle stages but observed a much greater variance when comparing green to red cells [75]. Lich-tenthaller et al. especially considered and corrected for the chlorophylls in their equations, but they are based on the analysis of various plants with another carotenoid composition and without astaxanthin. Both photometric approaches assume that astaxanthin accounts for about 80% of all carotenoids, which is not true for various stress stages of *H. pluvialis* cells, and an absorption coefficient  $A_{1\text{cm}}^{1\%}$  of 1980 [100mL/(g\*cm)] for the total xanthophylls [100] was assumed. Apart from the mentioned unsuitability for precise measurement of astaxanthin, it might result in a further misestimation as it also does not distinguish between the diastereomers. UHPLC-PDA analysis showed an increase in all diastereomers over the measurement periods. The relative proportion of 9Z- and 13Z-astaxanthin increased slightly initially, whereas the proportion of the di-Z-isomers decreased constantly. Gong et al. observed similar correlations and reported a steady increase of total astaxanthin and its isomers during cultivation but no significant difference in the relative proportion of 9Z- and 13Z-astaxanthin during the astaxanthin accumulation phase [125]. Both photometric approaches include the geometric isomers. However, their different proportions and absorption coefficients are neglected. Maximum extinction is generally reduced and shifted to shorter wavelengths in Z-isomers of carotenoids [54, 79]. Therefore, the exact determination of astaxanthin, including the absorption characteristics of its isomers, in complex matrices, with other carotenoids and chromophores



of unknown portions and extinction properties is a delicate task. Recent methods circumvent these problems by measuring at higher wavelengths (530 nm in DMSO), where the absorption of most carotenoids, except for astaxanthin, is near zero [48, 59, 77]. Minor deviations might still occur because of the named issues with geometrical isomers. Another possibility is to use Gauss peak spectra methods to estimate carotenoids and astaxanthin [140, 141]. The different isomer spectra can be taken into account here.

Photometric methods provided a reasonably good estimate of the total astaxanthin content at a given time point near the end of a stress period. Only minor deviations between 0.2 and 4.0% from the UHPLC-PDA-based measurements occurred. However, comparison with samples taken at an earlier stage of cultivation resulted in deviations up to 30%, with the potential for even greater discrepancy. Without further insights into the cell composition, such methods should only be used to estimate differences in astaxanthin content of the same cultures. Astaxanthin in differently cultivated *H. pluvialis* algae, strains, or even processed samples should not be compared because photometric measurements cannot specifically distinguish between isomers, other carotenoids, and chlorophylls.

### Shelf life of astaxanthin containing samples

Astaxanthin-rich biomass is often stored prior to extraction and quantification. Generally, astaxanthin is highly reactive. It reacts with oxygen and forms various auto-oxidation products with shifted absorption maxima [142] and different absorption coefficients, leading to lower extinction. Moreover, isomerization reactions of carotenoids are induced by incubation at elevated temperatures also in the absence of solvents [106]. Although this effect generally depends on the height of the temperature [58, 67, 102, 104, 105, 107], longer storage at lower temperatures may result in similar isomerization effects. To achieve reproducible results, astaxanthin losses should be minimized during storage. Therefore, the stability of free astaxanthin standard in acetone was examined at various temperatures to characterize its vulnerability without further protection. Furthermore, dried and non-dried *H. pluvialis* biomass was investigated at different temperatures and in the presence and absence of oxygen to find storage conditions that reduce astaxanthin losses and storage costs.

**Free astaxanthin standard.** Free all-*E*-astaxanthin standard with a concentration of 1 µg/mL in acetone was stored at -80°C, -20°C, 4°C, and room temperature for 833 days in the dark. At room temperature, a decrease of 6% and 12% after 10 days and 41 days was observed, respectively. The concentration of samples stored in cooler conditions remained constant during this period. After 833 days, the sample stored at room temperature had lost 93% of its initial concentration, and the sample stored at 4°C had lost 27%. For storage at -80°C and -20°C no major changes in optical density were observed. These results indicate partial prevention of astaxanthin degradation by temperature reduction. This assumption is supported by other studies in which increased degradation of astaxanthin was observed at elevated temperatures [76, 143, 144].

**Non-disrupted *H. pluvialis* biomass concentrated in residual medium.** *H. pluvialis* biomass suspended in a nutrient depleted liquid medium with a concentration of 40 g/L was stored at 4°C in the dark. The measured all-*E*-astaxanthin content decreased to 93 and 83% of its initial value of 0.99±0.01% w/w (n = 6) when the samples were measured after 104 and 489 days, respectively. Similar protection of astaxanthin in frozen cells of *H. pluvialis* after 672 days was observed by Miao et al., who reported a loss of less than 15% astaxanthin [76]. *H. pluvialis* aplanospores have a rigid, multilayered cell wall that protects the alga from unfavorable environmental conditions [145, 146], which might impair oxygen diffusion into the cell and thus astaxanthin oxidation.



#### Lyophilized and non-disrupted *H. pluvialis* biomass exposed to ambient atmosphere.

An aliquot of the same biomass was lyophilized and stored under ambient air atmosphere at 4°C. The all-*E*-astaxanthin content was  $0.95 \pm 0.01\%$  w/w ( $n = 3$ ) directly after freeze-drying, but it decreased to 69% and 32% of this initial value when the samples were measured 108 and 489 days later, respectively. These findings are similar to those of Ahmed et al., who reported 35% astaxanthin degradation in lyophilized *H. pluvialis* after 20 weeks in non-vacuum conditions [144]. Again, the relatively high temperature and direct oxygen exposure probably promoted astaxanthin degradation. The protective sheath of the cell wall might have failed due to its desiccation compared to the previous experiments.

**Lyophilized and non-disrupted *H. pluvialis* biomass partially exposed to ambient atmosphere.** Aliquots of the same lyophilized samples as before were vacuum-sealed directly after freeze-drying. They were exposed to ambient air immediately, 7, 108, and 489 days later. These samples were measured altogether on day 489. The all-*E*-astaxanthin recoveries were 32, 44, 70, and 83% of the initial value, respectively (Fig 10 and S1 Table). The di-*Z*-isomers were generally most abundant, followed by 9*Z*- and 13*Z*-astaxanthin. Their total amount decreased the longer the sample was exposed to ambient air. However, their proportion in relation to the total astaxanthin content was similar. Exposure to oxygen has been reported to negatively affect astaxanthin during storage of *H. pluvialis* [76, 143, 144], e.g., Raposo et al. observed an improvement in astaxanthin degradation in spray-dried samples when stored under nitrogen or vacuum atmosphere compared to storage under air [71]. The small losses still observed in this experiment might be due to reactions with residual oxygen in the cells or the atmosphere of the packaging. Lyophilization was performed at 37 Pa, and no atmosphere change was applied.

**Dried and disrupted *H. pluvialis* biomass sealed and exposed to ambient air.** Two sealed bags of *H. pluvialis* powder were stored at -21°C in the dark. One of them was opened, exposed to ambient air, and closed tightly again without changing the atmosphere. The astaxanthin content of both samples was measured after two and a half years. The all-*E*-astaxanthin content was  $3.98 \pm 0.04\%$  w/w ( $n = 4$ ) and  $3.46 \pm 0.04\%$  w/w ( $n = 5$ ) in the sealed and the opened sample, respectively (S1 Table). Compared to the closed sample, 9*Z*- and 13*Z*-astaxanthin

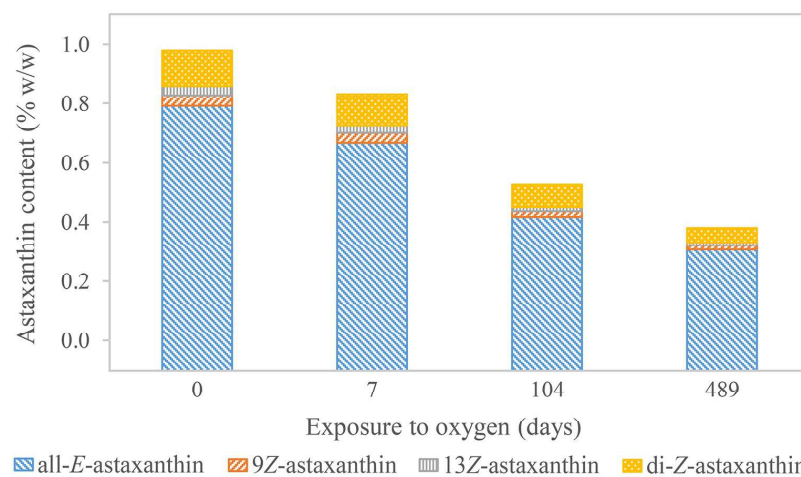


**Fig 10.** Astaxanthin content in lyophilized *H. pluvialis* biomass. It was exposed to ambient atmosphere for different periods of time and measured after 489 days.

<https://doi.org/10.1371/journal.pone.0278504.g010>



decreased by 12% and 22%, respectively, in the opened sample, while the sum of the di-*Z*-isomers increased by 14%. Related to total astaxanthin, all-*E*-, 9*Z*-, and 13*Z*-astaxanthin were not significantly different, and only the proportion of the di-*Z*-isomers increased from  $5.9 \pm 0.1$  ( $n = 4$ ) to  $7.7 \pm 0.3\%$  ( $n = 5$ ). As described above, oxidation of astaxanthin is probably the reason for its general decrease in the opened sample. Compared to the previously analyzed lyophilized samples stored without a protective atmosphere at 4°C, a beneficial effect of the reduced temperature was observed, as total astaxanthin content decreased less.

## Conclusion

A method for astaxanthin quantification was developed to accurately determine astaxanthin from a variety of *H. pluvialis* biomass, extracts, and formulations. Specifically, the following method parameters considered: Enzymolysis, extraction, and extract processing. Besides all-*E*-astaxanthin, the diastereomers 9*Z*-, 13*Z*- and two di-*Z*-isomers of astaxanthin were detected. In natural samples, the measurement precision of all-*E*-astaxanthin was determined with a maximum coefficient of variation of 1.1%, whereas it was below 10% regarding the diastereomers. Generally, linear correlations of biomass to astaxanthin content were determined in the extraction phase between 1.8 µg/mL and up to 30 µg/mL all-*E*-astaxanthin. It was demonstrated that an optimal concentration for quantification depended on the sample type and composition. Optimal cholesterol esterase concentration was dependent on astaxanthin concentration and biomass composition, but 2.0 units were generally sufficient in the outlined quantification range. The robustness of the method was demonstrated for ethanolic extracts of *H. pluvialis* obtained from SC-CO<sub>2</sub> extraction. Direct quantification from liquid-liquid extracts was corrected for volume aberrations and dilatations during solvent mixing.

Based on our research, we recommend starting with between 0.5 and 2.0 mg of astaxanthin-containing biomass. The initial experiment can be performed with 2.0 units of cholesterol esterase and an incubation time of 0.75 hours. The settings of the enzymolysis can be adapted depending on the type of the sample, i.e., fresh or dried biomass or extracts. For *H. pluvialis* samples, the stress level and thus estimated astaxanthin content must be considered. Different sample amounts should be processed to examine the approximate astaxanthin concentration and the influence of cellular components and to assure compliance with extraction limits. Enzyme amount and concentration can be adapted in a second measurement set if necessary. Special attention has to be paid to the correct calibration and quantification.

## Supporting information

**S1 Table. Overview of the astaxanthin content in the various experiments.**  
(PDF)

**S2 Table. Overview of the astaxanthin content determined in ethanolic SC-CO<sub>2</sub> extracts.**  
(PDF)

## Acknowledgments

This study was supported by Sea & Sun Technology GmbH, especially Dr. Stefan Hindersin and Clemens Elle, who provided various batches of differently processed *H. pluvialis* biomass.

## Author Contributions

**Conceptualization:** Inga K. Koopmann, Annemarie Kramer, Antje Labes.

**Data curation:** Inga K. Koopmann.



**Formal analysis:** Inga K. Koopmann.

**Funding acquisition:** Antje Labes.

**Investigation:** Inga K. Koopmann.

**Methodology:** Inga K. Koopmann, Annemarie Kramer.

**Project administration:** Annemarie Kramer.

**Supervision:** Annemarie Kramer, Antje Labes.

**Validation:** Inga K. Koopmann.

**Visualization:** Inga K. Koopmann.

**Writing – original draft:** Inga K. Koopmann.

**Writing – review & editing:** Inga K. Koopmann, Annemarie Kramer, Antje Labes.

## References

1. Britton G, Liaaen-Jensen S, Pfander H, editors. Carotenoids: Handbook. Basel: Springer Basel AG; 2004. <https://doi.org/10.1007/978-3-0348-7836-4>
2. National Center for Biotechnology Information. PubChem Compound Summary for CID 5281224, Astaxanthin. <https://pubchem.ncbi.nlm.nih.gov/compound/Astaxanthin>. Accessed 07.06.2022.
3. Del Campo JA, Rodríguez H, Moreno J, Vargas MÁ, Rivas J, Guerrero MG. Accumulation of astaxanthin and lutein in *Chlorella zofingiensis* (Chlorophyta). Appl Microbiol Biotechnol. 2004; 64: 848–854. <https://doi.org/10.1007/s00253-003-1510-5> PMID: 14689249
4. Abe K, Hattori H, Hirano M. Accumulation and antioxidant activity of secondary carotenoids in the aerial microalga *Coelastrrella striolata* var. *multistriata*. Food Chem. 2007; 100: 656–661. <https://doi.org/10.1016/j.foodchem.2005.10.026>
5. Orosa M, Torres E, Fidalgo P, Abalde J. Production and analysis of secondary carotenoids in green algae. J Appl Phycol. 2000; 12: 553–556.
6. Zhang DH, Lee YK, Ng ML, Phang SM. Composition and accumulation of secondary carotenoids in *Chlorococcum* sp. J Appl Phycol. 1997; 9: 147–155.
7. Czeuczuga B. Carotenoids in *Euglena rubida* mainx. Comp Biochem Physiol. 1974; 48B: 349–354.
8. Czeuczuga B. Characteristic carotenoids in some phytobentos species in the coastal area of the Adriatic Sea. Acta Soc Bot Pol. 1986; 55: 601–609.
9. Müller T, Bleiß W, Martin CD, Rogaschewski S, Fuhr G. Snow algae from northwest Svalbard: their identification, distribution, pigment and nutrient content. Polar Biol. 1998; 20: 14–32.
10. Procházková L, Remias D, Holzinger A, Řezanka T, Nedbalová L. Ecophysiological and ultrastructural characterisation of the circumpolar orange snow alga *Sanguina aurantia* compared to the cosmopolitan red snow alga *Sanguina nivaloides* (Chlorophyta). Polar Biol. 2021; 44: 105–117. <https://doi.org/10.1007/s00300-020-02778-0> PMID: 33519055
11. Shah MR, Liang Y, Cheng JJ, Daroch M. Astaxanthin-Producing Green Microalga *Haematococcus pluvialis*: From Single Cell to High Value Commercial Products. Front Plant Sci. 2016; 7: 1–28. <https://doi.org/10.3389/fpls.2016.00531> PMID: 27200009
12. Kopecký J, Schoefs B, Loest K, Štys D, Pulz O. Microalgae as a source for secondary carotenoid production: a screening study. Algal Stud. 2000; 98: 153–168. [https://doi.org/10.1127/algol\\_stud/98/2000/153](https://doi.org/10.1127/algol_stud/98/2000/153)
13. Pawar PR, Velani S, Kumari S, Lali AM, Prakash G. Isolation and optimization of a novel thraustochytrid strain for DHA rich and astaxanthin comprising biomass as aquafeed supplement. 3 Biotech. 2021; 11: 1–10. <https://doi.org/10.1007/s13205-020-02616-4> PMID: 33489688
14. Aki T, Hachida K, Yoshinaga M, Katai Y, Yamasaki T, Kawamoto S, et al. Thraustochytrid as a potential source of carotenoids. J Am Oil Chem Soc. 2003; 80: 789–794. <https://doi.org/10.1007/s11746-003-0773-2>
15. Park H, Kwak M, Seo J, Ju J, Heo S, Park S, et al. Enhanced production of carotenoids using a Thraustochytrid microalgal strain containing high levels of docosahexaenoic acid-rich oil. Bioprocess Biosyst Eng. 2018; 41: 1355–1370. <https://doi.org/10.1007/s00449-018-1963-7> PMID: 29948212



16. Yokoyama A, Izumida H, Miki W. Production of Astaxanthin and 4-Ketozeaxanthin by the Marine Bacterium, *Agrobacterium aurantiacum*. Biosci Biotechnol Biochem. 1994; 58: 1842–1844. <https://doi.org/10.1271/bbb.58.1842>
17. Tsubokura A, Yoneda H, Mizuta H. *Paracoccus carotinifaciens* sp. nov., a new aerobic Gram-negative astaxanthin-producing bacterium. Int J Syst Biol. 1999; 277–282.
18. Yokoyama A, Miki W, Izumida H, Shizuri Y. New trihydroxy-keto-carotenoids isolated from an astaxanthin-producing marine bacterium. Biosci Biotechnol Biochem. 1996; 60: 200–203. <https://doi.org/10.1271/bbb.60.200> PMID: 27299394
19. Osanjo GO, Muthike EW, Tsuma L, Okoth MW, Lünsdorf H, Abraham W-R, et al. A salt lake extremophile, *Paracoccus bogoriensis* sp. nov., efficiently produces xanthophyll carotenoids. Afr J Microbiol Res. 2009; 3: 426–433.
20. Iizuka H, Nishimura Y. Microbiological studies on petroleum and natural gas. X. Carotenoid pigments of hydrocarbon-utilizing bacteria. J Gen Appl Microbiol. 1969; 15: 127–134.
21. Calo P, de Miguel T, Sieiro C, Velazquez JB, Villa TG. Ketocarotenoids in halobacteria: 3-hydroxy-echinenone and *trans*-astaxanthin. J Appl Bacteriol. 1995; 79: 282–285. <https://doi.org/10.1111/j.1365-2672.1995.tb03138.x>
22. Andrewes AG, Phaff HJ, Starr MP. Carotenoids of *Phaffia rhodozyma*, a red-pigmented fermenting yeast. Phytochemistry. 1976; 1003–1007.
23. Tran TN, Tran Q-V, Huynh HT, Hoang N-S, Nguyen HC, Ngo D-N. Astaxanthin Production by Newly Isolated *Rhodospiridium toruloides*: Optimization of Medium Compositions by Response Surface Methodology. Not Bot Horti Agrobot Cluj-Napoca. 2018; 47: 320–327. <https://doi.org/10.15835/nbha4711361>
24. Seybold A, Goodwin T. Occurrence of astaxanthin in the flower petals in *Adonis annua*. Nature. 1959; 184: 1714–1715.
25. Li Y, Gong F, Guo S, Yu W, Liu J. *Adonis amurensis* Is a Promising Alternative to *Haematococcus* as a Resource for Natural Esterified (3S,3'S)-Astaxanthin Production. Plants. 2021; 10: 1–15. <https://doi.org/10.3390/plants10061059> PMID: 34070556
26. Di Mascio P, Kaiser S, Sies H. Lycopene as the most efficient biological carotenoid singlet oxygen quencher. Arch Biochem Biophys. 1989; 274: 532–538. [https://doi.org/10.1016/0003-9861\(89\)90467-0](https://doi.org/10.1016/0003-9861(89)90467-0) PMID: 2802626
27. Conn PF, Schalch W, Truscott TG. The singlet oxygen and carotenoid interaction. J Photochem Photobiol B Biol. 1991; 11: 41–47. [https://doi.org/10.1016/1011-1344\(91\)80266-k](https://doi.org/10.1016/1011-1344(91)80266-k) PMID: 1791493
28. Miki W. Biological functions and activities of animal carotenoids. Pure Appl Chem. 1991; 63: 141–146.
29. Shimidzu N, Goto M, Miki W. Carotenoids as Singlet Oxygen Quenchers in Marine Organisms. Fish Sci. 1996; 62: 134–137. <https://doi.org/10.2331/fishsci.62.134>
30. Liu J, Zhang X, Sun Y, Lin W. Antioxidative capacity and enzyme activity in *Haematococcus pluvialis* cells exposed to superoxide free radicals. Chin J Oceanol Limnol. 2010; 28: 1–9. <https://doi.org/10.1007/s00343-010-9244-6>
31. Rodrigues E, Mariutti LRB, Mercadante AZ. Scavenging Capacity of Marine Carotenoids against Reactive Oxygen and Nitrogen Species in a Membrane-Mimicking System. Mar Drugs. 2012; 10: 1784–1798. <https://doi.org/10.3390/md10081784> PMID: 23015774
32. Liu X, Shibata T, Hisaka S, Osawa T. Astaxanthin inhibits reactive oxygen species-mediated cellular toxicity in dopaminergic SH-SY5Y cells via mitochondria-targeted protective mechanism. Brain Res. 2009; 1254: 18–27. <https://doi.org/10.1016/j.brainres.2008.11.076> PMID: 19101523
33. Chen Y-Y, Lee P-C, Wu Y-L, Liu L-Y. *In Vivo* Effects of Free Form Astaxanthin Powder on Anti-Oxidation and Lipid Metabolism with High-Cholesterol Diet. PLOS ONE. 2015; 10: e0134733. <https://doi.org/10.1371/journal.pone.0134733> PMID: 26262684
34. Jiang X, Chen L, Shen L, Chen Z, Xu L, Zhang J, et al. *Trans*-astaxanthin attenuates lipopolysaccharide-induced neuroinflammation and depressive-like behavior in mice. Brain Res. 2016; 1649: 30–37. <https://doi.org/10.1016/j.brainres.2016.08.029> PMID: 27559013
35. Xue Y, Qu Z, Fu J, Zhen J, Wang W, Cai Y, et al. The protective effect of astaxanthin on learning and memory deficits and oxidative stress in a mouse model of repeated cerebral ischemia/reperfusion. Brain Res Bull. 2017; 131: 221–228. <https://doi.org/10.1016/j.brainresbull.2017.04.019> PMID: 28479214
36. Farruggia C, Kim M-B, Bae M, Lee Y, Pham TX, Yang Y, et al. Astaxanthin exerts anti-inflammatory and antioxidant effects in macrophages in NRF2-dependent and independent manners. J Nutr Biochem. 2018; 62: 202–209. <https://doi.org/10.1016/j.jnutbio.2018.09.005> PMID: 30308382
37. Sharma K, Sharma D, Sharma M, Sharma N, Bidve P, Prajapati N, et al. Astaxanthin ameliorates behavioral and biochemical alterations in *in-vitro* and *in-vivo* model of neuropathic pain. Neurosci Lett. 2018; 674: 162–170. <https://doi.org/10.1016/j.neulet.2018.03.030> PMID: 29559419



38. Brendler T, Williamson EM. Astaxanthin: How much is too much? A safety review. *Phytother Res*. 2019; 33: 3090–3111. <https://doi.org/10.1002/ptr.6514> PMID: 31788888
39. European Food Safety Authority. Scientific Opinion on the safety of astaxanthin-rich ingredients (AstaREAL A1010 and AstaREAL L10) as novel food ingredients. *EFSA J*. 2014; 12: 1–34.
40. Capelli B, Bagchi D, Cysewski GR. Synthetic astaxanthin is significantly inferior to algal-based astaxanthin as an antioxidant and may not be suitable as a human nutraceutical supplement. *Nutrafoods*. 2013; 12: 145–152. <https://doi.org/10.1007/s13749-013-0051-5>
41. Edwards JA, Bellion P, Beilstein P, Rumbeli R, Schierle J. Review of genotoxicity and rat carcinogenicity investigations with astaxanthin. *Regul Toxicol Pharmacol*. 2016; 75: 5–19. <https://doi.org/10.1016/j.yrtph.2015.12.009> PMID: 26713891
42. Lorenz RT, Cysewski GR. Commercial potential for *Haematococcus* microalgae as a natural source of astaxanthin. *Trends Biotechnol*. 2000; 18: 160–167. [https://doi.org/10.1016/S0167-7799\(00\)01433-5](https://doi.org/10.1016/S0167-7799(00)01433-5)
43. Olaizola M. Commercial production of astaxanthin from *Haematococcus pluvialis* using 25,000-liter outdoor photobioreactors. *J Appl Phycol*. 2000; 12: 499–506.
44. Torzillo G, Goksan T, Faraloni C, Kopecky J, Masojidek J. Interplay between photochemical activities and pigment composition in an outdoor culture of *Haematococcus pluvialis* during the shift from the green to red stage. *J Appl Phycol*. 2003; 15: 127–136. <https://doi.org/10.1023/A:1023854904163>
45. Affalo C, Meshulam Y, Zarka A, Boussiba S. On the relative efficiency of two- vs. one-stage production of astaxanthin by the green alga *Haematococcus pluvialis*. *Biotechnol Bioeng*. 2007; 98: 300–305. <https://doi.org/10.1002/bit.21391> PMID: 17318905
46. Rao R, Sarada AR, Baskaran V, Ravishankar GA. Identification of Carotenoids from Green Alga *Haematococcus pluvialis* by HPLC and LC-MS (APCI) and Their Antioxidant Properties. *J Microbiol Biotechnol*. 2009; 19: 1333–1341.
47. Wang J, Han D, Sommerfeld MR, Lu C, Hu Q. Effect of initial biomass density on growth and astaxanthin production of *Haematococcus pluvialis* in an outdoor photobioreactor. *J Appl Phycol*. 2013; 25: 253–260. <https://doi.org/10.1007/s10811-012-9859-4>
48. Liyanaarachchi VC, Nishshanka GKSH, Premaratne RGMM, Ariyadasa TU, Nimarshana PHV, Malik A. Astaxanthin accumulation in the green microalga *Haematococcus pluvialis*: Effect of initial phosphate concentration and stepwise/continuous light stress. *Biotechnol Rep*. 2020; 28: e00538. <https://doi.org/10.1016/j.btre.2020.e00538> PMID: 33294401
49. Miao F, Lu D, Li Y, Zeng M. Characterization of astaxanthin esters in *Haematococcus pluvialis* by liquid chromatography–atmospheric pressure chemical ionization mass spectrometry. *Anal Biochem*. 2006; 352: 176–181. <https://doi.org/10.1016/j.ab.2006.03.006> PMID: 16597431
50. Holtin K, Kuehnle M, Rehbein J, Schuler P, Nicholson G, Albert K. Determination of astaxanthin and astaxanthin esters in the microalgae *Haematococcus pluvialis* by LC–(APCI)MS and characterization of predominant carotenoid isomers by NMR spectroscopy. *Anal Bioanal Chem*. 2009; 395: 1613–1622. <https://doi.org/10.1007/s00216-009-2837-2> PMID: 19466394
51. Grewe C, Griehl C. Time- and media-dependent secondary carotenoid accumulation in *Haematococcus pluvialis*. *Biotechnol J*. 2008; 3: 1232–1244. <https://doi.org/10.1002/biot.200800067> PMID: 18683169
52. Miao F, Lu D, Zhang C, Zuo J, Geng Y, Hu H, et al. The synthesis of astaxanthin esters, independent of the formation of cysts, highly correlates with the synthesis of fatty acids in *Haematococcus pluvialis*. *Sci China C Life Sci*. 2008; 51: 1094–1100. <https://doi.org/10.1007/s11427-008-0141-6> PMID: 19093083
53. Harker M, Tsavalos AJ, Young AJ. Autotrophic growth and carotenoid production of *Haematococcus pluvialis* in a 30 liter air-lift photobioreactor. *J Ferment Bioeng*. 1996; 82: 113–118. [https://doi.org/10.1016/0922-338X\(96\)85031-8](https://doi.org/10.1016/0922-338X(96)85031-8)
54. Zechmeister L. *Cis-trans* Isomerization and Stereochemistry of Carotenoids and Diphenyl-polyenes. *Chem Rev*. 1944; 34: 267–344. <https://doi.org/10.1021/cr60108a004>
55. Yuan J-P, Chen F. Purification of *trans*-astaxanthin from a high-yielding astaxanthin ester-producing strain of the microalga *Haematococcus pluvialis*. *Food Chem*. 2000; 68: 443–448.
56. Yuan J-P, Chen F. Hydrolysis Kinetics of Astaxanthin Esters and Stability of Astaxanthin of *Haematococcus pluvialis* during Saponification. *J Agric Food Chem*. 1999; 47: 31–35. <https://doi.org/10.1021/jf980465x> PMID: 10563844
57. Yuan J-P, Chen F. Chromatographic Separation and Purification of *trans*-Astaxanthin from the Extracts of *Haematococcus pluvialis*. *J Agric Food Chem*. 1998; 46: 3371–3375. <https://doi.org/10.1021/jf980039b>
58. Euglert G, Vecchi M. *trans/cis* Isomerization of Astaxanthin Diacetate/Isolation by HPLC. and Identification by <sup>1</sup>H-NMR. Spectroscopy of Three Mono-*cis*- and Six Di-*cis*-Isomers. *Helv Chim Acta*. 1980; 63: 1711–1718. <https://doi.org/10.1002/hlca.19800630640>



59. Casella P, Iovine A, Mehariya S, Marino T, Musmarra D, Molino A. Smart Method for Carotenoids Characterization in *Haematococcus pluvialis* Red Phase and Evaluation of Astaxanthin Thermal Stability. *Antioxidants*. 2020; 9: 1–17. <https://doi.org/10.3390/antiox9050422> PMID: 32414186
60. Subramanian B, Tchoukanova N, Djaoued Y, Pelletier C, Ferron M, Robichaud J. Investigations on the geometrical isomers of astaxanthin: Raman spectroscopy of conjugated polyene chain with electronic and mechanical confinement: Investigations on the geometrical isomers of astaxanthin. *J Raman Spectrosc*. 2014; 45: 299–304. <https://doi.org/10.1002/jrs.4459>
61. Moretti VM, Mentasti T, Bellagamba F, Luzzana U, Caprino F, Turchini GM, et al. Determination of astaxanthin stereoisomers and colour attributes in flesh of rainbow trout (*Oncorhynchus mykiss*) as a tool to distinguish the dietary pigmentation source. *Food Addit Contam*. 2006; 23: 1056–1063.
62. Renstrøm B, Borch G, Skulberg OM, Liaaen-Jensen S. Optical purity of (3S,3'S)-astaxanthin from *Haematococcus pluvialis*. *Phytochemistry*. 1981; 20: 2561–2564.
63. Zhao X, Liu H, Zhang X, Zhang G, Zhu H. Astaxanthin from *Haematococcus pluvialis* Microencapsulated by Spray Drying: Characterization and Antioxidant Activity. *J Am Oil Chem Soc*. 2019; 96: 93–102. <https://doi.org/10.1002/aocs.12170>
64. Sarada R, Vidhyavathi R, Usha D, Ravishankar GA. An Efficient Method for Extraction of Astaxanthin from Green Alga *Haematococcus pluvialis*. *J Agric Food Chem*. 2006; 54: 7585–7588. <https://doi.org/10.1021/jf060737t> PMID: 17002425
65. Boussiba S, Vonshak A. Astaxanthin Accumulation in the Green Alga *Haematococcus pluvialis*. *Plant Cell Physiol*. 1991; 32: 1077–1082.
66. Kulikov EA, Kulikova IS, Vasilov RG, Selishcheva AA. The Effect of the Solvent Nature and Lighting on Isomerization and Oxidative Degradation of Astaxanthin. *Biophysics*. 2020; 65: 433–442. <https://doi.org/10.1134/S0006350920030112>
67. Yuan J-P, Chen F. Isomerization of *trans*-Astaxanthin to *cis*-Isomers in Organic Solvents. *J Agric Food Chem*. 1999; 47: 3656–3660. <https://doi.org/10.1021/jf981319u> PMID: 10552699
68. Yuan J-P, Gong X-D, Chen F. Separation and Analysis of Carotenoids and Chlorophylls in *Haematococcus lacustris* by High-Performance Liquid Chromatography Photodiode Array Detection. *J Agric Food Chem*. 1997; 45: 1952–1956. <https://doi.org/10.1021/jf970002b>
69. Cifuentes AS, González MA, Vargas S, Hoeneisen M, González N. Optimization of biomass, total carotenoids and astaxanthin production in *Haematococcus pluvialis* Flotow strain Steptoe (Nevada, USA) under laboratory conditions. *Biol Res*. 2003; 36: 343–357. <https://doi.org/10.4067/S0716-97602003000300006> PMID: 14631867
70. Kang CD, Sim SJ. Selective Extraction of Free Astaxanthin from *Haematococcus* Culture Using a Tandem Organic Solvent System. *Biotechnol Prog*. 2007; 23: 866–871. <https://doi.org/10.1021/bp0700354> PMID: 17567038
71. Raposo MFJ, Morais AMMB, Morais RMSC. Effects of spray-drying and storage on astaxanthin content of *Haematococcus pluvialis* biomass. *World J Microbiol Biotechnol*. 2012; 28: 1253–1257. <https://doi.org/10.1007/s11274-011-0929-6> PMID: 22805845
72. Dong S, Huang Y, Zhang R, Wang S, Liu Y. Four Different Methods Comparison for Extraction of Astaxanthin from Green Alga *Haematococcus pluvialis*. *Sci World J*. 2014; 2014: 1–7. <https://doi.org/10.1155/2014/694305> PMID: 24574909
73. Jaime L, Rodríguez-Meizoso I, Cifuentes A, Santoyo S, Suarez S, Ibáñez E, et al. Pressurized liquids as an alternative process to antioxidant carotenoids' extraction from *Haematococcus pluvialis* microalgae. *LWT—Food Sci Technol*. 2010; 43: 105–112. <https://doi.org/10.1016/j.lwt.2009.06.023>
74. Reyes FA, Mendiola JA, Ibáñez E, del Valle JM. Astaxanthin extraction from *Haematococcus pluvialis* using CO<sub>2</sub>-expanded ethanol. *J Supercrit Fluids*. 2014; 92: 75–83. <https://doi.org/10.1016/j.supflu.2014.05.013>
75. Boussiba S, Fan L, Vonshak A. Enhancement and determination of astaxanthin accumulation in green alga *Haematococcus pluvialis*. *Methods Enzymol*. 1992; 213: 386–391.
76. Miao F, Geng Y, Lu D, Zuo J, Li Y. Stability and changes in astaxanthin ester composition from *Haematococcus pluvialis* during storage. *Chin J Oceanol Limnol*. 2013; 31: 1181–1189. <https://doi.org/10.1007/s00343-013-2105-3>
77. Li Y, Miao F, Geng Y, Lu D, Zhang C, Zeng M. Accurate quantification of astaxanthin from *Haematococcus* crude extract spectrophotometrically. *Chin J Oceanol Limnol*. 2012; 30: 627–637. <https://doi.org/10.1007/s00343-012-1217-5>
78. de Bruijn WJC, Weesepeel Y, Vincken J-P, Gruppen H. Fatty acids attached to all-*trans*-astaxanthin alter its *cis-trans* equilibrium, and consequently its stability, upon light-accelerated autoxidation. *Food Chem*. 2016; 194: 1108–1115. <https://doi.org/10.1016/j.foodchem.2015.08.077> PMID: 26471660



79. Bjerkeng B, Følling M, Lagocki S, Storebakken T, Olli JJ, Alsted N. Bioavailability of all-*E*-astaxanthin and *Z*-isomers of astaxanthin in rainbow trout (*Oncorhynchus mykiss*). *Aquaculture*. 1997; 157: 63–82. [https://doi.org/10.1016/S0044-8486\(97\)00146-4](https://doi.org/10.1016/S0044-8486(97)00146-4)
80. Orona-Navar A, Aguilar-Hernández I, Cerdán-Pasarán A, López-Luke T, Rodríguez-Delgado M, Cárdenas-Chávez DL, et al. Astaxanthin from *Haematococcus pluvialis* as a natural photosensitizer for dye-sensitized solar cell. *Algal Res*. 2017; 26: 15–24. <https://doi.org/10.1016/j.algal.2017.06.027>
81. Chen H-M, Meyers SP. A rapid quantitative method for determination of astaxanthin pigment concentration in oil extracts. *J Am Oil Chem Soc*. 1984; 61: 1045–1047. <https://doi.org/10.1007/BF02636215>
82. An G-H, Schuman DB, Johnson EA. Isolation of *Phaffia rhodozyma* Mutants with Increased Astaxanthin Content. *Appl Environ Microbiol*. 1989; 55: 116–124. <https://doi.org/10.1128/AEM.55.1.116-124.1989>
83. Gomez PI, Inostroza I, Pizarro M, Perez J. From genetic improvement to commercial-scale mass culture of a Chilean strain of the green microalga *Haematococcus pluvialis* with enhanced productivity of the red ketocarotenoid astaxanthin. *AoB Plants*. 2013; 5: plt026. <https://doi.org/10.1093/aobpla/plt026> PMID: 23789055
84. Jin H, Lao YM, Zhou J, Zhang HJ, Cai ZH. Simultaneous determination of 13 carotenoids by a simple C18 column-based ultra-high-pressure liquid chromatography method for carotenoid profiling in the astaxanthin-accumulating *Haematococcus pluvialis*. *J Chromatogr A*. 2017; 1488: 93–103. <https://doi.org/10.1016/j.chroma.2017.01.088> PMID: 28179080
85. Su F, Xu H, Yang N, Liu W, Liu J. Hydrolytic efficiency and isomerization during de-esterification of natural astaxanthin esters by saponification and enzymolysis. *Electron J Biotechnol*. 2018; 34: 37–42. <https://doi.org/10.1016/j.ejbt.2018.05.002>
86. Toomey MB, McGraw KJ. Modified Saponification and HPLC Methods for Analyzing Carotenoids from the Retina of Quail: Implications for Its Use as a Nonprimate Model Species. *Investig Ophthalmology Vis Sci*. 2007; 48: 3976–3982. <https://doi.org/10.1167/jovs.07-0208> PMID: 17724175
87. Galarza JI, Arredondo Vega BO, Villón J, Henríquez V. Deesterification of astaxanthin and intermediate esters from *Haematococcus pluvialis* subjected to stress. *Biotechnol Rep*. 2019; 23: e00351. <https://doi.org/10.1016/j.btre.2019.e00351> PMID: 31312607
88. Doria E, Temporiti MEE, Damiani MC, Popovich CA, Leonardi PI, Nielsen E. Influence of Light Stress in the Accumulation of Xanthophylls and Lipids in *Haematococcus Pluvialis* Grown under Autotrophic or Mixotrophic Conditions. *J Mar Biol Aquac*. 2018; 4: 30–35. <https://doi.org/10.15436/2381-0750.18.1799>
89. Nobre B, Marcelo F, Passos R, Beirão L, Palavra A, Gouveia L, et al. Supercritical carbon dioxide extraction of astaxanthin and other carotenoids from the microalga *Haematococcus pluvialis*. *Eur Food Res Technol*. 2006; 223: 787–790. <https://doi.org/10.1007/s00217-006-0270-8>
90. Lietz G, Henry CJK. A modified method to minimise losses of carotenoids and tocopherols during HPLC analysis of red palm oil. *Food Chem*. 1997; 60: 109–117. [https://doi.org/10.1016/S0308-8146\(96\)00319-6](https://doi.org/10.1016/S0308-8146(96)00319-6)
91. Jacobs PB, LeBoeuf RD, McCommas SA, Tauber JD. The cleavage of carotenoid esters by cholesterol esterase. *Comp Biochem Physiol Part B Comp Biochem*. 1982; 72: 157–160. [https://doi.org/10.1016/0305-0491\(82\)90027-X](https://doi.org/10.1016/0305-0491(82)90027-X)
92. Denery JR, Dragull K, Tang CS, Li QX. Pressurized fluid extraction of carotenoids from *Haematococcus pluvialis* and *Dunaliella salina* and kavalactones from *Piper methysticum*. *Anal Chim Acta*. 2004; 501: 175–181. <https://doi.org/10.1016/j.aca.2003.09.026>
93. Zhao Y, Guan F, Wang G, Miao L, Ding J, Guan G, et al. Astaxanthin Preparation by Lipase-Catalyzed Hydrolysis of Its Esters from *Haematococcus pluvialis* Algal Extracts. *J Food Sci*. 2011; 76: C643–C650. <https://doi.org/10.1111/j.1750-3841.2011.02119.x> PMID: 22417348
94. Huang J, Yang Z, Zhu R, Qian X, Wang Y, Li Y, et al. Efficient heterologous expression of an alkaline lipase and its application in hydrolytic production of free astaxanthin. *Biotechnol Biofuels*. 2018; 11: 1–12. <https://doi.org/10.1186/s13068-018-1180-2> PMID: 29983744
95. Nagao T, Fukami T, Horita Y, Komemushi S, Sugihara A, Shimada Y. Enzymatic enrichment of astaxanthin from *Haematococcus pluvialis* cell extracts. *J Am Oil Chem Soc*. 2003; 80: 975–981. <https://doi.org/10.1007/s11746-003-0806-x>
96. Dong H, Li X, Xue C, Mao X. Astaxanthin preparation by fermentation of esters from *Haematococcus pluvialis* algal extracts with *Stenotrophomonas* species. *Biotechnol Prog*. 2016; 32: 649–656. <https://doi.org/10.1002/btpr.2258> PMID: 26949202
97. Lorenz T. HPLC and spectrophotometric analysis of carotenoids from *Haematococcus* algae powder. 2001 pp. 1–10. Report No.: BioAstin/NatuRose TM Technichal Bulletin.



98. Fuji Chemical Industry Co., Ltd. Spectrophotometric and HPLC Analysis Method for Determining Astaxanthin Content in AstaRealR-P2AF. 1918 pp. 1–18.
99. Cyanotech Corporation. Analysis of Natural Astaxanthin Derived from *Haematococcus* Microalgae in Astaxanthin Oleoresin, Astaxanthin Gelcaps, Astaxanthin Beadlets, and *Haematococcus* Biomass. pp. 1–22.
100. Lichtenthaler HK. Chlorophylls and Carotenoids: Pigments of Photosynthetic Biomembranes. *Methods Enzymol.* 1987; 148: 350–382.
101. Ruiz-Domínguez MC, Espinosa C, Paredes A, Palma J, Jaime C, Vilchez C, et al. Determining the Potential of *Haematococcus pluvialis* Oleoresin as a Rich Source of Antioxidants. *Molecules.* 2019; 24: 1–17. <https://doi.org/10.3390/molecules24224073> PMID: 31717936
102. Honda M, Takahashi N, Kuwa T, Takehara M, Inoue Y, Kumagai T. Spectral characterisation of Z-isomers of lycopene formed during heat treatment and solvent effects on the E/Z isomerisation process. *Food Chem.* 2015; 171: 323–329. <https://doi.org/10.1016/j.foodchem.2014.09.004> PMID: 25308676
103. Zechmeister L. *Cis-Trans Isomeric Carotenoids Vitamins A and Arylpolynes.* Vienna: Springer; 1962. <https://doi.org/10.1007/978-3-7091-5548-6>
104. Murakami K, Honda M, Takemura R, Fukaya T, Kubota M, Wahyudiono, et al. The thermal Z-isomerization-induced change in solubility and physical properties of (all-E)-lycopene. *Biochem Biophys Res Commun.* 2017; 491: 317–322. <https://doi.org/10.1016/j.bbrc.2017.07.103> PMID: 28735868
105. Murakami K, Honda M, Wahyudiono, Kanda H, Goto M. Thermal isomerization of (all-E)-lycopene and separation of the Z-isomers by using a low boiling solvent: Dimethyl ether. *Sep Sci Technol.* 2017; 52: 2573–2582. <https://doi.org/10.1080/01496395.2017.1374412>
106. Aman R, Schieber A, Carle R. Effects of Heating and Illumination on *Trans-Cis* Isomerization and Degradation of  $\beta$ -Carotene and Lutein in Isolated Spinach Chloroplasts. *J Agric Food Chem.* 2005; 53: 9512–9518. <https://doi.org/10.1021/jf050926w> PMID: 16302770
107. Honda M, Sowa T, Kawashima Y. Thermal- and Photo-Induced Isomerization of All-E - and Z-Isomer-Rich Xanthophylls: Astaxanthin and Its Structurally-Related Xanthophylls, Adonirubin, and Adonixanthin. *Eur J Lipid Sci Technol.* 2020; 1900462: 1–9. <https://doi.org/10.1002/ejlt.201900462>
108. Liu X, Osawa T. *Cis* astaxanthin and especially 9-*cis* astaxanthin exhibits a higher antioxidant activity *in vitro* compared to the all-*trans* isomer. *Biochem Biophys Res Commun.* 2007; 357: 187–193. <https://doi.org/10.1016/j.bbrc.2007.03.120> PMID: 17416351
109. Uwajima T, Terada O. Purification and Properties of Cholesterol Esterase from *Pseudomonas fluorescens*. *Agric Biol Chem.* 1976; 40: 1957–1964. <https://doi.org/10.1080/00021369.1976.10862345>
110. Takeda Y, Aono R, Doukyu N. Purification, characterization, and molecular cloning of organic-solvent-tolerant cholesterol esterase from cyclohexane-tolerant *Burkholderia cepacia* strain ST-200. *Extremophiles.* 2006; 10: 269–277. <https://doi.org/10.1007/s00792-005-0494-8> PMID: 16463077
111. Yuan J-P, Chen F. Kinetics for the reversible isomerization reaction of *trans*-astaxanthin. *Food Chem.* 2001; 73: 131–137. [https://doi.org/10.1016/S0308-8146\(01\)00107-8](https://doi.org/10.1016/S0308-8146(01)00107-8)
112. Qin A, Hoffman DE, Munk P. Excess volumes of mixtures of alkanes with carbonyl compounds. *J Chem Eng Data.* 1992; 37: 55–61. <https://doi.org/10.1021/je00005a018>
113. Honda M, Kodama T, Kageyama H, Hibino T, diono W, Kanda H, et al. Enhanced solubility and reduced crystallinity of carotenoids,  $\beta$ -carotene and astaxanthin, by Z-isomerization. *Eur J Lipid Sci Technol.* 2018; 120: 1–8. <https://doi.org/10.1002/ejlt.201800191>
114. Honda M, Watanabe Y, Murakami K, Takemura R, Fukaya T, Wahyudiono, et al. Thermal isomerization pre-treatment to improve lycopene extraction from tomato pulp. *LWT.* 2017; 86: 69–75. <https://doi.org/10.1016/j.lwt.2017.07.046>
115. Saha SK, McHugh E, Hayes J, Moane S, Walsh D, Murray P. Effect of various stress-regulatory factors on biomass and lipid production in microalga *Haematococcus pluvialis*. *Bioresour Technol.* 2013; 128: 118–124. <https://doi.org/10.1016/j.biortech.2012.10.049> PMID: 23196231
116. Sarada R, Tripathi U, Ravishankar GA. Influence of stress on astaxanthin production in *Haematococcus pluvialis* grown under different culture conditions. *Process Biochem.* 2002; 37: 623–627. [https://doi.org/10.1016/S0032-9592\(01\)00246-1](https://doi.org/10.1016/S0032-9592(01)00246-1)
117. Recht L, Zarka A, Boussiba S. Patterns of carbohydrate and fatty acid changes under nitrogen starvation in the microalgae *Haematococcus pluvialis* and *Nannochloropsis* sp. *Appl Microbiol Biotechnol.* 2012; 94: 1495–1503. <https://doi.org/10.1007/s00253-012-3940-4> PMID: 22361859
118. Howles PN, Hui DY. Cholesterol Esterase. 1st ed. In: Mansbach CM, Tso P, Kuksis A, editors. *Intestinal Lipid Metabolism.* 1st ed. Boston, MA: Springer; 2001. pp. 119–134.
119. Chen Q, Sternby B, Nilsson A. Hydrolysis of triacylglycerol arachidonic and linoleic acid ester bonds by human pancreatic lipase and carboxyl ester lipase. *Biochim Biophys Acta BBA—Lipids Lipid Metab.* 1989; 1004: 372–385.



120. Sugihara A, Shimada Y, Nomura A, Terai T, Imayasu M, Nagai Y, et al. Purification and Characterization of a Novel Cholesterol Esterase from *Pseudomonas aeruginosa*, with Its Application to Cleaning Lipid-stained Contact Lenses. *Biosci Biotechnol Biochem*. 2002; 66: 2347–2355.
121. Hui DY, Howles PN. Carboxyl ester lipase: structure-function relationship and physiological role in lipid-protein metabolism and atherosclerosis. *J Lipid Res*. 2002; 43: 2017–2030. <https://doi.org/10.1194/jlr.R200013-jlr200> PMID: 12454261
122. Ben Ali Y, Carrière F, Verger R, Petry S, Muller G, Abousalham A. Continuous monitoring of cholesterol oleate hydrolysis by hormone-sensitive lipase and other cholesterol esterases. *J Lipid Res*. 2005; 46: 994–1000. <https://doi.org/10.1194/jlr.M400509-JLR200> PMID: 15716583
123. Gargouri Y, Julien R, Pieroni G, Verger R, Sarda L. Studies on the inhibition of pancreatic and microbial lipases by soybean proteins. *J Lipid Res*. 1984; 25: 1214–1221. [https://doi.org/10.1016/S0022-2275\(20\)34465-5](https://doi.org/10.1016/S0022-2275(20)34465-5) PMID: 6542933
124. Gargouri Y, Julien R, Sugihara A, Verger R, Sarda L. Inhibition of pancreatic and microbial lipases by proteins. *Biochim Biophys Acta BBA—Lipids Lipid Metab*. 1984; 795: 326–331. [https://doi.org/10.1016/0005-2760\(84\)90082-1](https://doi.org/10.1016/0005-2760(84)90082-1)
125. Gong F, Zhang C, Zhang L, Liu J. Changes of carotenoids contents and analysis of astaxanthin geometrical isomerization in *Haematococcus pluvialis* under outdoor high light conditions. *Aquac Res*. 2020; 51: 770–778. <https://doi.org/10.1111/are.14427>
126. Krichnavaruk S, Shotipruk A, Goto M, Pavasant P. Supercritical carbon dioxide extraction of astaxanthin from *Haematococcus pluvialis* with vegetable oils as co-solvent. *Bioresour Technol*. 2008; 99: 5556–5560. <https://doi.org/10.1016/j.biortech.2007.10.049> PMID: 18068354
127. Machmudah S, Shotipruk A, Goto M, Sasaki M, Hirose T. Extraction of Astaxanthin from *Haematococcus pluvialis* Using Supercritical CO<sub>2</sub> and Ethanol as Entrainer. *Ind Eng Chem Res*. 2006; 45: 3652–3657. <https://doi.org/10.1021/ie051357k>
128. Pan J-L, Wang H-M, Chen C-Y, Chang J-S. Extraction of astaxanthin from *Haematococcus pluvialis* by supercritical carbon dioxide fluid with ethanol modifier: Supercritical CO<sub>2</sub> fluid extraction of astaxanthin from microalgae. *Eng Life Sci*. 2012; 12: 638–647. <https://doi.org/10.1002/elsc.201100157>
129. Amin MdA, Halder R, Ghosh C, Jana B, Bhattacharyya K. Effect of alcohol on the structure of cytochrome C: FCS and molecular dynamics simulations. *J Chem Phys*. 2016; 145: 1–8. <https://doi.org/10.1063/1.4972065> PMID: 28010091
130. Nandi S, Parui S, Halder R, Jana B, Bhattacharyya K. Interaction of proteins with ionic liquid, alcohol and DMSO and in situ generation of gold nano-clusters in a cell. *Biophys Rev*. 2018; 10: 757–768. <https://doi.org/10.1007/s12551-017-0331-1> PMID: 29147940
131. Deshpande A, Nimsadkar S, Mande SC. Effect of alcohols on protein hydration: crystallographic analysis of hen egg-white lysozyme in the presence of alcohols. *Acta Crystallogr D Biol Crystallogr*. 2005; 61: 1005–1008. <https://doi.org/10.1107/S0907444905009364> PMID: 15983424
132. Ormanoudis C, Dakos C, Panayiotou C. Volumetric Properties of Binary Mixtures. 2. Mixtures of n-Hexane with Ethanol and i-Propanol. *J Chem Eng Data*. 1991; 36: 39–42.
133. Qin A, Hofmann DE, Munk P. Excess volumes of mixtures of some alkyl esters and ketones with alcohols. *Collect Czech Chem Commun*. 1993; 58: 2625–2641.
134. Miyano Y, Hayduk W. Solubilities of n-butane gas and densities for acetone-methanol, acetone-ethanol, and acetone-propanol solvent solutions. *J Chem Eng Data*. 1986; 31: 81–83. <https://doi.org/10.1021/je00043a023>
135. Dortmund Data Bank, 2022, [www.ddbst.com](http://www.ddbst.com).
136. Schoefs B, Rmiki N-E, Rachadi J, Lemoine Y. Astaxanthin accumulation in *Haematococcus* requires a cytochrome P450 hydroxylase and an active synthesis of fatty acids. *FEBS Lett*. 2001; 500: 125–128. [https://doi.org/10.1016/S0014-5793\(01\)02596-0](https://doi.org/10.1016/S0014-5793(01)02596-0)
137. Álvarez CE, Vardanega R, Salinas-Fuentes F, Ramírez JP, Muñoz WB, Jiménez-Rondón D, et al. Effect of CO<sub>2</sub> Flow Rate on the Extraction of Astaxanthin and Fatty Acids from *Haematococcus pluvialis* Using Supercritical Fluid Technology. *Molecules*. 2020; 25: 1–17.
138. Gamlieli-Bonshtein I, Korin E, Cohen S. Selective separation of *cis-trans* geometrical isomers of  $\beta$ -carotene via CO<sub>2</sub> supercritical fluid extraction. *Biotechnol Bioeng*. 2002; 80: 169–174. <https://doi.org/10.1002/bit.10357> PMID: 12209772
139. Watanabe Y, Honda M, Higashiura T, Fukaya T, Machmudah S, Wahyudiono, et al. Rapid and Selective Concentration of Lycopene Z-isomers from Tomato Pulp by Supercritical CO<sub>2</sub> with Co-solvents. *Solvent Extr Res Dev Jpn*. 2018; 25: 47–57. <https://doi.org/10.15261/serdj.25.47>
140. Küpper H, Seibert S, Parameswaran A. Fast, Sensitive, and Inexpensive Alternative to Analytical Pigment HPLC: Quantification of Chlorophylls and Carotenoids in Crude Extracts by Fitting with Gauss Peak Spectra. *Anal Chem*. 2007; 79: 7611–7627. <https://doi.org/10.1021/ac070236m> PMID: 17854156



141. Thrane J-E, Kyle M, Striebel M, Haande S, Grung M, Rohrlack T, et al. Spectrophotometric Analysis of Pigments: A Critical Assessment of a High-Throughput Method for Analysis of Algal Pigment Mixtures by Spectral Deconvolution. PLOS ONE. 2015; 10: e0137645. <https://doi.org/10.1371/journal.pone.0137645> PMID: [26359659](https://pubmed.ncbi.nlm.nih.gov/26359659/)
142. Etoh H, Suhara M, Tokuyama S, Kato H, Nakahigashi R, Maejima Y, et al. Auto-Oxidation Products of Astaxanthin. J Oleo Sci. 2012; 61: 17–21. <https://doi.org/10.5650/jos.61.17> PMID: [22188802](https://pubmed.ncbi.nlm.nih.gov/22188802/)
143. Niamnuy C, Devahastin S, Soponronnarit S, Vijaya Raghavan GS. Kinetics of astaxanthin degradation and color changes of dried shrimp during storage. J Food Eng. 2008; 87: 591–600. <https://doi.org/10.1016/j.jfoodeng.2008.01.013>
144. Ahmed F, Li Y, Fanning K, Netzel M, Schenk PM. Effect of drying, storage temperature and air exposure on astaxanthin stability from *Haematococcus pluvialis*. Food Res Int. 2015; 74: 231–236. <https://doi.org/10.1016/j.foodres.2015.05.021> PMID: [28411988](https://pubmed.ncbi.nlm.nih.gov/28411988/)
145. Hagen C, Siegmund S, Braune W. Ultrastructural and chemical changes in the cell wall of *Haematococcus pluvialis* (Volvocales, Chlorophyta) during aplanospore formation. Eur J Phycol. 2002; 37: 217–226. <https://doi.org/10.1017/S0967026202003669>
146. Damiani MC, Leonardi PI, Pieroni OI, Cáceres EJ. Ultrastructure of the cyst wall of *Haematococcus pluvialis* (Chlorophyceae): wall development and behaviour during cyst germination. Phycologia. 2006; 45: 616–623. <https://doi.org/10.2216/05-27.1>









## Chapter II

Optimization of Astaxanthin Recovery in the Downstream Process of *Haematococcus pluvialis*



Article

# Optimization of Astaxanthin Recovery in the Downstream Process of *Haematococcus pluvialis*

Inga K. Koopmann <sup>1,2</sup> , Simone Möller <sup>1,2</sup>, Clemens Elle <sup>2</sup>, Stefan Hindersin <sup>2</sup>, Annemarie Kramer <sup>1</sup> and Antje Labes <sup>1,\*</sup> 

<sup>1</sup> ZAIT, Bio and Food Technology, Faculty Energy and Biotechnology, Flensburg University of Applied Sciences, 24943 Flensburg, Germany; inga.koopmann@hs-flensburg.de (I.K.K.); simone.moeller@lactotec.de (S.M.); annemarie.kramer@hs-flensburg.de (A.K.)

<sup>2</sup> Sea & Sun Technology GmbH, 24610 Trappenkamp, Germany; elle@sea-sun-tech.com (C.E.); hindersin@sea-sun-tech.com (S.H.)

\* Correspondence: antje.labes@hs-flensburg.de



**Citation:** Koopmann, I.K.; Möller, S.; Elle, C.; Hindersin, S.; Kramer, A.; Labes, A. Optimization of Astaxanthin Recovery in the Downstream Process of *Haematococcus pluvialis*. *Foods* **2022**, *11*, 1352. <https://doi.org/10.3390/foods11091352>

Academic Editors: Yanwen Wang and Guoxun Chen

Received: 12 April 2022

Accepted: 3 May 2022

Published: 6 May 2022

**Publisher's Note:** MDPI stays neutral with regard to jurisdictional claims in published maps and institutional affiliations.



**Copyright:** © 2022 by the authors. Licensee MDPI, Basel, Switzerland. This article is an open access article distributed under the terms and conditions of the Creative Commons Attribution (CC BY) license (<https://creativecommons.org/licenses/by/4.0/>).

**Abstract:** Astaxanthin derived from *Haematococcus pluvialis* is a valuable metabolite applied in a wide range of products. Its extraction depends on a sophisticated series of downstream process steps, including harvesting, disruption, drying, and extraction, of which some are dependent on each other. To determine the processes that yield maximum astaxanthin recovery, bead milling, high-pressure homogenization, and no disruption of *H. pluvialis* biomass were coupled with spray-drying, vacuum-drying, and freeze-drying in all possible combinations. Eventually, astaxanthin was extracted using supercritical CO<sub>2</sub>. Optimal conditions for spray-drying were evaluated through the design of experiments and standard least squares regression (feed rate: 5.8 mL/min, spray gas flow: 400 NL/h, inlet temperature: 180 °C). Maximal astaxanthin recoveries were yielded using high-pressure homogenization and lyophilization (85.4%). All combinations of milling or high-pressure homogenization and lyophilization or spray-drying resulted in similar recoveries. Bead milling and spray-drying repeated with a larger spray-dryer resulted in similar astaxanthin recoveries compared with the laboratory scale. Smaller astaxanthin recoveries after the extraction of vacuum-dried biomass were mainly attributed to textural changes. Evaluation of these results in an economic context led to a recommendation for bead milling and spray-drying prior to supercritical CO<sub>2</sub> extraction to achieve the maximum astaxanthin recoveries.

**Keywords:** isomerization; UHPLC-PDA-MS; microalgae; carotenoids; disruption; drying; supercritical CO<sub>2</sub> extraction; economic feasibility

## 1. Introduction

Astaxanthin (3,3'-dihydroxy- $\beta,\beta'$ -carotene-4,4'-dione), a secondary ketocarotenoid, can reduce (photo-)oxidative stress by scavenging a variety of radicals and quenching singlet oxygen [1–6]. This strong antioxidant capability applies in vivo and in vitro [7–12]. Astaxanthin has been used as a nutritional supplement, food and feed additive, and in cosmetics. Beneficial health effects, such as cardiovascular disease prevention and improved immune response, have been associated with astaxanthin consumption. The approval of astaxanthin from natural sources for human consumption has been granted in many countries worldwide, with recommended daily intakes of up to 24 mg/day permitted by the United States Food and Drug Administration [13]. Although it can be produced synthetically, its natural form has gained interest with respect to consumer demands [14,15]. Various organisms have the potential to accumulate astaxanthin. Its biosynthesis has mainly been observed in microalgae [16–24], but also in a few protists [25–27], bacteria [28–32], archaea [33], as well as yeasts [34,35], and very few plant species [36,37]. A major source for the biotechnological production of astaxanthin is the green alga *Haematococcus pluvialis* [24,38]. It forms flagellated, motile cells under optimal environmental conditions. These



transform into spherical, non-motile aplanospores, which accumulate astaxanthin under stress conditions such as high light irradiation or nutrient deficiency [24,39–43]. *H. pluvialis* can accumulate 1.9% to 7.0% astaxanthin of its dry weight [44–49].

Astaxanthin often has to be extracted from whole-cell biomass to meet legal and processing demands, e.g., raw materials free from cellular debris are needed for cosmetics or feed additive production. Therefore, elaborate downstream processing is necessary, which may constitute a large part of the total production costs [50–53]. Depending on the purity desired, it generally comprises four or more steps: harvesting the biomass, cell disruption, drying, and the extraction of astaxanthin [50]. Harvesting comprises biomass concentration to reduce the volume in further processes.

Disruption is necessary to facilitate later accessibility during the extraction [54,55], because the aplanospores of *H. pluvialis* have a very thick and rigid cell wall, limiting extractability [56–58]. The disrupted biomass is dried to enhance its shelf life and prepare for extraction, which is the last step. Various methods have been described to achieve these different goals, and some even combine them. Their applicability on an industrial scale is often limited. E.g., chemical extraction approaches using methanol, ethanol, acetone, acetonitrile, hexane or hydrochloric acid may be suitable on a laboratory scale [58–61], but are restricted in human applications due to possible health risks, product degradation [61,62], and environmental issues. Physical and biological treatments using sonication, microwaves, autoclaving, ionic liquids, enzymatic treatment or germination [59,62–66] often lack efficiency, are difficult to upscale, or are too expensive. Simple mechanical disruption processes such as milling [38,53] or high-pressure homogenization (HPH) [67,68] are possible, but risk astaxanthin degradation. Additionally, HPH is quite expensive.

Combined disruption and extraction have been described with generally recognized as safe (GRAS) solvents [69,70], but the selectivity of these extraction processes is limited, compared with, e.g., supercritical CO<sub>2</sub> (SC-CO<sub>2</sub>) extraction. Drying techniques such as freeze-drying (FD), spray-drying (SD), and belt-drying have been applied for further dehydration of the biomass [53,71–73]. In all these processes, attention must be paid to product degradation [74], because astaxanthin is prone to oxidation [75]. This is especially important when working at higher temperatures. Final astaxanthin extraction can be achieved with various solvents. Reductions in the use of fossil-based solvents is an important environmental goal. It must also be considered that consumers demand increasing standards of sustainability, eco-friendliness and product safety. SC-CO<sub>2</sub> extraction enables the gentle, selective, and efficient recovery of astaxanthin from other, polar compounds and cell biomass while being non-toxic, aseptic, and environmentally friendly. Accordingly, many authors have proposed SC-CO<sub>2</sub> extraction for safe and environmentally friendly production of astaxanthin-containing oleoresins [54,55,76–86].

Of the named processes, bead milling (BM), SD, and SC-CO<sub>2</sub> extraction are commonly applied and discussed for the industrial and pilot-scale production of astaxanthin, as well as for economic assessments [50,52,53,73,87]. Many of those processes have been investigated individually concerning their efficiency and, most importantly, their astaxanthin recovery. Nevertheless, only a few studies have combined the various processes used in downstream processing. Therefore, this study combined different disruption and drying methods for *H. pluvialis* biomass in all possible combinations.

## 2. Materials and Methods

### 2.1. Chemicals and Reagents

Analytical-grade acetone, petroleum ether and hypergrade acetonitrile were obtained from Merck (Darmstadt, Germany). Ethanol and Tris(hydroxymethyl) aminomethane (TRIS) ( $\geq 99.9\%$ ) were provided by Carl Roth (Karlsruhe, Germany), and formic acid (99% ULC/MS) by Biosolve (Valkenswaard, The Netherlands). Cholesterol esterase from *Pseudomonas* sp. was purchased from MP Biomedicals (Eschwege, Germany). All-E-astaxanthin standard in its free form (SML0982,  $\geq 97\%$ , 3S,3'S, from *Blakslea trispora*) was



obtained from Sigma-Aldrich (Taufkirchen, Germany), and astaxanthin monopalmitate (1017, 3RS, 3'RS) was provided by CaroteNature (Münsingen, Switzerland).

## 2.2. *Haematococcus Pluvialis* Cultivation

*Haematococcus pluvialis* (proprietary strain of Sea & Sun Technology, Trappenkamp, Germany) was cultivated indoors in a glass tube system of 1500 L under artificial light conditions (LED tubes, 24 h) at  $23 \pm 1$  °C. The cells were cultivated in BG11 medium consisting of 17.6 mM NaNO<sub>3</sub>, 0.18 mM K<sub>2</sub>HPO<sub>4</sub> · 3 H<sub>2</sub>O, 0.3 mM MgSO<sub>4</sub> · 7 H<sub>2</sub>O, 0.25 mM CaCl<sub>2</sub> · 2 H<sub>2</sub>O, 0.031 mM citric acid, 0.023 mM ferric ammonium citrate, 0.003 mM Na<sub>2</sub>EDTA · 2H<sub>2</sub>O, 0.19 mM NaCO<sub>3</sub> and 1 mL/L trace metal solution made of 1.0 mM H<sub>3</sub>BO<sub>3</sub>, 1.0 mM MnSO<sub>4</sub> · H<sub>2</sub>O, 1.00 mM ZnSO<sub>4</sub> · 7 H<sub>2</sub>O, 0.01 mM (NH<sub>4</sub>)<sub>6</sub>Mo<sub>7</sub>O<sub>24</sub> · 4 H<sub>2</sub>O and 0.1 mM CuSO<sub>4</sub> · 5 H<sub>2</sub>O until nitrogen was completely depleted. Subsequently, the cells were transferred to a 3000 L glass tube system, operated in a greenhouse (Gönnebek, Germany), and exposed to direct sunlight to induce astaxanthin production. The cells were cultivated in the greenhouse until the astaxanthin content reached its highest level. The cells were harvested by centrifugation (Clara 80, Alfa Laval, Lund, Sweden). The harvested biomass had a final concentration of  $179.9 \pm 0.05$  g/L ( $n = 3$ ).

## 2.3. Downstream Processing—Laboratory Scale

### 2.3.1. Disruption of *H. pluvialis* Biomass

Two disruption methods, i.e., bead milling (BM) and high-pressure homogenization (HPH), were compared.

An agitator bead mill (Dyno-Mill KDL A, Willy A. Bachofen AG, Muttentz, Switzerland) was used for cell disruption by BM. The grinding chamber had a volume of 600 mL and was filled to 85% with grinding beads (0.8–1.0 mm diameter, 83% ZrO<sub>2</sub> and 17% CeO<sub>2</sub>). It was cooled by cold water flowing through a double jacket, resulting in a biomass temperature between 36 °C and 44 °C in the outlet. The separation gap width was 0.2 mm. The peripheral speed for the agitator discs (64 mm diameter) was 14 m/s. The throughput was between 10.5 L/h and 12.0 L/h, resulting in average dwell times between 1.4 and 1.7 min for one passage. All batches were milled three times, and samples were taken after each passage. The aliquots were homogenized after the experiment and stored at  $-21$  °C, prior to astaxanthin analysis and further processing.

For HPH, the biomass with a concentration of 180 g/L was diluted 1 to 4 with water and filtered. This was the highest concentration homogenizable with this device. The biomass was filtered through 50 µm polyamide gauze. Four aliquots of 500 to 600 mL were homogenized twice separately at approximately 80 MPa (EmulsiFlex-C3, Avestin, Mannheim, Germany). Samples were taken and measured before and after each disruption step. Cell disintegration and dry weight were determined directly after the experiments. The aliquots were homogenized after the experiment and stored at  $-21$  °C, prior to astaxanthin analysis or further processing.

### 2.3.2. Drying of *H. pluvialis* Biomass

Three drying techniques were compared: spray-drying (SD), freeze-drying (FD), and vacuum-drying (VD).

SD conditions were assessed by the design of experiments for optimal experimental parameters to dry 200 mL continuously agitated, non-disrupted *H. pluvialis* biomass (concentration 99.4 g/L) at the laboratory scale with a mini spray-dryer B-191 (Büchi, Essen, Germany) for maximization of the biomass and astaxanthin yield. Therefore, the amount of dried biomass in the collection container and its astaxanthin content were measured and used independently as dependent variables. Three independent variables were chosen and tested in ten different scenarios at distinct points: spray gas flow was applied at 400 and 500 NL/h, product flow rate at 5%, 10%, and 15%  $\pm$  2.7, 5.8, and 8.7 mL/min, respectively, and inlet temperature at 160 and 180 °C. In three further runs, the temperature was reduced to 140 and 120 °C, and spray gas flow was increased to 600 NL/h in one run. The experi-



ment using the parameters that were later considered optimal was repeated, resulting in 14 experiments. An overview of the different process conditions can be found in Table S1. Hot air volume flow was maintained constant at 25 m<sup>3</sup>/h throughout all experiments.

The obtained results were analyzed using JMP PRO software version 15.0.0. Data were regressed using standard least squares with different models, namely, linear ((Equation (1)) and quadratic (Equation (2)), as well as quadratic combined with interaction terms (response surface model) (Equation (3)).  $Y$  is the yield,  $a$  is the intercept,  $b_i$ ,  $c_i$ , and  $d_{ij}$  are model coefficients, and  $X_i$  and  $X_j$  represent the model regressors.

$$Y = a + \sum_{i=1}^3 b_i X_i \quad (1)$$

$$Y = a + \sum_{i=1}^3 b_i X_i + \sum_{i=1}^3 c_i X_i^2 \quad (2)$$

$$Y = a + \sum_{i=1}^3 b_i X_i + \sum_{i=1}^3 c_i X_i^2 + \sum_{i=1}^2 \sum_{j=i+1}^3 d_{ij} X_i X_j \quad (3)$$

The adjusted coefficients of determination were used to compare the three different models. The model with the highest adjusted coefficient of determination was then optimized numerically via a gradient descent algorithm on the yield. T-tests were applied to identify the statistical significance of the model parameters. The described approaches were carried out, regressing the biomass and astaxanthin contents. The results of both estimations were combined with approximate optimal parameters for astaxanthin recovery with regard to degradation and biomass yield. These parameters were verified by applying them to the drying process of the same biomass slurry in the same concentration and diluted to 50 g/L. Another *H. pluvialis* batch with a concentration of 200 g/L was used as a reference. These concentrations reflected those used in the following SD experiments. The spray nozzle temperature was regulated with an external circulation thermostat at 40 °C.

Using the optimal parameters obtained from the design of experiments, SD in the final experiment was performed using a mini spray-dryer B-191 (Büchi, Essen, Germany). Conditions were set to 180 °C inlet temperature, product flow of 5.8 mL/min, spray gas flow of 400 NL/h, and ventilation of 25 m<sup>3</sup>/h. The spray nozzle was tempered with an external circulation thermostat at 40 °C. Three aliquots of 200 mL of non-disrupted, milled, and high-pressure homogenized samples were used (179.9, 176.0, and 45.5 g/L, respectively). Biomass recoveries were determined in the different compartments of the spray-dryer, namely, the spray tower, the joint, the cyclone, and the collection vessel by weighing them before and after drying. Astaxanthin and dry mass content were determined in the *H. pluvialis* powder recovered from the collection vessel. This powder was also used for SC-CO<sub>2</sub> extraction.

FD was performed with multiple aliquots taken from each differently disrupted batch. Three aliquots of milled biomass were used with approximately 7.04 g biomass each, and six aliquots of the samples that were disintegrated by HPH, equaling approximately 1.82 g biomass each, were applied. For comparison, three 40 mL aliquots of concentrated and non-disrupted biomass, equaling approximately 7.20 g, were used. All were poured into aluminum bowls for FD. They had a filling height of approximately 0.8 cm and were frozen at −80 °C prior to FD (Alpha 1–4, Christ, Osterode, Germany) for 12 h at 37 Pa.

VD was performed in a vacuum chamber (Vacutherm, Heraeus instruments, Hanau, Germany). Sample preparation was accomplished in the same way as for FD. In the first step, the temperature in the vacuum chamber was set to 40 °C and approximately 5–15 kPa (main drying). In the second step, the temperature was increased to 50 °C, and the vacuum was reduced to approximately 3–8 kPa (secondary drying). The samples were dried until reaching constant weight. The six samples with the higher cell concentration were dried together over 24 h with 1:1 main and secondary drying. The high-pressure homogenized



samples were dried in duplets due to their higher water content over 12 h with 1:1 main and secondary drying.

### 2.3.3. Supercritical CO<sub>2</sub> Extraction of Astaxanthin

Subsequently,  $125 \pm 2$  mg dried *H. pluvialis* powder of the previous experiments were homogenized with approximately  $1.1 \pm 0.2$  g glass beads and filled in a 5 mL extraction vessel. A plain layer of beads was placed on the exit of the cartridge. On top of that layer, more beads and the weighed biomass were placed alternately and gently stirred. SC-CO<sub>2</sub> extraction was performed with an MV-10 ASFE system (Waters, Milford, MA, USA) at 35 MPa and 6.0 mL/min CO<sub>2</sub> flow for 30 min with 1.5 mL/min ethanol as a co-solvent and an additional 0.5 mL/min ethanol as make-up solvent after depressurization at 50 °C.

Afterwards, drying and depressurization of the sample were performed in three steps, each taking two minutes: First, the co- and make-up solvent flow were reduced to zero and the pressure to 20 MPa. Second, CO<sub>2</sub> flow was reduced to 5 mL/min, and the pressure was reduced to 15 MPa. Third, CO<sub>2</sub> flow was reduced to 2 mL/min, and pressure was reduced to 10 MPa. Extract volume was determined by weighing, assuming a density of 0.79 kg/L, and verified by volumetric measurements. Aliquots were transferred for astaxanthin quantification. The residual extract was dried in a rotary evaporator at 40 °C and 17.8 kPa. The extract was resuspended in acetone and transferred into a weighed amber vial. Acetone was evaporated at 40 °C under a gentle stream of nitrogen, and the weight of dried extract was determined. Recoveries of astaxanthin in SC-CO<sub>2</sub> extracts were calculated by comparing them to the astaxanthin content of the applied biomass before extraction.

### 2.4. Downstream Processing—Pilot Scale

Another batch of biomass was used exclusively in these experiments. This was disrupted similarly as described for the laboratory scale, using the same agitator bead mill with the same specifications as used before. The biomass was concentrated to a density of 15–18% *w/v*. The biomass throughput was set to 10 L/h, and three passages of the whole biomass were performed. The disrupted biomass was recovered in a light-protected stainless-steel vessel. The milled biomass was dried in a spray-dryer (Anhydro MS150, SPX FLOW, Charlotte, NC, USA) at 180 °C and a feed flow rate of 5 L/h. The biomass slurry was stirred to prevent agglomerations and clogging of the spray nozzle. The nozzle pressure was set to 0.3 MPa, and the outlet temperature was set to 90 °C. The resulting powder was collected in a stainless-steel pot at the end of the cyclone. The powder was vacuum-sealed and stored at −21 °C in the dark.

### 2.5. Disintegration Rate

The cell disintegration rate was determined visually by microscopic methods. Intact cells were counted at least in triplets before and after disruption in a Neubauer improved (BM samples) and a Fuchs–Rosenthal (HPH samples) cell counting chamber and were related to each other.

### 2.6. Dry Weight

Dry weight of the wet samples was determined after washing the samples with distilled water and drying them in a moisture analyzer MA 50/1.X2.A (Radwag, Hilden, Germany) at 140 °C until reaching constant weight (method adapted as per the manufacturer's recommendation). Dry weight after FD and VD was determined by measuring the respective sample weight and calculating the dry weight with the help of the dry weight content of the wet biomass. Dry weight after SD was measured with 0.5 to 1.0 g sample in a moisture analyzer (MA 50/1.X2.A, Radwag, Hilden, Germany) at 140 °C until reaching constant weight. Residual moisture of all dried samples was smaller than 9%, and thus considered negligible.



## 2.7. Astaxanthin Analysis

Astaxanthin analysis was performed after each process step, according to Koopmann et al. [88], with adaptations to the differently processed biomasses as follows: wet biomass with known concentrations was weighed into lysis tubes type C (Analytik Jena, Jena, Germany) with less than 300  $\mu\text{L}$  and final amounts of 0.3–2.0 mg *H. pluvialis* dry mass. Dry biomass was adjusted when dried by SD or FD. Biomass dehydrated by VD was treated equally, but it was weighed into type G bead tubes (Macherey Nagel, Düren, Germany). All samples were filled up to 500  $\mu\text{L}$  with acetone, and cells were disrupted for 3 min in a swing mill (MM 2000, Retsch, Haan, Germany) at 27 Hz. Subsequently, centrifugation at  $10,000 \times g$  and separation of carotenoid containing acetone from the residual biomass were performed. Extraction with 500  $\mu\text{L}$  fresh acetone, disruption, and separation were repeated twice until the residual biomass and the acetone were colorless.

For de-esterification, the combined supernatant was filled up to 3 mL with acetone. Ethanolic SC-CO<sub>2</sub> extracts were directly added to the reaction mixture in volumes of 100 to 1000  $\mu\text{L}$  and filled up with acetone to 3 mL. Then, 2 mL of 50 mM TRIS buffer (pH 7 at 21 °C) and 600  $\mu\text{L}$  cholesterol esterase solution with a concentration of 3.3 U/mL suspended in the same buffer were added. The tubes were incubated at 37 °C in a water bath and mixed gently every 10 min. Astaxanthin was recovered by liquid–liquid extraction with 2 mL of petroleum ether. The mixture was shaken vigorously for 10 s to ameliorate astaxanthin transfer into the petroleum ether. Subsequent phase separation was enhanced by centrifugation at  $3,000 \times g$  for 1 min. The upper, astaxanthin-containing layer was filtered through a 0.45  $\mu\text{m}$  PTFE filter, and either measured directly or stored for one night at  $-21$  °C prior to analysis.

Extracts were vortexed and ultrasonicated for 20–30 s before analysis if stored overnight previously. Qualification and quantification of astaxanthin were performed by ultra-high-performance liquid chromatography (UHPLC). This was performed on an ACQUITY Arc system (Waters, Milford, MA, USA) coupled with a UV/Vis detector (2998 PDA Detector, Waters, Milford, MA, USA) and a mass spectrometer (Acquity QDa Detector, Waters, Milford, MA, USA), using a C18-column (Cortecs C18 2.7  $\mu\text{m}$ , 90 Å,  $3.0 \times 100$  mm, Waters, Milford, MA, USA) operated at 40 °C. The injection volume was 5  $\mu\text{L}$ . A gradient of H<sub>2</sub>O (A) and acetonitrile (B) was applied (0 min 70% A, 4 min 10% A, 9 min 0% A, 11.5 min 70% A until 15 min) with 0.1% formic acid added to both solvents. Flow velocity was 0.5 mL/min. Optical spectra were measured in a range of 200 to 800 nm, and astaxanthin data were analyzed and quantified at 474 nm. The mass spectrometer with electrospray ionization was operated in positive mode with a cone voltage of 15 V and a probe temperature of 600 °C, measuring in a range of 150 to 1250  $m/z$ . For further accuracy, the mass of astaxanthin was observed by selected ion recording at 598  $m/z$   $[\text{M} + \text{H}]^+$ . The volume dilatation of the petroleum ether phase after liquid–liquid extraction was considered to quantify astaxanthin, de-esterified in the presence or absence of ethanol.

For identification and quantification, 0.5 to 54.8  $\mu\text{g}$  free all-*E*-astaxanthin, and 1.0 to 62.6  $\mu\text{g}$  astaxanthin monopalmitate were processed like in de-esterification, and astaxanthin was quantified with UHPLC-PDA. However, in the case of the free all-*E*-astaxanthin standard, the cholesterol esterase solution was replaced with the same amount of TRIS buffer. A proportion of 69.4% *w/w* astaxanthin was assumed for the quantification of ester-derived, free astaxanthin. Peaks with a corresponding UV/Vis absorption spectrum [89–93] accompanied by peaks with the mass of astaxanthin in SIR were assigned to the *Z*-isomers 9*Z*- and 13*Z*-astaxanthin and several di-*Z*-isomers. The latter are difficult to differentiate without further validation; therefore, they were summed and consecutively termed di-*Z*-isomers. Quantities of all diastereomers were estimated using the quantification of all-*E*-astaxanthin, corrected by factors adjusting the different extinction coefficients published by Bjerkeng et al. [94], namely, 1.20 for 9*Z*-astaxanthin, 1.56 for 13*Z*-astaxanthin, and 1.11 for the di-*Z*-isomers.



Linear regression of the calibration data was performed by the ordinary least squares method, and the significance of the deviation of the y-intercepts from zero was evaluated by *t*-tests [88]. Tests on significant deviations were calculated using mean difference tests with a level of significance of  $\sigma = 0.05$ .

### 2.8. Evaluation of Significance

All disruption processes and SD were performed at least in triplicates using identical biomass batches. FD and VD were performed once to multiple times with triplets to sextets of the samples in separated containers. SC-CO<sub>2</sub> extraction was performed once with all differently processed and dried samples. Astaxanthin analysis of each individual sample was performed in triplicates after each process step. Tests on significant deviations were calculated by mean difference tests with a level of significance of  $\sigma = 0.05$ .

### 2.9. Effort Estimation

An effort estimation was performed to assess the technical and economic feasibility of cell disruption and drying of *Haematococcus pluvialis* biomass. Therefore, the following aspects were evaluated: biomass and astaxanthin recovery rate, cell disruption efficiency (for BM and HPH), residual moisture (for SD and FD), acquisition costs, workload, usability of the equipment, power consumption, hygienic aspects, throughput, sample pre-treatment and scalability. The disruption efficiency refers to comparable disruption grades of algal cells, i.e., after three and one passages in the bead mill and high-pressure homogenizer, respectively. The acquisition costs refer to the costs incurred when purchasing the equipment. The workload includes the time needed for assembly and disassembly, pretreatment/processing of the biomass, as well as cleaning and sanitization steps after usage. Technical data (power, hygienic data, etc.) were obtained from the manufacturer's data sheets, assuming to use the same devices as those used in the experiments of this study. SD was calculated only based on the pilot-scale spray dryer (Anhydro MS150, SPX FLOW, Charlotte, NC, USA). Only for FD, a scaled device was used for calculation of the technical data (DW-50ND, Drawell Scientific Instrument, Chongqing, China). Usability was evaluated based on the assessment of the complexity of setting up, dismantling, and sanitizing the machines, the simplicity of operation, and what prerequisites, in terms of the level of training of the staff, must be met in order to competently operate the machines. Some process parameters were defined for comparability of the processes: the dry weight of the harvested biomass was defined to be 150 g/L and the working volume was 50 L.

## 3. Results and Discussion

Astaxanthin extraction from *H. pluvialis* requires disruption and drying as preparation for SC-CO<sub>2</sub> extraction. To evaluate the efficiency of each step regarding the final astaxanthin yield, different disruption and drying methods were compared. Various combinations of the procedures followed by SC-CO<sub>2</sub> extraction were assessed to optimize the overall astaxanthin recovery (Figure 1). For all experiments, one initial batch of *H. pluvialis* biomass was used. After each process step, astaxanthin concentration and process parameters such as the disruption rate or residual moisture were determined. Precise astaxanthin concentrations and diastereomer distribution data are given in Table S2. All process steps were evaluated economically. This study aimed to find the optimal combination of process steps for maximum astaxanthin yields at minimal costs.



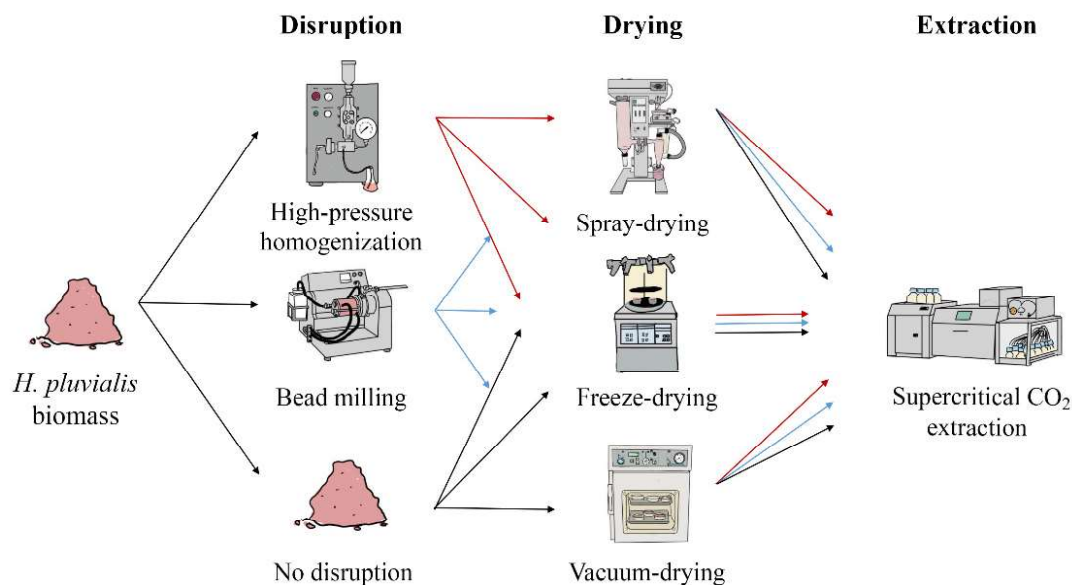


**Figure 1.** Process steps for the optimization of astaxanthin recovery in the downstream process of *H. pluvialis*.

### 3.1. Disruption of *H. pluvialis* Biomass

The hypothesis of facilitated astaxanthin extraction by cell disruption was tested by starting the downstream processing with high-pressure homogenization (HPH) or bead milling (BM).

#### 3.1.1. High-Pressure Homogenization

The disruption efficiency of HPH was  $81.1 \pm 3.7\%$  ( $n = 4$ ) after the first and  $92.4 \pm 1.6\%$  ( $n = 4$ ) after the second passage at circa 80 MPa. Slightly lower disruption rates of *H. pluvialis* by HPH were observed by Praveenkumar et al. at 68.9 MPa. They showed the decreases in intact cells to be 45%, 20%, and 11% after one, two, and three passages, respectively. However, increases in pressure to 137.9 and 206.8 MPa did not result in higher disintegration rates [67]. Chen et al. observed disruption rates of over 90% at 70 MPa at *H. pluvialis* concentrations of 3% to 5% and one to three HPH passages [68]. A correlation of HPH disruption efficiency with increasing pressure has also been shown for various other microalgae [95], whereas no effect of varying pressure on the disruption rate has been observed in *Nannochloropsis* sp. between 30 and 150 MPa [96]. Higher disruption efficiency with decreasing biomass concentration has been observed for microalgae and *Escherichia coli* cells [97,98]. Kleinig et al. suggested, among other things, the lower viscosity to be the actual cause [97]. Direct comparison of the disruption rate of different *H. pluvialis* batches even at similar conditions may result in significant variances due to differently rigid cell walls. Moreover, the cells in these experiments were frozen prior to HPH, which might have destabilized cell wall integrity.

Homogenization generates heat. In these experiments, the temperature rose from 21 °C to 39.3 °C ( $n = 2$ ) in the first and from  $26.7 \pm 1.53$  °C ( $n = 4$ ) to  $36.8 \pm 3.6$  °C ( $n = 4$ ) in the second pass. This reflects increases of 2.3 °C and 1.3 °C per 10 MPa after the first and second pass, respectively. Increases of 2.2 °C and 2.5 °C per 10 MPa have been reported in other studies as well [99,100]. Heating of the cell suspension might influence astaxanthin stability. At elevated temperatures, carotenoids oxidize and degrade [71,101,102] and



isomerize in solvents [89,103–107] but also without [108]. The temperature may locally be well above the mentioned increase, because it emerges by the dissipation of mechanical energy into heat when the suspension collides with the impact ring [109]. Nevertheless, only short exposure to these conditions did not result in astaxanthin deterioration. Total astaxanthin content was  $2.73 \pm 0.15\%$  w/w ( $n = 6$ ) before and  $2.67 \pm 0.14\%$  w/w ( $n = 12$ ) after two passages of HPH. Before the disruption, astaxanthin was composed of 84.9% all-*E*-astaxanthin, 4.2% 9*Z*-astaxanthin, and 3.61% 13*Z*-astaxanthin, and the di-*Z*-isomers had a proportion of 7.3% (Figure 2). Standard deviations for the single isomers and the number of replicates are provided in Table S2. HPH did not significantly influence the abundance of the geometric isomers. Neither significant astaxanthin degradation nor isomerization were observed compared with the unprocessed biomass; therefore, HPH can be generally assumed as a gentle disruption method. An essential factor might be the very short exposure to unfavorable conditions, which does not significantly harm astaxanthin.

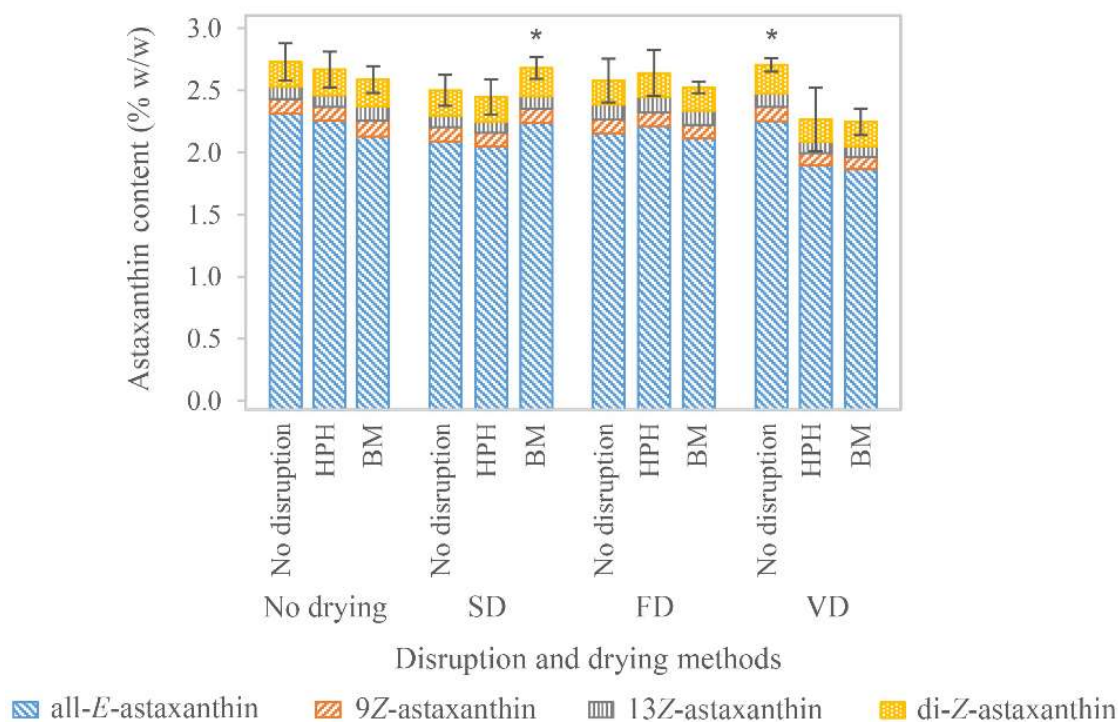


**Figure 2.** Astaxanthin content in *H. pluvialis* biomass after various disruption and drying processes. Standard deviation is indicated for total astaxanthin. Stars indicate significant differences ( $p < 0.05$ ) from samples dried with the same process. Further significant differences are provided in Table S2.

Due to device specifications, the biomass had been diluted prior to HPH. Thus, the subsequent drying processes of high-pressure homogenized cells were performed with the diluted biomass. This dilution step is not desirable on industrial-scale processing because it requires repeated dehydration of the biomass, which is cost- and energy-intensive. It could be prevented on a larger scale, e.g., by high-pressure homogenizers that can cope with higher concentrated biomasses.



### 3.1.2. Bead Milling

BM of biomass resulted in cell disruption of  $32.4 \pm 13.3\%$  ( $n = 3$ ),  $60.2 \pm 20.3\%$  ( $n = 3$ ), and  $78.5 \pm 11.3\%$  ( $n = 3$ ) after the first, second, and third passage, respectively. Disruption after three cycles of BM was not significantly different from one and two passes of HPH. Cell disruption requires a certain amount of energy. This is often referred to as stress intensity when the specific energy of an individual stress event is considered [110,111]. In agitator bead mills, this energy transfer depends on the applied beads (size and material), their filling level, speed of the agitator discs, the mill geometry, and the viscosity of the sample [112–116]. The throughput and the number of passages influence the dwell time of the product. In turn, the dwell time impacts the duration that a cell is exposed to milling conditions and how often a cell is exposed to a stress event (stress number). Together, stress intensity and number have a major influence on the disintegration rate [111]. Some of the mentioned factors, such as the flow rate, may have contrasting effects on the disruption efficiency, however [117], and should not be oversimplified. In this study, most factors were constant due to a fixed setup. The disruption degree was significantly enhanced by multiple passages, confirming the mentioned influence of the stress number [112,113,116,118,119].

Comparisons with the disruption degree of other milled algae [112–114,116–118] are complicated due to the variety of influence factors. In addition to those already mentioned, cell characteristics influence their stability [120,121] and play an important role in disintegration [112,116,117]. Nevertheless, 78.5% disrupted cells are a good first approach, considering the rigid cell wall of *H. pluvialis* [57].

The deviation in the disruption rates within the repetitions indicates inhomogeneities, with varying mixing degrees. Consistent disintegration might be improved by using less concentrated algae slurries, because more highly concentrated algae slurries often exhibit higher viscosity and are accompanied by higher energy requirements for pumping [122] and difficulties in mixing [114].

The temperature of the algae paste increased up to 40, 42, and 44 °C after the first, second, and third run, respectively. Cooling of the slurry was performed during the passages, in order to prevent a higher temperature rise. Nevertheless, the increasing viscosity of the paste resulted in slightly elevated temperatures. Generally, the temperature increases throughout the process can be explained by dissipative mechanic energy. It depends on flow rate [115], agitation speed [112], bead filling and size, as well as sample concentration. Temperature is one possibly detrimental factor for astaxanthin stability. However, as long as the average dwell time, and thus, exposure, to higher temperatures is short, the milling process does not necessarily influence astaxanthin negatively, as it can also be concluded from the obtained results. Total astaxanthin content was  $2.73 \pm 0.15\%$   $w/w$  ( $n = 6$ ) before and  $2.59 \pm 0.11\%$   $w/w$  ( $n = 8$ ) after three passages of milling (Figure 2); however, it was not significantly different. All-*E*-astaxanthin decreased significantly by about 8.1%, whereas 13*Z*-astaxanthin increased by 17.5%. The absolute proportion of the remaining diastereomers did not change significantly. BM has been assessed as a mild process step for recovering proteins, especially when maintaining their proper function is intended [116,118,123]. Therefore, it should not negatively affect pigments such as carotenoids.

### 3.2. Drying of *H. pluvialis* Biomass

Further dehydration of the biomass is necessary for SC-CO<sub>2</sub> extraction. Drying biomass is a critical process step as it is often energy-intensive and a potential harm for astaxanthin, because the biomass is already disrupted. The exposure to oxygen is enhanced by high surface areas necessary for evaporation. The latter is also promoted by high temperatures, which supports astaxanthin degradation. Three drying processes were compared regarding their influence on astaxanthin content: 1. Freeze-drying (FD): A method using low temperatures and a protective atmosphere. 2. Vacuum-drying (VD): A similar method operating at slightly elevated temperature and reduced oxygen atmosphere. 3. Spray-drying (SD): A frequently used alternative that utilizes high temperatures and air



throughput to dry the biomass. The influence of the previous disruption on the subsequent drying step was investigated for all methods.

### 3.2.1. Freeze-Drying

FD is widely used to solidify fragile pharmaceutical agents [124] because it is generally considered a mild drying process that maintains the activity of processed substances. FD of *H. pluvialis* resulted in total astaxanthin recoveries of 94.5%, 97.6%, and 98.8% in non-disrupted biomass and samples disrupted by BM and HPH, respectively. However, none of the deviations were considered significant (Figure 2). FD has already been used for algae biomass rich in carotenoids. In *Chlorella vulgaris*, FD was reported superior to hot-air-drying for carotenoid recovery. Nevertheless, only about 43% carotenoid recovery was obtained [125]. FD of *Phaeodactylum tricornutum* did not result in significant carotenoid losses [126]. In fruits and vegetables, recoveries of lycopene (11% to 48%),  $\beta$ -carotene (27% and 56%), and lutein (34%) were described after FD [127–129], indicating different vulnerabilities of various carotenoids to FD and possibly also surrounding conditions. Zhao et al. observed significantly higher astaxanthin recoveries in freeze-dried *H. pluvialis* extracts than vacuum or otherwise dried samples [130]. Overall, the extensive exclusion of oxygen and low drying temperatures possibly provide protective conditions for astaxanthin. Regarding the diastereomers, some minor differences were observed. All-*E*-astaxanthin decreased 6.9% in the non-disrupted lyophilized samples; however, its proportion to the other isomers was unaffected. Similar results were achieved by Cong et al., who lyophilized astaxanthin-rich krill and reported about a 10% loss of all-*E*-astaxanthin [131]. They also observed a simultaneous decrease in 9*Z*- and 13*Z*-astaxanthin, although their losses were only 6.6% and 3.6%, respectively [131]. In the lyophilized samples of this experiment, a significant decrease in 9*Z*-astaxanthin and also the di-*Z*-isomers was observed in the previously milled samples. In contrast, in non-disrupted and high-pressure homogenized samples, 13*Z*-astaxanthin increased up to 35%, whereas in the former, only its relative proportion changed significantly. This can be attributed to isomerization reactions during the drying process. Although isomerization has been reported to increase at higher temperatures [89,103–108], minor changes at lower temperatures are still possible. The texture of all samples was a cake with large pores, which was loose, fluffy, and easy to disintegrate, as it is typical for freeze-dried samples.

### 3.2.2. Spray-Drying

SD of *H. pluvialis* is a widely applied drying method [53,73]. However, the combination of high temperatures and oxygen exposure, which is enhanced by the surface enlargement during the spray process, increases its potential for astaxanthin degradation. SD also exhibits a variety of setting options. Design of experiment and model estimation and selection were performed to find optimal conditions for drying the specific target. The influence of the obtained parameters was tested for significant influences on yield and astaxanthin degradation. Spray gas pressure, product flow, and inlet temperature were varied at constant biomass concentration and airflow. The amount of the obtained biomass in the collection vessel and its astaxanthin content were measured. The highest biomass amount of 4.93 g, corresponding to 25.1% recovery of the total biomass of the sample, was obtained at a spray gas flow of 400 NL/h, 10% feed rate, and 180 °C. The lowest biomass amount of 0.18 g, corresponding to 0.90% recovery, was obtained at a spray gas flow of 600 NL/h, 10% feed rate, and 180 °C (Table S1). Three different models were estimated to find the best description and optimize the SD conditions. When the parameters were fitted regarding biomass yield, the quadratic model, including the interaction terms, described the results best when comparing the adjusted coefficients of determination (Table 1).



**Table 1.** Estimated model coefficients, *p*-values, and optimized parameters regarding maximal biomass yield. Significant *p*-values ( $\sigma = 0.05$ ) are highlighted in bold.

	Linear Model		Quadratic Model		Quadratic Model + Interactions	
	Coefficient	<i>p</i> -Value	Coefficient	<i>p</i> -Value	Coefficient	<i>p</i> -Value
A (Intercept)	7.175		27.5392		−23.6551	
b <sub>1</sub> (S <sup>a</sup> )	−0.0178	<b>0.0006</b>	−0.0848	0.212	−0.0349	0.48853
b <sub>2</sub> (F <sup>b</sup> )	0.0294	0.2422	−0.0326	0.9482	−6.4457	<b>0.01817</b>
b <sub>3</sub> (T <sup>c</sup> )	0.0196	0.7315	−0.0295	0.9082	0.7736	0.07361
c <sub>1</sub> (S <sup>2</sup> )			0.0001	0.3117	0.0001	0.06927
c <sub>2</sub> (F <sup>2</sup> )			0.0031	0.8963	−0.0661	<b>0.04148</b>
c <sub>3</sub> (T <sup>2</sup> )			0.0001	0.859	−0.002	0.08029
d <sub>12</sub> (S*F)					0.0044	<b>0.02337</b>
d <sub>13</sub> (S*T)					−0.0008	<b>0.04314</b>
d <sub>23</sub> (F*T)					0.0337	<b>0.02003</b>
R <sup>2</sup>	0.7739		0.8085		0.9612	
R <sup>2</sup> adjusted	0.7061		0.6444		0.8739	
Optimized parameters						
F	15		15		10.4	
S	400		400		400	
T	180		180		180	

<sup>a</sup> S, spray gas flow (NL/h); <sup>b</sup> F, product feed rate (%); <sup>c</sup> T, inlet temperature (°C).

The model does not allow accurate assessment of the single parameters, but it shows the importance of the interaction terms ( $p < 0.05$ ). Interactions between the different settings in SD have been assumed [132–134]. This is plausible because a higher feed rate reduces temperature as more water evaporates. A higher feed rate also influences the spray behavior, and the difference in droplet size probably also influences the temperature. Consequently, the quadratic model, including the interaction terms, was chosen to describe SD behavior best regarding biomass yield. Generally, the highest temperature (180 °C) was assessed to be optimal in terms of yield in all models. Such positive effects were also observed in the SD of other products [132,135] and differently concentrated microalgae samples. In the latter, the highest yields were reported at 220 °C compared with 170 °C and 120 °C [136]. Higher drying temperatures result in faster evaporation and likely less biomass sticking to the walls of the device and thus higher proportions reaching the collection vessel.

Lower spray gas flows have been considered to improve product yields in SD by increasing particle size and facilitating capturing by centrifugal forces in the cyclone [133]. A similar correlation was confirmed here, as the lowest volume flow was considered optimal in all models, even though a significant influence of this parameter could only be observed in the linear model.

A higher product feed rate has been described to result in smaller yields; however, at lower temperatures than used in these experiments [134]. A higher feed rate will eventually result in lower yields when the drying capacity of the spray-dryer is overloaded. The feed rate range in these experiments was limited. Thus, this tendency is not reflected by the models. Again, the data from the quadratic model, including the interaction terms, were considered most reliable. Thus, a medium feed rate of 10.4%, 5.8 mL/min, was assumed optimal.

Astaxanthin content decreased only slightly after drying in most samples (Table S2). Before drying, total astaxanthin amount of the biomass was  $1.32 \pm 0.03\%$  *w/w* ( $n = 3$ ). After drying, the highest total astaxanthin contents of 1.22% *w/w*, obtained at a spray flow of 400 NL/h, 10 to 15% feed rate, and 160 to 180 °C, were not very different from the astaxanthin content before drying. The lowest astaxanthin content of  $0.91 \pm 0.03\%$  *w/w* ( $n = 3$ ) was obtained at a spray flow of 600 NL/h, 10% feed rate, and 180 °C. However, most of the astaxanthin proportions did not differ from each other, impeding proper model



evaluation (Table S3). These findings indicate an almost negligible influence of many SD conditions on astaxanthin content. No effect on isomer composition was observed and is in agreement with Leach et al., who investigated  $\beta$ -carotene in microencapsulated and spray-dried *Dunaliella salina* [137].

SD at the previously considered optimal parameters (10% feed rate, 400 NL/h spray flow, 180 °C inlet temperature) resulted in  $1.14 \pm 0.07\%$   $w/w$  ( $n = 3$ ) total astaxanthin. This was only slightly different from the maximum result. Therefore, the parameters optimizing the biomass yield were considered best for the subsequent experiments. They were applied once more to evaluate the influence of water content in the sample by drying 200 mL of the same biomass diluted to 5%  $w/v$  dry mass and 200 mL of another batch of biomass at 20%  $w/v$  dry mass. Results were 2.58 g and 6.13 g biomass in the collection vessel, corresponding to 24.6% and 15.2% recovery. It might be concluded that higher dry matter content negatively influences the yield in SD. However, a converse correlation was observed by the manufacturer of the spray-dryer, who reported higher yields in dried microalgae samples with a concentration of 17%  $w/w$  than 9%  $w/w$  and assumed the bigger particles beneficial in separation [136]. Bigger droplets do not dry as fast as smaller ones, and might also be more likely to stick to the walls of the device instead of being transported into the collection container, which could be the reason for the lower yield in these experiments. Nevertheless, a recovery of 15.2% was acceptable for the planned experiments and meant a sufficient absolute biomass quantity for subsequent downstream processing. Further optimization was not performed. However, on an industrial scale, the biomass recovery after drying is crucial and has to be enhanced.

Using the optimal parameters obtained from the design of experiments, spray-drying with the same biomass as used in the other drying experiments was performed. Total astaxanthin recovered after SD decreased to 91.6% and 91.7% in non-disrupted biomass and samples disrupted by HPH, respectively. This loss was mainly attributed to a decrease in all-*E*-astaxanthin. The losses observed after SD were higher than after FD. Ahmed et al. described an even more pronounced effect of 29% less astaxanthin in spray-dried than in freeze-dried *H. pluvialis* samples immediately after drying [71]. Other studies showed a significant decrease in carotenoids in spray-dried *Phaeodactylum tricornutum* [126] and *Rhodotorula glutinis* [138]. Total astaxanthin content in the milled biomass stayed constant after SD at the laboratory scale as well as the pilot scale. In the latter, total astaxanthin content in non-disrupted samples was 2.15%  $w/w$  and decreased to 2.01%, 2.00%, and 1.88%  $w/w$  in samples milled one, two, and three times, respectively. Spray-dried samples exhibited 1.85%  $w/w$  total astaxanthin, which was insignificantly different from all milled samples but significantly lower than in the non-disrupted biomass. All diastereomers were unaffected by SD at the pilot scale, whereas at the laboratory scale, a decrease in 9Z- and 13Z-astaxanthin was accompanied by an increase in all-*E*-astaxanthin, indicating isomerization reactions. No obvious isomerization has been reported in  $\beta$ -carotene during SD [137]. Generally, the deteriorating effect of exposure to 180 °C at the inlet was not as severe as expected. This was confirmed by other studies, which even observed higher astaxanthin recovery with increasing SD temperatures [72,102]. However, the reverse correlation was reported for  $\beta$ -carotene from *Dunaliella salina*. Here, an increase to 265 °C in inlet and 120 °C in outlet temperature during SD caused a reduced recovery of  $\beta$ -carotene, which was only diminished by a lower feed concentration or microencapsulation [137]. Such effects of feed concentration were not observed in these experiments. Overall, the rapid drying process and product cooling by evaporation reduced carotenoid oxidation and degradation, as also assumed by Leach et al. [137]. Thus, SD is not as devastating as expected regarding the astaxanthin content and remains an option for the downstream processing of *H. pluvialis*.

Spray-dried biomass mostly had a powdery texture. In previously high-pressure homogenized samples, smaller spheres of 1 to 4 mm in diameter were formed. They had a loose coherence and easily disintegrated. They were also observed in two milled samples to a smaller extent. Biomass recovery throughout the spray-dryer was similar for



non-disrupted and milled biomass. The biomass recovered in the collection vessel was not significantly different in all experiments. It was  $20.63 \pm 0.49\%$  ( $n = 3$ ),  $21.49 \pm 6.28\%$  ( $n = 3$ ) and  $25.42 \pm 3.24\%$  ( $n = 3$ ) for non-disrupted, high-pressure homogenized and milled samples, respectively. However, drying of high-pressure homogenized samples resulted in a heavier loaded cyclone and a less loaded spray tower compared with milled and non-disrupted biomass. The loading for non-disrupted and milled samples was highly similar; thus, the disruption and accompanying changes in viscosity seemed not to influence the drying and adhesion behavior in the device. More likely, the dilution of the biomass affects it, because this was the only significantly different parameter. For optimal total astaxanthin recovery, biomass yield is equally important. In FD and VD, biomass losses to the walls of the vessels are negligible. However, the surface to which biomass can stick is much larger in SD, and although biomass can be scraped off after drying, greater biomass and astaxanthin losses are very likely; material that is stuck to the wall of the spray tower is exposed to higher temperatures over a longer time, and astaxanthin is more likely to degrade here. These issues have to be addressed in the optimization of SD processes, as well as in economic evaluations. The use of modifiers or (micro)encapsulation with various wall materials has been reported to affect carotenoid losses, yields, and antioxidant activity during drying and/or subsequent storage beneficially [68,139,140].

### 3.2.3. Vacuum-Drying

VD has been reported to affect plant and algae bioactive compounds less detrimentally than drying with heat steps [141,142]. The texture of the dried biomass was very dense. It was a rigid and even rubbery cake that was hardly disintegrable. Total astaxanthin recovery after VD was 86.8% and 84.9% in samples disrupted by BM and HPH, respectively. Astaxanthin in non-disrupted biomass was not significantly affected by VD. The extensive exclusion of oxygen and only slightly elevated temperatures were intended to reduce the oxidation of astaxanthin during VD. However, this only applied to the non-disrupted samples. Again, the intact, rigid cell wall of *H. pluvialis* probably protects astaxanthin from environmental influences, resulting in lower degradation.

The diastereomers were generally more affected in the disrupted samples. In milled biomass, the proportion of 9Z- and 13Z-astaxanthin decreased, whereas in high-pressure homogenized samples, the proportion of 13Z-astaxanthin increased significantly. In non-disrupted biomass, the proportional decrease in all-E-astaxanthin was accompanied by an increase in the di-Z-isomers.

Comparing all the different drying processes, higher total astaxanthin recovery was observed in non-disrupted and vacuum-dried samples than in non-disrupted and freeze- or spray-dried samples. This may be because of the more compact sample during VD, reducing the surface area and thus possible reactions of astaxanthin with residual environmental oxygen. However, disrupted biomass yielded the lowest recoveries in VD. Here, the longer and direct exposure of astaxanthin to the drying conditions might cause enhanced degradation. Overall, the best results were obtained from milled and spray-dried biomass, whereas milled or high-pressure homogenized freeze-dried biomass was equally promising. These findings indicate that BM and HPH are suitable disintegration methods, and SD and FD are both appropriate for drying disrupted *H. pluvialis* biomass without severe astaxanthin losses. Astaxanthin recoveries obtained after the different combinations of disruption and drying methods are shown in Figure 2.

### 3.3. Supercritical CO<sub>2</sub> Extraction of Astaxanthin

Astaxanthin was still bound to the disrupted biomass of *H. pluvialis* after the drying processes. SC-CO<sub>2</sub> extraction was performed to separate and concentrate astaxanthin. Total astaxanthin recovery was lowest in the SC-CO<sub>2</sub> extracts of non-disrupted *H. pluvialis* biomass. Here,  $10.40 \pm 0.23\%$  ( $n = 3$ ),  $14.72 \pm 0.37\%$  ( $n = 3$ ), and  $14.32 \pm 0.28\%$  ( $n = 3$ ) of total astaxanthin were extracted from spray-dried, lyophilized, and vacuum-dried biomass, respectively. An overview of all recoveries is shown in Figure 3. Standard deviations of



samples were evaluated for triplets or quartets. Diastereomer composition can be found in Table S2. The low recovery can be explained by the poor extractability of intact *H. pluvialis* cells. Generally, mass transfer in SC-CO<sub>2</sub> extraction of plant material is improved when the transport resistance across cell walls and/or membranes is reduced [143]. Here, SC-CO<sub>2</sub> could hardly penetrate the rigid cell wall, and solution and transfer of astaxanthin were impeded. This suggests that cell disruption is a key component in the downstream processing of *H. pluvialis*. Comparing only these non-disrupted samples, extractability from vacuum-dried and lyophilized biomass was similar, whereas it was significantly lower from spray-dried biomass. This might be because of the vacuum damaging some of the cells and thus facilitating extractability slightly.

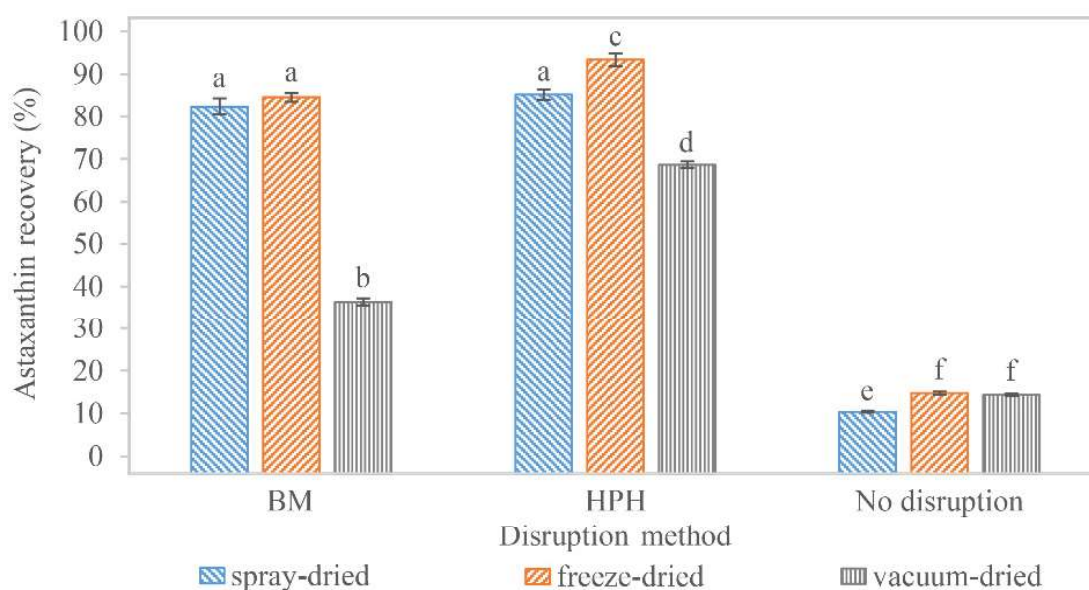


**Figure 3.** Astaxanthin recovery in supercritical fluid extracts of differently disrupted and dried *H. pluvialis* biomass. Significant differences ( $p < 0.05$ ) of the samples are indicated by different letters.

Extracts of milled samples that were spray-dried, lyophilized and vacuum-dried reached recoveries of  $82.41 \pm 1.96\%$  ( $n = 3$ ),  $84.61 \pm 1.03\%$  ( $n = 3$ ), and  $36.45 \pm 0.84\%$  ( $n = 3$ ) total astaxanthin, respectively, as compared with their counterparts prior to extraction. No significant difference in extractability was observed in samples that had been lyophilized or spray-dried. The significantly lower extractability of vacuum-dried samples was possibly caused by the texture of the biomass. Different models describe mass transfer in SC-CO<sub>2</sub> extraction. Very simplified, molecules at the solid to supercritical fluid interface are extracted first. If these are washed out, mass transfer is additionally determined by the solute diffusivity within the solid (through pores) to the interface [143,144]. The accessibility of astaxanthin in this step was probably easier in spray-dried and lyophilized biomasses, which had a porous texture with a high surface, whereas vacuum-dried biomass was very dense and solid.

Total astaxanthin yields in extracts of high-pressure homogenized samples were  $85.25 \pm 1.21$  ( $n = 4$ ),  $93.38 \pm 1.49$  ( $n = 3$ ), and  $68.68 \pm 0.78\%$  ( $n = 3$ ) of previously spray-dried, lyophilized, and vacuum-dried samples, respectively. The lower extractability of the vacuum-dried samples can be explained similarly to the milled samples. The higher extractability of lyophilized samples might be due to the effect of breaking residual intact cells by the vacuum and an even looser texture than that obtained after SD. The higher



extractability of (lyophilized and vacuum-dried) high-pressure homogenized biomass compared to their bead milled counterparts might be because of their higher disruption degree, and thus, easier accessibility of astaxanthin during SC-CO<sub>2</sub> extraction.

Altogether, the extracts of high-pressure homogenized samples that were freeze-dried yielded the highest astaxanthin recoveries, closely followed by high-pressure homogenized samples that were spray-dried and milled samples that were either spray- or freeze-dried. Between the latter, no significant difference was observed. Comprehensive literature on optimal SC-CO<sub>2</sub> extraction conditions for astaxanthin recovery from *H. pluvialis* is available, and the influences of pressure, temperature, flow rate, and co-solvents have been discussed [78–82,84–86]. Nevertheless, these experiments showed that pre-processing of the samples was equally essential. Positive effects of cell disruption on carotenoid recovery have already been indicated in general and in SC-CO<sub>2</sub> extraction [119,145]. Nobre et al. reported total carotenoid recoveries of 91.8% in lyophilized, crushed (vibratory mill), and SC-CO<sub>2</sub>-extracted *H. pluvialis* [54]. This is similar to the results shown here for high-pressure homogenized cells. Nobre et al. and Valderrama et al. also stressed the impact of the crushing intensity and SC-CO<sub>2</sub> extraction conditions on extractability [54,55]. This facilitated mass transfer of astaxanthin into SC-CO<sub>2</sub> due to prior cell disruption could also be confirmed. Moreover, drying affects extractability if it enhances the coherence of the biomass, as observed in the vacuum-dried samples. The observed astaxanthin recoveries were generally correlated with the extract yields.

Total astaxanthin was concentrated 1.35- to 4.15-fold in evaporated SC-CO<sub>2</sub> extracts compared with the concentration in the biomass of the corresponding samples. Thereby, the concentration of all diastereomers increased significantly in all extracts except for one (non-disrupted and spray-dried). However, the composition of the different isomers changed. In all extracts, the proportion of all-*E*-astaxanthin increased, whereas the proportion of other diastereomers decreased (Table S2). This effect was significant for the majority of diastereomers and samples. Álvarez et al. reported even higher all-*E*- and 9*Z*-astaxanthin proportions in their SC-CO<sub>2</sub> extracts. However, they did not include the di-*Z*-isomers [78]. Other studies indicated higher *Z*/*E*-ratios of various carotenoids in supercritical fluid extracts due to their higher solubility [145–147]. Selective extractability is also dependent on SC-CO<sub>2</sub> extraction parameters [148,149] and isomerization during extraction [150], but was not confirmed in the SC-CO<sub>2</sub> extraction of *H. pluvialis* at different temperatures and pressures [78]. Moreover, isomerization in the later analysis cannot be excluded, and might lead to higher 9*Z*- and di-*Z*-astaxanthin isomer shares [88]. Although the exact influence of various process conditions on isomer ratios was not precisely evaluated, SC-CO<sub>2</sub> extraction likely affects the composition of astaxanthin diastereomers in the resulting extracts.

### 3.4. Overall Astaxanthin Yield

Regarding the whole process, maximum astaxanthin yield was recovered after SC-CO<sub>2</sub> extraction when using HPH combined with FD (85.4%) or SD (81.6%). Similar results were obtained using BM and SD (79.0%) or FD (78.1%). VD did not result in good recoveries for all samples, possibly because of the discussed change in sample texture, i.e., high-pressure homogenized (60.5%), milled (30.9%), and non-disrupted (14.0%), respectively. No good recovery rates were obtained from non-disrupted samples, regardless of the drying process (FD 13.7% and SD 9.4%). It can be concluded that SC-CO<sub>2</sub> extraction yielded the best results when the biomass was disintegrated before extraction, with as few cells remaining intact as possible. VD resulted in textural changes in the biomass, which deteriorated the efficiency of SC-CO<sub>2</sub> extraction. However, BM and HPH combined with SD and FD and subsequent SC-CO<sub>2</sub> extraction of *H. pluvialis* biomass resulted in similarly high astaxanthin yields. Thus, all these processes might be applicable in downstream processing regarding astaxanthin maximization (Table 2), but biomass yields, acquisition, labor, and operating costs also have to be considered.



**Table 2.** Total astaxanthin recovery after SC-CO<sub>2</sub> extraction compared with the initial astaxanthin content of the sample, depending on the previous disruption and drying methods.

Disruption	Drying	Recovery (%)
No disruption	Freeze-drying	13.7 ± 0.35
No disruption	Spray-drying	9.4 ± 0.21
No disruption	Vacuum-drying	14.0 ± 0.27
Milling	Freeze-drying	78.1 ± 0.95
Milling	Spray-drying	79.0 ± 1.88
Milling	Vacuum-drying	30.9 ± 0.71
High-pressure homogenization	Freeze-drying	85.4 ± 1.36
High-pressure homogenization	Spray-drying	81.6 ± 1.56
High-pressure homogenization	Vacuum-drying	60.5 ± 0.69

### 3.5. Effort Estimation

An effort estimation to assess technical and economic feasibility of cell disruption and drying of *Haematococcus pluvialis* biomass was performed. Such evaluations of the practical application of the proposed methods and their technical and economic feasibility are crucial in setting up a commercial realization of an astaxanthin production process. We demonstrated astaxanthin losses in every combination of the methods for cell disruption and drying. Some of these losses can be attributed insufficient cell disruption. Hardly any astaxanthin was extracted from unbroken *H. pluvialis* cells. Hence, choosing the right disruption method is essential for the profitability of commercial astaxanthin productions. The difference in the astaxanthin yields between the individual full processes (disruption and subsequent drying) was rather small. Accordingly, no clear recommendation for a specific process can be based on the astaxanthin recovery rates only. Other evaluation criteria need to be considered (Table 3).

**Table 3.** Comparison of technical data of the used disruption and drying devices. n.a., not applicable.

	Cell Disruption		Biomass Drying	
	Bead Mill	High-Pressure Homogenizer	Spray-Dryer	Freeze-Dryer
Throughput	10 L/h	3 L/h	5 L/h	0.4 L/h
Power consumption	4 kW	4 kW	5 kW	4.5 kW
Disruption efficiency	high	high	n.a.	n.a.
Residual moisture	n.a.	n.a.	<9%	<9%
Time for setup	<0.5 h	<0.5 h	1 h	<0.5 h
Time for processing	15 h	50 h	10 h <sup>a</sup> /30 h <sup>b</sup>	120 h <sup>a</sup> /360 h <sup>b</sup>
Cleaning time	1 h	<1 h	1–2 h	<0.5 h
Cleaning procedure	simple	very simple	difficult	very simple
Overall workload	32 h	61 h	12 h	2 h
Product sanitization	n.a.	n.a.	very high	high
Usability	simple	simple	moderate	simple
Scalability	yes	yes	yes	yes
Acquisition costs	EUR 70,000	EUR 40,000	EUR 250,000	EUR 27,000

<sup>a</sup> when BM is used for cell disruption; <sup>b</sup> when HPH is used for cell disruption.

For cell disruption, both methods are rather similar with respect to the effort: the acquisition costs for a pilot-scale bead mill are around EUR 70,000. Here, an actual throughput of 3.3 L/h was considered, because three passages of the biomass are necessary for adequate disruption rates. A comparable HPH system costs around EUR 40,000. Both methods have a similar throughput and are scalable for commercial processes. User-friendliness is also given as both devices are easy to use. The cleaning times and the respective cleaning effort



are also similar. The power consumption of both devices is also the same, as well as the performance at equal throughput. However, there are also significant differences between the two approaches. The BM requires three runs to achieve a high level of cell disruption (~78%). HPH only needs one passage for the same level of disruption (~81%). The second passage increases the disruption rate to ~92%. Therefore, the disruption efficiency of the HPH can be regarded as higher than that of the BM. HPH can be a very time-consuming process. The material had to be processed first to remove clumps or other coarse pieces (biofilm residues), because HPH is prone to clogging by impurities or non-uniform particle sizes. This process can be time-consuming, depending on the amount and the condition of the biomass, and might be a major bottleneck to the HPH of *H. pluvialis* cells.

For HPH, the biomass density should not be higher than 50 g/L. Therefore, the biomass had to be diluted first. Assuming a biomass density after harvesting of 150 g/L, a dilution factor of three is needed. This increases a working volume of 50 to 150 L, causing a subsequent three-fold increase in disruption time for HPH compared with BM. That also increases costs for the following drying step. Assuming that the BM needs three runs and the HPH needs one run, the duration of the cell disruption is more than three times higher with HPH compared with BM. Accordingly, the overall working time and thereby the overall labor costs rise. Thus, BM is more efficient regarding working time and energetic costs. The cleaning procedures of both devices were a bit different. For cleaning the HPH, water was pumped through the system followed by disinfecting agents. The cleaning of the BM was a bit more complex due to the disassembling and reattachment of all product contacting parts, including the beads that had to be cleaned separately. In contrast to the cleaning procedure of HPH, the cleaning step for the BM took longer because every part was cleaned manually. However, this can result in a higher degree of cleanliness. Although the initial costs are higher, and the disruption efficiencies can be lower, we recommend BM for cell disruption on a larger scale because the overall working time, labor costs, as well as the overall power consumption are lower compared with a process that uses HPH. It is also important to consider that BM has many interacting parameters and still further optimization potential.

Regarding astaxanthin recovery, the drying process was most efficient using SD or FD. VD resulted in higher astaxanthin degradation and lower extractability in the SC-CO<sub>2</sub> extraction, and was therefore not included in the effort estimation. Both SD and FD showed similar content of residual moisture in the biomass after drying (<9%). Each process is already used for largescale production, which proves the scalability, e.g., FD is used to produce plant-based foods [151,152] and SD is used to produce a variety of products in the food and beverage industry, e.g., milk powder, soy protein, etc. [153]. Using FD, the process of drying can take several hours for one batch. In contrast, with SD, the material is dried immediately when it passes through the machine. However, because the operation of the FD is very simple and the device works without the necessity of constant supervision, workload and labor costs are reduced compared with other approaches. Nevertheless, FD cannot be operated continuously. This means that depending on the volume of biomass and the size of the FD, several cycles might be necessary. This increases the workload and the overall drying time. In that case, the disrupted algal biomass must be stored temporarily, implicating additional time and space requirements. The cleaning effort for SD was higher because the entire interior as well as the pipes were in contact with the biomass and needed to be cleaned. The biomass accumulated in the machine during the drying process was collected entirely in the pilot-scale process and only from the collection vessel in the laboratory-scale experiments. This is why the losses of biomass during pilot-scale SD were lower than at the laboratory scale and assumed similar to FD. With FD, only the trays that contained the biomass needed to be cleaned. Therefore, the cleaning time was approximately 3 times longer with SD. The main disadvantage of FD is power consumption for freezing, sublimation, condensation, and creating a vacuum in comparison to heat-drying processes [154]. Thus, the power consumption of FD was calculated to be 11 times higher in comparison with SD. Similar results were obtained in a study that



compared the costs and energy demand of SD and FD of 100 kg *H. pluvialis* biomass. Here, FD has been shown to be more than 7 times more energy-consuming than SD [71]. As shown, astaxanthin recovery rates were similar after FD and SD. FD might be more suitable regarding the stability and shelf life of astaxanthin [71]; however, this is negligible when the samples are quickly further processed. The high temperatures of up to 180 °C inside the drying vessel and an outlet temperature of 80–90 °C that were applied for SD led to a high degree of sanitization in the resulting product. In cases of potential presence of bacteria and fungi in the biomass, this step improves the product quality and food safety. SD is not a sterilizing process, even for non-spore-forming organisms, but will substantially reduce bacterial populations in products [155,156]. If the machines are regularly maintained and fully functional, no high level of education or specialist knowledge is required to operate them. Although the initial costs are higher, for a larger scale, we recommend using a spray-dryer for biomass drying because the overall working time, labor costs, and overall power consumption are lower compared with a process that uses FD.

Publications focusing on the larger-scale production of astaxanthin most often used a disruption step and SD. Some describe a similar set up of BM and SD followed by SC-CO<sub>2</sub> [53,157]. Li et al. changed their order and used SD prior to an airflow pulverizer for disintegration, and did not include an additional extraction step [52]. Pérez-Lopez et al. only used SD prior to SC-CO<sub>2</sub> extraction, but omitted a disintegration step [87]. Based on the results of this article, we highly recommend a disruption step for easier extractability, and thus higher astaxanthin recoveries. For the complete downstream process, BM followed by SD of *H. pluvialis* biomass was estimated as optimal pretreatment for SC-CO<sub>2</sub> extraction when additionally considering economic parameters.

#### 4. Conclusions

Various downstream process steps were combined in all possible combinations and the astaxanthin recovery was assessed. A disruption of *H. pluvialis* was necessary to facilitate SC-CO<sub>2</sub> extraction. Neither BM nor HPH influenced the total astaxanthin content significantly, thus only their ability to disrupt the biomass efficiently had a possible influence in the later extraction. Here, HPH resulted in a 14% higher disruption degree and lower variance. Favorable SD conditions concerning astaxanthin recovery and biomass yield were determined with design of experiments and standard least squares regression. The impacts of SD and FD on the astaxanthin content was generally low or even negligible; only VD resulted in a considerable decrease of 13% to 15% total astaxanthin and a change in the texture of the samples, which impeded SC-CO<sub>2</sub> extraction. Considering the whole process chain, the highest astaxanthin recovery of 85.4% was achieved using HPH and FD; however, all process combinations involving a disruption process and SD or FD resulted in similarly good results. FD and HPH are quite expensive. Therefore, BM was combined with spray-drying on larger scale. The results concerning the astaxanthin recovery were comparable to those on laboratory scale. However, also economic parameters have to be taken into consideration. The feasibility studies showed that BM combined with SD can also be recommended in an economic context.

**Supplementary Materials:** The following supporting information can be downloaded at: <https://www.mdpi.com/article/10.3390/foods11091352/s1>, Table S1: Overview of process parameters and results of the conducted experiments for model regression and evaluation in spray-drying, Table S2: Content and proportion of astaxanthin and its diastereomers after various processing steps, Table S3: Estimated model coefficients, p-values and optimized parameters regarding maximal astaxanthin yield in spray-drying.

**Author Contributions:** Conceptualization, I.K.K., S.M., A.K., C.E. and S.H.; methodology, I.K.K. and S.M.; validation, I.K.K.; formal analysis, I.K.K.; investigation, I.K.K., S.M., C.E. and S.H.; data curation, I.K.K.; writing—original draft preparation, I.K.K., C.E. and S.M.; writing—review and editing, A.L., A.K., S.H., I.K.K., C.E. and S.M.; visualization, I.K.K.; supervision, A.K. and S.H.; project administration, A.K.; funding acquisition, A.L. All authors have read and agreed to the published version of the manuscript.



**Funding:** This research is part of the project Grenzland INNOVATIV Schleswig Holstein [innovative border region Schleswig Holstein] and was funded by the German Federal Ministry of Education and Research (BMBF) in context of “Innovative Hochschule” [innovative university]. We acknowledge financial support by Land Schleswig-Holstein within the funding program Open Access-Publikationsfonds.

**Institutional Review Board Statement:** Not applicable.

**Conflicts of Interest:** The authors Clemens Elle and Stefan Hindersin are fully employed and Inga K. Koopmann is marginally employed by the company Sea & Sun Technology GmbH. Simone Möller was marginally employed by the company Sea & Sun Technology GmbH. The funders had no role in the design of the study; in the collection, analyses, or interpretation of data; in the writing of the manuscript, or in the decision to publish the results.

## References

- Di Mascio, P.; Kaiser, S.; Sies, H. Lycopene as the most efficient biological carotenoid singlet oxygen quencher. *Arch. Biochem. Biophys.* **1989**, *274*, 532–538. [\[CrossRef\]](#)
- Conn, P.F.; Schalch, W.; Truscott, T.G. The singlet oxygen and carotenoid interaction. *J. Photochem. Photobiol. B Biol.* **1991**, *11*, 41–47. [\[CrossRef\]](#)
- Miki, W. Biological functions and activities of animal carotenoids. *Pure Appl. Chem.* **1991**, *63*, 141–146. [\[CrossRef\]](#)
- Shimidzu, N.; Goto, M.; Miki, W. Carotenoids as singlet oxygen quenchers in marine organisms. *Fish. Sci.* **1996**, *62*, 134–137. [\[CrossRef\]](#)
- Liu, J.; Zhang, X.; Sun, Y.; Lin, W. Antioxidative capacity and enzyme activity in *Haematococcus pluvialis* cells exposed to superoxide free radicals. *Chin. J. Oceanol. Limnol.* **2010**, *28*, 1–9. [\[CrossRef\]](#)
- Rodrigues, E.; Mariutti, L.R.B.; Mercadante, A.Z. Scavenging capacity of marine carotenoids against reactive oxygen and nitrogen species in a membrane-mimicking system. *Mar. Drugs* **2012**, *10*, 1784–1798. [\[CrossRef\]](#)
- Liu, X.; Shibata, T.; Hisaka, S.; Osawa, T. Astaxanthin inhibits reactive oxygen species-mediated cellular toxicity in dopaminergic SH-SY5Y cells via mitochondria-targeted protective mechanism. *Brain Res.* **2009**, *1254*, 18–27. [\[CrossRef\]](#)
- Chen, Y.-Y.; Lee, P.-C.; Wu, Y.-L.; Liu, L.-Y. In vivo effects of free form astaxanthin powder on anti-oxidation and lipid metabolism with high-cholesterol diet. *PLoS ONE* **2015**, *10*, e0134733. [\[CrossRef\]](#)
- Jiang, X.; Chen, L.; Shen, L.; Chen, Z.; Xu, L.; Zhang, J.; Yu, X. Trans-astaxanthin attenuates lipopolysaccharide-induced neuroinflammation and depressive-like behavior in mice. *Brain Res.* **2016**, *1649*, 30–37. [\[CrossRef\]](#)
- Xue, Y.; Qu, Z.; Fu, J.; Zhen, J.; Wang, W.; Cai, Y.; Wang, W. The protective effect of astaxanthin on learning and memory deficits and oxidative stress in a mouse model of repeated cerebral ischemia/reperfusion. *Brain Res. Bull.* **2017**, *131*, 221–228. [\[CrossRef\]](#)
- Farruggia, C.; Kim, M.-B.; Bae, M.; Lee, Y.; Pham, T.X.; Yang, Y.; Han, M.J.; Park, Y.-K.; Lee, J.-Y. Astaxanthin exerts anti-inflammatory and antioxidant effects in macrophages in NRF2-dependent and independent manners. *J. Nutr. Biochem.* **2018**, *62*, 202–209. [\[CrossRef\]](#) [\[PubMed\]](#)
- Sharma, K.; Sharma, D.; Sharma, M.; Sharma, N.; Bidve, P.; Prajapati, N.; Kalia, K.; Tiwari, V. Astaxanthin ameliorates behavioral and biochemical alterations in in-vitro and in-vivo model of neuropathic pain. *Neurosci. Lett.* **2018**, *674*, 162–170. [\[CrossRef\]](#) [\[PubMed\]](#)
- Brendler, T.; Williamson, E.M. Astaxanthin: How much is too much? A safety review. *Phytother. Res.* **2019**, *33*, 3090–3111. [\[CrossRef\]](#) [\[PubMed\]](#)
- Capelli, B.; Bagchi, D.; Cysewski, G.R. Synthetic astaxanthin is significantly inferior to algal-based astaxanthin as an antioxidant and may not be suitable as a human nutraceutical supplement. *Nutraceuticals* **2013**, *12*, 145–152. [\[CrossRef\]](#)
- Edwards, J.A.; Bellion, P.; Beilstein, P.; Rumbeli, R.; Schierle, J. Review of genotoxicity and rat carcinogenicity investigations with astaxanthin. *Regul. Toxicol. Pharmacol.* **2016**, *75*, 5–19. [\[CrossRef\]](#)
- Del Campo, J.A.; Rodríguez, H.; Moreno, J.; Vargas, M.Á.; Rivas, J.; Guerrero, M.G. Accumulation of astaxanthin and lutein in *Chlorella zofingiensis* (Chlorophyta). *Appl. Microbiol. Biotechnol.* **2004**, *64*, 848–854. [\[CrossRef\]](#)
- Abe, K.; Hattori, H.; Hirano, M. Accumulation and antioxidant activity of secondary carotenoids in the aerial microalga *Coelastrum striolatum* var. *multistriatum*. *Food Chem.* **2007**, *100*, 656–661. [\[CrossRef\]](#)
- Orosa, M.; Torres, E.; Fidalgo, P.; Abalde, J. Production and analysis of secondary carotenoids in green algae. *J. Appl. Phycol.* **2000**, *12*, 553–556. [\[CrossRef\]](#)
- Zhang, D.H.; Lee, Y.K.; Ng, M.L.; Phang, S.M. Composition and accumulation of secondary carotenoids in *Chlorococcum* sp. *J. Appl. Phycol.* **1997**, *9*, 147–155. [\[CrossRef\]](#)
- Czczuga, B. Carotenoids in *Euglena rubida* mainx. *Comp. Biochem. Physiol.* **1974**, *48B*, 349–354. [\[CrossRef\]](#)
- Czczuga, B. Characteristic carotenoids in some phytobentos species in the coastal area of the Adriatic Sea. *Acta Soc. Bot. Pol.* **1986**, *55*, 601–609. [\[CrossRef\]](#)
- Müller, T.; Bleiß, W.; Martin, C.D.; Rogaschewski, S.; Fuhr, G. Snow algae from northwest Svalbard: Their identification, distribution, pigment and nutrient content. *Polar Biol.* **1998**, *20*, 14–32. [\[CrossRef\]](#)



23. Procházková, L.; Remias, D.; Holzinger, A.; Řezanka, T.; Nedbalová, L. Ecophysiological and ultrastructural characterisation of the circumpolar orange snow alga *Sanguina aurantia* compared to the cosmopolitan red snow alga *Sanguina nivaloides* (Chlorophyta). *Polar Biol.* **2021**, *44*, 105–117. [\[CrossRef\]](#) [\[PubMed\]](#)
24. Shah, M.R.; Liang, Y.; Cheng, J.J.; Daroch, M. Astaxanthin-producing green microalga *Haematococcus pluvialis*: From single cell to high value commercial products. *Front. Plant. Sci.* **2016**, *7*, 531. [\[CrossRef\]](#) [\[PubMed\]](#)
25. Pawar, P.R.; Velani, S.; Kumari, S.; Lali, A.M.; Prakash, G. Isolation and optimization of a novel thraustochytrid strain for DHA rich and astaxanthin comprising biomass as aquafeed supplement. *3 Biotech.* **2021**, *11*, 71. [\[CrossRef\]](#)
26. Aki, T.; Hachida, K.; Yoshinaga, M.; Katai, Y.; Yamasaki, T.; Kawamoto, S.; Kakizono, T.; Maoka, T.; Shigeta, S.; Suzuki, O.; et al. Thraustochytrid as a potential source of carotenoids. *J. Am. Oil Chem. Soc.* **2003**, *80*, 789–794. [\[CrossRef\]](#)
27. Park, H.; Kwak, M.; Seo, J.; Ju, J.; Heo, S.; Park, S.; Hong, W. Enhanced production of carotenoids using a thraustochytrid microalgal strain containing high levels of docosahexaenoic acid-rich oil. *Bioprocess. Biosyst. Eng.* **2018**, *41*, 1355–1370. [\[CrossRef\]](#)
28. Yokoyama, A.; Izumida, H.; Miki, W. Production of astaxanthin and 4-ketozeaxanthin by the marine bacterium, *Agrobacterium aurantiacum*. *Biosci. Biotechnol. Biochem.* **1994**, *58*, 1842–1844. [\[CrossRef\]](#)
29. Tsubokura, A.; Yoneda, H.; Mizuta, H. *Paracoccus carotinifaciens* sp. nov., a new aerobic gram-negative astaxanthin-producing bacterium. *Int. J. Syst. Biol.* **1999**, *49 Pt 1*, 277–282. [\[CrossRef\]](#)
30. Yokoyama, A.; Miki, W.; Izumida, H.; Shizuri, Y. New trihydroxy-keto-carotenoids isolated from an astaxanthin-producing marine bacterium. *Biosci. Biotechnol. Biochem.* **1996**, *60*, 200–203. [\[CrossRef\]](#)
31. Osanjo, G.O.; Muthike, E.W.; Tsuma, L.; Okoth, M.W.; Lünsdorf, H.; Abraham, W.-R.; Dion, M.; Timmis, K.N.; Golyshin, N.; Mulaa, F.J. A salt lake extremophile, *Paracoccus bogoriensis* sp. nov., efficiently produces xanthophyll carotenoids. *Afr. J. Microbiol. Res.* **2009**, *3*, 426–433.
32. Iizuka, H.; Nishimura, Y. Microbiological studies on petroleum and natural Gas. X. Carotenoid pigments of hydrocarbon-utilizing bacteria. *J. Gen. Appl. Microbiol.* **1969**, *15*, 127–134. [\[CrossRef\]](#)
33. Calo, P.; de Miguel, T.; Sieiro, C.; Velazquez, J.B.; Villa, T.G. Ketocarotenoids in halobacteria: 3-hydroxy-echinenone and trans-astaxanthin. *J. Appl. Bacteriol.* **1995**, *79*, 282–285. [\[CrossRef\]](#)
34. Andrewes, A.G.; Phaff, H.J.; Starr, M.P. Carotenoids of *Phaffia rhodozyma*, a red-pigmented fermenting yeast. *Phytochemistry* **1976**, *15*, 1003–1007. [\[CrossRef\]](#)
35. Tran, T.N.; Tran, Q.-V.; Huynh, H.T.; Hoang, N.-S.; Nguyen, H.C.; Ngo, D.-N. Astaxanthin production by newly isolated *Rhodospiridium toruloides*: Optimization of medium compositions by response surface Methodology. *Not. Bot. Horti Agrobot. Cluj-Napoca* **2018**, *47*, 320–327. [\[CrossRef\]](#)
36. Seybold, A.; Goodwin, T. Occurrence of astaxanthin in the flower petals in *Adonis annua*. *Nature* **1959**, *184*, 1714–1715. [\[CrossRef\]](#)
37. Li, Y.; Gong, F.; Guo, S.; Yu, W.; Liu, J. *Adonis amurensis* is a promising alternative to *Haematococcus* as a resource for natural esterified (3S,3'S)-astaxanthin production. *Plants* **2021**, *10*, 1059. [\[CrossRef\]](#)
38. Lorenz, R.T.; Cysewski, G.R. Commercial potential for *Haematococcus* microalgae as a natural source of astaxanthin. *Trends Biotechnol.* **2000**, *18*, 160–167. [\[CrossRef\]](#)
39. Zhang, C.; Liu, J.; Zhang, L. Cell cycles and proliferation patterns in *Haematococcus pluvialis*. *Chin. J. Oceanol. Limnol.* **2017**, *35*, 1205–1211. [\[CrossRef\]](#)
40. Borowitzka, M.A.; Huisman, J.M.; Osborn, A. culture of the astaxanthin-producing green alga *Haematococcus pluvialis*. *J. Appl. Phycol.* **1991**, *3*, 295–304. [\[CrossRef\]](#)
41. Kobayashi, M.; Kurimura, Y.; Kakizono, T.; Nishio, N.; Tsuji, Y. Morphological changes in the life cycle of the green alga *Haematococcus pluvialis*. *J. Ferment. Bioeng.* **1997**, *84*, 94–97. [\[CrossRef\]](#)
42. Boussiba, S.; Vonshak, A. Astaxanthin accumulation in the green alga *Haematococcus pluvialis*. *Plant. Cell Physiol.* **1991**, *32*, 1077–1082. [\[CrossRef\]](#)
43. Boussiba, S. Carotenogenesis in the green alga *Haematococcus pluvialis*: Cellular physiology and stress response. *Physiol. Plant.* **2000**, *108*, 111–117. [\[CrossRef\]](#)
44. Olaizola, M. Commercial production of astaxanthin from *Haematococcus pluvialis* using 25,000-liter outdoor photobioreactors. *J. Appl. Phycol.* **2000**, *12*, 499–506. [\[CrossRef\]](#)
45. Torzillo, G.; Goksan, T.; Faraloni, C.; Kopecky, J.; Masojidek, J. Interplay between photochemical activities and pigment composition in an outdoor culture of *Haematococcus pluvialis* during the shift from the green to red stage. *J. Appl. Phycol.* **2003**, *15*, 127–136. [\[CrossRef\]](#)
46. Afalo, C.; Meshulam, Y.; Zarka, A.; Boussiba, S. On the relative efficiency of two- vs. one stage production of astaxanthin by the green alga *Haematococcus pluvialis*. *Biotechnol. Bioeng.* **2007**, *98*, 300–305. [\[CrossRef\]](#)
47. Rao, R.; Sarada, A.R.; Baskaran, V.; Ravishankar, G.A. Identification of carotenoids from green alga *Haematococcus pluvialis* by HPLC and LC-MS (APCI) and their antioxidant properties. *J. Microbiol. Biotechnol.* **2009**, *19*, 1333–1341.
48. Wang, J.; Han, D.; Sommerfeld, M.R.; Lu, C.; Hu, Q. Effect of initial biomass density on growth and astaxanthin production of *Haematococcus pluvialis* in an outdoor photobioreactor. *J. Appl. Phycol.* **2013**, *25*, 253–260. [\[CrossRef\]](#)
49. Liyanaarachchi, V.C.; Nishshanka, G.K.S.H.; Premaratne, R.G.M.M.; Ariyadasa, T.U.; Nimarshana, P.H.V.; Malik, A. Astaxanthin accumulation in the green microalga *Haematococcus pluvialis*: Effect of initial phosphate concentration and stepwise/continuous light stress. *Biotechnol. Rep.* **2020**, *28*, e00538. [\[CrossRef\]](#)



50. Rodríguez-Sifuentes, L.; Marszalek, J.E.; Hernández-Carbajal, G.; Chuck-Hernández, C. Importance of downstream processing of natural astaxanthin for pharmaceutical application. *Front. Chem. Eng.* **2021**, *2*, 29. [\[CrossRef\]](#)
51. 't Lam, G.P.; Vermuë, M.H.; Eppink, M.H.M.; Wijffels, R.H.; van den Berg, C. Multi-product microalgae biorefineries: From concept towards reality. *Trends Biotechnol.* **2018**, *36*, 216–227. [\[CrossRef\]](#) [\[PubMed\]](#)
52. Li, J.; Zhu, D.; Niu, J.; Shen, S.; Wang, G. An economic assessment of astaxanthin production by large scale cultivation of *Haematococcus pluvialis*. *Biotechnol. Adv.* **2011**, *29*, 568–574. [\[CrossRef\]](#) [\[PubMed\]](#)
53. Panis, G.; Carreon, J.R. Commercial astaxanthin production derived by green alga *Haematococcus pluvialis*: A microalgae process model and a techno-economic assessment all through production line. *Algal Res.* **2016**, *18*, 175–190. [\[CrossRef\]](#)
54. Nobre, B.; Marcelo, F.; Passos, R.; Beirão, L.; Palavra, A.; Gouveia, L.; Mendes, R. Supercritical carbon dioxide extraction of astaxanthin and other carotenoids from the microalga *Haematococcus pluvialis*. *Eur. Food Res. Technol.* **2006**, *223*, 787–790. [\[CrossRef\]](#)
55. Valderrama, J.O.; Perrut, M.; Majewski, W. Extraction of astaxanthine and phycocyanine from microalgae with supercritical carbon dioxide. *J. Chem. Eng. Data* **2003**, *48*, 827–830. [\[CrossRef\]](#)
56. Damiani, M.C.; Leonardi, P.I.; Pieroni, O.I.; Cáceres, E.J. Ultrastructure of the cyst wall of *Haematococcus pluvialis* (Chlorophyceae): Wall development and behaviour during cyst germination. *Phycologia* **2006**, *45*, 616–623. [\[CrossRef\]](#)
57. Hagen, C.; Siegmund, S.; Braune, W. Ultrastructural and chemical changes in the cell wall of *Haematococcus pluvialis* (Volvocales, Chlorophyta) during aplanospore formation. *Eur. J. Phycol.* **2002**, *37*, 217–226. [\[CrossRef\]](#)
58. Sarada, R.; Vidhyavathi, R.; Usha, D.; Ravishankar, G.A. An efficient method for extraction of astaxanthin from green alga *Haematococcus pluvialis*. *J. Agric. Food Chem.* **2006**, *54*, 7585–7588. [\[CrossRef\]](#)
59. Ruen-ngam, D.; Shotipruk, A.; Pavasant, P. Comparison of extraction methods for recovery of astaxanthin from *Haematococcus pluvialis*. *Sep. Sci. Technol.* **2010**, *46*, 64–70. [\[CrossRef\]](#)
60. Dong, S.; Huang, Y.; Zhang, R.; Wang, S.; Liu, Y. Four different methods comparison for extraction of astaxanthin from green alga *Haematococcus pluvialis*. *Sci. World J.* **2014**, *2014*, 694305. [\[CrossRef\]](#)
61. Jaime, L.; Rodríguez-Meizoso, I.; Cifuentes, A.; Santoyo, S.; Suarez, S.; Ibáñez, E.; Señorans, F.J. Pressurized liquids as an alternative process to antioxidant carotenoids' extraction from *Haematococcus pluvialis* microalgae. *LWT-Food Sci. Technol.* **2010**, *43*, 105–112. [\[CrossRef\]](#)
62. Mendes-Pinto, M.M.; Raposo, M.F.J.; Bowen, J.; Young, A.J.; Morais, R. Evaluation of different cell disruption processes on encysted cells of *Haematococcus pluvialis*: Effects on astaxanthin recovery and implications for bio-availability. *J. Appl. Phycol.* **2001**, *13*, 19–24. [\[CrossRef\]](#)
63. Zou, T.-B.; Jia, Q.; Li, H.-W.; Wang, C.-X.; Wu, H.-F. Response surface methodology for ultrasound-assisted extraction of astaxanthin from *Haematococcus pluvialis*. *Mar. Drugs* **2013**, *11*, 1644–1655. [\[CrossRef\]](#) [\[PubMed\]](#)
64. Bauer, A.; Minceva, M. Direct extraction of astaxanthin from the microalgae *Haematococcus pluvialis* using liquid–liquid chromatography. *RSC Adv.* **2019**, *9*, 22779–22789. [\[CrossRef\]](#)
65. Praveenkumar, R.; Lee, K.; Lee, J.; Oh, Y.-K. Breaking dormancy: An energy-efficient means of recovering astaxanthin from microalgae. *Green Chem.* **2015**, *17*, 1226–1234. [\[CrossRef\]](#)
66. Choi, S.-A.; Oh, Y.-K.; Lee, J.; Sim, S.J.; Hong, M.E.; Park, J.-Y.; Kim, M.-S.; Kim, S.W.; Lee, J.-S. High-efficiency cell disruption and astaxanthin recovery from *Haematococcus pluvialis* cyst cells using room-temperature imidazolium-based ionic liquid/water mixtures. *Bioresour. Technol.* **2019**, *274*, 120–126. [\[CrossRef\]](#)
67. Praveenkumar, R.; Lee, J.; Vijayan, D.; Lee, S.Y.; Lee, K.; Sim, S.J.; Hong, M.E.; Kim, Y.-E.; Oh, Y.-K. Morphological change and cell disruption of *Haematococcus pluvialis* cyst during high-pressure homogenization for astaxanthin recovery. *Appl. Sci.* **2020**, *10*, 513. [\[CrossRef\]](#)
68. Chen, L.; Liu, X.; Li, D.; Chen, W.; Zhang, K.; Chen, S. Preparation of stable microcapsules from disrupted cell of *Haematococcus pluvialis* by spray drying. *Int. J. Food Sci. Technol.* **2016**, *51*, 1834–1843. [\[CrossRef\]](#)
69. Irshad, M.; Myint, A.A.; Hong, M.E.; Kim, J.; Sim, S.J. One-pot, simultaneous cell wall disruption and complete extraction of astaxanthin from *Haematococcus pluvialis* at room temperature. *ACS Sustain. Chem. Eng.* **2019**, *7*, 13898–13910. [\[CrossRef\]](#)
70. Boonnoun, P.; Kurita, Y.; Kamo, Y.; Wahyudiono; Machmudah, S.; Okita, Y.; Ohashi, E.; Kanda, H.; Goto, M. Wet extraction of lipids and astaxanthin from *Haematococcus pluvialis* by liquefied dimethyl ether. *J. Nutr. Food Sci.* **2014**, *4*, 1–4. [\[CrossRef\]](#)
71. Ahmed, F.; Li, Y.; Fanning, K.; Netzel, M.; Schenk, P.M. Effect of drying, storage temperature and air exposure on astaxanthin stability from *Haematococcus pluvialis*. *Food Res. Int.* **2015**, *74*, 231–236. [\[CrossRef\]](#) [\[PubMed\]](#)
72. Raposo, M.F.J.; Morais, A.M.M.B.; Morais, R.M.S.C. Effects of spray-drying and storage on astaxanthin content of *Haematococcus pluvialis* biomass. *World J. Microbiol. Biotechnol.* **2012**, *28*, 1253–1257. [\[CrossRef\]](#) [\[PubMed\]](#)
73. Li, X.; Wang, X.; Duan, C.; Yi, S.; Gao, Z.; Xiao, C.; Agathos, S.N.; Wang, G.; Li, J. Biotechnological production of astaxanthin from the microalga *Haematococcus pluvialis*. *Biotechnol. Adv.* **2020**, *43*, 107602. [\[CrossRef\]](#) [\[PubMed\]](#)
74. Molina Grima, E.; Belarbi, E.-H.; Acien Fernández, F.G.; Robles Medina, A.; Chisti, Y. Recovery of microalgal biomass and metabolites: Process options and economics. *Biotechnol. Adv.* **2003**, *20*, 491–515. [\[CrossRef\]](#)
75. Etoh, H.; Suhara, M.; Tokuyama, S.; Kato, H.; Nakahigashi, R.; Maejima, Y.; Ishikura, M.; Terada, Y.; Maoka, T. Auto-oxidation products of astaxanthin. *J. Oleo Sci.* **2012**, *61*, 17–21. [\[CrossRef\]](#)
76. Díaz-Reinoso, B.; Moure, A.; Domínguez, H.; Parajó, J.C. Supercritical CO<sub>2</sub> extraction and purification of compounds with antioxidant activity. *J. Agric. Food Chem.* **2006**, *54*, 2441–2469. [\[CrossRef\]](#)



77. Perrut, M. Supercritical fluid applications: Industrial developments and economic issues. *Ind. Eng. Chem. Res.* **2000**, *39*, 4531–4535. [\[CrossRef\]](#)
78. Álvarez, C.E.; Vardanega, R.; Salinas-Fuentes, F.; Ramírez, J.P.; Muñoz, W.B.; Jiménez-Rondón, D.; Meireles, M.A.A.; Mezquita, P.C.; Ruiz-Domínguez, M.C. Effect of CO<sub>2</sub> flow rate on the extraction of astaxanthin and fatty acids from *Haematococcus pluvialis* using supercritical fluid technology. *Molecules* **2020**, *25*, 6044. [\[CrossRef\]](#)
79. Krichnavaruk, S.; Shotipruk, A.; Goto, M.; Pavasant, P. Supercritical carbon dioxide extraction of astaxanthin from *Haematococcus pluvialis* with vegetable oils as co-solvent. *Bioresour. Technol.* **2008**, *99*, 5556–5560. [\[CrossRef\]](#)
80. Machmudah, S.; Shotipruk, A.; Goto, M.; Sasaki, M.; Hirose, T. Extraction of astaxanthin from *Haematococcus pluvialis* using supercritical CO<sub>2</sub> and ethanol as entrainer. *Ind. Eng. Chem. Res.* **2006**, *45*, 3652–3657. [\[CrossRef\]](#)
81. Molino, A.; Mehariya, S.; Iovine, A.; Larocca, V.; Di Sanzo, G.; Martino, M.; Casella, P.; Chianese, S.; Musmarra, D. Extraction of astaxanthin and lutein from microalga *Haematococcus pluvialis* in the red phase using CO<sub>2</sub> supercritical fluid extraction technology with ethanol as co-solvent. *Mar. Drugs* **2018**, *16*, 432. [\[CrossRef\]](#) [\[PubMed\]](#)
82. Pan, J.-L.; Wang, H.-M.; Chen, C.-Y.; Chang, J.-S. Extraction of astaxanthin from *Haematococcus pluvialis* by supercritical carbon dioxide fluid with ethanol modifier: Supercritical CO<sub>2</sub> fluid extraction of astaxanthin from microalgae. *Eng. Life Sci.* **2012**, *12*, 638–647. [\[CrossRef\]](#)
83. Reyes, F.A.; Mendiola, J.A.; Ibañez, E.; del Valle, J.M. Astaxanthin extraction from *Haematococcus pluvialis* using CO<sub>2</sub>-expanded ethanol. *J. Supercrit. Fluids* **2014**, *92*, 75–83. [\[CrossRef\]](#)
84. Sanzo, G.; Mehariya, S.; Martino, M.; Larocca, V.; Casella, P.; Chianese, S.; Musmarra, D.; Balducchi, R.; Molino, A. Supercritical carbon dioxide extraction of astaxanthin, lutein, and fatty acids from *Haematococcus pluvialis* microalgae. *Mar. Drugs* **2018**, *16*, 334. [\[CrossRef\]](#) [\[PubMed\]](#)
85. Thana, P.; Machmudah, S.; Goto, M.; Sasaki, M.; Pavasant, P.; Shotipruk, A. Response surface methodology to supercritical carbon dioxide extraction of astaxanthin from *Haematococcus pluvialis*. *Bioresour. Technol.* **2008**, *99*, 3110–3115. [\[CrossRef\]](#) [\[PubMed\]](#)
86. Wang, L.; Yang, B.; Yan, B.; Yao, X. Supercritical fluid extraction of astaxanthin from *Haematococcus pluvialis* and its antioxidant potential in sunflower oil. *Innov. Food Sci. Emerg. Technol.* **2012**, *13*, 120–127. [\[CrossRef\]](#)
87. Pérez-López, P.; González-García, S.; Jeffryes, C.; Agathos, S.N.; McHugh, E.; Walsh, D.; Murray, P.; Moane, S.; Feijoo, G.; Moreira, M.T. Life cycle assessment of the production of the red antioxidant carotenoid astaxanthin by microalgae: From lab to pilot scale. *J. Clean. Prod.* **2014**, *64*, 332–344. [\[CrossRef\]](#)
88. Koopmann, I.K.; Kramer, A.; Labes, A. Development and validation of reliable astaxanthin quantification from natural sources. *PLoS ONE* **2022**, submitted.
89. Euglert, G.; Vecchi, M. *Trans*./*Cis* isomerization of astaxanthin diacetate/isolation by HPLC. and identification by <sup>1</sup>H-NMR. spectroscopy of three mono-*cis*- and six di-*cis*-isomers. *Helv. Chim. Acta* **1980**, *63*, 1711–1718. [\[CrossRef\]](#)
90. Casella, P.; Iovine, A.; Mehariya, S.; Marino, T.; Musmarra, D.; Molino, A. Smart method for carotenoids characterization in *Haematococcus pluvialis* red phase and evaluation of astaxanthin thermal stability. *Antioxidants* **2020**, *9*, 422. [\[CrossRef\]](#)
91. Subramanian, B.; Tchoukanova, N.; Djaoued, Y.; Pelletier, C.; Ferron, M.; Robichaud, J. Investigations on the geometrical isomers of astaxanthin: Raman spectroscopy of conjugated polyene chain with electronic and mechanical confinement: Investigations on the geometrical isomers of astaxanthin. *J. Raman Spectrosc.* **2014**, *45*, 299–304. [\[CrossRef\]](#)
92. de Bruijn, W.J.C.; Weesepoel, Y.; Vincken, J.-P.; Gruppen, H. Fatty acids attached to all-*trans*-astaxanthin alter its *cis*–*trans* equilibrium, and consequently its stability, upon light-accelerated autoxidation. *Food Chem.* **2016**, *194*, 1108–1115. [\[CrossRef\]](#) [\[PubMed\]](#)
93. Kulikov, E.A.; Kulikova, I.S.; Vasilov, R.G.; Selishcheva, A.A. The effect of the solvent nature and lighting on isomerization and oxidative degradation of astaxanthin. *Biophysics* **2020**, *65*, 433–442. [\[CrossRef\]](#)
94. Bjerkeng, B.; Følling, M.; Lagocki, S.; Storebakken, T.; Olli, J.J.; Alsted, N. Bioavailability of all-*E*-astaxanthin and *Z*-isomers of astaxanthin in rainbow trout (*Oncorhynchus mykiss*). *Aquaculture* **1997**, *157*, 63–82. [\[CrossRef\]](#)
95. Spiden, E.M.; Yap, B.H.J.; Hill, D.R.A.; Kentish, S.E.; Scales, P.J.; Martin, G.J.O. Quantitative evaluation of the ease of rupture of industrially promising microalgae by high pressure homogenization. *Bioresour. Technol.* **2013**, *140*, 165–171. [\[CrossRef\]](#) [\[PubMed\]](#)
96. Yap, B.H.J.; Dumsday, G.J.; Scales, P.J.; Martin, G.J.O. Energy evaluation of algal cell disruption by high pressure homogenisation. *Bioresour. Technol.* **2015**, *184*, 280–285. [\[CrossRef\]](#) [\[PubMed\]](#)
97. Kleinig, A.R.; Mansell, C.J.; Nguyen, Q.D.; Badalyan, A.; Middelberg, A.P.J. Influence of broth dilution on the disruption of *Escherichia coli*. *Biotechnol. Technol.* **1995**, *9*, 759–762. [\[CrossRef\]](#)
98. Halim, R.; Rupasinghe, T.W.T.; Tull, D.L.; Webley, P.A. Mechanical cell disruption for lipid extraction from microalgal biomass. *Bioresour. Technol.* **2013**, *140*, 53–63. [\[CrossRef\]](#)
99. Middelberg, A.P.J. Microbial cell disruption by high-pressure homogenization. In *Downstream Processing of Proteins*; Desai, M.A., Ed.; Methods in Biotechnology; Humana Press: Totowa, NJ, USA, 2000; Volume 9, pp. 11–21.
100. Brookman, J.S.G. Mechanism of cell disintegration in a high pressure homogenizer. *Biotechnol. Bioeng.* **1974**, *16*, 371–383. [\[CrossRef\]](#)
101. Miao, F.; Geng, Y.; Lu, D.; Zuo, J.; Li, Y. Stability and changes in astaxanthin ester composition from *Haematococcus pluvialis* during storage. *Chin. J. Oceanol. Limnol.* **2013**, *31*, 1181–1189. [\[CrossRef\]](#)
102. Niamnuy, C.; Devahastin, S.; Soponronnarit, S.; Vijaya Raghavan, G.S. Kinetics of astaxanthin degradation and color changes of dried shrimp during storage. *J. Food Eng.* **2008**, *87*, 591–600. [\[CrossRef\]](#)



103. Yuan, J.-P.; Chen, F. Isomerization of *trans*-astaxanthin to *cis*-isomers in organic solvents. *J. Agric. Food Chem.* **1999**, *47*, 3656–3660. [\[CrossRef\]](#)
104. Honda, M.; Takahashi, N.; Kuwa, T.; Takehara, M.; Inoue, Y.; Kumagai, T. Spectral characterisation of Z-isomers of lycopene formed during heat treatment and solvent effects on the E/Z isomerisation process. *Food Chem.* **2015**, *171*, 323–329. [\[CrossRef\]](#) [\[PubMed\]](#)
105. Murakami, K.; Honda, M.; Takemura, R.; Fukaya, T.; Kubota, M.; Wahyudiono; Kanda, H.; Goto, M. The thermal Z-isomerization-induced change in solubility and physical properties of (all-E)-lycopene. *Biochem. Biophys. Res. Commun.* **2017**, *491*, 317–322. [\[CrossRef\]](#) [\[PubMed\]](#)
106. Murakami, K.; Honda, M.; Wahyudiono; Kanda, H.; Goto, M. Thermal isomerization of (all-E)-lycopene and separation of the Z-isomers by using a low boiling solvent: Dimethyl ether. *Sep. Sci. Technol.* **2017**, *52*, 2573–2582. [\[CrossRef\]](#)
107. Honda, M.; Sowa, T.; Kawashima, Y. Thermal- and photo-induced isomerization of all-E- and Z-isomer-rich xanthophylls: Astaxanthin and its structurally-related xanthophylls, adonirubin, and adonixanthin. *Eur. J. Lipid Sci. Technol.* **2020**, *122*, 1900462. [\[CrossRef\]](#)
108. Aman, R.; Schieber, A.; Carle, R. Effects of heating and illumination on *trans-cis* isomerization and degradation of  $\beta$ -carotene and lutein in isolated spinach chloroplasts. *J. Agric. Food Chem.* **2005**, *53*, 9512–9518. [\[CrossRef\]](#)
109. Floury, J.; Desrumaux, A.; Lardières, J. Effect of high-pressure homogenization on droplet size distributions and rheological properties of model oil-in-water emulsions. *Innov. Food Sci. Emerg. Technol.* **2000**, *1*, 127–134. [\[CrossRef\]](#)
110. Kwade, A. Determination of the most important grinding mechanism in stirred media mills by calculating stress intensity and stress number. *Powder Technol.* **1999**, *105*, 382–388. [\[CrossRef\]](#)
111. Kwade, A.; Schwedes, J. Breaking Characteristics of different materials and their effect on stress intensity and stress number in stirred media mills. *Powder Technol.* **2002**, *122*, 109–121. [\[CrossRef\]](#)
112. Suarez Garcia, E.; Lo, C.; Eppink, M.H.M.; Wijffels, R.H.; van den Berg, C. Understanding mild cell disintegration of microalgae in bead mills for the release of biomolecules. *Chem. Eng. Sci.* **2019**, *203*, 380–390. [\[CrossRef\]](#)
113. Doucha, J.; Lívanský, K. Influence of processing parameters on disintegration of *Chlorella* cells in various types of homogenizers. *Appl. Microbiol. Biotechnol.* **2008**, *81*, 431–440. [\[CrossRef\]](#) [\[PubMed\]](#)
114. Postma, P.R.; Miron, T.L.; Olivieri, G.; Barbosa, M.J.; Wijffels, R.H.; Eppink, M.H.M. Mild disintegration of the green microalgae *Chlorella vulgaris* using bead milling. *Bioresour. Technol.* **2015**, *184*, 297–304. [\[CrossRef\]](#) [\[PubMed\]](#)
115. Mogren, H.; Lindblom, M.; Hedenskog, G. Mechanical disintegration of microorganisms in an industrial homogenizer. *Biotechnol. Bioeng.* **1974**, *16*, 261–274. [\[CrossRef\]](#)
116. Postma, P.R.; Suarez-Garcia, E.; Safi, C.; Yonathan, K.; Olivieri, G.; Barbosa, M.J.; Wijffels, R.H.; Eppink, M.H.M. Energy efficient bead milling of microalgae: Effect of bead size on disintegration and release of proteins and carbohydrates. *Bioresour. Technol.* **2017**, *224*, 670–679. [\[CrossRef\]](#)
117. Montalescot, V.; Rinaldi, T.; Touchard, R.; Jubeau, S.; Frappart, M.; Jaouen, P.; Bourseau, P.; Marchal, L. Optimization of bead milling parameters for the cell disruption of microalgae: Process modeling and application to *Porphyridium cruentum* and *Nannochloropsis oculata*. *Bioresour. Technol.* **2015**, *196*, 339–346. [\[CrossRef\]](#)
118. Suarez Garcia, E.; van Leeuwen, J.; Safi, C.; Sijtsma, L.; Eppink, M.H.M.; Wijffels, R.H.; van den Berg, C. Selective and energy efficient extraction of functional proteins from microalgae for food applications. *Bioresour. Technol.* **2018**, *268*, 197–203. [\[CrossRef\]](#)
119. Irshad, M.; Hong, M.E.; Myint, A.A.; Kim, J.; Sim, S.J. Safe and complete extraction of astaxanthin from *Haematococcus pluvialis* by efficient mechanical disruption of cyst cell wall. *Int. J. Food Eng.* **2019**, *15*, 10. [\[CrossRef\]](#)
120. Wang, C.; Lan, C.Q. Effects of shear stress on microalgae—A review. *Biotechnol. Adv.* **2018**, *36*, 986–1002. [\[CrossRef\]](#)
121. Alhattab, M.; Kermanshahi-Pour, A.; Brooks, M.S.-L. Microalgae disruption techniques for product recovery: Influence of cell wall composition. *J. Appl. Phycol.* **2019**, *31*, 61–88. [\[CrossRef\]](#)
122. Wileman, A.; Ozkan, A.; Berberoglu, H. Rheological properties of algae slurries for minimizing harvesting energy requirements in biofuel production. *Bioresour. Technol.* **2012**, *104*, 432–439. [\[CrossRef\]](#) [\[PubMed\]](#)
123. Postma, P.R.; Pataro, G.; Capitoli, M.; Barbosa, M.J.; Wijffels, R.H.; Eppink, M.H.M.; Olivieri, G.; Ferrari, G. Selective extraction of intracellular components from the microalga *Chlorella vulgaris* by combined pulsed electric field–temperature treatment. *Bioresour. Technol.* **2016**, *203*, 80–88. [\[CrossRef\]](#) [\[PubMed\]](#)
124. Kasper, J.C.; Winter, G.; Friess, W. Recent advances and further challenges in lyophilization. *Eur. J. Pharm. Biopharm.* **2013**, *85*, 162–169. [\[CrossRef\]](#) [\[PubMed\]](#)
125. Stramarkou, M.; Papadaki, S.; Kyriakopoulou, K.; Krokida, M. Effect of drying and extraction conditions on the recovery of bioactive compounds from *Chlorella vulgaris*. *J. Appl. Phycol.* **2017**, *29*, 2947–2960. [\[CrossRef\]](#)
126. Ryckebosch, E.; Muylaert, K.; Eeckhout, M.; Ruysen, T.; Foubert, I. Influence of drying and storage on lipid and carotenoid stability of the microalga *Phaeodactylum tricornutum*. *J. Agric. Food Chem.* **2011**, *59*, 11063–11069. [\[CrossRef\]](#)
127. Chang, C.-H.; Lin, H.-Y.; Chang, C.-Y.; Liu, Y.-C. Comparisons on the antioxidant properties of fresh, freeze-dried and hot-air-dried tomatoes. *J. Food Eng.* **2006**, *77*, 478–485. [\[CrossRef\]](#)
128. Vanamala, J.; Cobb, G.; Turner, N.D.; Lupton, J.R.; Yoo, K.S.; Pike, L.M.; Patil, B.S. Bioactive compounds of grapefruit (*Citrus paradisi* cv. rio red) respond differently to postharvest irradiation, storage, and freeze drying. *J. Agric. Food Chem.* **2005**, *53*, 3980–3985. [\[CrossRef\]](#)



129. Simonne, A.H.; Smith, M.; Weaver, D.B.; Vail, T.; Barnes, S.; Wei, C.I. Retention and changes of soy isoflavones and carotenoids in immature soybean seeds (Edamame) during processing. *J. Agric. Food Chem.* **2000**, *48*, 6061–6069. [\[CrossRef\]](#)
130. Zhao, X.; Zhang, X.; Fu, L.; Zhu, H.; Zhang, B. Effect of extraction and drying methods on antioxidant activity of astaxanthin from *Haematococcus pluvialis*. *Food Bioprod. Process.* **2016**, *99*, 197–203. [\[CrossRef\]](#)
131. Cong, X.-Y.; Miao, J.-K.; Zhang, H.-Z.; Sun, W.-H.; Xing, L.-H.; Sun, L.-R.; Zu, L.; Gao, Y.; Leng, K.-L. Effects of drying methods on the content, structural isomers, and composition of astaxanthin in antarctic krill. *ACS Omega* **2019**, *4*, 17972–17980. [\[CrossRef\]](#)
132. Focaroli, S.; Mah, P.T.; Hastedt, J.E.; Gitlin, I.; Oscarson, S.; Fahy, J.V.; Healy, A.M. A Design of experiment (DoE) approach to optimise spray drying process conditions for the production of trehalose/leucine formulations with application in pulmonary delivery. *Int. J. Pharm.* **2019**, *562*, 228–240. [\[CrossRef\]](#) [\[PubMed\]](#)
133. Ståhl, K.; Claesson, M.; Lilliehorn, P.; Lindén, H.; Bäckström, K. The effect of process variables on the degradation and physical properties of spray dried insulin intended for inhalation. *Int. J. Pharm.* **2002**, *233*, 227–237. [\[CrossRef\]](#)
134. Broadhead, J.; Rouan, S.K.E.; Hau, I.; Rhodes, C.T. The Effect of process and formulation variables on the properties of spray-dried  $\beta$ -Galactosidase. *J. Pharm. Pharmacol.* **1994**, *46*, 458–467. [\[CrossRef\]](#) [\[PubMed\]](#)
135. Gu, B.; Linehan, B.; Tseng, Y.-C. Optimization of the Büchi B-90 spray drying process using central composite design for preparation of solid dispersions. *Int. J. Pharm.* **2015**, *491*, 208–217. [\[CrossRef\]](#)
136. Büchi Application Note No. 245/2016, Spray Drying of Microalgae. 2016. Available online: <https://www.buchi.com/en/knowledge/applications/spray-drying-microalgae> (accessed on 11 April 2022).
137. Leach, G.; Oliveira, G.; Morais, R. Spray-drying of *Dunaliella salina* to produce  $\beta$ -carotene rich powder. *J. Ind. Microbiol. Biotechnol.* **1998**, *20*, 82–85. [\[CrossRef\]](#)
138. Bhosale, P.; Jogdand, V.V.; Gadre, R.V. Stability of  $\beta$ -Carotene in spray dried preparation of *Rhodotorula glutinis* mutant 32. *J. Appl. Microbiol.* **2003**, *95*, 584–590. [\[CrossRef\]](#)
139. Corrêa-Filho, L.C.; Lourenço, M.M.; Moldão-Martins, M.; Alves, V.D. Microencapsulation of  $\beta$ -carotene by spray drying: Effect of wall material concentration and drying inlet temperature. *Int. J. Food Sci.* **2019**, *2019*, 8914852. [\[CrossRef\]](#)
140. Bustamante, A.; Masson, L.; Velasco, J.; del Valle, J.M.; Robert, P. Microencapsulation of *H. pluvialis* oleoresins with different fatty acid composition: Kinetic stability of astaxanthin and alpha-tocopherol. *Food Chem.* **2016**, *190*, 1013–1021. [\[CrossRef\]](#)
141. Larrosa, A.P.Q.; Comitre, A.A.; Vaz, L.B.; Pinto, L.A.A. Influence of air temperature on physical characteristics and bioactive compounds in vacuum drying of *Arthrospira spirulina*: *Spirulina* dried in vacuum dryer. *J. Food Process. Eng.* **2017**, *40*, e12359. [\[CrossRef\]](#)
142. Karasu, S.; Kilicli, M.; Baslar, M.; Arici, M.; Sagdic, O.; Karaagacli, M. Dehydration kinetics and changes of bioactive compounds of tulip and poppy petals as a natural colorant under vacuum and oven conditions: Best drying condition of tulip and poppy petals. *J. Food Process. Preserv.* **2015**, *39*, 2096–2106. [\[CrossRef\]](#)
143. Brunner, G. *Gas Extraction*; Topics in Physical Chemistry; Springer: Berlin/Heidelberg, Germany, 1994; Volume 4, ISBN 978-3-662-07382-7.
144. Huang, Z.; Shi, X.; Jiang, W. Theoretical models for supercritical fluid extraction. *J. Chromatogr. A* **2012**, *1250*, 2–26. [\[CrossRef\]](#) [\[PubMed\]](#)
145. Gamlieli-Bonshtein, I.; Korin, E.; Cohen, S. Selective separation of *cis-trans* geometrical isomers of  $\beta$ -carotene via CO<sub>2</sub> supercritical fluid extraction. *Biotechnol. Bioeng.* **2002**, *80*, 169–174. [\[CrossRef\]](#) [\[PubMed\]](#)
146. Watanabe, Y.; Honda, M.; Higashiura, T.; Fukaya, T.; Machmudah, S.; Wahyudiono; Kanda, H.; Goto, M. Rapid and selective concentration of lycopene Z-isomers from tomato pulp by supercritical CO<sub>2</sub> with co-solvents. *Solvent Extr. Res. Dev. Jpn.* **2018**, *25*, 47–57. [\[CrossRef\]](#)
147. Mendes, R.L.; Nobre, B.P.; Cardoso, M.T.; Pereira, A.P.; Palavra, A.F. Supercritical carbon dioxide extraction of compounds with pharmaceutical importance from microalgae. *Inorganica Chim. Acta* **2003**, *356*, 328–334. [\[CrossRef\]](#)
148. Gomez, P.I.; Inostroza, I.; Pizarro, M.; Perez, J. From genetic improvement to commercial-scale mass culture of a Chilean strain of the green microalga *Haematococcus pluvialis* with enhanced productivity of the red ketocarotenoid astaxanthin. *AOB Plants* **2013**, *5*, plt026. [\[CrossRef\]](#)
149. Nobre, B.P.; Palavra, A.F.; Pessoa, F.L.P.; Mendes, R.L. Supercritical CO<sub>2</sub> extraction of *trans*-lycopene from Portuguese tomato industrial waste. *Food Chem.* **2009**, *116*, 680–685. [\[CrossRef\]](#)
150. Yi, C.; Shi, J.; Xue, S.J.; Jiang, Y.; Li, D. Effects of supercritical fluid extraction parameters on lycopene yield and antioxidant activity. *Food Chem.* **2009**, *113*, 1088–1094. [\[CrossRef\]](#)
151. Bhatta, S.; Stevanovic Janezic, T.; Ratti, C. Freeze-drying of plant-based foods. *Foods* **2020**, *9*, 87. [\[CrossRef\]](#)
152. Nowak, D.; Jakubczyk, E. The freeze-drying of foods—The characteristic of the process course and the effect of its parameters on the physical properties of food materials. *Foods* **2020**, *9*, 1488. [\[CrossRef\]](#)
153. Filková, I.; Huang, L.X.; Mujumdar, A.S. Industrial spray drying systems. In *Handbook of Industrial Drying*; CRC Press: Boca Raton, FL, USA, 2006; pp. 215–256.
154. Ratti, C. Hot air and freeze-frying of high-value foods: A review. *J. Food Eng.* **2001**, *49*, 311–319. [\[CrossRef\]](#)
155. Blázquez, E.; Rodríguez, C.; Ródenas, J.; Saborido, N.; Solà-Ginés, M.; Pérez de Rozas, A.; Campbell, J.M.; Segalés, J.; Pujols, J.; Polo, J. Combined effects of spray-drying conditions and postdrying storage time and temperature on *Salmonella choleraesuis* and *Salmonella typhimurium* survival when inoculated in liquid porcine plasma. *Lett. Appl. Microbiol.* **2018**, *67*, 205–211. [\[CrossRef\]](#) [\[PubMed\]](#)



- 
156. LiCari, J.J.; Potter, N.N. Salmonella survival during spray drying and subsequent handling of skim milk powder. II. Effects of drying conditions. *J. Dairy Sci.* **1970**, *53*, 871–876. [[CrossRef](#)]
  157. Zgheib, N.; Saade, R.; Khallouf, R.; Takache, H. Extraction of astaxanthin from microalgae: Process design and economic feasibility study. *IOP Conf. Ser. Mater. Sci. Eng.* **2018**, *323*, 012011. [[CrossRef](#)]







# **Chapter III**

**Screening of a Thraustochytrid Strain Collection for Carotenoid and Squalene Production  
Characterized by Cluster Analysis, Comparison of 18S rRNA Gene Sequences, Growth  
Behavior, and Morphology**





## Article

# Screening of a Thraustochytrid Strain Collection for Carotenoid and Squalene Production Characterized by Cluster Analysis, Comparison of 18S rRNA Gene Sequences, Growth Behavior, and Morphology

Inga K. Koopmann , Bettina A. Müller and Antje Labes \*

ZAiT, Center for Analytics in Technology Transfer of Bio and Food Technology Innovations, Flensburg University of Applied Sciences, 24943 Flensburg, Schleswig-Holstein, Germany

\* Correspondence: antje.labes@hs-flensburg.de

**Abstract:** Carotenoids and squalene are important terpenes that are applied in a wide range of products in foods and cosmetics. Thraustochytrids might be used as alternative production organisms to improve production processes, but the taxon is rarely studied. A screening of 62 strains of thraustochytrids *sensu lato* for their potential to produce carotenoids and squalene was performed. A phylogenetic tree was built based on 18S rRNA gene sequences for taxonomic classification, revealing eight different clades of thraustochytrids. Design of experiments (DoE) and growth models identified high amounts of glucose (up to 60 g/L) and yeast extract (up to 15 g/L) as important factors for most of the strains. Squalene and carotenoid production was studied by UHPLC-PDA-MS measurements. Cluster analysis of the carotenoid composition partially mirrored the phylogenetic results, indicating a possible use for chemotaxonomy. Strains in five clades produced carotenoids. Squalene was found in all analyzed strains. Carotenoid and squalene synthesis was dependent on the strain, medium composition and solidity. Strains related to *Thraustochytrium aureum* and *Thraustochytriidae* sp. are promising candidates for carotenoid synthesis. Strains closely related to *Schizochytrium aggregatum* might be suitable for squalene production. *Thraustochytrium striatum* might be a good compromise for the production of both molecule groups.



**Citation:** Koopmann, I.K.; Müller, B.A.; Labes, A. Screening of a Thraustochytrid Strain Collection for Carotenoid and Squalene Production Characterized by Cluster Analysis, Comparison of 18S rRNA Gene Sequences, Growth Behavior, and Morphology. *Mar. Drugs* **2023**, *21*, 204. <https://doi.org/10.3390/md21040204>

Academic Editor: Rob Keyzers

Received: 27 February 2023

Revised: 20 March 2023

Accepted: 22 March 2023

Published: 24 March 2023



**Copyright:** © 2023 by the authors. Licensee MDPI, Basel, Switzerland. This article is an open access article distributed under the terms and conditions of the Creative Commons Attribution (CC BY) license (<https://creativecommons.org/licenses/by/4.0/>).

**Keywords:** Stramenopiles; *Thraustochytrium*; *Ulkenia*; *Schizochytrium*; *Oblongichytrium*; Labyrinthulomycetes; chemotaxonomy; microscopy; growth models; cluster analysis

## 1. Introductions

Carotenoids and squalene belong to the very heterogeneous group of terpenes, sharing the building block isoprene. Carotenoids are tetra- or polyterpenes, comprise over 500 known chemical structures [1] and are produced by a variety of organisms [2–4]: mainly plants [5], (micro)algae [6–10], bacteria [11–14], archaea [15,16], fungi [17,18] and protists [19–21]. Many carotenoids offer protective properties against photooxidative stress by quenching reactive oxygen and nitrogen species, photosensitizers, and free radicals [22–27]. Antioxidant and anti-inflammatory activities were also observed in vivo [25,28–32], and beneficial effects regarding various health aspects have been described [33–35]. This led to the application of carotenoids mainly as food and feed supplements but also as nutraceuticals, pharmaceuticals, and in cosmetics [36]. Many carotenoids can be chemically synthesized, but increasing consumer awareness towards sustainable and environmentally friendly products has led to a higher demand for biotechnological production [36]. Many carotenoid-producing organisms do not synthesize large amounts of these substances or are not suitable for high-density cultivation. Thus, biotechnological production processes often suffer from low yields.

Squalene is a triterpene that is ubiquitous in higher organisms. It is abundant in human skin surface lipids [37] and an intermediate in sterol biosynthesis in plants and



animals [38,39]. It is mainly used in cosmetics as an antioxidant and hydrating agent [40,41] but also in pharmaceuticals, e.g., as an adjuvant in vaccines [42–44], in nutraceuticals, and food products [42]. It is highly abundant in the liver of certain shark species [45–49], from which it was also first isolated [50]. It can also be extracted from various fruits, legumes, grains, seeds, and nuts, especially from olives and amaranth seeds [51–55]. Although plant-based resources have a growing market share, some squalene is still derived from endangered sharks, which has been heavily criticized. As the market size value of squalene is expected to continue to grow in the coming years [41,42], a sustainable and easily scalable resource for squalene must be found.

Different optimization approaches are necessary to improve the efficiency of carotenoid and squalene production. The selection of an optimal production organism is one of them. Thraustochytrids is a promising group of organisms, being a family of marine unicellular organisms. They are eukaryotic, saprobic protists and occur ubiquitously in the marine ecosystem. Thraustochytrids play an important part in the microbial loop as nutrient recyclers and act as partners in various relationships with algae and other marine organisms [56,57]. The taxonomy of the thraustochytrids still needs clarification. Since their first description in 1934 [58], their classification has changed, from belonging to fungi to oomycetes [59] and finally to a phylogenetic group of its own together with the labyrinthulids in the polyphyletic kingdom of Protista [60]. 18S rRNA gene comparison confirmed their independency from oomycetes, and they were associated with the stramenopiles [61,62]. On a lower taxonomic level, the assignment of various strains to different orders and genera has been repeatedly revisited, still in recent years [62–68].

Some strains are successfully used for the production of long-chain  $\omega$ -3-fatty acids, especially docosahexaenoic acid (DHA) (C22:6), at laboratory [69–75] and industrial scale [76]. Thraustochytrids are further known for the synthesis of squalene [69–71,77–79] and carotenoids, particularly astaxanthin,  $\beta$ -carotene, canthaxanthin, echinenone, and phoenicoxanthin [19–21,63,64,74,80–83]. The heterotrophic cultivation is a major advantage over microalgae, the main carotenoid-synthesizing organisms in large-scale biotechnological production. Microalgae have to be grown phototrophically in most cases, which means high operational effort and costs. Thraustochytrids have a great potential to reach high cell densities of up to 170 g/L [84,85] and can be cultivated in fermentation processes using various waste streams [69–71,86]. Therefore, an optimization of the production rate of carotenoids and squalene in comparison to established processes is very likely. Nevertheless, there is still a lack of knowledge regarding this very heterogeneous group of organisms. The fact that today's production strains are mainly members of the genus *Schizochytrium* shows that the diversity of this group is not fully used [76].

A few production strains and those commonly used in the laboratory are fairly well described. Still, for the vast diversity of thraustochytrids, only few coherent datasets combine taxonomic data with optimal cultivation parameters, morphology, and secondary metabolite patterns [63,64,87]. Such combined datasets have been used and proposed to improve the understanding and quality of taxonomic arrangements [63,64] and provide better access to industrial applicability. A major problem in this specific group is the high variability in morphology and metabolite patterns, partly also depending on different cultivation parameters.

This work aims to present a better and more coherent picture of this group by a multilevel screening of a strain collection of marine thraustochytrids. We used design of experiment (DoE) and modeling tools to explain the growth of various strains. 18S rRNA gene-based phylogeny was correlated with the production of various carotenoids and squalene, and microscopic morphology. The objective was to show and describe that strains similar at molecular level have similar growth characteristics, morphology, and metabolite patterns with a specific focus on squalene and carotenoids. This picture shall enable and simplify the classification and cultivation of new and not studied strains, not least to test their applicability on an industrial scale for producing valuable substances.



## 2. Results

### 2.1. Molecular Identification

The 18S rRNA sequences were compared with those in the GenBank database using the Basic Local Alignment Search Tool (BLAST). The majority of strains of the collection were assigned to already described genera of the Thraustochytriaceae, namely *Thraustochytrium* spp., *Ulkenia* spp., *Thraustochytriidae* sp., *Schizochytrium aggregatum*, and *Oblongichytrium minutum* (Table S1). Only one group of strains (N6421, N6422, N6423, N6424, N6523) was closer related to *Paranamyces uniporus* (NCBI accession number MT731025.1), which belongs to the Rhizophydiales. This group was not used for the final alignment and tree formation. The phylogenetic tree (Figure 1) contained two main clades and the outgroup. One contained members of the Thraustochytriaceae and most of the strains from the collection. The other one contained members of the Thraustochytriaceae and Labyrinthulaceae. Only two strains from the collection (N5995 and 5996) were located here, being closely related to *Oblongichytrium minutum* (AB022108.1). Within the branches of the two clades, many of the strains of the collection had little or no evolutionary distance. Twenty of the strains were closely related to *Thraustochytrium kinnei* with only small or no evolutionary distance to each other. For strain N1694d, the sequence was already available (*T. kinnei* L34668.1) [61]. The 18S rRNA gene sequence of this strain (here with number N1694d) was similar but not identical. Amplification of 18S rRNA genes of most strains related to *S. aggregatum* was not possible with primers T18S1F and T18S5R. Only shorter segments were amplified.

### 2.2. Growth Studies

Design of experiment, model estimation, and selection were performed to find optimal cultivation conditions for the thraustochytrids and to compare their growth behavior. Three models (Equations (1)–(3)) were estimated and compared to find the best description for growth at a constant salt concentration (15 g/L): In the simplest model (Equation (1)/model 1), the quadratic influence of all parameters was considered. Model 2 (Equation (2)) reduced the quadratic influences to those of glucose and yeast extract and included the interaction term of yeast extract and glucose. Model 3 (Equation (3)) included further interaction terms.

In total, the experiment was performed with 30 strains. Some strains did not grow at all (*T. kinnei* 1438e, *U. profunda* N5976, N5629e) or not sufficiently for model estimation (*U. profunda* N5905). These strains were excluded from the model evaluation. The models of the remaining 26 strains were summarized and compared by the median of the adjusted coefficients of determination. The highest values were reached by model 3, followed by model 2 and model 1, with a median of the adjusted  $R^2$  of 0.904, 0.775, and 0.689, respectively. Comparing the adjusted coefficients of determination directly, the third model (Equation (3)) scored a higher adjusted  $R^2$  for 65% of the strains. The best-describing model varied for some of the clusters detected in the phylogenetic tree. *U. visurgensis* N6000b and Sakar 7 were best described by model 1. *U. visurgensis* N5589c, N5594d, and *U. profunda* N5658a were best described by model 2. *Thraustochytriidae* sp. N4994d, N4995d, and N5670c, *T. kinnei* N1709d, N1694d, 14766c, 1465d, 1462d, and 3041c, and *T. aggregatum* 4992b and 154f were best described by model 3. The coefficients of determination and  $p$ -values of all models can be found in the supplement (Table S2). Model 1 showed that the quadratic influence of pH or phosphate had no significant influence on the growth, except for one strain, and was not further evaluated. Due to the reduction of the degrees of freedom by the addition of interaction terms, model 3 did not display many parameters as significant. Thus, for a general impression of the importance of the parameters and better clarity and comparability, model 2 was chosen to carefully compare all strains with an adjusted  $R^2 \geq 0.7$  and a significant  $p$ -value ( $\sigma = 0.05$ ). These were *U. visurgensis* Sakar7, N6000b, N5589c, N5594d, *Thraustochytriidae* sp. N4994d, N4995d, N5670c, *T. aureum* N6007e, N6006d, *T. kinnei* N1709d, N1694d, N1476c, 1462d, *T. aggregatum* 4992b, and 154f.





**Figure 1.** Phylogenetic tree based on 18S rRNA genes created using the maximum-likelihood method and the Tamura–Nei nucleotide substitution model. The final dataset contained 1378 base positions. Bootstrap values are shown for 1000 replicates. Type strains are marked with a “T”. Strains that were reclassified in this study are marked with an asterisk. Strains from the mFSC collection are highlighted bold. Accession numbers, names of taxa and strain labels are shown for the sequences retrieved from GenBank. Strains with no calculated evolutionary distance are on the same branch.

Glucose and yeast extract addition had a generally positive influence on growth. The linear parameter for yeast extract concentration was considered significant ( $\sigma = 0.05$  or



$\sigma = 0.01$ ) for 93% of the tested strains, followed by glucose with a significant linear influence on the growth of 73% of the named strains. The quadratic coefficients of both (glucose and yeast extract) were most often slightly negative but insignificant. The parameters for the interaction of glucose and yeast extract were primarily small but positive. It was considered significant for the growth of 27% of the strains. This resulted in predicted high optimal concentrations of up to the maximum of glucose (60 g/L) and yeast extract (15 g/L) for most strains (Table 1 and Table S3). *U. visurgensis* Sakar 7 and N6000b showed lower optimized glucose concentrations of 46 and 32 g/L, respectively. Strain N6000b also had a lower optimized yeast extract value of 10.1 g/L. Likewise, the optimization for the results of *Thraustochytriidae* sp. N4995d and *T. aggregatum* 154f indicated that lower glucose and yeast extract concentrations were optimal. The influence of the pH value and the addition of phosphate was considered significant only in under 15% of the strains. The coefficient of the pH value was negative for most strains, whereas the coefficient for the addition of phosphate was balanced positive and negative. Thus, the optimized pH was the minimum of 6.5 for all strains except for *T. aggregatum* 154f. The optimized additional phosphate concentration was either 0 or 0.5 g/L.

**Table 1.** Estimated model coefficients, *p*-values, and optimized parameters of model 2 for four exemplary strains regarding maximal biomass yield. Significant *p*-values are indicated with \*\* ( $\sigma = 0.01$ ) and \* ( $\sigma = 0.05$ ). The variance of the yield is given for a 0.95 confidence interval.

	<i>T. aureum</i> N6006d		<i>U. visurgensis</i> N5594d		<i>Thraustochytriidae</i> sp. N4994d		<i>T. kinnei</i> N1694d	
	Coefficient	<i>p</i> -Value	Coefficient	<i>p</i> -Value	Coefficient	<i>p</i> -Value	Coefficient	<i>p</i> -Value
a	−39.2		66.8		188.4		236.5	
b <sub>1</sub> (G <sup>a</sup> )	−0.4	0.0009 **	−0.01	0.0030 **	0.7	0.0014 **	0.09	<0.0001 **
b <sub>2</sub> (Y <sup>b</sup> )	69.0	0.0137 *	−4.4	0.00055 **	6.5	<0.0001 **	2.91	<0.0001 **
b <sub>3</sub> (pH)	−6.5	0.9614	−4.4	0.6555	−24.8	0.0397 *	−28.9	0.0086 **
b <sub>4</sub> (P <sup>c</sup> )	246.7	0.5375	−13.4	0.5185	−30.0	0.1807	−66.2	0.0058 **
c <sub>1</sub> (G <sup>2</sup> )	0.05	0.7913	0.01	0.5328	−0.01	0.2596	−0.01	0.5564
c <sub>2</sub> (Y <sup>2</sup> )	−5.0	0.1615	0.5	0.0222 *	−0.3	0.2000	−0.1	0.4664
d <sub>12</sub> (G*Y)	1.5	0.0200 *	0.03	0.02682	0.1	0.0060 *	0.16	0.0002 **
R <sup>2</sup>	0.9140		0.9322		0.9761		0.9533	
R <sup>2</sup> adj.	0.8281		0.8643		0.9482		0.9667	
<i>p</i> -value	0.0029		0.0013		0.0002		<0.0001	
Optimized parameters								
G	60		60		60		60	
Y	15		15		15		15	
pH	6.5		6.5		6.5		6.5	
P	0.5		0		0.5		0.5	
Y <sup>d</sup>	25.9 ± 15.9		2.2 ± 0.6		2.8 ± 0.7		3.4 ± 0.6	

<sup>a</sup> G, Glucose (g/L), <sup>b</sup> Y, Yeast extract (g/L), <sup>c</sup> P, KH<sub>2</sub>PO<sub>4</sub> addition (g/L), <sup>d</sup> Y, Yield (g/L).

Many of the strains that were clearly better described by model 3 (*S. aggregatum* N2820a, 5999, 561bx, *T. aureum* N5998, 5986, *O. minutum* 5996, and *T. striatum* N5997) still showed a growth optimum at 50–60 g/L glucose, but some had a lower optimum for yeast extract (*T. aureum* N5998, 5986, and *O. minutum* 5996). Only *T. kinnei* 1465d, 3041c, and *O. minutum* N5995 had a growth maximum at lower glucose (0 and 26 g/L) and varying yeast extract concentration (15 and 0.5 g/L).

*T. aureum* N6006d, N6007e, 5985, *T. aggregatum* 4992b, 154f, and *T. striatum* N5997 yielded the highest biomasses of all strains. Their average yield varied between 4 and 7 g/L. All these strains grew best on DoE medium 8 or 9 (Table S4). The highest yield of 27 g/L was obtained from N6007e on medium 8, regardless of the salt concentration. *Thraustochytriidae* sp. N4995d and *S. aggregatum* 561bx, and 5999 yielded just over 2 g/L on average. Most of the other strains yielded less than 2 g/L.



Sixteen of the analyzed strains were additionally cultivated on media with a higher salinity. Model 2 was extended by the linear influence of salt concentration. A slightly but significant negative influence ( $\sigma = 0.05$ ) was found in *Thraustochytriidae* sp. N4995d. A significant positive influence ( $\sigma = 0.01$ ) was observed in *O. minutum* N5995, *U. visurgensis* Sakar7, and *U. profunda* N5905 and N5629e. The effect was particularly clear for the latter two. These strains only grew on one of the 15 media with a lower salt concentration (DoE 13 and 3, respectively) and on most of the media with a higher salt concentration of 30 g/L. Of the media with the higher salt concentration, they yielded the highest biomass on media 13 and 6, respectively.

### 2.3. Target Molecules

The occurrence of various carotenoids and squalene was analyzed in the strains. The following carotenoids were detected by comparison with standards: astaxanthin, astaxanthin monopalmitate, phoenicoxanthin, canthaxanthin, 9Z-canthaxanthin, echinenone, lycopene, and  $\beta$ -carotene. Neither lutein, zeaxanthin, antheraxanthin, nor rhodoxanthin were observed in comparison to the standards. Diastereomers of astaxanthin were also detected. Carotenoids were found in all tested strains except for those closely related to *T. kinnei* (1462d, 1465d, N1476c, N1694d, N1709d), *T. aggregatum* (154f, N4992b), and *O. minutum* (N5995). Squalene was detected in all strains.

### 2.4. Cluster Analysis of Carotenoid Composition

A comparison of the carotenoid composition (Figure 2, Table S5 and S6) by k-means and hierarchical cluster analysis (Figure 3) indicated eight different clusters of strains.

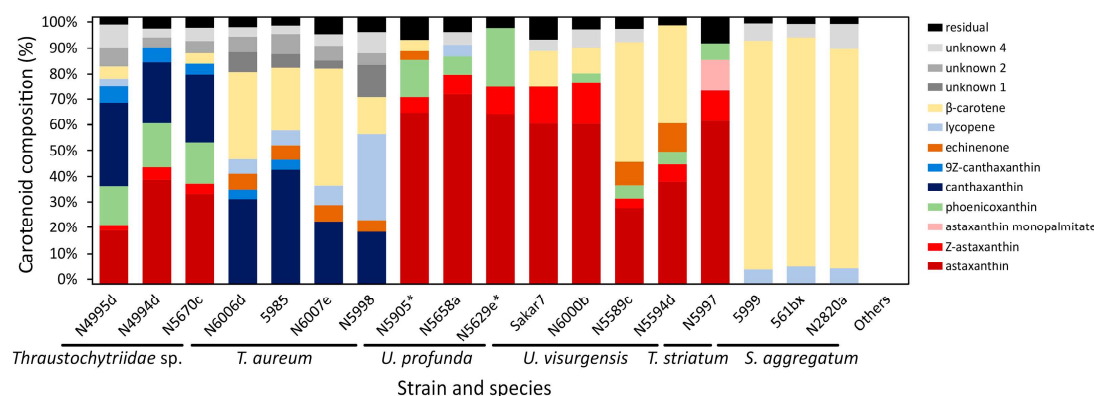


**Figure 2.** Carotenoid composition of the analyzed strains. Mean values of the individual experiments from each strain whose share in the total carotenoids exceeded 3% are displayed individually (Table S5). Diastereomers of astaxanthin are summarized as “Z-astaxanthin”. “Others” comprises all tested strains assigned to *T. kinnei* (N1694d, 1462d, 1465d, N1476c, N1709d, 3041c), *T. aggregatum* (4992b, 154f), and *O. minutum* (N5995). Strains that grew only on media with high salinity are marked with asterisks.



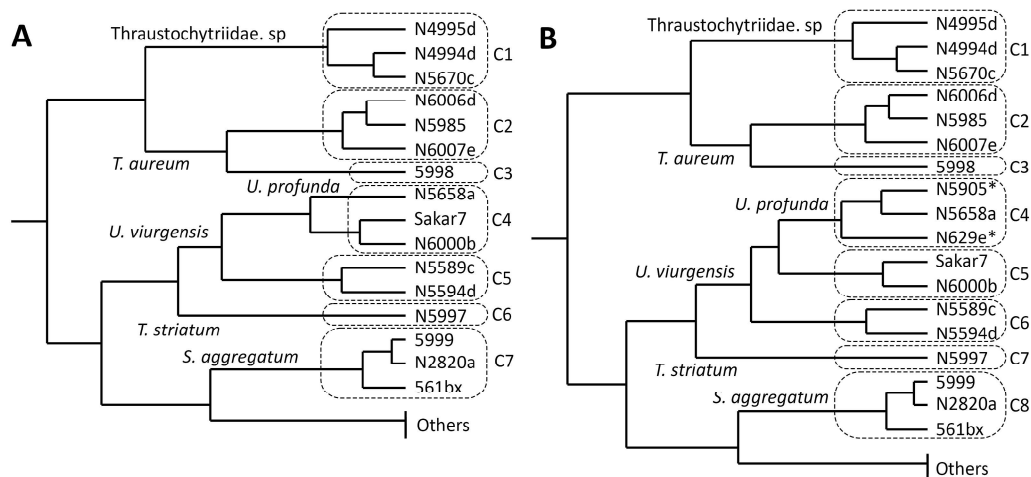


**Figure 3.** Hierarchical clustering of the analyzed strains based on their carotenoid profiles. Clusters calculated by k-means algorithm were highlighted by dashed boxes. (A) Clusters excluding carotenoid patterns of *U. profunda* N5629e and N5905. (B) Clusters including carotenoid patterns of *U. profunda* N5629e and N5905 (marked with asterisks) cultivated on media with a high salt concentration. “Others” comprises all tested strains assigned to *T. kinnei* (N1694d, 1462d, 1465d, N1476c, N1709d, 3041c), *T. aggregatum* (4992b, 154f), and *O. minutum* (N5995).

The first cluster was characterized by a balanced ratio of astaxanthin and canthaxanthin (cluster means of 30% and 28%, respectively) and some phoenicoxanthin (cluster mean of 16%). It contained all strains closely related to *Thraustochytriidae* sp. The second cluster comprised three of the four strains closely related to *T. aureum*, characterized by major proportions of canthaxanthin (cluster mean of 32%) and  $\beta$ -carotene (cluster mean of 35%). The fourth strain of this group (*T. aureum* N5998) was, from a phylogenetic view, closely related to two of the strains from that cluster. It was only associated with that cluster because of still comparably high canthaxanthin (cluster mean of 18%) and  $\beta$ -carotene values (cluster mean of 14%). However, it was not included, mainly because of its outstanding lycopene proportion. It was the highest of all strains at 34%. The fourth and fifth cluster contained all strains closely related to *Ulkenia* species. The fourth clustered *U. profunda* N5658a and *U. visurgensis* Sakar7 and 6000d and displayed predominantly a high astaxanthin content (cluster mean of 64%). The fifth was characterized by astaxanthin (cluster mean of 33%) and  $\beta$ -carotene (cluster mean of 42%) and contained *U. visurgensis* N5589c and N5594d. *T. striatum* N5997 had a separate position in the tree but was located in close proximity to the *Ulkenia* clusters. It had a similar astaxanthin proportion (cluster mean of 62%), but produced also an astaxanthin ester, which could not be found in any of the other strains. The last comparable cluster comprised strains closely related to *S. aggregatum* with a high proportion of  $\beta$ -carotene (cluster mean of 88%). Strains closely related to *T. kinnei*, *T. aggregatum*, and *O. minutum* were clustered because no carotenoids were detected.

#### 2.5. Cluster Analysis of Carotenoid Composition, including Strains with a High Salt Affinity

Comparison of carotenoid profiles emerging on media with high (30 g/L) and low (15 g/L) salt concentration showed only small differences between the same strain (Table S7 and Figure S1). *U. profunda* N5629e and N5905 did produce almost no biomass on media with a salt concentration of 15 g/L. Therefore, their carotenoid patterns were evaluated only by the biomass grown on the media with the higher salinity. They were similar to those of *U. profunda* N5658a (Figure 2). Inclusion in cluster analysis resulted in the division of cluster 4 (Figure 3). All strains related to *U. profunda* (N5658a, N5629e, N5905) now clustered with a higher mean



of astaxanthin (67%) and some phoenicoxanthin (cluster mean of 15%). *U. visurgensis* N6000b and Sakar7 formed a separate cluster with mainly astaxanthin (cluster mean of 60%) and  $\beta$ -carotene (cluster mean of 12%). *U. visurgensis* N5594d and N5589c remained unaffected.

## 2.6. Target Molecule Content and Yield in the DoE Studies

Mean total carotenoid content varied between 0 and 246  $\mu\text{g/g}$  (maximum in *T. aureum* 5985). Clusters 1 and 2 comprised the strains with the highest carotenoid content, whereas squalene was generally more abundant in *T. striatum* N5997 and some *Ulkenia* strains (Figure 4). It has to be noted that these values are means over all the various media used in the DoE. Strains performed better on some of the individual media. e.g., *Thraustochytriidae* sp. N4994d, *T. aureum* N6006d, N6007e, and *U. visurgensis* Sakar7, N5589c showed a higher carotenoid content on medium 8 than in the mix or on the other individually tested media. *T. aureum* 5985 possessed the highest total carotenoid content of 307  $\mu\text{g/g}$  on medium 9. Most strains related to *Thraustochytriidae* sp. and *T. aureum* also produced high biomass. Thus, the carotenoid yield was also high and resulted in 6 mg/L for *T. aureum* 5985 on medium 9.

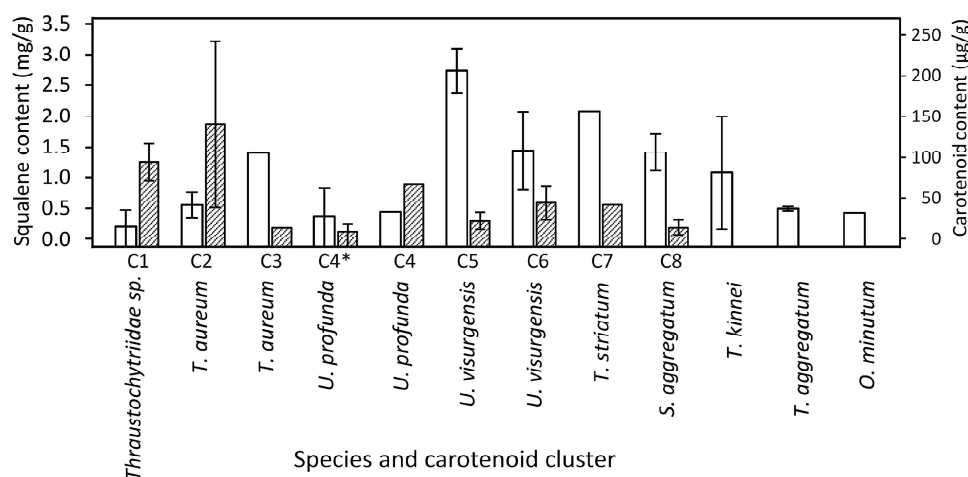


**Figure 4.** Mean squalene (empty bars) and carotenoid (shaded bars) content of strains belonging to the same carotenoid cluster (Figure 3B). Strains that grew only on media with high salinity are marked with asterisks. Whiskers indicate the standard deviation between the different strains of a cluster. Dry weight was approximated using data from the other trials.

The mean squalene content varied between 0.02 mg/g (*Thraustochytriidae* sp. N4995d) and 3 mg/g (*U. visurgensis* N6000b). The highest squalene contents observed were 13 mg/g and 12 mg/g in *T. striatum* N5997 on medium 11, and in *O. minutum* N5995 on medium 14 with a high salt concentration, respectively.

## 2.7. Regression Analysis of Target Molecules

For a more detailed insight into the carotenoid and squalene synthesis based on the dependency of the media composition, target molecules in *T. striatum* N5997 were analyzed on all media from the DoE except for number 8, on which it did not grow. In addition, the growth regression was repeated to find a model that described growth better than the previously obtained models (model 1-3). The resulting regression had an adjusted  $R^2$  of 0.8819. Due to few degrees of freedom, only the optimized parameters were evaluated, but not their individual influences. Model optimization indicated that the maximum glucose concentration (60 g/L) and a small yeast extract concentration (3.9 g/L) maximized the biomass yield (Table 2). Optimization of squalene content resulted in a minimum glucose



concentration and maximum yeast extract concentration. An intermediate glucose and yeast extract concentration was considered advantageous for squalene yield.

Carotenoids found in *T. striatum* N5997 were mainly astaxanthin, its diastereomers, and an ester (85.4% of the carotenoids in total). Phoenicoxanthin (6.3%), lycopene (2.6%),  $\beta$ -carotene (1.5%), canthaxanthin and its diastereomer (1.2%), and two unknown carotenoids (2.9%) were observed to a smaller extent. Carotenoid composition changed slightly depending on the medium composition (Table S8 and Figure S2). In contrast to squalene, a high glucose (48–60 g/L) but minimal yeast extract concentration (0.5 g/L) was found to be beneficial in optimizing total and individual carotenoid content. The highest absolute carotenoid yield was predicted at maximum glucose and minimum yeast extract concentration.

**Table 2.** Model quality and optimized parameters of models for growth, carotenoid, and squalene production in *T. striatum* N5997. Dry weight was approximated using data from the other trials.

	Target Molecule Content					Target Molecule Yield			
	Biomass Yield (g/L)	Squalene (mg/g)	Total Carotenoids ( $\mu$ g/g)	Total Astaxanthin ( $\mu$ g/g)	Phoenico-Xanthin ( $\mu$ g/g)	Squalene (mg/L)	Total Carotenoids (mg/L)	Total Astaxanthin (mg/L)	Phoenico-Xanthin (mg/L)
R <sup>2</sup>	0.9578	0.9887	0.8909	0.8956	0.9891	0.8530	0.9600	0.9622	0.9476
R <sup>2</sup> adj.	0.8819	0.9705	0.7164	0.7288	0.9644	0.5884	0.8601	0.8676	0.8532
p-value	0.0061	0.0002	0.0446	0.0403	0.0014	0.1052	0.0215	0.0194	0.0103
Optimized parameters									
G <sup>a</sup>	60	0	48.7	48.4	60	29.9	60	60	60
Y <sup>b</sup>	3.9	15	0.5	0.5	0.5	8.2	0.5	0.5	0.5
pH	7.6	7.6	7.6	7.6	7.6	7.6	7.6	7.6	7.6
P <sup>c</sup>	0.5	0	0.5	0.5	0.5	0.3	0.5	0.5	0.5
Y <sup>d</sup>	23.2 $\pm$ 7.5	34.8 $\pm$ 5.7	125.0 $\pm$ 47.4	120.1 $\pm$ 44.5	8.3 $\pm$ 1.1	40.0 $\pm$ 25.0	1.7 $\pm$ 0.6	1.5 $\pm$ 0.5	0.12 $\pm$ 0.04

<sup>a</sup> G, Glucose (g/L), <sup>b</sup> Y, Yeast extract (g/L), <sup>c</sup> P, KH<sub>2</sub>PO<sub>4</sub> addition (g/L), <sup>d</sup> Y, Yield.

## 2.8. Effect of the Medium Composition on the Target Molecules

A selection of strains was used to replicate the experiment on media 6, 9, and 15. Medium 9 was chosen because the highest biomass for most of the strains was yielded here. Medium 15 was most similar to the optimized parameters for a high carotenoid content. Medium 6 was chosen for its reduced glucose and medium yeast extract content, which were thought to increase squalene content while promoting growth, as suggested by the optimized media in the regression of *T. striatum* N5997.

Cell dry weight (CDW) was determined in those strains that yielded the highest biomasses on medium 9 (N6007e, 5985, N6006d, 5996, N2820a, 5999). The mean CDW was 34.8  $\pm$  6.1% *w/w*. The highest amount of extract was obtained from *T. aureum* N6006d and 5985 and from *S. aggregatum* 5999 and N2820a on media 9 and 15 (Table S9). These extracts had a fatty appearance.

Carotenoid content varied between 0 and 346.1  $\mu$ g/g in the different strains and media (Figure 5). For all strains except *Thraustochytriidae* sp. N5670c and N4994d, the highest carotenoid content was measured when grown on medium 15, with maximum values of 343 and 346  $\mu$ g/g in *T. aureum* N6006d and 5985, respectively. The carotenoid compositions were consistent with those described in the cluster analysis. The media nevertheless had an influence on the exact carotenoid composition (Figure 6 and Table S10).



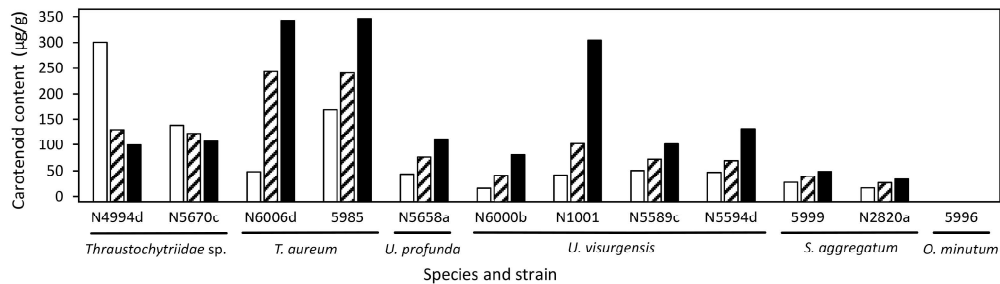


**Figure 5.** Carotenoid content in selected strains grown on DoE media 6 (empty bars), 9 (shaded bars), and 15 (filled bars).

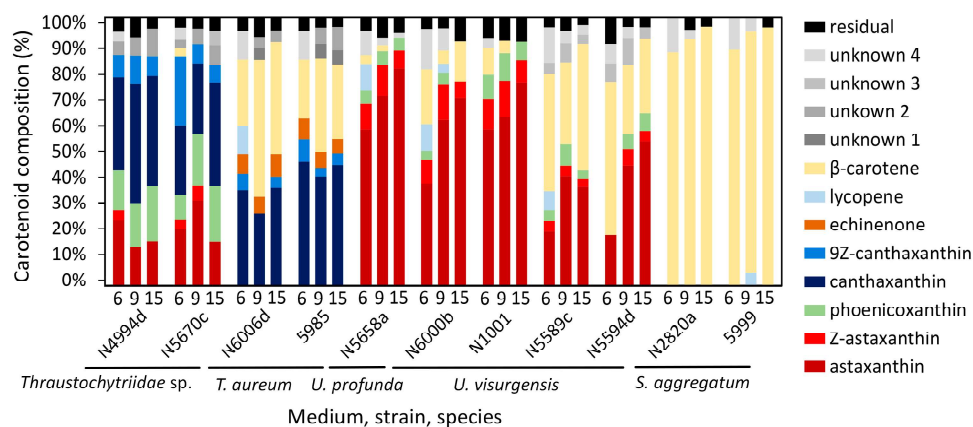


**Figure 6.** Carotenoid composition of the analyzed strains cultivated on medium 6, 9, and 15. Individually displayed are only carotenoids whose contribution to the total carotenoids was above 3% (Table S10). Diastereomers of astaxanthin are summarized as “Z-astaxanthin”.

The highest squalene content was most often reached on medium 6 (Figure 7). *S. aggregatum* N2820a and 5999 showed especially high squalene content on medium 6 but a generally low carotenoid content. The highest squalene content was 10.4 mg/g in *S. aggregatum* N2820a. *T. aureum* N6006d and 5985 as well as *Thraustochytriidae* sp. N5670c and N4994d showed the opposite pattern with generally high carotenoid but low squalene contents.

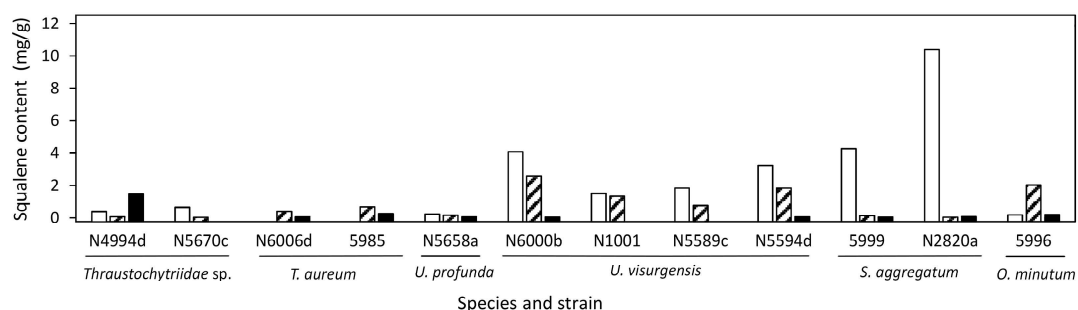


**Figure 7.** Squalene content in selected strains grown on DoE medium 6 (empty bars), 9 (shaded bars), and 15 (filled bars).



## 2.9. Comparison of Biomass Yield and Target Molecule Content in Cultures Cultivated in Liquid and on Solid Medium

Representative strains of four species with a high carotenoid production were chosen for a comparative study. *Thraustochytriidae* sp. N4994d, *T. aureum* N6006d, *U. profunda* N5658a, and *U. visurgensis* N1001 were cultivated on DoE medium 7 either in liquid or solid culture. In liquid culture, biomass densities of 1.1, 1.0, 0.6, and 0.7 g/L were reached for N4994d, N6006d, N5658a, and N1001, respectively. On solid medium, the CDW of the cultures scraped from the agar was 25.0, 30.7, 29.7, and 28.1% *w/w*, and biomass yields of 1.4, 1.8, 1.5, and 1.3 g/L were harvested for strains N4994d, N6006d, N5658a, and N1001, respectively. Extract yield was higher on the solid media (Table S9). The carotenoid content varied from 16 µg/g in N6006d in liquid medium to 218 µg/g in N4994d on solid medium (Figure 8). The carotenoid compositions of the strains cultivated on solid medium were similar to those observed in the previous experiment. *U. visurgensis* N1001 fitted to the other strains of the genus *Ulkenia*. A higher carotenoid content was measured in all strains cultivated on solid medium than in liquid medium. It was 1.3-fold higher in *U. profunda* N5658a and 3.8-fold higher in *T. aureum* N6006d. The carotenoid patterns changed according to the cultivation condition (Figure 8 and Table S11). The percentage of  $\beta$ -carotene increased in all strains when cultivated in liquid medium, whereas the percentage of astaxanthin, phenicoxanthin, and canthaxanthin decreased. *Thraustochytriidae* sp. N4994d exhibited the greatest differences in carotenoid composition when the cultivation medium was changed.

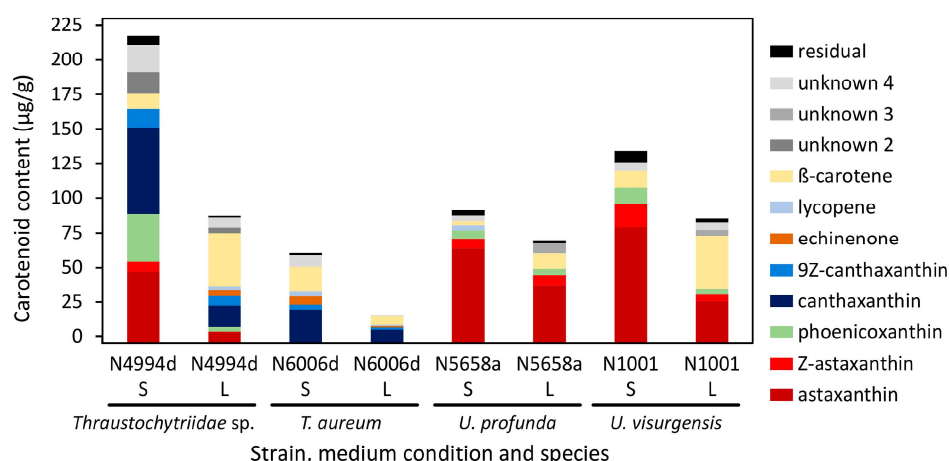


**Figure 8.** Carotenoid content and composition of four different strains cultivated on DoE medium 7 either in liquid (L) culture or on solid medium (S). Individually displayed are only carotenoids whose contribution to the total carotenoids was above 3% (Table S11). Diastereomers of astaxanthin are summarized as “Z-astaxanthin”.

Squalene content was similar in all strains except for N1001. For N4994d, N6006d, and N5658a, it varied between 0.3 and 0.7 mg/g when cultivated on solid medium and between 2.8 and 2.9 mg/g when cultivated in liquid medium. *U. visurgensis* N1001 showed higher contents of 6.0 and 8.6 mg/g when cultivated on solid and in liquid medium, respectively. Squalene was between 1.4 and 9.0 times higher when the cultivation was performed in liquid medium.

## 2.10. Unknown Metabolites

Besides those carotenoids that were identified by the comparison with standards, six other substances might be classified as carotenoids. Four of them exceeded the threshold of 3% applied for the cluster analysis and carotenoid patterns.



Unknown 1 was only present in all species belonging to *T. aureum*. Its retention time was very similar to that of phoenicoxanthin (9.0 min) but had a different absorption spectrum with a single maximum at 448 nm (Table 3). Unknowns 2 and 3 were present in various species. Retention times were at 10.4 and 14.8 min. They had similar UV/Vis absorption maxima as echinenone (461 nm and 462 nm, retention time at 16.5 min). The mass spectrum of unknown 2 had two main peaks at  $m/z$  566.4 and  $m/z$  549.8. Unknown 4 was present in *T. aureum*, *Thraustochytriidae* sp., *Ulkenia* spp., and *S. aggregatum*. Its retention time was 21.9 min, and it was close to that of astaxanthin monopalmitate and  $\beta$ -carotene. It had a characteristic UV/Vis absorption spectrum with two peaks and a shoulder and maxima at 461 nm and 489 nm.

**Table 3.** Retention times, UV/Vis absorption maxima, and masses of unknown substances found by UHPLC-PDA-MS chromatography in extracts of Thraustochytriaceae species. 1–4 carotenoids (assignment to strains and media in Tables S5–S8, S10, and S11), A–D porphyrins.

Substance	Retention Time (min)	$\lambda_{\max}$ (nm)	$m/z$	Species
Unknown 1	9.0	448	$584.3 \pm 1.1, 802.7 \pm 0.2$	<i>T. aureum</i>
Unknown 2	10.4	461	$549.8 \pm 0.7, 566.4 \pm 1.2$	<i>Ulkenia</i> spp., <i>Thraustochytriidae</i> sp., <i>T. aureum</i>
Unknown 3	14.8	462	n.d. <sup>1</sup>	<i>Ulkenia</i> spp., <i>Thraustochytriidae</i> sp., <i>T. striatum</i>
Unknown 4	21.9	461, 489, 439sh	n.d.	<i>Ulkenia</i> spp., <i>Thraustochytriidae</i> sp., <i>T. striatum</i> , <i>S. aggregatum</i>
Unknown A	5.9	415, 548, 582	n.d.	<i>O. minutum</i> N5995
Unknown B	6.3	400, 502, 538	n.d.	<i>O. minutum</i> N5995
Unknown C	6.8	401, 504, 538, 574, 628	$563.4 \pm 0.02$	<i>O. minutum</i> N5995
Unknown D	8.9	404, 508, 542	n.d.	<i>O. minutum</i> N5995

<sup>1</sup> n.d. = not detectable.

One group of substances was present in *O. minutum* N5995. It was only observed on DoE medium 14 with a high salt concentration. The substances had a very characteristic UV/Vis absorption spectrum. These were porphyrins rather than carotenoids. The substance with the highest peak (retention time at 6.8 min) had one large maximum at 401 nm and further small maxima at 504, 538, 574, and 628 nm. The main observed mass was  $m/z$  563.4, accompanied by further substances with similar absorption spectra.

## 2.11. Morphology

The studied strains differed in their morphology. Cell size varied from approximately 2 to 80  $\mu\text{m}$ , and different cell shapes were observed. Cell size and form varied not only between the different strains but also changed after the cultivation of the same strain in different media. All strains were compared after growth in B1TMG (2.5 mL), the basal medium and positive control for the subsequent growth and optimization studies. Most strains exhibited healthy cells in this medium (Figure 9). All strains had a wide cell size distribution at all observed growth phases. Strains closely related to *Ulkenia* spp. (Figure 9A–F) showed many globose cells with highly refractive cell walls. In *U. profunda* N5658a and *U. visurgensis* N5594d and Sakar 7, “hatching” cells were observed, i.e., the inner part of a cell slowly left its cell wall through a small spot (Figure 9D,E). The cell wall remained nearly intact. The resulting protoplasts were perfectly globose and did not resemble an amoeba. This behavior was observed in mature and comparably large cells. *T. aureum* N6006d and N6007e (Figure 9S,T) also formed round cells but were more densely packed. Their cell walls were not as refractive as in *Ulkenia* spp. except for some larger cells ( $>25 \mu\text{m}$ ). *T. aureum* 5985 (Figure 9U) differed from the other two strains with generally larger and more irregular cells. *T. kinnei* N1694d and N1476c (Figure 9O,P) formed more clusters with fewer single cells. The cells of *S. aggregatum* 561bx, N2820a, and 5999 (Figure 9I–K) had a granular sub-structure. *S. aggregatum* 561bx, in particular, showed intracellular bodies. Single cells of *S. aggregatum* were among the largest observed (30–50  $\mu\text{m}$ ), and dense clusters of cells with difficult to distinguish and irregularly shaped cells were observed in medium 3. *O. minutum* N5995 and especially 5996 (Figure 9M,N)



formed clusters of comparably small cells. In cultures of *T. striatum* N5997 (Figure 9L), the largest cells up to 80  $\mu\text{m}$  were observed. Its cells exhibited finer and coarser substructures and vacuole-like compartments. *Thraustochytriidae* sp. N5670c and N4994d (Figure 9Q,R) were more dispersed and showed smaller agglomerates with smaller cells and cellular structures that might have been small sporangia (10–15  $\mu\text{m}$ ). Their substructure was very fine and smooth. All the named strains formed some agglomerates. *T. aggregatum* 4992b and N4930a (Figure 9G,H) differed from them by their very equally distributed small or medium-sized cells compared to the other strains.

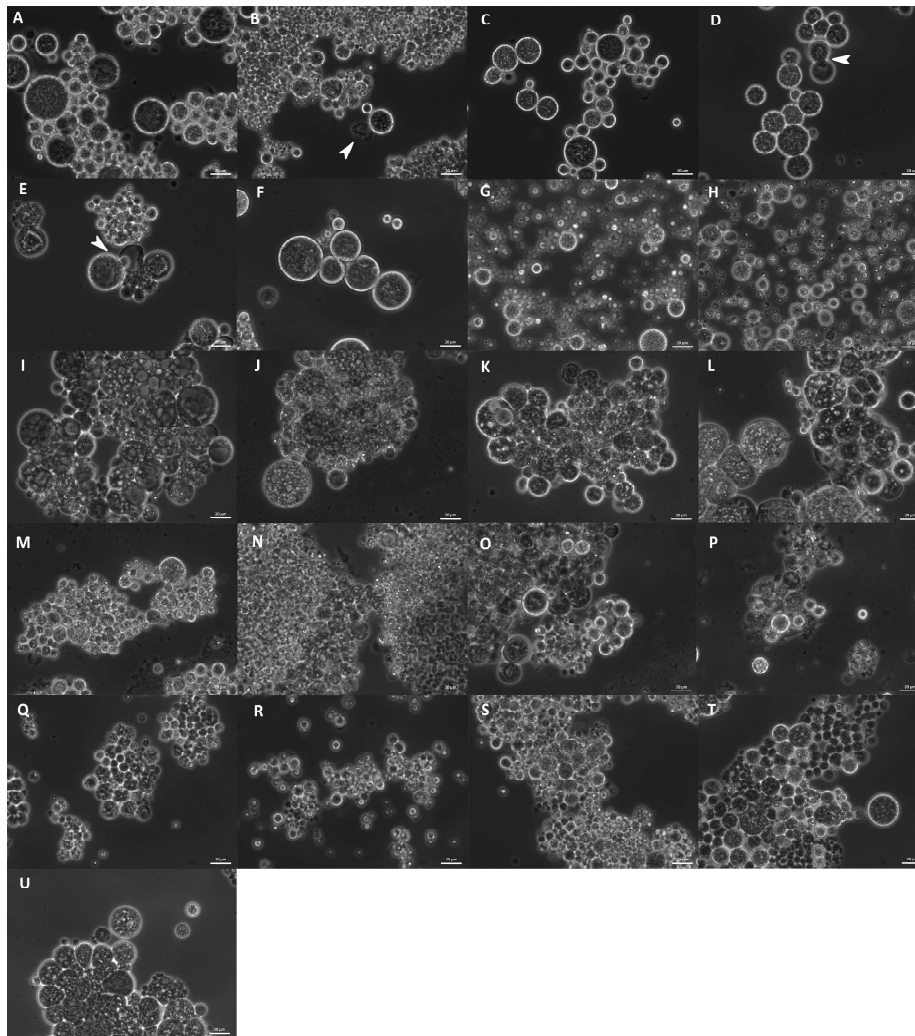


**Figure 9.** Morphology of various strains observed in BITMG medium after cultivation in microtiter plates. *U. profunda* N5905 (A), N5658a (B), *U. visurgensis* 6000b (C), Sakar7 (D), N5594d (E), N5589c (F), *T. aggregatum* 4992b (G), N4930a (H), *S. aggregatum* 561bx (I), N2820a (J), 5999 (K), *T. striatum* 5997 (L), *O. minutum* N5995 (M), 5996 (N), *T. kinnei* N1694d (O), 1476c (P), *Thraustochytriidae* sp. N5670c (Q), N4994d (R), *T. aureum* N6006d (S), N6007e (T), and 5985 (U). Arrowheads indicate “hatching” cells and their cell wall remnants. All figures are in identical scale, scale bars show 20  $\mu\text{m}$ .



When comparing the morphology of strains grown under different nutrient conditions (Figures S3–S6), it was not possible to clearly detect patterns in morphological change between the different media and strains. The formation of agglomerates generally increased in the DoE media. *T. aggregatum* N4930a, 4992b mainly remained dispersed. Strains related to *S. aggregatum* showed clusters of amorphous cells, especially in medium 3. Irregularly shaped cells were more frequently detected in media 3 and 6 compared to the other media for most strains. Some phenomena were observed in the different genera, which might underline their taxonomic peculiarities.

In addition to *Ulkenia* spp., “hatching” cells were observed in *T. striatum* N5997 and *T. kinnei* N1694d. These cells were mature and comparably large. Thus, the remaining cell wall remnants were also comparably large (up to 20 µm) and often slightly deformed. Similar empty cell walls were also observed in *T. aureum* N6007e (Figure S5T) but without the phenomenon of “hatching” cells. Microscopic observation suggests the development of sporangia only in a few strains. Few cells containing several spore-like cells were observed (Figure 10), e.g., in *T. aureum* N6006d and N6007e, *S. aggregatum* 561bx, N2820a, and 5999, *T. striatum* N5997, and *Thraustochytriidae* sp. N5670c. However, flagella as proof for zoospores were not observed, possibly due to the resolution. It might be that only aplanospores were built. These sporangia were also observed in the 7-day-old cultures used for inoculation, in *T. striatum* N5997, *T. aureum* N6006d and N6007e, *Thraustochytriidae* sp. N4994d, N4995d, and N5670c, and *U. visurgensis* 5594d.

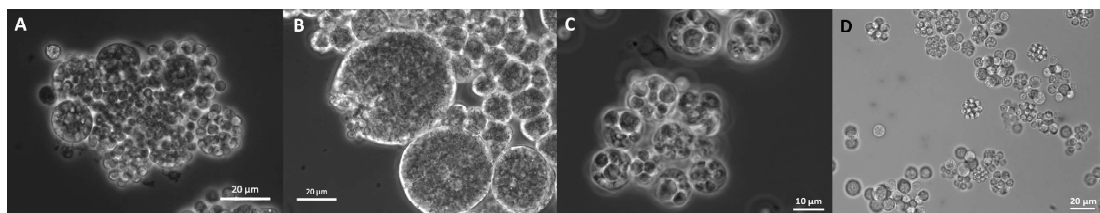


**Figure 10.** Sporangia in *T. aureum* N6006d (medium 12) (A), *T. striatum* N5997 (B1TMG, inoculation culture) (B), *Thraustochytriidae* N5670c (B1TMG) (C), and N4994d (B1TMG, inoculation culture) (D).

Most strains formed an ectoplasmic net (EN) on the bottom of the well. Intact and whole structures of ENs were only visible in the cultures analyzed by inverted microscopy (Figure 11A). It was observed in *S. aggregatum* 561bx, N2820a, 5999, *O. minutum* N5995, 5996, *T. aureum* N6006d, N6007e, *T. kinnei* N1476c, N1694d, and *T. striatum* N5997. Additionally, *S. aggregatum* 561bx, N2820a, 5999, and *O. minutum* N5995 formed a knot-like structure within their EN. Those structures were smaller than any cells in the culture and showed the same light refraction in the microscope as the EN (Figure 11A,B).

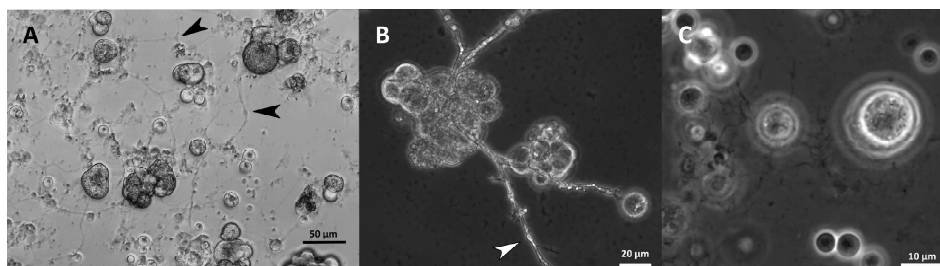


**Figure 11.** EN with knot-like structures in *S. aggregatum* 561bx (medium 3, analyzed by inverted microscopy) (A), and 5999 (medium 12) (B), fine EN of *O. minutum* 5996 (medium 12) (C). Black and white arrowheads indicate knot-like structures in the net.



Structures that appeared like “empty cells” or membranes were observed. Their size varied, but they were primarily small ( $<10\ \mu\text{m}$ ) and round without deformations (Figure 12A). They seemed primarily empty but sometimes contained smaller spheres or thread-like structures (Figure 12B,C). They appeared in all analyzed species and most strains with varying abundance. Thin, elongated, and branched cellular substructures were observed exclusively in *O. minutum* N5995 and in the strains that were closely related to *T. kinnei*. They sometimes appeared together with very small, globose granules. The structures were found in medium 12 and, to a lesser extent, in medium 14 (Figure 12E). They also occurred in *T. kinnei* N1709d and 3041c in the cultures used for inoculation of the experiments in B1TMG (Figure 12D).

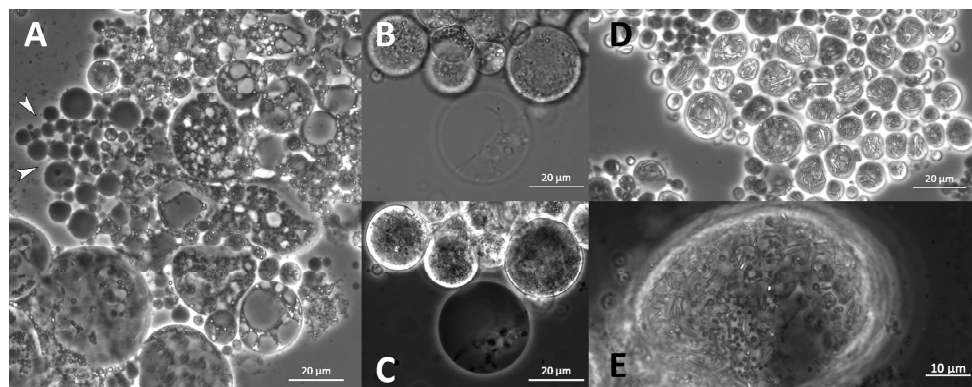


**Figure 12.** Empty cell structures indicated with white arrowheads observed in B1TMG inoculation cultures of *T. striatum* N5997 (A) and *T. kinnei* N1694d in bright-field (B) and phase-contrast microscopy (C). Oblong cellular substructures in *T. kinnei* 3041c (B1TMG, inoculation culture) (D) and together with small granules in N1694d (medium 12) (E).

In some media, the cells exhibited round or oval vacuole-like inclusions, pushing the protoplast to the edge of the cell, resulting in a ring or crescent shape (Figure 13). They appeared in all analyzed species and most strains with varying but primarily low abundance.

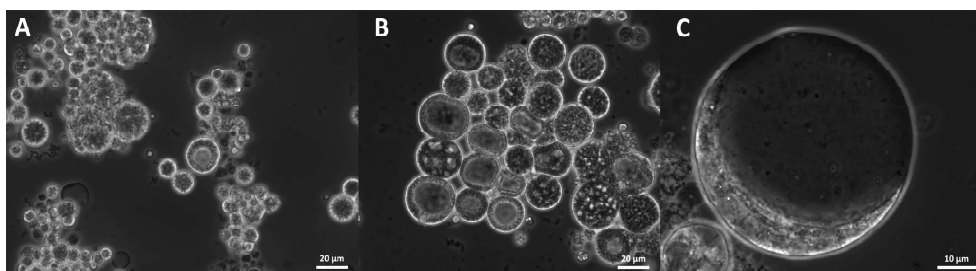


**Figure 13.** Ring-shaped cell interior of *T. aureum* N6007e (medium 12) (A), *U. visurgensis* N5594d (medium 12) (B), and crescent-shaped cell interior of *T. striatum* N5997 (medium 14) (C).

A polymer-like structure was observed (Figure 14). Mostly it floated on the medium surface of some culture wells and was even macroscopically perceptible. This structure consisted of small subglobose grains, which were also visible on the surface of the cells and surrounded them. It was noticed in all analyzed strains related to *S. aggregatum*, *T. aureum*, *T. aggregatum*, *Thraustochytriidae* sp., *T. kinnei*, and *T. striatum*, but only in some related to *O. minutum* (N5995) and *Ulkenia* spp. (*U. profunda* N5658a, *U. visurgensis* N6000b, Sakar7). It occurred predominantly in medium 3 and to a lesser extent in the other DoE media but never in B1TMG.



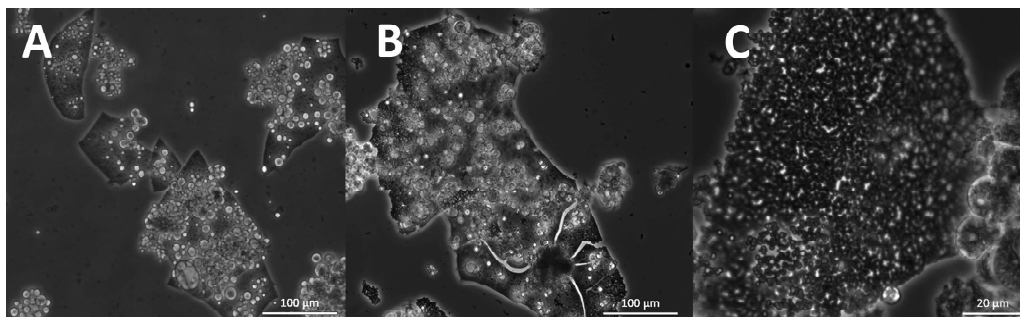


**Figure 14.** Polymer-like structure in *T. aureum* N6007e (medium 12) (A), *T. kinnei* N1476c (medium 3) (B), and *T. striatum* N5997 (medium 3) (C).

A further characteristic was observed in all strains related to *T. aggregatum*. They showed a distinct color switch from pale white to brownish-red on some of the solid media of the DoE. The color was media- and time-dependent, as some cultures were initially white and turned red over time, although not in a gradual color change but in a sharp transition.

### 3. Discussion

Uncertain or outdated strain denomination in the literature is a common problem in Thraustochytriaceae research. Many strains are not characterized at species level or are even assigned to the wrong genus. There is high uncertainty, especially regarding the genus *Schizochytrium*. Many of the strains used today still are addressed as members of the genus *Schizochytrium*, although 18S rRNA data reveal a closer relationship to *Aurantiochytrium* sp. than to *Schizochytrium sensu stricto* as proposed by Yokoyama and Honda in 2007 [63]. Accordingly, some strains used for comparison, whose 18S rRNA sequences were obtained from the GenBank database or publications, were reclassified according to their closest relatives, where appropriate. All strains whose 18S rRNA sequences were reviewed by comparison with the dataset are marked with an asterisk in the following text and can be found in Table S12 and the phylogenetic tree (Figure 1), where possible.

#### 3.1. Molecular Identification

The strains of the collection were assigned to eight different clades within the Thraustochytriaceae. One group of strains was closer related to the Rhizophydiales. The phylogenetic tree obtained is essentially similar to those in recent publications [63–65,78,87–91]. It was divided into two main clades, one containing only Thraustochytriaceae and one comprising Thraustochytriaceae and the Labyrinthulaceae. Strains N557a and N1694d were assigned to *S. aggregatum* and *T. kinnei*, respectively. This corresponds to their previous classification [61,62,92].

#### 3.2. Growth Studies

For most strains, glucose and yeast extract concentrations up to the maximum level were considered best for optimal growth. The linear influence of yeast extract was most important, as it was significant for the growth of 93% of the tested strains. This is in agreement with studies for various members of the Thraustochytriaceae. Stefánsson et al. reported in a similar experiment that the influence of the yeast extract was the most positive and only significant factor in their growth model for an isolate (St5) possibly closely related to *T. kinnei* [87]. *T. aureum* ATCC 34304 was reported to show highest growth at maximum yeast extract (2.5 g/L), peptone (2.5 g/L), and glucose (30 g/L) concentration [93]. Previous studies from Bahnweg, who worked in part with strains of the former KMPB collection, indicated higher nitrogen levels in the form of L-glutamate to generally increase the maximum yield of various strains and genera [92]. Optimal growth for most strains



studied here was predicted at the highest yeast extract concentration of 15 g/L used in the experiments, indicating that their optimum might be even higher. In a model developed for *Aurantiochytrium* sp. UMACC-T023\*, the sum of maximum yeast extract (20 g/L) and peptone (20 g/L) concentrations was considered optimal for high growth. However, here the glucose concentration was considered best for growth at its minimum of 10 g/L [94]. In this study, a significant influence of the glucose concentration on growth was observed for nearly 75% of the strains. Maximum glucose concentrations of up to 60 g/L were predicted to be optimal for most of the strains. Again, the fact that this was the highest concentration used and the insignificance of the quadratic term in the model for glucose concentration indicated that the optimum growth of the strains might be achieved well above 60 g/L glucose. The aforementioned isolate St5 was shown to reach optimal biomass at a glucose concentration of 77.6 g/L [87] and *Aurantiochytrium* sp. ONC-T18\* at 60 g/L [95]. *Schizochytrium* sp. G13/2S still grew well between 100 and 200 g/L [96]. Gupta et al. reported optimum growth of *T. aureum* AMCQS5-5\* when cultivated in media containing 40 g/L glucose, though no clear change between 5 and 100 g/L [74].

The C/N ratio was shown to be important, and the highest growth was achieved at C/N between 2 and 4 [74]. Similarly, a low C/N ratio of 5 was advantageous over higher ratios for the growth of *A. limacinum* ICTSG-17\* [19] and *Aurantiochytrium* sp. ATCC 26185\* [97]. Comparably high C/N ratios of 27.2 and 54.4 increased the growth of *Aurantiochytrium* sp. ATCC PRA-276 as opposed to a ratio of 4 [97]. These differences show that an optimal C/N ratio is possibly very strain-specific and the optimal value also seems to depend on the nitrogen source [74]. In these experiments, the C/N ratio was not regressed, but most of the strains evaluated by regression model two favored high glucose and yeast extract concentrations, indicating a positive influence of a comparably lower C/N ratio.

Thraustochytrids appear to be euryhaline. Optimal salt concentration for growth varied between 2.0% and 2.5% NaCl in various Thraustochytriaceae [92,98] or 25 and 30 practical salinity units (PSU) in several strains of *Aurantiochytrium* sp. [99]. *T. aureum* grew best between 15 and 20 g/L salt concentration [93,100,101]. *Aurantiochytrium* sp. ONC-T18\* grew best on a lower salt concentration of 2 g/L [95]. The highest cell dry weight in *A. limacinum* ICTSG-17\* was reached in a medium prepared with seawater, but the growth did not decrease much with lower salinity. It was even able to grow at 0‰ [19]. Other authors showed that growth was inhibited by very low salt concentrations [102]. Few strains, which belonged to *T. aureum* and *S. aggregatum*, were able to grow at 0.1% NaCl and not very well [92]. In contrast, several Thraustochytriaceae grew optimally at salinity levels between 3.5 and 4.2‰ and survived even higher concentrations [102,103]. Our results revealed no significant difference in growth of most strains depending on a salinity between 1.5‰ and 3.0‰. Only some species belonging to the genus *Ulkenia* showed a significant need for a higher salt concentration. Bahnweg did not show this for an *Ulkenia* strain [92], but this might be species and strain dependent. Adaption to the condition might also influence growth (see below).

The influence of the initial pH was not considered significant for most strains in the tested range between pH 6.5 and 7.6. This is similar to results of Stefánsson et al., who found a positive but insignificant effect of the pH on the growth of their isolate St5 between pH 6 and 8 [87]. The highest biomass of *A. limacinum* ICTSG-17\* was measured in a pH range of 6–7 [19]. In several other strains of *Aurantiochytrium*, the optimum was between 6.5 and 7.5 [99]. Bahnweg observed optima between 6.0 and 8.0 for various Thraustochytriaceae strains [92]. Some authors mentioned an increase in pH in a pH-uncontrolled environment [19,104], which could be confirmed here.

The addition of phosphate ( $\text{KH}_2\text{PO}_4$ ) did not influence the growth of the strains significantly. Its effect was not uniform either. Stefánsson et al. reported a negative but insignificant influence of the  $\text{KH}_2\text{PO}_4$  concentration between 0 and 0.1 g/L on the growth of their isolate [87].

A replacement of the media components might further enhance growth. For example, glycerol improved the growth in various Thraustochytriaceae [74,105]. Optimal nitrogen



sources were discussed. Those of marine origin were reported to increase growth compared to yeast extract and tryptone [87]. Temperature and light influenced growth as well [92,99,103]. Various Thraustochytriaceae were shown to have a quite wide temperature range (9–30 °C), except for some Antarctic isolates [92].

Regression quality of the growth data of some strains and genera was limited. Insufficient adaptation of the strains to the new media might have biased the data. All DoE trials were inoculated from the same liquid medium, so the strains had to adapt to some more than others, changing their ability to grow and produce metabolites. The change of medium solidity also influenced growth at otherwise constant parameters. For example, *U. profunda* N5905 did not grow on the solid media with a low (15 g/L) salt concentration but in the same media provided in the liquid form prepared for the morphological observations. It was inoculated from a stock medium with a salt concentration of 30 g/L, and the shock of low salt concentration and solid medium was possibly too high. In contrast, it was able to adapt to the liquid environment. It was observed (data not published) that a rapid change in medium composition and solidity inhibited the growth of some strains, whereas they were able to adapt to more gradual changes, especially if grown in liquid media. We assume that the thraustochytrids can adapt to various environmental conditions if given the chance.

Screening many novel isolates and strains with varying characteristics and needs is challenging. Reduced factorial design of experiments combined with regression analysis was a valuable tool for approaching the strain collection. An impression of growth-promoting parameters was obtained. For a robust regression and to increase accuracy, a sufficient number of experiments must be performed to also evaluate the influence of interaction terms.

### 3.3. Comparison of Growth Analysis and Taxonomy

The screening was designed to determine and compare the growth behavior of possibly closely related strains. As nearly all strains preferred the media with high glucose and yeast extract concentration, a distinction was difficult. Coherent deviating behavior was found in both analyzed strains of *U. visurgensis*: Sakar 7 and N6000b, and of *T. aggregatum*: 4992b and 154f. They were closely related, showed intermediate glucose optima and, with the exception of Sakar7, intermediate yeast extract optima. Strains N5905, N5976, N5658a, and N5629e were closely related to *U. profunda* based on the molecular taxonomy. N5905, N5976, and N5629e did nearly not grow on solid media with a salt concentration of 15 g/L. When the medium was supplied with 30 g/L salt, N5905 and N5629e yielded the highest biomass on media with low or very low glucose and yeast extract concentrations. Similarly, *U. profunda* N5658a had comparably low glucose and yeast extract maxima. All these strains were closely related, indicating unique characteristics of *U. profunda*.

Most strains yielded mean biomass yields of below 2 g/L. *T. aureum* N6006d, N6007e, and 5985, as well as *T. aggregatum* 4992b, 154f, and *T. striatum* N5997 yielded higher mean biomasses of above 4 g/L. The strains belonging to *T. aureum* and *T. striatum* were more closely related to each other than to *T. aggregatum* based on the 18S rRNA phylogeny. *T. aureum* N5998, which was identical to N6006d and N6007e based on its 18S rRNA genes, yielded a much lower medium biomass of below 2 g/L. Thus, characteristics may be very strain specific. Based on the obtained growth results, a precise and well-distinguished differentiation of all the tested strains is difficult. The growth parameters are not suitable to support the taxonomic classification.

### 3.4. Carotenoids

The production chain of carotenoids in thraustochytrids was proposed to include  $\beta$ -carotene,  $\beta$ -cryptoxanthin, echinenone, hydroxyechinenone, canthaxanthin, zeaxanthin, phoenicoxanthin, adonixanthin and astaxanthin [21,80,83]. The following carotenoids were found in species of the Thraustochytriaceae: astaxanthin, canthaxanthin, echinenone,  $\beta$ -carotene, and rarely also lutein, zeaxanthin, lycopene, and astaxanthin esters and iso-



mers [21,74,81,82,97,106–108]. Although there are few comparative datasets for the carotenoid patterns of thraustochytrids [63,64], individual strains have been described.

Astaxanthin, phoenicoxanthin, echinenone, and  $\beta$ -carotene have been reported in *Ulkenia* sp. SEK 214\* and ATCC 28207\* [64]. This is similar to the carotenoids observed in these experiments in all strains closely related to *Ulkenia* species. Additionally, small proportions of lycopene and an unknown carotenoid were observed in *U. profunda* N5658a.

*Schizochytrium sensu stricto* (e.g., *S. aggregatum* ATCC 28209\*, *Schizochytrium* sp. SEK210\*, *Schizochytrium* sp. SEK 345\*) was reported to form light yellow colonies with  $\beta$ -carotene only [63]. This is in general agreement with the results obtained for the strains closely related to the named species. However, besides  $\beta$ -carotene, small proportions of lycopene and an unknown carotenoid were observed. The strains produced a total carotenoid content of up to 49  $\mu\text{g/g}$ .

*T. aureum* was reported to contain up to 44  $\mu\text{g/g}$  of carotenoids but without further differentiation [109]. *T. aureum* AMCQS5-5\* and AMCQS5-3\* produced primarily canthaxanthin, followed by echinenone and  $\beta$ -carotene with a total of up to 68.5  $\mu\text{g/g}$  and no astaxanthin [74]. This is largely consistent with the results obtained in this study. Here, mainly canthaxanthin and  $\beta$ -carotene but also echinenone were observed. A total carotenoid content of up to 346  $\mu\text{g/mg}$  was measured depending on the medium.

There was also little information on carotenoids in strains closely related to *Thraustochytriidae* sp. N4994d, N4995d, N5670c, such as *Labyrinthulochytrium* spp., whose colonies were reported to be grayish white [110,111], possibly depending on the medium. Strains N4994d, N4995d, and N5670c were also colorless on some DoE media. Another related strain found was *Phycophthorum* sp. RT2316-16\* [112]. It contained mainly canthaxanthin (86.5–87.4%), followed by astaxanthin and  $\beta$ -carotene in similar proportions, depending on the cultivation conditions [106]. It reached a total carotenoid content from 64 to above 200  $\mu\text{g/g}$  [106,112,113]. Canthaxanthin also had the highest proportion of carotenoids in *Thraustochytriidae* sp. N4994d, N4995d, and N5670c in the form of all-*E*-canthaxanthin and 9*Z*-canthaxanthin, followed by astaxanthin and phoenicoxanthin, indicating a possible relationship to *Phycophthorum* sp. RT2316-16\*.

The analyzed carotenoids in *T. striatum* N5997 were mainly astaxanthin (mean of 85% in total), followed by significantly lower proportions of phoenicoxanthin, canthaxanthin, lycopene,  $\beta$ -carotene, and two unknown components. *T. striatum* N5997 had a mean carotenoid content of 42  $\mu\text{g/g}$  in the DoE and a maximum content of 69  $\mu\text{g/g}$  (medium 15). Yokoyama et al. [63] analyzed *T. striatum* ATCC 24473\* and found the same carotenoids except for lycopene. In the same strain, up to 600  $\mu\text{g/g}$  astaxanthin under pH stress conditions was reported. Additionally, zeaxanthin, canthaxanthin, echinenone,  $\beta$ -cryptoxanthin, and  $\beta$ -carotene occurred [114]. In *T. striatum* AL16\*, mainly astaxanthin and zeaxanthin, and up to 12  $\mu\text{g/g}$  of total carotenoids were detected [115]. Singh et al. analyzed *T. striatum* S7\* and reported astaxanthin (67  $\mu\text{g/g}$ ) as main carotenoid, followed by canthaxanthin (20  $\mu\text{g/g}$ ), echinenone (17  $\mu\text{g/g}$ ), and  $\beta$ -carotene (11  $\mu\text{g/g}$ ) [81].

Yokoyama et al. observed canthaxanthin, echinenone, and  $\beta$ -carotene in *Oblongichytrium* sp. SEK347\* [63], but no carotenoids were measured in *O. minutum* N5995 and 5996.

Astaxanthin, phoenicoxanthin, canthaxanthin, echinenone, and  $\beta$ -carotene were identified in *Aurantiochytrium* sp. ATCC 26185\* and *Aurantiochytrium* sp. ATCC PRA-276 with maximum values of 77 and 180  $\mu\text{g/g}$  total carotenoids, respectively. Their carotenoid profiles varied with the culture conditions [97]. Burja et al. measured  $\beta$ -carotene, echinenone, canthaxanthin, zeaxanthin, and astaxanthin in their strain *Aurantiochytrium* sp. ONC-T18\* [95]. Major carotenoids in *Aurantiochytrium* sp. S31\* (ATCC 20888) were either  $\beta$ -carotene and astaxanthin [104] or astaxanthin, canthaxanthin, and echinenone [74]. In *Aurantiochytrium* sp. AMCQS1-9\*, only  $\beta$ -carotene was reported [74], although phylogeny implied a close relationship to *Aurantiochytrium*\* sp. S31. Astaxanthin, phoenicoxanthin, canthaxanthin, echinenone, and  $\beta$ -carotene were observed in *Aurantiochytrium* CHN-1\* with a total of almost 450  $\mu\text{g/g}$  [82].



The genus *Aurantiochytrium* seems very potent concerning carotenoid production, although the reported results vary. This clade might be much larger than previously assumed and is currently not very well structured. A clearer organization of the contained species and strains and carotenoid production under coherent conditions need to be achieved for further insight into the applicability of chemotaxonomy in this clade. Meanwhile, other thraustochytrids may be underexplored concerning their carotenoid synthesis potential. *T. aureum* and *Thraustochytriidae* sp. had the highest mean measured carotenoid content and comprised the strains with the highest carotenoid content of all on individual media: *T. aureum* 5985 produced 346 µg/g of carotenoids (medium 15) and *Thraustochytriidae* sp. N4994d 300 µg/g (medium 6). Most strains belonging to *T. aureum* produced comparably high biomasses, and thus the total carotenoid production was high. The clade of *T. striatum* might also contain good carotenoid production strains. As indicated by comparison with the literature, exact yields might be strain specific but also dependent on the culture conditions and may be improved.

#### 3.4.1. Cluster Analysis of Carotenoid Composition

Cluster analysis of carotenoid composition detected nine main carotenoid clusters. *U. profunda* N5905 and N5629e carotenoid data were limited to salt condition media, as these strains grew mainly on media with a high salt concentration. The dendrogram obtained by hierarchical clustering mirrored k-means clusters and added a level of detail. The k-means clusters were comparable to the clades created by the phylogenetic tree based on 18S rRNA gene sequences.

Direct comparison of the clusters based on the carotenoids with the phylogenetic tree revealed high similarities. All strains closely related to *Thraustochytriidae* sp. were clustered, as well as those belonging to *Ulkenia* spp., *S. aggregatum*, and *T. aureum*. *T. striatum* N5997 was placed close to the *Ulkenia* species, which is also evident in the phylogenetic tree. Its phylogenetic relationship to *Thraustochytriidae* sp. was not displayed by the dendrogram based on carotenoid patterns. The division of the *Ulkenia* species into different subgroups based on their carotenoid profiles is generally similar to the 18S rRNA data. Adding the strains that only grew on a higher salt concentration increased the robustness of the clustering. *U. profunda* N5658a, N5905, and N5629e formed one clade in both dendrograms. In *U. visurgensis*, two slightly separated clades (Sakar 7 and N6000b/N5594d and N5589c) were identified by both methods. A difference was the separation of *T. aureum* N5998 from the other members of this group, especially from N6006d and N6007e. These three strains were taxonomically identical on an 18S rRNA basis.

On a greater scale, strains belonging to *Thraustochytriidae* sp. and *T. aureum* built one larger clade based on carotenoid profiles, and *T. striatum* N5997 clustered close to *Ulkenia* spp. However, in the molecular phylogeny, *Thraustochytriidae* sp. was most related to *Ulkenia* spp., which together shared a common ancestor with *T. striatum*. *T. aureum* was least related to all of them. *S. aggregatum* species were clearly distinct from all other clades based on 18S rRNA and carotenoid-based taxonomy.

Carotenoid patterns might support phylogenetic studies and help assign strains to a particular genus or even species. However, chemotaxonomic markers alone cannot explain the relationship between the different clades. Fossier Marchan et al. [116] stated in their review that the genus *Thraustochytrium* does not form a monophyletic group and that no common carotenoid profiles were observed. We agree with the first part and argue that the phylogenetic classification of not only the genus *Thraustochytrium*, but also the entire family of Thraustochytriaceae needs a comprehensive and coherent revision. However, we also conclude that the carotenoid profiles are coherent enough to provide chemotaxonomic support to an 18S rRNA gene and morphology-based approach. Carotenoid compositions of individual strains of a species were similar, but the detailed composition changed depending on the medium. Thus, an agreement on how to collect such data must be reached. The detailed individual carotenoid composition and yield of a strain, and to some



extent its growth behavior, might help to further distinguish strains with highly similar 18S rRNA sequences, providing an approach for a polyphasic taxonomy.

### 3.4.2. Carotenoid Regression

Strain *T. striatum* N5997 was characterized by a relatively constant carotenoid production on most DoE media. Therefore, it was chosen for closer identification of carotenoid production parameters. The optimized regression for growth showed a high affinity for glucose but low yeast extract concentration. Shene et al. showed the highest growth in *T. striatum* AL16\* at a maltose concentration of 60 g/L compared to lower concentrations [115]. In *T. striatum* ATCC 24473\*, the highest biomass was yielded between glucose concentrations of 30 and 40 g/L and 4 and 20 g/L yeast extract and peptone [114,117]. The growth of *T. striatum* N5997 was even inhibited by high yeast extract concentrations.

Maximum content of most carotenoids was predicted at high glucose (48.4–60 g/L) and minimum yeast extract concentration (0.5 g/L), at maximum pH (6.7), and maximum phosphate addition (0.5 g/L). Similarly, higher carotenoid yields in *T. striatum* AL16\* at increasing maltose levels were demonstrated [115]. Xiao et al. demonstrated increasing astaxanthin content in the cells using either maximum glucose concentration (100 g/L) or low yeast extract and peptone concentration (2–4 g/L) in *T. striatum* ATCC 24473\*. They also showed that astaxanthin yield decreased at glucose concentrations higher than 50 g/L because of decreasing cell mass [114]. This was not shown here, possibly because the experiments were limited to glucose concentrations of 60 g/L. A high carbon-to-nitrogen (C/N) ratio seemed favorable for a high carotenoid content.

The carotenoids changed depending on the C/N ratio in *Aurantiochytrium* sp. S31\* (ATCC 20888). Particularly high (75:5) and low (75:30) C/N ratios resulted in high carotenoid content (85–89 µg/g). The high ratio also caused a shift in the carotenoid pattern in favor of astaxanthin, the proportion of which exceeded that of β-carotene [104]. Such a drastic change in carotenoid composition was not observed in our experiments. Furlan et al. [97] reported that generally lower C/N ratios favored a high carotenoid concentration in batch cultures and that changes in cultivation conditions impacted the carotenoid profiles of *Aurantiochytrium* sp. ATCC 26185\* and ATCC PRA-276. Increased production of carotenoids and fatty acids under stress conditions like nitrogen starvation is also known in various microalgae [118]. Like in microalgae, carotenoid production in thraustochytrids seems to be correlated with the production of fatty acids [113], and factors influencing fatty acid production are likely to influence carotenoid production as well.

Increasing KH<sub>2</sub>PO<sub>4</sub> concentration (up to 0.5 g/L) was reported to have a beneficial influence on the carotenoid concentration of *Aurantiochytrium* sp. S31\* and also to change the proportion of individual carotenoids [104]. The prediction for optimal carotenoid content and yield in *T. striatum* N5997 indicated the maximum phosphate level as favorable.

Carotenoid production might be further improved, and carotenoid profiles might be manipulated by the replacement of, e.g., the carbon source [74,104,106,115]. It also depends on environmental factors such as temperature and aeration and is likely to be influenced by light [19,21,114]. Overall, the carotenoid pattern varied with changing medium composition. Such a varying composition was also reported in *T. striatum* S7\* and other Thraustochytriaceae during cultivation [81–83,112]. Finding the optimal time for harvesting is another approach to maximizing carotenoid yield.

### 3.5. Squalene

Squalene has been observed mainly in *Aurantiochytrium* sp. [69–71,119–123], and to minor extents in *Schizochytrium* sp. ACEM 6063 [124], strains closely related to *T. aureum*, *T. striatum*, *Oblongichytrium* sp., *Parietichytrium* sp., *Botryochytrium* sp., and *Ulkenia* sp. [120]. Squalene was found in all strains analyzed in this study. Thus, the majority of the family of Thraustochytriaceae might be able to produce squalene under certain circumstances. The highest squalene contents observed were 13 mg/g and 12 mg/g in *T. striatum* N5997 on medium 11 and *O. minutum* N5995 on medium 16 with a high salt concentration,



respectively, and 10.4 mg/g in *S. aggregatum* N2820a on medium 6. This is less than the 317 mg/g found in *Aurantiochytrium* sp. [120]. Still, it might be worth examining other members of the Thraustochytriaceae for squalene production and optimizing cultivation parameters further, especially as growth and biomass density are equally important for high total yields, as also Aasen et al. [80] stated. To our knowledge there has been no description of squalene in *T. kinnei*, and *T. aggregatum*. The results show that even within clades of closely related species, the variance in productivity may be high. High differences in squalene production by closely related strains belonging to *Aurantiochytrium* and *Hondea* were described [125].

Studies showed that squalene synthesis depends on the nitrogen source and that yeast extract concentrations of 2.5 or 6 g/L were optimal concerning squalene content and yield in *Aurantiochytrium* sp.\* [121,126]. However, evaluating such values in isolation from other parameters is difficult. A mixture of different nitrogen sources positively influenced squalene content and yield in *Aurantiochytrium*\* sp. BR-MP4-A1 [121]. The model developed for *T. striatum* N5997 generally implied a higher yeast extract concentration of 15 g/L as beneficial for high squalene content. However, such a high yeast extract concentration did not increase the biomass yield, and thus optimal squalene yield was estimated at 8.2 g/L yeast extract. The opposite correlation was shown for the glucose concentration. Here, the squalene content was predicted to be high when no glucose was provided in the medium, but growth was low. This contrasts studies that found glucose concentrations of 20–30 g/L to be optimal for squalene yield and content in *A. mangrovei* and *Aurantiochytrium* sp.\* [79,126]. Again, a cross-genus comparison must be considered with caution.

There are also contrasting studies about the temporary course of squalene formation. Squalene content was reported to increase over 1 to 8 days of the experiment [122] or to decrease slightly between day 4 and 12 [119]. Other studies showed a rapidly decreasing squalene content after the initial stage of cultivation [79,127], which was correlated to lipid accumulation [127]. Increased squalene and carotenoid content were reported in *A. limacinum* B4D1\* by adding methanol or butanol, which was correlated to a change in lipid composition, especially a decrease in docosahexaenoic acid (DHA) [108,128]. Squalene is the first step in sterol synthesis [124] and necessary for membrane building. Squalene synthesis was correlated to other factors such as temperature, carbon and nitrogen source, dissolved oxygen, and NaCl concentration [124,126], some of which also impacted the lipid profiles [129]. Squalene synthesis is very likely connected to fatty acid and carotenoid synthesis. A deeper understanding of the interrelations and corresponding optimization could improve productivity even further. The activation and inhibition of certain enzymes in the metabolic pathways of squalene is another approach to improving its production [79,130]. It is likely that optimal conditions regarding relative and total squalene productivity also vary between the different species of the Thraustochytriaceae, as seen in the different literature results.

### 3.6. Comparison of Growth and Target Molecule Synthesis on Solid and in Liquid Medium

Several strains were tested on their biomass, squalene, and carotenoid productivity in liquid and solid cultures. In liquid culture, the maximum cell density achieved was 1.1 g/L in *Thraustochytriidae* sp. N4994d. Between 4.0 and 7.9 g/L was reported for *T. aureum* ATCC 34304 [93,100,131–133]. Cultivation of *Aurantiochytrium* sp.\* yielded biomass densities between 6.25 and 27 g/L [94,134–137] but also up to 154 g/L [72]. Generally higher biomass densities of up to 65–200 g/L and productivities of around 5–8 g/L\*h were reported for *A. limacinum* and *Schizochytrium* sp. [84,85,96]. Other genera of the Thraustochytriaceae, e.g., *Ulkenia*, *Oblongichytrium*, *Botryochytrium*, and species such as *T. kinnei* and *T. aggregatum* have been scarcely studied for their productivity. For the strains studied here (N4994d, N6006d, N5658a, and N1001), the biomass density on solid medium was higher than in liquid culture. On solid medium, a maximum yield of 1.8 g/L was reached (*T. aureum* N6006d on medium 7). The best-growing strain in the DoE yielded 27 g/L (*T. aureum* N6007e on medium 8). The higher productivity and density of thraustochytrids on solid



media might be correlated to their natural behavior in the marine environment. They build biofilms and decompose marine detritus, and increasing cell densities were measured on decaying matter [138–140]. A biofilm-based cultivation approach might be useful to enhance productivity, reduce media volumes, space for cultivation, and thus increase production efficacy. Such cultivation designs have already been proposed for microalgae cultivation [141–144].

The production of the target molecules depended on the state of the medium. Generally, more carotenoids were produced on solid medium but less squalene and vice versa. Moreover, the carotenoid profile of the strains changed. A solid medium might also be a stress factor because the availability of nutrients and oxygen availability is limited to diffusion. The close proximity of the cells might induce competition for resources and space. Lower water availability and air exposure might lead to dry stress. An increased production of carotenoids might be a countermeasure.

### 3.7. Effect of the Medium Composition on the Metabolites

Comparison of the target molecule content of selected strains on three different media (DoE 6, 9, and 15) showed that for most strains, the highest carotenoid contents were yielded in the medium with high glucose and low yeast extract concentration (medium 15). The squalene content was generally lower under these conditions, as predicted by the carotenoid regression and optimization of *T. striatum* N5997. In contrast, squalene and carotenoid content in the medium with low glucose and yeast extract concentration (medium 6) were higher and lower, respectively. Thus, conditions that support squalene synthesis obstructed carotenoid synthesis and vice versa. *Thraustochytriidae* sp. N5670c and N4994d were an exception to this pattern as the highest measured carotenoid levels were observed in medium 6, indicating that exceptions to that rule are possible.

Medium 15, which favored the production of carotenoids, generally also influenced the extract yield positively, indicating a positive correlation between fatty acids and carotenoid synthesis. The highest extract yields were obtained from *T. aureum* N6006d and 5985. The fatty extracts show that these strains from this clade might be used as a co-producer of fatty acids and carotenoids. Various authors already revealed a high fatty acid and docosahexaenoic acid content in *T. aureum* [93,100,131–133,145].

Farnesyl pyrophosphate is a starting point for the synthesis of carotenoids, and squalene and sterols. Likewise, the common precursor acetyl-CoA is also the starting point for fatty acid synthesis [80,108]. Environmental and nutritional conditions might induce a switching between all those pathways. In addition, carotenoid patterns changed depending on the medium composition, showing that understanding the underlying mechanisms is crucial for exact predictions.

Evaluation has shown that carotenoid synthesis in thraustochytrids was dependent on the strain and the medium composition. Strains belonging to *T. aureum* and *Thraustochytriidae* sp. synthesized a high carotenoid content and might be promising genera for biotechnological carotenoid production. However, in *T. aureum*, large differences between some of the strains were observed. Strains belonging to *S. aggregatum* produced relatively more squalene than the other strains.

It seemed that carotenoid and squalene production somehow canceled each other, both in terms of their dependency on opposing medium composition and condition and depending on the production capability of the strain. Most strains that produced higher amounts of squalene did not synthesize high amounts of carotenoids and vice versa. *Ulkenia* spp. and *T. striatum* represented a compromise between squalene and carotenoid synthesis, but *T. striatum* yielded higher biomass.

### 3.8. Unknown Metabolites

Unknown substances with absorption properties in the visible spectrum were detected, and some of them were assigned to further carotenoids: Unknown 1 had a similar absorption spectrum and mass to micromonal [1,146], but this carotenoid was described in the



green algal order Mamiellales [147] but not in thraustochytrids. Unknown 2 and 3 had a UV/Vis absorption spectrum similar to echinenone and adonixanthin [1,148]. In unknown 2, the mass peak at  $m/z$  566.4 resembled the exact mass of 2- or 3-hydroxyechinenone of  $m/z$  567.42  $[M+H]^+$ . The second mass peaks at  $m/z$  549.8 might have resulted from cleavage of the hydroxyl group and is similar to the exact mass of echinenone of  $m/z$  551.43  $[M+H]^+$ . 2 and 3-hydroxyechinenone have a similar  $\lambda_{\max}$  to echinenone [1,148]. 3-hydroxyechinenone and 3'-hydroxyechinenone were described as intermediates in the astaxanthin synthesis pathway in vitro [149], which was accepted and adapted for cyanobacteria and thraustochytrids [83,148]. Because of similarities of the masses, unknown 2 might be 3-hydroxyechinenone or 3'-hydroxyechinenone but cannot be further differentiated. Unknown 3 might be either adonixanthin or an enantiomer or constitutional isomer of hydroxyechinenone, but it is questionable because of missing reliable mass data. It was excluded that these substances were diastereomers of echinenone, since the retention times of the Z-forms are usually longer than that of the all-E-form. The occurrence of these substances is plausible because they are part of the carotenoid metabolism. Unknown 4 had a characteristic double peak with a shoulder. It was similar to those of  $\gamma$ -carotene and rubixanthin [1,148,150]. Due to its late retention time and the fact that  $\gamma$ -carotene might be part of the carotenoid synthesis chain as in *Xanthophyllomyces dendrorhous* [151,152], it is more likely to be  $\gamma$ -carotene.

One group of substances with similar and very characteristic UV/Vis absorption spectra was only present in *O. minutum* N5995. Unknown C is possibly protoporphyrin IX. Its main observed mass was  $m/z$  563.33, which is similar to the mass of protoporphyrin IX with  $m/z$  563.27  $[M+H]^+$ . Their absorption spectra were also similar [153–155]. It was accompanied by smaller peaks with similar absorption spectra, which were possibly also porphyrins [156–158].

### 3.9. Morphology

The different Thraustochytriaceae were heteromorphic. One major characteristic of the genus *Ulkenia* is its amoeboid cell stage. Its cell wall either disappears or the protoplast leaves the cell wall through a small opening [64]. This was observed in strains closely related to *U. visurgensis* and *U. profunda*. It was described that species belonging to the genus of *Ulkenia* only formed small colonies [64], which was basically confirmed here. *Ulkenia* was also characterized by a highly refractive cell boundary in these experiments. It has been described in the literature as having a discrete cell wall, which was thin during growth, but also thick membranes were observed [64,159,160]. *T. aureum* was described to form large conglomerates [161] with globose or subglobose cells [101] and diameters up to 17 [101] or 65  $\mu\text{m}$  [161]. Except for the larger diameters, these observations were confirmed here. *Schizochytrium aggregatum* forms cell clusters and globose cells with diameters between 6 and 12  $\mu\text{m}$  [162]. These may grow by its special ability to perform successive binary division [63] and were described to end in an amorphous mass by Goldstein and Belsky [162]. In this experiment, *S. aggregatum* 561bx, N2820a, and 5999 formed large cell clusters, sometimes with larger individual cells than reported in literature. In some media, mainly number 3, bipartition was observed by the appearance of such amorphous cell clusters. In B1TMG, intracellular bodies were observed in all three strains. These might have been the described vacuole-like structures or lipid bodies. *Schizochytrium sensu lato*, especially *Aurantiochytrium*, is known for its high fatty acid content [163]. Reports about fatty acids in *S. aggregatum* are scarce, nevertheless they have been described, although not in high amounts [132,164]. Yokoyama and Honda described that *Oblongichytrium* sp. formed large cell clusters and was characterized mainly by the ellipsoidal form of its zoospores [63]. In these experiments, *O. minutum* N5995 and 5996 also formed large cell clusters, but no zoospores were observed. Both strains, especially 5996, were characterized by their generally small cells. *T. kinnei* (N1476c, N1694d) formed large cell agglomerates, whereas almost no cell clusters were observed in *T. aggregatum* (N4930a, 4992b) and only very few in *Thraustochytriidae* sp. (N5670c and N4994d). The older studies



on the Thraustochytriaceae, which investigated *T. aggregatum* [160,165] among others, were mostly performed with pollen cultures, which are not comparable to the experimental design here. Goldstein already summarized the problem of varying morphology under different culture conditions in 1973 [166].

Residual cell walls were found in several strains and genera. The literature distinguishes between two types of persistent cell walls: the cell wall that remains after the release of a protoplast and the persistent cell wall after the release of zoospores. The remaining cell wall after protoplast release was reported in *Ulkenia* sp. [64], which was also observed in this study. Likewise, at least some of the cell walls observed in *T. striatum* N5997 are likely due to this phenomenon. All described protoplasts were perfectly round and indistinguishable from other cells once they completely had left the cell wall. The amoeboid form described for *Ulkenia* spp. and *T. striatum* [64,167,168] was not observed. In *T. striatum*, disappearing and persistent cell walls after the release of zoospores were reported [169–171]. Therefore, the observed walls might be attributed to the release of protoplasts and spores. Empty cell walls in the cultures of *T. aureum* N6007e and *T. kinnei* N1476c might also be persistent sporangial walls like described for *T. aureum* and *T. kinnei* [101,172,173]. In *T. kinnei*, hatching cells were observed, which has not yet been described in the literature.

Sporangia were observed only rarely in most strains. Exceptions were *Thraustochytriidae* sp. N5670c and N4994d but with very small sporangia. Their closest relative in the phylogenetic analysis was *Labyrinthulochytrium* spp. To date, only two strains, *Labyrinthulochytrium arktikum* and *halotidis*, have been described. They reproduced by binary division and formed even smaller sporangia (7.8–8.9 µm) than observed here, containing three to eight zoospores [110,111].

Zoospores were not observed at all. According to Goldstein and Belsky, zoospores keep their swimming motility for 15 min to 3 h after their release from the zoosporangium [162]. Iida et al. reported that they saw zoospores only in the early growth phase of *T. aureum* but not anytime later [100]. It is therefore likely that the timing of microscopy (13 days after inoculation) was too late. Thraustochytriaceae can also produce aplanospores, just like *Aplanochytrium* [67,174]. So, it is possible that under the given conditions, only aplanospores were released, which would explain the very small cells in some of the cultures.

Structures that resembled smaller “empty cells” floated freely in the medium of most strains. However, their refraction was slightly different, they were perfectly round and closed, whereas the previously described cell walls often were irregularly shaped and damaged.

Generally, Thraustochytriaceae are known to form an ectoplasmic net (EN) [63,64,67,161,174–176], which could be confirmed. Compared to ENs in the literature, the nets obtained in these experiments seemed underdeveloped, which might be attributable to the nutrient-rich media. ENs play a part in digestion and nutrient intake [176–178]. They were finer when no food source was present, and nutrient concentration in the medium was high [175]. Knot-like features in the ENs of *Schizochytrium* and *Oblongichytrium* were observed. Iwata and Honda described that the EN of *Schizochytrium* thickens once it attaches to a food source [175]. Similar knot-like features have been recorded in *T. striatum*, *T. kinnei*, and *Aplanochytrium* sp., but the authors did not describe the structure [67,176]. In strains related to *T. kinnei* and *O. minutum*, oblong, branched cellular substructures were observed. Weete et al. documented similar structures in *Aurantiochytrium* sp. ATCC 26185\*. They discussed that these structures were associated with lipid bodies and lipid synthesis and showed that they became internalized in the growing lipid bodies [179].

Vacuole-like substructures were observed in different strains. Similar compartments were described in *Schizochytrium sensu stricto*, *Oblongichytrium*, *Aurantiochytrium*, and *Mucochytrium quahogii*. However, the authors could not define their function [63,180,181].

Taxonomy based on morphology only was not possible in this group. Although strains from the same clade had a similar appearance even under different medium conditions and sometimes showed very specific characteristics, cross-clade assessment was difficult. Strains that were only distantly related shared common traits, which were not present in closer relatives. Moreover, the expression of many features depended on the medium, but the variability of different strains under different conditions also aggravated classification.



### 3.10. Synopsis

Most of the analyzed Thraustochytriaceae were located in the first major branch of the phylogenetic tree.

Eleven strains belonged to the genus *Ulkenia sensu stricto*, as described by Yokoyama et al. [64]. They were divided into two main branches, as also described elsewhere [62,64,87,89–91,99]. One contained strains closely related to *U. profunda*, and the other contained strains near *U. visurgensis*. Carotenoid cluster analysis revealed three main clusters containing *Ulkenia* spp. with high similarity to the phylogenetic tree. One of them contained the strains belonging to *U. profunda*, while the other two contained strains related to *U. visurgensis*. Morphology showed some unique properties of this genus, such as “hatching” and perfectly globose cells. Three strains belonging to *Ulkenia* spp. showed a significant need for higher salinities for growth in the DoE experiments, which was especially pronounced in two strains belonging to *U. profunda* (N5905 and N5629e).

*Thraustochytrium* is a polyphyletic genus and contained most (33) of the analyzed strains in four different clades, belonging to the species *T. kinnei*, *aureum*, *striatum*, and *aggregatum*. Although they were distributed across the phylogenetic tree, the general placement of each clade was consistent with literature data.

Strains related to *T. kinnei* synthesized medium amounts of squalene but no carotenoids. Their morphology was most often unobtrusive with the special characteristics of oblong, branched cellular substructures under certain conditions. *T. kinnei* was most closely related to *S. aggregatum* in this phylogeny and elsewhere [87,89–91]. Strains related to *S. aggregatum* resembled *T. kinnei* only in that carotenoid production was low and squalene content was intermediate. They differed in that *S. aggregatum* had higher biomass yields. They were quite distinct from the other clades based on 18S rRNA phylogeny and carotenoid cluster analysis.

Most strains in the clade of *T. aureum* excelled by high biomass yield, high carotenoid content, but very low squalene content. Possibly, they are also potent fatty acid producers. *T. striatum* N5997 was the closest relative to strains of this clade. The closest neighbors (based on 18S rRNA genes) to *T. striatum* were the clades of *T. aureum*, *Thraustochytriidae* sp., and *Ulkenia*. Similar relationships were also reported by other authors [65,78,81,87,90]. *T. striatum* N5997 also showed a comparably high biomass yield and carotenoid content. In contrast to *T. aureum*, it exhibited elevated squalene levels. However, its carotenoid composition was more similar to strains belonging to *Ulkenia*, which was distantly related. Like in *Ulkenia* spp., the phenomenon of “hatching” cells was observed in *T. striatum*. Due to their high biomass and carotenoid yields, *T. aureum* and *T. striatum* might be interesting for further investigation. *T. aggregatum* was quite isolated in the phylogeny, which was also displayed by other researchers [63,64,78,87–89]. It synthesized no carotenoids but was characterized by a rapid color change from white to red at varying cultivation conditions and small and well-dispersed cells in the morphological observations. Therefore, its distant position in the 18S rRNA sequence-based phylogeny was reinforced by its other characteristics.

Three strains assigned to *Thraustochytriidae* sp. were in the first instance related to *Labyrinthulochytrium* spp. and more distantly related to *Phycophthorum* sp. and *Ulkenia* spp. They were also closely related to *Thraustochytriidae* sp. M4-103\*, which was shown to be related to *L. halotidis* and *Ulkenia* spp. [88]. However, a closer proximity of *L. halotidis* to *T. kinnei* than to *U. profunda* was also described [68,88,182]. The carotenoid patterns of strains related to *Thraustochytriidae* sp. were shown to be similar to those of members of *T. aureum*, although their phylogenetic relationships were quite distant.

Strains classified as *O. minutum* were located in the second major branch of the dendrogram. A clear phylogenetic distinction from most of the other members of Thraustochytriaceae has been reported quite often [63–65,78,87–90]. No carotenoids were measured in these strains, but the production of substances that were assigned to porphyrins was observed. *O. minutum* was rearranged in 2007, formerly known as *Schizochytrium minutum* [63]. Based on the recorded characteristics, it was very different from the strains assigned to *S. aggregatum*, which produced small amounts of carotenoids, differed in morphology, and were located in the other major branch of the phylogenetic tree.



## 4. Materials and Methods

### 4.1. Chemicals and Reagents

Analytical grade acetone (SupraSolv) and acetonitrile (hypergrade) were obtained from Merck (Darmstadt, Germany). Ethanol and tris(hydroxymethyl)aminomethane (TRIS) ( $\geq 99.9\%$ ) were provided by Carl Roth (Karlsruhe, Germany), and formic acid (99% ULC/MS) by Biosolve (Valkenswaard, Netherlands). Standards of all-*E*-astaxanthin (SML0982,  $\geq 97\%$ ), all-*E*-canthaxanthin (PHR1239, 96.7%), all-*E*-lutein (PHR1699, 85.6%), all-*E*- $\beta$ -carotene (PHR1239, 97.6%), and squalene (442785, analytical standard) were provided by Sigma-Aldrich (Taufkirchen, Germany). All-*E*-zeaxanthin (10009992,  $\geq 98\%$ ) was provided by Cayman Chemical (Ann Arbor, MI, USA). All-*E*-lycopene (0031,  $\geq 95\%$ ), all-*E*-echinenone (0283,  $\geq 95\%$ ), 9*Z*-canthaxanthin (0380.1,  $\geq 95\%$ ), all-*E*-phoenicoxanthin (0391), all-*E*-antheraxanthin (0231,  $\geq 95\%$ ), all-*E*-violaxanthin (0259,  $\geq 95\%$ ), all-*E*-rhodoxanthin (0424,  $\geq 95\%$ ), and astaxanthin monopalmitate (1017,  $\geq 95\%$ ) were obtained from CaroteNature (Münsingen, Switzerland).

Premium Sea Salt was obtained from Dupla Marin (Grafschaft-Gelsdorf, Germany), yeast extract, meat peptone, agar,  $\text{NaHCO}_3$ ,  $\text{MnCl}_2 \times 4 \text{H}_2\text{O}$ , cobalamin, biotin, and thiamin hydrochloride were provided by Carl Roth (Karlsruhe, Germany).  $\text{MgSO}_4 \times 7 \text{H}_2\text{O}$ ,  $\text{KH}_2\text{PO}_4$ ,  $\text{FeCl}_3 \times 6 \text{H}_2\text{O}$  9 mg/L,  $\text{ZnSO}_4 \times 7 \text{H}_2\text{O}$ ,  $\text{CoSO}_4 \times 7 \text{H}_2\text{O}$ ,  $\text{CuSO}_4 \times 5 \text{H}_2\text{O}$ ,  $\text{NaOH}$  ( $\geq 98\%$ ), and  $\text{HCl}$  (37%) were obtained from Merck (Darmstadt, Germany), and riboflavin from AppliChem (Darmstadt, Germany).

### 4.2. Culture Collection

The 60 strains used were all part of the former “Kultursammlung mariner Pilze Bremerhaven” (KMPB) of the Alfred-Wegener-Institut für Polar und Meeresforschung (Bremerhaven, Germany). It was originally established in the 1970s and contains strains, some of which have already been described [61,62,88,92,105,168,183–186]. This collection is now part of the Flensburg strain collection of marine fungi (mFSC). The following strains were used: 154f\*, 561bx\*, 1450d, 1462d\*, 1465d\*, 1471d, 1471f, 1472e, 1473e, 1476b, 1485a, 1518e, 1526d, 1527a, 1527c, 1531c, 3041c\*, 4992b\*, 5985\*, 5996\*, 5999\*, N557a, N561b, N1001, N1438e\*, N1476c\*, N1694d\* (accession number: L34668), N1709d\*, N2820a\*, N2845c, N4930a, N4930b, N4994b, N4994d\*, N4995d\*, N5589c\*, N5594d\*, N5629e\*, N5658a\*, N5661, N5670c\*, N5676f, N5905\*, N5976\*, N5995\*, N5997\*, N5998\*, N6000b\*, N6001b, N6002a, N6005a, N6006d\*, N6006e, N6007e\*, N6421, N6422, N6423, N6424, N6523, and Sakar7\*. The asterisks indicate the 30 strains used for 18S rRNA gene analysis, growth and terpene studies. All other strains were analyzed only regarding their 18S rRNA genes. Some strains were analyzed in earlier works [187,188].

### 4.3. Culture Media, Cultivation, and Harvest

The following media were used for the maintenance of the cultures: B1TM, B1TMG and AS. The basis of B1TM was adapted according to Gupta et al. [189] and included sea salt 30 g/L, yeast extract 1 g/L, meat peptone 1 g/L, trace element solution 1 mL/L and vitamin mix 1 mL/L. B1TMG included sea salt 15 g/L, yeast extract 5 g/L, meat peptone 5 g/L, glucose 10 g/L, trace element solution 1 mL/L, and vitamin mix 1 mL/L. The AS medium included sea salt 28.5 g/L, glucose 1 g/L, casein peptone 1.8 g/L, trace element solution 1 mL/L and vitamin mix 1 mL/L. Its pH was adjusted to 6.9 with 1 M  $\text{HCl}$  before sterilization. Media for the design of experiments (see below) were prepared likewise but with agar 12 g/L. Their pH was adjusted with 1 M  $\text{NaOH}$  or 1 M  $\text{HCl}$ .

The trace element mix was adapted from Lee Chang et al. [190]:  $\text{MgSO}_4 \times 7 \text{H}_2\text{O}$  200 mg/L,  $\text{KH}_2\text{PO}_4$  200 mg/L,  $\text{NaHCO}_3$  100 mg/L,  $\text{MnCl}_2 \times 4 \text{H}_2\text{O}$  9 mg/L,  $\text{FeCl}_3 \times 6 \text{H}_2\text{O}$  9 mg/L,  $\text{ZnSO}_4 \times 7 \text{H}_2\text{O}$  1 mg/L,  $\text{CoSO}_4 \times 7 \text{H}_2\text{O}$  0.34 mg/L, and  $\text{CuSO}_4 \times 5 \text{H}_2\text{O}$  0.2 mg/L. It was prepared by autoclaving a stock solution of each component individually and combining them under sterile conditions to the final concentration. The vitamin mix was prepared based on Bahnweg [92] for a final concentration in the medium of: cobalamin 5  $\mu\text{g/L}$ , biotin 10  $\mu\text{g/L}$ , thiamin hydrochloride 10  $\mu\text{g/L}$ , and riboflavin 10  $\mu\text{g/L}$ . All vitamins were prepared



individually in stock solutions. Filter sterilized (0.2 µm) stocks were combined and diluted to their final concentrations with sterile millipore water. Trace elements and vitamins were added sterilely to the culture media after autoclaving and cooling.

The used strains were defrosted from cryopreservation (−80 °C) and suspended in either 20 mL B1TM, B1TMG or AS liquid medium, and brought into culture in Erlenmeyer flasks. They were incubated at 20 °C and 70 rpm for 7–14 days in the dark. If the growth was sufficient, i.e., the medium had become turbid or visible pellets had been formed, the first passage was performed after seven days. Otherwise, the cultures were cultivated under the same conditions until observable growth. The inoculation volume for each passage was 1 mL. The cultures were passaged every 7–9 days until the culture was either harvested for DNA analysis or used to inoculate the design of experiment (DoE) media and morphology experiments. For DNA analysis, either an aliquot of 1 mL was taken from the culture and transferred to a reaction tube, or the whole broth was transferred to a 20 mL Falcon tube and centrifuged at  $1000 \times g$  for 5 min. Subsequently, most of the supernatant was removed; the cell pellet was resuspended and transferred to a reaction tube. Storage until the next steps was at −21 °C.

For inoculation of the DoE, 400 µL of the 7–9 day old culture was transferred on each petri dish containing one of the described DoE media (see below). The same medium used for the liquid cultures served as a positive in form of solid agar. B1TMG was used as positive control for N6006d, 561bx, 154f, N4995d, N2820a, N4994d, N6007e, N1694d, N5998, N1709d, 1465d, N1476c, 4992b, 5985, 5999, N5658a, N5997, N5594d, 3041c, N5589c, N5976, N5670c, and Sakar7. B1TM was used for N5995, N5629e, N5905 and AS was used for 5996 and N6000b. Cultures were incubated for 13 days in the dark at 20 °C. Subsequent harvesting was performed by scraping the biomass with a spatula and weighing directly into lysis tubes type C (Macherey Nagel, Düren, Germany). The biomass was deep-frozen at −21 °C until further processing.

#### 4.4. 18S rRNA Gene Characterization and Phylogeny

In a first step, DNA was extracted from the harvested cell pellet. Therefore, the Quick-DNA Microprep Kit (Zymo Research, Freiburg, Germany) was used, and an adapted version of the protocol “solid tissue samples” was followed. First, 100–150 µL biomass was added to 500 µL Genomic Lysis Buffer from the kit in a lysis reaction tube type C (Analytik Jena, Jena, Germany). Cell disruption was performed using a vibration mill (Retsch GmbH, Haan, Germany) at a frequency of 27 Hz and a duration of  $2 \times 3$  min with a break of 30 s in between. The lysate was centrifuged at  $10,000 \times g$  for 5 min. Further steps were executed according to the manufacturer’s protocol.

The PCR reaction mixture consisted of the following components: 25 µL DreamTaq Green PCR Master Mix (Thermo Scientific, Waltham, MA, USA), 23 µL nuclease-free water (Carl Roth, Karlsruhe, Germany), 1 µL DNA template, 0.5 µL forward primer (100 µM) and 0.5 µL reverse primer (100 µM). For PCR, primers T18S1F and T18S5R [95] were used. The amplification was performed similarly as described by Burja et al. [95], using a Mastercycler gradient thermocycler (Eppendorf, Hamburg, Germany). Initial denaturation was at 95 °C for 180 s. Thirty cycles were performed of 30 s at 95 °C, 30 s at 56 °C (annealing), and 90 s at 72 °C. Final extension was conducted at 72 °C for 10 min. The PCR products were checked by gel electrophoresis, and well-amplified sequences were sequenced by Sanger sequencing. Non-sufficient PCR products were discarded, and the original DNA was again amplified with primers F and RA2 [191] with the identical PCR program and FA1 [191] and SR-11 [192] with an adapted annealing temperature at 49 °C. Sanger sequencing was carried out at the Institute for Clinical Molecular Biology (IKMB) at Kiel University. In addition to the primers used for PCR, the following primers were used for sequencing: FA2, FA3, R, RA1, RA3 [191], and SR-6 [192].

The sequences were assembled with ChromasPro (version 2.1.9, Technelysium Pty Ltd., South Brisbane, Australia). In addition to these sequencing data, 18S rRNA gene sequences from closely related species found by a BLAST search, further members of the families of the



Thraustochytriaceae and Labyrinthulaceae and strains used as outgroup\* were retrieved from the GenBank database. They were added to the alignment and the phylogenetic tree to increase robustness and informative value, and to enable a well-founded and meaningful discussion (NCBI accession numbers AB022103.1, AB022104.1, AB022106.1, AB022108.1, AB022109.1, AB022110.1, AB022111.1, AB022112.1, AB022113.1, AB022116.1, AB126669.1, AB290355.1, AB290575.1, AB290576.1, AB290577.1, AB355410.1, AB355411.1, AB355412.1, AB636147.1, AB810962.1, AB810968.1, AB810969.1, AB810977.1, AB973514.1, AB973517.1, AB973524.1, AB973531.1, AB973545.1, AB973546.1, AB973561.1, AB973564.1, AB973565.1, AJ415519.1\*, AJ519935.1, AY705753.2, DQ023615.1, DQ367049.1, DQ367050.1, DQ374149.1, EF114348.1, FJ004948.1, FJ821482.1, FJ799799.1, FR875335.2, GQ452862.1\*, HQ228958.1, HQ228964.1, HQ228969.1, HQ228980.1, JQ281514.1\*, JX993839.1, JX993841.1, KF500513.1, KT598545.1, KT598546.1, KT716334.1, KX160007.1, KX379459.1, KX430103.1, L34054.1, L34668.1, MF872140.1, MG099001.1, MG799152.1\*, MK615597.1, MN382127.1, MT484273.1, and U21338.1). All successfully assembled sequences that belonged to the Thraustochytriaceae were aligned using the Clustal W algorithm. The phylogenetic tree was based on the maximum-likelihood algorithm and the nucleotide substitution model by Tamura and Nei [193]. Missing gaps were treated by partial deletion, i.e., positions with less than 95% site coverage were eliminated. The final dataset contained 86 sequences and 1378 base positions. The phylogeny was tested using the Bootstrap method with 1000 replicates and rooted using the outgroup. Alignment and tree building were performed with MEGA 11 (Molecular Evolutionary Genetics Analysis version 11, Tamura, Stecher, and Kumar 2021 [194]). All obtained sequences were deposited in the NCBI GenBank database under accession numbers given in Table S1.

#### 4.5. Design of Experiment and Model Regression—Growth Studies

A two-step approach was used to determine the optimal growth parameters. First, a series of different media was created using a statistical experimental design. The recipes were prepared as solid media, inoculated, and incubated with different strains. Different models were calculated based on the biomass yield and compared. The most applicable model was used to evaluate the growth behavior of the different strains.

For the design of experiments, four variables were chosen: Glucose (0–60 g/L), yeast extract (0.5–15 g/L), pH (6.5–7.6), and additional potassium dihydrogen phosphate (0–0.5 g/L) to a base concentration of approximately 0.06 mg/L. In an additional set of experiments, which was used only for a smaller number of strains, the salt concentration (15–30 g/L) was used as a further variable (Table 4). Constant parameters were temperature (20 °C), trace element solution (1 mL/L), vitamin mix (1 mL/L), agar (12 g/L), and, for the first set of experiments, salt concentration (15 g/L). It was expected that some strains were oligotroph, so the design was established in two subsets: For better coverage of the area with lower concentrated media components, the first subset of 6 media was calculated with reduced media components, using a Latin hypercube algorithm and space-filling design. The second subset of six additional media was created with the above concentrations and a space-filling design (all JMP PRO, version 16.0.0, SAS Institute Inc., Cary, NC, USA). Additionally, three runs with nearly extreme (high or low) amounts of glucose and yeast were added (Table 4 No. 13, 14, 15). As a response, the biomass yield was used.

The obtained results were regressed using the standard least squares method with different models (JMP PRO). All experiments executed without further addition of salt were regressed by the following two approaches: quadratic (Equation (1)), reduced quadratic including one interaction term (glucose and yeast extract) (Equation (2)), and reduced quadratic including the interaction terms of glucose and yeast, glucose and pH, glucose and phosphate, yeast extract and pH, and yeast extract and phosphate (Equation (3)).  $Y$  is the yield,  $X_1$  represents the glucose concentration,  $X_2$  the yeast extract concentration,  $X_3$  the pH, and  $X_4$  the phosphate concentration.  $a$  is the intercept,  $b_i$ ,  $c_i$ , and  $d_{ij}$  are model coefficients.



**Table 4.** Overview of media composition of the experimental design for growth model establishment. Asterisks indicate media additionally prepared with a salt concentration of 30 g/L.

Number	Glucose(g/L)	Yeast Extract (g/L)	KH <sub>2</sub> PO <sub>4</sub> (g/L)	pH
1	10.0	2.3	0.50	6.9
2	2.0	1.4	0.00	7.3
3	0.0	3.2	0.40	7.6
4	4.0	5.0	0.21	6.5
5	6.0	0.5	0.30	7.5
6 *	8.0	4.1	0.10	7.2
7	27.5	14.8	0.05	6.7
8 *	58.8	12.9	0.08	7.6
9	55.4	6.1	0.46	7.4
10	32.9	11.7	0.21	7.0
11	16.4	11.0	0.44	7.4
12	46.8	8.8	0.32	7.0
13 *	0.5	0.5	0.20	7.2
14 *	0.5	15.0	0.28	7.0
15 *	60.0	0.5	0.15	7.3

$$Y = a + \sum_{i=1}^4 b_i X_i + \sum_{i=1}^4 c_i X_i^2 \quad (1)$$

$$Y = a + \sum_{i=1}^4 b_i X_i + \sum_{i=1}^2 c_i X_i^2 + d_{12} X_1 X_2 \quad (2)$$

$$Y = a + \sum_{i=1}^4 b_i X_i + \sum_{i=1}^2 c_i X_i^2 + d_{12} X_1 X_2 + d_{13} X_1 X_3 + d_{14} X_1 X_4 + d_{23} X_2 X_3 + d_{24} X_2 X_4 \quad (3)$$

The adjusted coefficients of determination were used to compare the different models. T-tests were applied to identify the statistical significance of the model parameters. The generally best describing-model was model 2. It was chosen for deeper investigation, and the influence of the parameters on yield was tested for significance. The gradient descent algorithm was used to numerically calculate the optimal medium composition. Different strains were compared by their predicted optimized yield. The influence of the salt concentration (regressor  $X_5$ ) on the growth of the strains was analyzed by the extension of model 2 by the linear influence of the salt concentration (Equation (4)) and by direct comparison of the growth on DoE media 6, 8, 13, 14, 15 with a low (15 g/L) and high (30 g/L) salt concentration.

$$Y = a + \sum_{i=1}^5 b_i X_i + \sum_{i=1}^2 c_i X_i^2 + d_{12} X_1 X_2 \quad (4)$$

#### 4.6. Extraction and UHPLC Analysis of Carotenoids and Squalene

The harvested biomass was disrupted in acetone to extract carotenoids and squalene. Therefore, up to 1.5 g of wet biomass was put into lysis tubes type C (Analytik Jena, Jena, Germany or Macherey Nagel, Düren, Germany). An amount of 500 µL acetone was added, and the cells were broken mechanically in a vibration mill (MM 2000, Retsch, Haan, Germany) at 27 Hz for 3 min. After subsequent centrifugation at  $10,000 \times g$ , the supernatant of the samples was transferred to a centrifuge tube, and 500 µL of fresh acetone was added to the lysis tube. This procedure was repeated until the supernatant and the residual biomass were colorless, but at least three times. The solvent of the combined supernatant was evaporated under a gentle stream of nitrogen at 40 °C. The remaining extract was dissolved in 250 to 500 µL acetone and filtered (0.45 µm, PTFE) into amber vials.

Qualification and quantification of carotenoids and squalene were performed by UHPLC using an ACQUITY Arc system by Waters (Milford, MA, USA) equipped with a sample manager (FTN-R), a quaternary solvent manager (R), an UV/Vis detector (2998



PDA Detector), and a mass spectrometer (Acquity QDa Detector). A C18-column (Cortecs C18 2.7  $\mu\text{m}$ , 90  $\text{\AA}$ ,  $3.0 \times 100$  mm, Waters, Milford, MA, USA) was operated at 40  $^{\circ}\text{C}$ . The injection volume was 5  $\mu\text{L}$ . The starting conditions were 70% millipore water (A) and 30% acetonitrile (B), containing 0.1% formic acid. Within 4 min, the gradient increased linearly to 90%B:10%A. This ratio was held isocratically for 5 min. Then B was increased linearly to 100% over 2.5 min and held for another 16.5 min. After a total of 28 min, the initial ratio was restored for 4 min to regenerate starting conditions. Flow velocity was 0.5 mL/min. Samples with a high extract content sometimes required additional cleaning of the column by running 100% acetonitrile at 60  $^{\circ}\text{C}$  for at least 30 min. Optical spectra were measured in a range of 200 to 800 nm, and carotenoid and squalene peaks were compared to the retention times of the standards. Data were analyzed and quantified at their determined absorbance maxima at 200 nm (squalene), 441 nm (violaxanthin), 448 nm (lutein and antheraxanthin), 452 nm ( $\beta$ -carotene), 454 nm (zeaxanthin), 461 nm (echinenone), 466 nm (9Z-canthaxanthin), 471 nm (lycopene), 475 nm (canthaxanthin), 477 nm (phoenicoxanthin and astaxanthin monopalmitate), 479 nm (astaxanthin), and 488 nm (rhodoxanthin). The mass spectrometer with electrospray ionization (ESI) was operated in positive mode with a cone voltage of 15 V and a probe temperature of 600  $^{\circ}\text{C}$ , measuring in a range of  $m/z$  150 to 1250. For further accuracy, the mass of selected carotenoids was observed by selected ion recording (SIR) at  $m/z$  537.4  $[\text{M}+\text{H}]^{+}$  ( $\beta$ -carotene), 551.4  $m/z$   $[\text{M}+\text{H}]^{+}$  (echinenone),  $m/z$  565.4  $[\text{M}+\text{H}]^{+}$  (canthaxanthin), and  $m/z$  597.4  $[\text{M}+\text{H}]^{+}$  (astaxanthin). Besides the major all-*E*-astaxanthin peak, peaks with UV/Vis absorption spectra corresponding to *Z*-astaxanthin isomers [195–200] that were additionally accompanied by peaks with the mass of astaxanthin in SIR were assigned to astaxanthin diastereomers. Their quantities were estimated using the quantification of all-*E*-astaxanthin, corrected by factors adjusting the different extinction coefficients published by Bjerkeng et al. [201], namely 1.20 for 9Z-astaxanthin, 1.56 for 13Z-astaxanthin, and 1.11 for the di-*Z*-isomers. Astaxanthin monopalmitate was detected by comparison of spectra and retention time with a standard. The carotenoid part was quantified using the calibration curve for all-*E*-astaxanthin. If no further information is given, the name of the carotenoid always stands for its all-*E*-isomer.

For identification and quantification, standards were used at concentrations of 0.2–50.0  $\mu\text{g/mL}$  in acetone. Calibration curves were adjusted to the concentration range of the substance in the samples. Blank acetone was applied for zero-value determination. Linear regression of the calibration data was performed by the ordinary least squares method, and the calibration was forced through zero. The content of unknown carotenoids was estimated by a mean calibration of all analyzed carotenoid standards. Dereplication was performed by comparison of retention times, UV/VIS absorption-, and mass spectra.

#### 4.7. Target Molecule Content, Composition, Cluster- and Regression Analysis

The ability of the strains to produce carotenoids and squalene was evaluated using samples from the growth studies. 1–4 plates per strain were selected based on the strongest coloration and the highest biomass for a detailed comparison. These were harvested separately from the others, and the biomass was directly transferred into lysis tubes after weighing. The biomass of all other plates was collected into one lysis tube after weighing. Samples were extracted and measured. For the calculation of target molecule content on a dry weight basis, a generalized cell dry weight (CDW) was assumed. It was determined in the experiments for the effect of medium composition (see below). The mean content of the target molecules was calculated using the harmonic mean. Cluster analysis of the obtained patterns was performed using the k-means algorithm and hierarchical clustering (JMP PRO). Due to possible differences in scale and variability, datasets were standardized for both approaches. For strain *T. striatum* N5997, all 15 plates were harvested and analyzed separately to regress squalene and carotenoid content ( $\mu\text{g/mg}$ ) and yield ( $\mu\text{g/L}$ ) on various growth parameters. To increase explanatory power, model 2 of the growth regression was extended if necessary. In this manner, models specifically adjusted to describe the growth and target molecule production of this specific strain were developed.



#### 4.8. Morphology

Strains from different clades in the created phylogenetic tree were used for morphological analysis (Sakar7, N6000b; N5994d, N5589c N5629e, N5905, N5658a; N5670c, N4994d; N6007e, N6006d; 561bx, N2820a, 5999; N147c, N1694d; N4930a, 4992b; N5997; 5996, N5995). To record their physiological appearance under different cultivation conditions (different amount of yeast extract, glucose, phosphate, and different pH), the experiment was performed in four liquid media derived from the DoE (number 3, 6, 12, and 14). B1TMG was used as a positive control. The experiment was carried out in 12 well microtiter plates with 2.5 mL medium per well. The inoculation was performed with 80  $\mu$ L from 7-day-old liquid stock cultures. To allow uniform air diffusion, the wells in the center of the plates functioned as blanks. The plates were incubated for 13 days in the dark at 20 °C without shaking. Subsequently, the first step was a microscopic evaluation using an inverted microscope (Eclipse TS100, Nikon, Tokyo, Japan). The plates remained sealed, and no samples were taken, so the reticular structures remained undamaged. In the next step, a conventional microscopic assessment (Carl Zeiss Microscopy GmbH, Jena, Germany) was carried out. Various criteria were considered for evaluating the morphology: cell size, cell form, agglomeration behavior, formation and properties of ectoplasmic nets (EN), the appearance of sporangia and spores, and extracellular and intracellular structures.

#### 4.9. Effect of Medium Composition on the Target Molecules

DoE experiments 6, 9, and 15 were repeated with selected strains (N5670c, N4994d, N6000b, N1001, N5589c, N5594d, N5658a, 5996, N2820a, 5999, N6006d, 5985) to quantify the target molecules on a CDW basis. They were performed similarly to the DoE but in multiple executions for a higher biomass yield. The biomass was harvested, measured, filled into micro-reaction tubes, and frozen at −80 °C before freeze-drying (Alpha 1–4, Christ, Osterode, Germany) for 24 h at 37 Pa. The weight of the biomass was recorded before and after drying, and CDW was calculated. Extraction and measurement of the target molecules were performed as described above.

#### 4.10. Comparison of Biomass Yield and Target Molecule Content in Cultures Cultivated in Liquid and on Solid Medium

To compare the biomass growth and carotenoid synthesis, selected strains (N6006d, N4994d, N5658a, N1001) were cultivated on medium 7 from the DoE. It was either prepared with 12, 14, and 18 g/L agar or without agar. Inoculation was performed similarly to the previous experiments from the liquid stock cultures. Liquid cultures inoculated with 1 mL from the stock culture were cultivated in Erlenmeyer flasks with 20 mL medium on an orbital shaker at 80 rpm. Solid and liquid cultures were incubated for 13 days in the dark and at 20 °C. Harvest of the cultures from the solid media was performed as described for the DoE. As no color difference between the solid media was visible, these were combined. The cultures from the flasks were transferred into centrifuge tubes and centrifuged for 5 min at 4000  $\times$  g. The supernatant was discarded and replaced with distilled water. The sample was resuspended by vortexing for 30–60 s. Centrifugation and washing steps were repeated twice. Afterward, the supernatant was discarded, the cell pellet was resuspended in 0.5 mL distilled water, transferred in glass tubes, and frozen at −80 °C prior to freeze-drying (Alpha 1–4, Christ, Osterode, Germany) for 24 h at 37 Pa.

### 5. Conclusions

The family of Thraustochytriaceae is very heterogeneous in its characteristics and traits. Although members possess many common features in their morphology, growth behavior, and metabolite patterns, these are not necessarily correlated to the phylogenetic clades based on 18S rRNA analysis. Within the described clades, some strains that were identical based on their 18S rRNA genes exhibited different characteristics. The carotenoid composition of *T. aureum* N5998 differed substantially from those of the other strains of this clade, although its 18S rRNA was genetically identical to two of them. We agree with



the statement of Dellero et al. [125] and argue that gene-based analysis, especially using the short 18S rRNA information, is not able to predict the exact behavior and potential of individual strains.

A deeper understanding of the relation of these organisms might be achieved mainly by two aspects: First, there needs to be an enhanced awareness of the variability of this group, and there is a necessity to precisely classify existing genera and species to allow coherent comparison. 18S rRNA analysis is a useful tool for a general classification in terms of family and genus. A rearrangement, as performed for species formerly belonging to *Ulkenia*, *Schizochytrium*, and *Thraustochytrium* [63,64,202], might also be helpful for other clades of the polyphyletic genus *Thraustochytrium* to allow better distinction. Second, the variety of Thraustochytriaceae is still underexplored. Recent discoveries of new genera, species [88,96,110,125,181,203], and strains, especially members of the genus *Aurantiochytrium*, were described [78,89,99,120,204]. Additionally, the high number and variability of novel isolates displayed in the phylogenetic tree published by Ueda et al. [91] indicates that the Thraustochytriaceae may contain more species and genera, which either have new characteristics or bridge the gaps between others. A comprehensive and correct denomination of novel species is crucial for a distinguished and meaningful discussion.

18S rRNA phylogenetic analysis allowed the distinction of the strains and assigned them to eight different clades. Carotenoid cluster analysis revealed that a fine classification at a species level was possible but failed to reflect the overall context of the phylogenetic tree based on 18S rRNA gene comparison. Strains belonging to *T. aureum* and *Thraustochytriidae* sp. showed the highest carotenoid content. Most strains of *T. aureum* also yielded high biomass. Squalene was found in variable concentrations in all strains. The conditions that favored carotenoid and squalene production were largely mutually exclusive. *T. striatum* N5997 produced squalene and carotenoids at intermediate levels and built high biomass, which might be a good compromise for a combined production.

The results of these experiments indicate that Thraustochytriaceae offer more potential for biotechnological applications than just the genus *Aurantiochytrium*. Closer examination of other clades for their ability to synthesize carotenoids, squalene, and fatty acids might help to find new production organisms. Subsequently, bioprocess, metabolic, and genetic engineering approaches will provide a basis for a sustainable production using the fascinating group of Thraustochytriaceae.

**Supplementary Materials:** The following supporting information can be downloaded at: <https://www.mdpi.com/article/10.3390/md21040204/s1>, Figure S1: Carotenoid composition of the analyzed strains grown on media with a high salinity (30 g/L); Figure S2: Carotenoid composition of *Thraustochytrium striatum* N5997 on various DoE media; Figure S3: Morphology of various strains observed in medium 3 after cultivation in microtiter plates; Figure S4: Morphology of various strains observed in medium 6 after cultivation in microtiter plates; Figure S5: Morphology of various strains observed in medium 12 after cultivation in microtiter plates; Figure S6: Morphology of various strains observed in medium 14 after cultivation in microtiter plates; Table S1: Assignment of the investigated strains based on sequence similarity to strains in the NCBI database on the basis of their 18S rRNA gene data; Table S2: Coefficients of determination and *p*-values of model 1–3 for the regression of growth data; Table S3: Estimated model coefficients, *p*-values, and optimized parameters of model 2 for all analyzed strains regarding maximal biomass yield; Table S4: Biomass yield of the analyzed strains on the DoE media; Table S5: Carotenoid content and proportion in the analyzed strains used for cluster analysis; Table S6: Cluster means of carotenoid composition obtained from k-means clustering; Table S7: Carotenoid content and proportion in the analyzed strains in the DoE with a high salt concentration (30 g/L); Table S8: Carotenoid and squalene content and carotenoid proportion in *T. striatum* N5997 depending on the medium composition; Table S9: Extract content in dependency of strain, medium composition and medium solidity; Table S10: Carotenoid content and proportion in strains cultivated on different solid media; Table S11: Carotenoid content and proportion in strains cultivated on medium 7 in either liquid medium (liquid) or in form of agar (solid); Table S12: Review of strains reported in the literature by comparison with the phylogenetic analysis of our study.



**Author Contributions:** Conceptualization, I.K.K.; methodology, I.K.K.; validation, I.K.K.; formal analysis, I.K.K.; investigation, I.K.K. and B.A.M.; data curation, I.K.K.; writing—original draft preparation, I.K.K. and B.A.M.; writing—review and editing, A.L., I.K.K. and B.A.M.; visualization, I.K.K.; supervision, A.L.; project administration, A.L.; funding acquisition, A.L. All authors have read and agreed to the published version of the manuscript.

**Funding:** This research is part of the project Grenzland INNOVATIV Schleswig Holstein [innovative border region Schleswig Holstein] and was funded by the German Federal Ministry of Education and Research (BMBF) in context of “Innovative Hochschule” [innovative university]. We acknowledge financial support by Land Schleswig-Holstein within the funding program Open Access-Publikationsfonds.

**Institutional Review Board Statement:** Not applicable.

**Informed Consent Statement:** Not applicable.

**Data Availability Statement:** Data is contained within the article and supplementary material.

**Acknowledgments:** We thank Jane Polglase and David Alderman for their comments on the morphology part of the manuscript. We thank the Institute of Clinical Molecular Biology in Kiel for providing Sanger sequencing as supported in part by the DFG Clusters of Excellence “Precision Medicine in Chronic Inflammation” and “ROOTS”. We thank T. Naujoks, D. Langfeldt and B. Löscher for technical support.

**Conflicts of Interest:** The authors declare no conflict of interest.

## References

1. Mercadante, A.Z.; Egeland, E.S. *Carotenoids: Handbook*; Britton, G., Liaaen-Jensen, S., Pfander, H., Eds.; Springer: Basel, Switzerland, 2004; ISBN 9783034878364.
2. Martínez-Cámara, S.; Ibañez, A.; Rubio, S.; Barreiro, C.; Barredo, J.-L. Main Carotenoids Produced by Microorganisms. *Encyclopedia* **2021**, *1*, 1223–1245. [\[CrossRef\]](#)
3. Lafarga, T.; Clemente, I.; Garcia-Vaquero, M. Carotenoids from microalgae. In *Carotenoids: Properties, Processing and Applications*; Galanakis, C.M., Ed.; Elsevier: Amsterdam, The Netherlands, 2020; pp. 149–187. ISBN 9780128170670.
4. Ram, S.; Mitra, M.; Shah, F.; Tirkey, S.R.; Mishra, S. Bacteria as an alternate biofactory for carotenoid production: A review of its applications, opportunities and challenges. *J. Funct. Foods* **2020**, *67*, 103867. [\[CrossRef\]](#)
5. Sun, T.; Rao, S.; Zhou, X.; Li, L. Plant carotenoids: Recent advances and future perspectives. *Mol. Hortic.* **2022**, *2*, 103867. [\[CrossRef\]](#)
6. Xu, Y.; Harvey, P.J. Carotenoid Production by *Dunaliella salina* under Red Light. *Antioxidants* **2019**, *8*, 123. [\[CrossRef\]](#) [\[PubMed\]](#)
7. Liu, J.; Sun, Z.; Gerken, H.; Liu, Z.; Jiang, Y.; Chen, F. *Chlorella zofingiensis* as an alternative microalgal producer of astaxanthin: Biology and industrial potential. *Mar. Drugs* **2014**, *12*, 3487–3515. [\[CrossRef\]](#)
8. Yuan, J.-P.; Chen, F.; Liu, X.; Li, X.-Z. Carotenoid composition in the green microalga *Chlorococcum*. *Food Chem.* **2002**, *76*, 319–325. [\[CrossRef\]](#)
9. Yi, Z.; Su, Y.; Cherek, P.; Nelson, D.R.; Lin, J.; Rolfsson, O.; Wu, H.; Salehi-Ashtiani, K.; Brynjolfsson, S.; Fu, W. Combined artificial high-silicate medium and LED illumination promote carotenoid accumulation in the marine diatom *Phaeodactylum tricornutum*. *Microb. Cell Fact.* **2019**, *18*, 209. [\[CrossRef\]](#)
10. Collins, A.M.; Jones, H.D.T.; Han, D.; Hu, Q.; Beechem, T.E.; Timlin, J.A. Carotenoid distribution in living cells of *Haematococcus pluvialis* (Chlorophyceae). *PLoS ONE* **2011**, *6*, e24302. [\[CrossRef\]](#)
11. Park, W.S.; Kim, H.-J.; Li, M.; Lim, D.H.; Kim, J.; Kwak, S.-S.; Kang, C.-M.; Ferruzzi, M.G.; Ahn, M.-J. Two Classes of Pigments, Carotenoids and C-Phycocyanin, in Spirulina Powder and Their Antioxidant Activities. *Molecules* **2018**, *23*, 2065. [\[CrossRef\]](#)
12. Vila, E.; Hornero-Méndez, D.; Azziz, G.; Lareo, C.; Saravia, V. Carotenoids from heterotrophic bacteria isolated from Fildes Peninsula, King George Island, Antarctica. *Biotechnol. Rep.* **2019**, *21*, e00306. [\[CrossRef\]](#)
13. Reis-Mansur, M.C.P.P.; Cardoso-Rurr, J.S.; Silva, J.V.M.A.; de Souza, G.R.; Da Cardoso, V.S.; Mansoldo, F.R.P.; Pinheiro, Y.; Schultz, J.; Lopez Balottin, L.B.; da Silva, A.J.R.; et al. Carotenoids from UV-resistant Antarctic *Microbacterium* sp. LEMMJ01. *Sci. Rep.* **2019**, *9*, 9554. [\[CrossRef\]](#)
14. Yokoyama, A.; Miki, W.; Izumida, H.; Shizuri, Y. New Trihydroxy-keto-carotenoids Isolated from an Astaxanthin-producing Marine Bacterium. *Biosci. Biotechnol. Biochem.* **1996**, *60*, 200–203. [\[CrossRef\]](#) [\[PubMed\]](#)
15. Calo, P.; de Miguel, T.; Sieiro, C.; Velazquez, J.B.; Villa, T.G. Ketocarotenoids in halobacteria: 3-hydroxy-echinenone and trans-astaxanthin. *J. Appl. Bacteriol.* **1995**, *79*, 282–285. [\[CrossRef\]](#)
16. Fang, C.-J.; Ku, K.-L.; Lee, M.-H.; Su, N.-W. Influence of nutritive factors on C<sub>50</sub> carotenoids production by *Haloferax mediterranei* ATCC 33500 with two-stage cultivation. *Bioresour. Technol.* **2010**, *101*, 6487–6493. [\[CrossRef\]](#) [\[PubMed\]](#)



17. Tran, T.N.; Tran, Q.-V.; Huynh, H.T.; Hoang, N.-S.; Nguyen, H.C.; Ngo, D.-N. Astaxanthin Production by Newly Isolated *Rhodospiridium toruloides*: Optimization of Medium Compositions by Response Surface Methodology. *Not. Bot. Horti Agrobot.* **2018**, *47*, 320–327. [CrossRef]
18. Andrewes, A.G.; Phaff, H.J.; Starr, M.P. Carotenoids of *Phaffia rhodozyma*, a red-pigmented fermenting yeast. *Phytochemistry* **1976**, *15*, 1003–1007. [CrossRef]
19. Pawar, P.R.; Velani, S.; Kumari, S.; Lali, A.M.; Prakash, G. Isolation and optimization of a novel thraustochytrid strain for DHA rich and astaxanthin comprising biomass as aquafeed supplement. *3 Biotech* **2021**, *11*, 71. [CrossRef] [PubMed]
20. Aki, T.; Hachida, K.; Yoshinaga, M.; Katai, Y.; Yamasaki, T.; Kawamoto, S.; Kakizono, T.; Maoka, T.; Shigeta, S.; Suzuki, O.; et al. Thraustochytrid as a potential source of carotenoids. *J. Am. Oil Chem. Soc.* **2003**, *80*, 789–794. [CrossRef]
21. Park, H.; Kwak, M.; Seo, J.; Ju, J.; Heo, S.; Park, S.; Hong, W. Enhanced production of carotenoids using a Thraustochytrid microalgal strain containing high levels of docosahexaenoic acid-rich oil. *Bioprocess Biosyst. Eng.* **2018**, *41*, 1355–1370. [CrossRef]
22. Viljanen, K.; Sundberg, S.; Ohshima, T.; Heinonen, M. Carotenoids as antioxidants to prevent photooxidation. *Eur. J. Lipid Sci. Technol.* **2002**, *104*, 353–359. [CrossRef]
23. Di Mascio, P.; Kaiser, S.; Sies, H. Lycopene as the most efficient biological carotenoid singlet oxygen quencher. *Arch. Biochem. Biophys.* **1989**, *274*, 532–538. [CrossRef]
24. Conn, P.F.; Schalch, W.; Truscott, T. The singlet oxygen and carotenoid interaction. *J. Photochem. Photobiol. B Biol.* **1991**, *11*, 41–47. [CrossRef]
25. Miki, W. Biological functions and activities of animal carotenoids. *Pure Appl. Chem.* **1991**, *63*, 141–146. [CrossRef]
26. Shimidzu, N.; Goto, M.; Miki, W. Carotenoids as Singlet Oxygen Quenchers in Marine Organisms. *Fish. Sci.* **1996**, *62*, 134–137. [CrossRef]
27. Rodrigues, E.; Mariutti, L.R.B.; Mercadante, A.Z. Scavenging capacity of marine carotenoids against reactive oxygen and nitrogen species in a membrane-mimicking system. *Mar. Drugs* **2012**, *10*, 1784–1798. [CrossRef] [PubMed]
28. Chen, Y.-Y.; Lee, P.-C.; Wu, Y.-L.; Liu, L.-Y. In Vivo Effects of Free Form Astaxanthin Powder on Anti-Oxidation and Lipid Metabolism with High-Cholesterol Diet. *PLoS ONE* **2015**, *10*, e0134733. [CrossRef]
29. Jiang, X.; Chen, L.; Shen, L.; Chen, Z.; Xu, L.; Zhang, J.; Yu, X. Trans-astaxanthin attenuates lipopolysaccharide-induced neuroinflammation and depressive-like behavior in mice. *Brain Res.* **2016**, *1649*, 30–37. [CrossRef]
30. Xue, Y.; Qu, Z.; Fu, J.; Zhen, J.; Wang, W.; Cai, Y.; Wang, W. The protective effect of astaxanthin on learning and memory deficits and oxidative stress in a mouse model of repeated cerebral ischemia/reperfusion. *Brain Res. Bull.* **2017**, *131*, 221–228. [CrossRef] [PubMed]
31. Darvin, M.E.; Lademann, J.; von Hagen, J.; Lohan, S.B.; Kolmar, H.; Meinke, M.C.; Jung, S. Carotenoids in Human Skin *In Vivo*: Antioxidant and Photo-Protectant Role against External and Internal Stressors. *Antioxidants* **2022**, *11*, 1451. [CrossRef]
32. Weaver, R.J.; Wang, P.; Hill, G.E.; Cobine, P.A. An *in vivo* test of the biologically relevant roles of carotenoids as antioxidants in animals. *J. Exp. Biol.* **2018**, *221*, jeb183665. [CrossRef] [PubMed]
33. Eggersdorfer, M.; Wyss, A. Carotenoids in human nutrition and health. *Arch. Biochem. Biophys.* **2018**, *652*, 18–26. [CrossRef]
34. Rao, A.V.; Rao, L.G. Carotenoids and human health. *Pharmacol. Res.* **2007**, *55*, 207–216. [CrossRef] [PubMed]
35. Johnson, E.J. The role of carotenoids in human health. *Nutr. Clin. Care* **2002**, *5*, 56–65. [CrossRef] [PubMed]
36. Grand View Research. Carotenoids Market Size, Share & Trends Analysis Report By Source (Natural, Synthetic), By Product (Beta-Carotene, Lutein, Lycopene, Astaxanthin, Zeaxanthin, Canthaxanthin), By Application, And Segment Forecasts, 2018–2025 GVR-1-68038-321-8. 2016. Available online: <https://www.grandviewresearch.com/industry-analysis/carotenoids-market> (accessed on 13 September 2022).
37. Passi, S.; de Pità, O.; Puddu, P.; Littarru, G.P. Lipophilic antioxidants in human sebum and aging. *Free Radic. Res.* **2002**, *36*, 471–477. [CrossRef]
38. Darnet, S.; Blary, A.; Chevalier, Q.; Schaller, H. Phytosterol Profiles, Genomes and Enzymes—An Overview. *Front. Plant Sci.* **2021**, *12*, 665206. [CrossRef] [PubMed]
39. Micera, M.; Botto, A.; Geddo, F.; Antoniotti, S.; Berteà, C.M.; Levi, R.; Gallo, M.P.; Querio, G. Squalene: More than a Step toward Sterols. *Antioxidants* **2020**, *9*, 688. [CrossRef]
40. Huang, Z.-R.; Lin, Y.-K.; Fang, J.-Y. Biological and pharmacological activities of squalene and related compounds: Potential uses in cosmetic dermatology. *Molecules* **2009**, *14*, 540–554. [CrossRef]
41. Grand View Research. Squalene Market Size, Share & Trends Analysis Report By Raw Material (Vegetable, Synthetic, Animal), By Application (Cosmetics, Pharmaceuticals), By Region, And Segment Forecasts, 2016–2024 978-1-68038-991-3. 2016. Available online: <https://www.grandviewresearch.com/industry-analysis/squalene-market> (accessed on 13 September 2022).
42. Grand View Research. Europe Squalene Market Size, Share & Trends Analysis Report By Source (Animal, Plant, Synthetic), By End Use (Pharmaceuticals, Personal Care & Cosmetics, Nutraceuticals, Food & Beverages), By Country, And Segment Forecasts, 2021–2030 GVR-4-68039-500-4. 2021. Available online: <https://www.grandviewresearch.com/industry-analysis/europe-squalene-market-report#> (accessed on 13 September 2022).
43. Del Giudice, G.; Fragarpane, E.; Bugarini, R.; Hora, M.; Henriksson, T.; Palla, E.; O’hagan, D.; Donnelly, J.; Rappuoli, R.; Podda, A. Vaccines with the MF59 adjuvant do not stimulate antibody responses against squalene. *Clin. Vaccine Immunol.* **2006**, *13*, 1010–1013. [CrossRef]



44. Reddy, L.H.; Couvreur, P. Squalene: A natural triterpene for use in disease management and therapy. *Adv. Drug Deliv. Rev.* **2009**, *61*, 1412–1426. [\[CrossRef\]](#) [\[PubMed\]](#)
45. Deprez, P.P.; Volkman, J.K.; Davenport, S.R. Squalene content and Neutral Lipid Composition of Livers from Deep-sea Sharks Caught in Tasmanian Waters. *Aust. J. Mar. Freshw. Res.* **1990**, *41*, 375–387. [\[CrossRef\]](#)
46. Blumer, M. Hydrocarbons in digestive tract and liver of a basking shark. *Science* **1967**, *156*, 390–391. [\[CrossRef\]](#)
47. Heller, J.H.; Heller, M.S.; Springer, S.; Clark, E. Squalene Content of Various Shark Livers. *Nature* **1957**, *179*, 919–920. [\[CrossRef\]](#)
48. Kayma, M.; Tsuchiya, Y.; Nevenzel, J.C. The Hydrocarbons of Shark Liver Oils. *Bull. Jpn. Soc. Sci. Fish.* **1969**, *35*, 653–664. [\[CrossRef\]](#)
49. Wetherbee, B.M.; Nichols, P.D. Lipid composition of the liver oil of deep-sea sharks from the Chatham Rise, New Zealand. *Comp. Biochem. Physiol. B Biochem. Mol. Biol.* **2000**, *125*, 511–521. [\[CrossRef\]](#)
50. Tsujimoto, M. A Highly Unsaturated Hydrocarbon In Shark Liver Oil. *J. Ind. Eng. Chem.* **1916**, *8*, 889–896. [\[CrossRef\]](#)
51. Beltrán, G.; Bucheli, M.E.; Aguilera, M.P.; Belaj, A.; Jimenez, A. Squalene in virgin olive oil: Screening of variability in olive cultivars. *Eur. J. Lipid Sci. Technol.* **2016**, *118*, 1250–1253. [\[CrossRef\]](#)
52. Owen, R.; Mier, W.; Giacosa, A.; Hull, W.; Spiegelhalter, B.; Bartsch, H. Phenolic compounds and squalene in olive oils: The concentration and antioxidant potential of total phenols, simple phenols, secoiridoids, lignans and squalene. *Food Chem. Toxicol.* **2000**, *38*, 647–659. [\[CrossRef\]](#) [\[PubMed\]](#)
53. Berganza, B.E.; Moran, A.W.; Rodríguez, M.G.; Coto, N.M.; Santamaría, M.; Bressani, R. Effect of variety and location on the total fat, fatty acids and squalene content of amaranth. *Plant Foods Hum. Nutr.* **2003**, *58*, 1–6. [\[CrossRef\]](#)
54. Ryan, E.; Galvin, K.; O'Connor, T.P.; Maguire, A.R.; O'Brien, N.M. Phytosterol, squalene, tocopherol content and fatty acid profile of selected seeds, grains, and legumes. *Plant Foods Hum. Nutr.* **2007**, *62*, 85–91. [\[CrossRef\]](#)
55. Maguire, L.S.; O'Sullivan, S.M.; Galvin, K.; O'Connor, T.P.; O'Brien, N.M. Fatty acid profile, tocopherol, squalene and phytosterol content of walnuts, almonds, peanuts, hazelnuts and the macadamia nut. *Int. J. Food Sci. Nutr.* **2004**, *55*, 171–178. [\[CrossRef\]](#)
56. Raghukumar, S. Ecology of the marine protists, the Labyrinthulomycetes (Thraustochytrids and Labyrinthulids). *Eur. J. Protistol.* **2002**, *38*, 127–145. [\[CrossRef\]](#)
57. Raghukumar, S.; Damare, V.S. Increasing evidence for the important role of Labyrinthulomycetes in marine ecosystems. *Bot. Mar.* **2011**, *54*, 3–11. [\[CrossRef\]](#)
58. Sparrow, F.K. Biological Observations on the Marine Fungi of Woods Hole Waters. *Biol. Bull.* **1936**, *70*, 236–263. [\[CrossRef\]](#)
59. Sparrow, F.K. *Aquatic Phycomycetes*, 2nd ed.; University of Michigan Press: Ann Arbor, MI, USA, 1960.
60. Olive, L.S. *The Mycetozoa*; Academic Press: New York, NY, USA, 1975; ISBN 9780125262507.
61. Cavalier-Smith, T.; Allsopp, M.T.E.P.; Chao, E.E. Thraustochytrids are chromists, not Fungi: 18S rRNA signatures of Heterokonta. *Phil. Trans. R. Soc. Lond. B* **1994**, *346*, 387–397. [\[CrossRef\]](#)
62. Honda, D.; Yokochi, T.; Nakahara, T.; Raghukumar, S.; Nakagiri, A.; Schaumann, K.; Higashihara, T. Molecular phylogeny of labyrinthulids and thraustochytrids based on the sequencing of 18S ribosomal RNA gene. *J. Eukaryot. Microbiol.* **1999**, *46*, 637–647. [\[CrossRef\]](#)
63. Yokoyama, R.; Honda, D. Taxonomic rearrangement of the genus *Schizochytrium* sensu lato based on morphology, chemotaxonomic characteristics, and 18S rRNA gene phylogeny (Thraustochytriaceae, Labyrinthulomycetes): Emendation for *Schizochytrium* and erection of *Aurantiochytrium* and *Oblongichytrium* gen. nov. *Mycoscience* **2007**, *48*, 199–211. [\[CrossRef\]](#)
64. Yokoyama, R.; Salleh, B.; Honda, D. Taxonomic rearrangement of the genus *Ulkenia* sensu lato based on morphology, chemotaxonomic characteristics, and 18S rRNA gene phylogeny (Thraustochytriaceae, Labyrinthulomycetes): Emendation for *Ulkenia* and erection of *Botryochytrium*, *Parietichytrium*, and *Sicyoidochytrium* gen. nov. *Mycoscience* **2007**, *48*, 329–341. [\[CrossRef\]](#)
65. Tsui, C.K.M.; Marshall, W.; Yokoyama, R.; Honda, D.; Lippmeier, J.C.; Craven, K.D.; Peterson, P.D.; Berbee, M.L. Labyrinthulomycetes phylogeny and its implications for the evolutionary loss of chloroplasts and gain of ectoplasmic gliding. *Mol. Phylogenet. Evol.* **2009**, *50*, 129–140. [\[CrossRef\]](#)
66. Tsui, C.K.M.; Vrijmoe, L.L.P. A Re-Visit to the Evolution and Ecophysiology of the Labyrinthulomycetes. In *Marine Ecosystems*; Cruzado, A., Ed.; InTech: London, UK, 2012; ISBN 978-953-51-0176-5.
67. Alderman, D.J.; Harrison, J.L.; Bremer, G.B.; Jones, E.B.G. Taxonomic revisions in the marine biflagellate fungi: The ultrastructural evidence. *Mar. Biol.* **1974**, *25*, 345–357. [\[CrossRef\]](#)
68. Leander, C.A.; Porter, D. The Labyrinthulomycota Is Comprised of Three Distinct Lineages. *Mycologia* **2001**, *93*, 459–464. [\[CrossRef\]](#)
69. Patel, A.; Rova, U.; Christakopoulos, P.; Matsakas, L. Mining of squalene as a value-added byproduct from DHA producing marine thraustochytrid cultivated on food waste hydrolysate. *Sci. Total Environ.* **2020**, *736*, 139691. [\[CrossRef\]](#) [\[PubMed\]](#)
70. Patel, A.; Rova, U.; Christakopoulos, P.; Matsakas, L. Simultaneous production of DHA and squalene from *Aurantiochytrium* sp. grown on forest biomass hydrolysates. *Biotechnol. Biofuels* **2019**, *12*, 255. [\[CrossRef\]](#) [\[PubMed\]](#)
71. Patel, A.; Liefeldt, S.; Rova, U.; Christakopoulos, P.; Matsakas, L. Co-production of DHA and squalene by thraustochytrid from forest biomass. *Sci. Rep.* **2020**, *10*, 1992. [\[CrossRef\]](#) [\[PubMed\]](#)
72. Janthanomsuk, P.; Verduyn, C.; Chauvatcharin, S. Improved docosahexaenoic acid production in *Aurantiochytrium* by glucose limited pH-auxostat fed-batch cultivation. *Bioresour. Technol.* **2015**, *196*, 592–599. [\[CrossRef\]](#)
73. Chen, C.-Y.; Yang, Y.-T. Combining engineering strategies and fermentation technology to enhance docosahexaenoic acid (DHA) production from an indigenous *Thraustochytrium* sp. BM2 strain. *Biochem. Eng. J.* **2018**, *133*, 179–185. [\[CrossRef\]](#)



74. Gupta, A.; Singh, D.; Barrow, C.J.; Puri, M. Exploring potential use of Australian thraustochytrids for the bioconversion of glycerol to omega-3 and carotenoids production. *Biochem. Eng. J.* **2013**, *78*, 11–17. [\[CrossRef\]](#)
75. Gupta, A.; Barrow, C.J.; Puri, M. Omega-3 biotechnology: Thraustochytrids as a novel source of omega-3 oils. *Biotechnol. Adv.* **2012**, *30*, 1733–1745. [\[CrossRef\]](#)
76. Gupta, A.; Barrow, C.J.; Puri, M. Multiproduct biorefinery from marine thraustochytrids towards a circular bioeconomy. *Trends Biotechnol.* **2022**, *40*, 448–462. [\[CrossRef\]](#)
77. Ishitsuka, K.; Koide, M.; Yoshida, M.; Segawa, H.; Leproux, P.; Couderc, V.; Watanabe, M.M.; Kano, H. Identification of intracellular squalene in living algae, *Aurantiochytrium mangrovei* with hyper-spectral coherent anti-Stokes Raman microscopy using a sub-nanosecond supercontinuum laser source. *J. Raman Spectrosc.* **2017**, *48*, 8–15. [\[CrossRef\]](#)
78. Otagiri, M.; Khalid, A.; Moriya, S.; Osada, H.; Takahashi, S. Novel squalene-producing thraustochytrids found in mangrove water. *Biosci. Biotechnol. Biochem.* **2017**, *81*, 2034–2037. [\[CrossRef\]](#)
79. Fan, K.W.; Aki, T.; Chen, F.; Jiang, Y. Enhanced production of squalene in the thraustochytrid *Aurantiochytrium mangrovei* by medium optimization and treatment with terbinafine. *World J. Microbiol. Biotechnol.* **2010**, *26*, 1303–1309. [\[CrossRef\]](#)
80. Aasen, I.M.; Ertesvåg, H.; Heggeset, T.M.B.; Liu, B.; Brautaset, T.; Vadstein, O.; Ellingsen, T.E. Thraustochytrids as production organisms for docosahexaenoic acid (DHA), squalene, and carotenoids. *Appl. Microbiol. Biotechnol.* **2016**, *100*, 4309–4321. [\[CrossRef\]](#) [\[PubMed\]](#)
81. Singh, D.; Gupta, A.; Wilkens, S.L.; Mathur, A.S.; Tuli, D.K.; Barrow, C.J.; Puri, M. Understanding response surface optimisation to the modeling of Astaxanthin extraction from a novel strain *Thraustochytrium* sp. S7. *Algal Res.* **2015**, *11*, 113–120. [\[CrossRef\]](#)
82. Carmona, M.L.; Naganuma, T.; Yamaoka, Y. Identification by HPLC-MS of carotenoids of the *Thraustochytrium* CHN-1 strain isolated from the Seto Inland Sea. *Biosci. Biotechnol. Biochem.* **2003**, *67*, 884–888. [\[CrossRef\]](#)
83. Armenta, R.E.; Burja, A.; Radianingtyas, H.; Barrow, C.J. Critical assessment of various techniques for the extraction of carotenoids and co-enzyme Q10 from the Thraustochytrid strain ONC-T18. *J. Agric. Food. Chem.* **2006**, *54*, 9752–9758. [\[CrossRef\]](#) [\[PubMed\]](#)
84. Pawar, P.R.; Lali, A.M.; Prakash, G. Integration of continuous-high cell density-fed-batch fermentation for *Aurantiochytrium limacinum* for simultaneous high biomass, lipids and docosahexaenoic acid production. *Bioresour. Technol.* **2021**, *325*, 124636. [\[CrossRef\]](#)
85. Bailey, R.B.; DiMasi, D.; Hansen, M.; Mirrasoul, P.J.; Ruecker, C.M.; Veeder, G.T., III; Kaneko, T.; Barclay, W.R. Enhanced Production of Lipids Containing Polyenoic Fatty Acid by Very High Density Cultures of Eukaryotic Microbes in Fermentors. U.S. Patent 6,607,900 B2, 19 August 2003.
86. Humhal, T.; Kastanek, P.; Jezkova, Z.; Cadkova, A.; Kohoutkova, J.; Branyik, T. Use of saline waste water from demineralization of cheese whey for cultivation of *Schizochytrium limacinum* PA-968 and *Japonochytrium marinum* AN-4. *Bioprocess Biosyst. Eng.* **2017**, *40*, 395–402. [\[CrossRef\]](#)
87. Stefánsson, M.Ö.; Baldursson, S.; Magnússon, K.P.; Eyþórsdóttir, A.; Einarsson, H. Isolation, Characterization and Biotechnological Potentials of Thraustochytrids from Icelandic Waters. *Mar. Drugs* **2019**, *17*, 449. [\[CrossRef\]](#)
88. Bongiorno, L.; Jain, R.; Raghukumar, S.; Aggarwal, R.K. *Thraustochytrium gaertnerium* sp. nov.: A new thraustochytrid stramenopile protist from mangroves of Goa, India. *Protist* **2005**, *156*, 303–315. [\[CrossRef\]](#)
89. Jaseera, K.V.; Kaladharan, P.; Vijayan, K.K.; Sandhya, S.V.; Antony, M.L.; Pradeep, M.A. Isolation and phylogenetic identification of heterotrophic thraustochytrids from mangrove habitats along the southwest coast of India and prospecting their PUFA accumulation. *J. Appl. Phycol.* **2019**, *31*, 1057–1068. [\[CrossRef\]](#)
90. Nakai, R.; Naganuma, T. Diversity and Ecology of Thraustochytrid Protists in the Marine Environment. In *Marine Protists*; Ohtsuka, S., Suzaki, T., Horiguchi, T., Suzuki, N., Not, F., Eds.; Springer: Tokyo, Japan, 2015; pp. 331–346. ISBN 978-4-431-55129-4.
91. Ueda, M.; Nomura, Y.; Doi, K.; Nakajima, M.; Honda, D. Seasonal dynamics of culturable thraustochytrids (Labyrinthulomycetes, Stramenopiles) in estuarine and coastal waters. *Aquat. Microb. Ecol.* **2015**, *74*, 187–204. [\[CrossRef\]](#)
92. Bahnweg, G. Studies on the Physiology of Thraustochytriales I. Growth Requirements and Nitrogen Nutrition of *Thraustochytrium* sp., *Japonochytrium* sp., *Ulkenia* spp., and *Labyrinthuloides* spp. *Veröff. Inst. Meeresforsch. Bremerh.* **1979**, *17*, 245–268.
93. Min, K.H.; Lee, H.H.; Anbu, P.; Chaulagain, B.P.; Hur, B.K. The effects of culture condition on the growth property and docosahexaenoic acid production from *Thraustochytrium aureum* ATCC 34304. *Korean J. Chem. Eng.* **2012**, *29*, 1211–1215. [\[CrossRef\]](#)
94. Sohedein, M.N.A.; Wan-Mohtar, W.A.A.Q.I.; Hui-Yin, Y.; Ilham, Z.; Chang, J.-S.; Supramani, S.; Siew-Moi, P. Optimisation of biomass and lipid production of a tropical thraustochytrid *Aurantiochytrium* sp. UMACC-T023 in submerged-liquid fermentation for large-scale biodiesel production. *Biocatal. Agric. Biotechnol.* **2020**, *23*, 101496. [\[CrossRef\]](#)
95. Burja, A.M.; Radianingtyas, H.; Windust, A.; Barrow, C.J. Isolation and characterization of polyunsaturated fatty acid producing *Thraustochytrium* species: Screening of strains and optimization of omega-3 production. *Appl. Microbiol. Biotechnol.* **2006**, *72*, 1161–1169. [\[CrossRef\]](#) [\[PubMed\]](#)
96. Ganuza, E.; Anderson, A.J.; Ratledge, C. High-cell-density cultivation of *Schizochytrium* sp. in an ammonium/pH-auxostat fed-batch system. *Biotechnol. Lett.* **2008**, *30*, 1559–1564. [\[CrossRef\]](#)
97. Furlan, V.J.M.; Batista, I.; Bandarra, N.; Mendes, R.; Cardoso, C. Conditions for the Production of Carotenoids by *Thraustochytrium* sp. ATCC 26185 and *Aurantiochytrium* sp. ATCC PRA-276. *J. Aquat. Food Prod. Technol.* **2019**, *28*, 465–477. [\[CrossRef\]](#)
98. Vishniac, H.S. Salt Requirements of Marine Phycomycetes. *Limnol. Oceanogr.* **1960**, *5*, 362–366. [\[CrossRef\]](#)
99. Kalidasan, K.; Viniithkumar, N.V.; Peter, D.M.; Dharani, G.; Dufossé, L. Thraustochytrids of Mangrove Habitats from Andaman Islands: Species Diversity, PUFA Profiles and Biotechnological Potential. *Mar. Drugs* **2021**, *19*, 571. [\[CrossRef\]](#)



100. Iida, I.; Nakahara, T.; Yokochi, T.; Kamisaka, Y.; Yagi, H.; Yamaoka, M.; Suzuki, O. Improvement of docosahexaenoic acid production in a culture of *Thraustochytrium aureum* by medium optimization. *J. Ferment. Bioeng.* **1996**, *81*, 76–78. [\[CrossRef\]](#)
101. Goldstein, S. Morphological variation and nutrition of a new monocentric marine fungus. *Arch. Mikrobiol.* **1963**, *45*, 101–110. [\[CrossRef\]](#) [\[PubMed\]](#)
102. Bremer, G.B. Physiological responses of some thraustochytrid fungi. *Veröff. Inst. Meeresforsch. Bremerh.* **1974**, *55*, 237–250.
103. Goldstein, S. Studies of a New Species of *Thraustochytrium* that Displays Light Stimulated Growth. *Mycologia* **1963**, *55*, 799–811. [\[CrossRef\]](#)
104. Chang, M.; Zhang, T.; Guo, X.; Liu, Y.; Liu, R.; Jin, Q.; Wang, X. Optimization of cultivation conditions for efficient production of carotenoid-rich DHA oil by *Schizochytrium* sp. S31. *Process Biochem.* **2020**, *94*, 190–197. [\[CrossRef\]](#)
105. Bahnweg, G. Studies on the Physiology of Thraustochytriales II. Carbon Nutrition of *Thraustochytrium* sp., *Schizochytrium* sp., *Japonochytrium* sp., *Ulkenia* spp., and *Labyrinthuloides* spp. *Veröff. Inst. Meeresforsch. Bremerh.* **1979**, *17*, 245–268.
106. Leyton, A.; Shene, C.; Chisti, Y.; Asenjo, J.A. Production of Carotenoids and Phospholipids by *Thraustochytrium* sp. in Batch and Repeated-Batch Culture. *Mar. Drugs* **2022**, *20*, 416. [\[CrossRef\]](#)
107. Atienza, G. Carotenoid analysis of locally isolated Thraustochytrids and their potential as an alternative fish feed for *Oreochromis niloticus* (Nile tilapia). *Mycosphere* **2012**, *3*, 420–428. [\[CrossRef\]](#)
108. Zhang, K.; Chen, L.; Liu, J.; Gao, F.; He, R.; Chen, W.; Guo, W.; Chen, S.; Li, D. Effects of butanol on high value product production in *Schizochytrium limacinum* B4D1. *Enzyme Microb. Technol.* **2017**, *102*, 9–15. [\[CrossRef\]](#)
109. Thom, L.T.; Hien, H.T.M.; Thu, N.T.H.; Tam, L.T.; Ha, N.C.; Hong, D.D. Optimization of cultivation conditions of the heterotrophic marine microalga *Thraustochytrium aureum* BT6 oriented to exploit bioactive compounds. *AJB* **2021**, *43*, 83–94. [\[CrossRef\]](#)
110. Hassett, B.T.; Gradinger, R. New Species of Saprobiic Labyrinthulea (=Labyrinthulomycota) and the Erection of a gen. nov. to Resolve Molecular Polyphyly within the Aplanochytrids. *J. Eukaryot. Microbiol.* **2018**, *65*, 475–483. [\[CrossRef\]](#) [\[PubMed\]](#)
111. Bower, S.M. *Labyrinthuloides haliotidis* n.sp. (Protozoa: Labyrinthomorpha), a pathogenic parasite of small juvenile abalone in a British Columbia mariculture facility. *Can. J. Zool.* **1987**, *65*, 1996–2007. [\[CrossRef\]](#)
112. Leyton, A.; Flores, L.; Shene, C.; Chisti, Y.; Larama, G.; Asenjo, J.A.; Armenta, R.E. Antarctic Thraustochytrids as Sources of Carotenoids and High-Value Fatty Acids. *Mar. Drugs* **2021**, *19*, 386. [\[CrossRef\]](#) [\[PubMed\]](#)
113. Valdebenito, D.; Urrutia, S.; Leyton, A.; Chisti, Y.; Asenjo, J.A.; Shene, C. Nitrogen Sources Affect the Long-Chain Polyunsaturated Fatty Acids Content in *Thraustochytrium* sp. RT2316-16. *Mar. Drugs* **2023**, *21*, 15. [\[CrossRef\]](#) [\[PubMed\]](#)
114. Xiao, R.; Li, X.; Leonard, E.; Tharayil, N.; Zheng, Y. Investigation on the effects of cultivation conditions, fed-batch operation, and enzymatic hydrolysate of corn stover on the astaxanthin production by *Thraustochytrium striatum*. *Algal Res.* **2019**, *39*, 101475. [\[CrossRef\]](#)
115. Shene, C.; Garcés, M.; Vergara, D.; Peña, J.; Claverol, S.; Rubilar, M.; Leyton, A. Production of Lipids and Proteome Variation in a Chilean *Thraustochytrium striatum* Strain Cultured under Different Growth Conditions. *Mar. Biotechnol.* **2019**, *21*, 99–110. [\[CrossRef\]](#)
116. Fossier Marchan, L.; Lee Chang, K.J.; Nichols, P.D.; Mitchell, W.J.; Polglase, J.L.; Gutierrez, T. Taxonomy, ecology and biotechnological applications of thraustochytrids: A review. *Biotechnol. Adv.* **2018**, *36*, 26–46. [\[CrossRef\]](#)
117. Xiao, R.; Li, X.; Zheng, Y. Comprehensive Study of Cultivation Conditions and Methods on Lipid Accumulation of a Marine Protist, *Thraustochytrium striatum*. *Protist* **2018**, *169*, 451–465. [\[CrossRef\]](#) [\[PubMed\]](#)
118. Shi, T.-Q.; Wang, L.-R.; Zhang, Z.-X.; Sun, X.-M.; Huang, H. Stresses as First-Line Tools for Enhancing Lipid and Carotenoid Production in Microalgae. *Front. Bioeng. Biotechnol.* **2020**, *8*, 610. [\[CrossRef\]](#)
119. Kaya, K.; Nakazawa, A.; Matsuura, H.; Honda, D.; Inouye, I.; Watanabe, M.M. Thraustochytrid *Aurantiochytrium* sp. 18W-13a Accumulates High Amounts of Squalene. *Biosci. Biotechnol. Biochem.* **2011**, *75*, 2246–2248. [\[CrossRef\]](#)
120. Nakazawa, A.; Kokubun, Y.; Matsuura, H.; Yonezawa, N.; Kose, R.; Yoshida, M.; Tanabe, Y.; Kusuda, E.; van Thang, D.; Ueda, M.; et al. TLC screening of thraustochytrid strains for squalene production. *J. Appl. Phycol.* **2014**, *26*, 29–41. [\[CrossRef\]](#)
121. Chen, G.; Fan, K.-W.; Lu, F.-P.; Li, Q.; Aki, T.; Chen, F.; Jiang, Y. Optimization of nitrogen source for enhanced production of squalene from thraustochytrid *Aurantiochytrium* sp. *New Biotechnol.* **2010**, *27*, 382–389. [\[CrossRef\]](#)
122. Hoang, M.H.; Ha, N.C.; Le Thom, T.; Tam, L.T.; Anh, H.T.L.; Thu, N.T.H.; Hong, D.D. Extraction of squalene as value-added product from the residual biomass of *Schizochytrium mangrovei* PQ6 during biodiesel producing process. *J. Biosci. Bioeng.* **2014**, *118*, 632–639. [\[CrossRef\]](#)
123. Jiang, Y.; Fan, K.-W.; Wong, R.T.-Y.; Chen, F. Fatty acid composition and squalene content of the marine microalga *Schizochytrium mangrovei*. *J. Agric. Food. Chem.* **2004**, *52*, 1196–1200. [\[CrossRef\]](#)
124. Lewis, T.E.; Nichols, P.D.; McMeekin, T.A. Sterol and squalene content of a docosahexaenoic-acid-producing thraustochytrid: Influence of culture age, temperature, and dissolved oxygen. *Mar. Biotechnol.* **2001**, *3*, 439–447. [\[CrossRef\]](#)
125. Dellerio, Y.; Cagnac, O.; Rose, S.; Seddiki, K.; Cussac, M.; Morabito, C.; Lupette, J.; Aiese Cigliano, R.; Sanseverino, W.; Kuntz, M.; et al. Proposal of a new thraustochytrid genus *Hondaea* gen. nov. and comparison of its lipid dynamics with the closely related pseudo-cryptic genus *Aurantiochytrium*. *Algal Res.* **2018**, *35*, 125–141. [\[CrossRef\]](#)
126. Zhang, A.; He, Y.; Sen, B.; Wang, W.; Wang, X.; Wang, G. Optimal NaCl Medium Enhances Squalene Accumulation in *Thraustochytrium* sp. ATCC 26185 and Influences the Expression Levels of Key Metabolic Genes. *Front. Microbiol.* **2022**, *13*, 900252. [\[CrossRef\]](#) [\[PubMed\]](#)



127. Ren, L.-J.; Sun, G.-N.; Ji, X.-J.; Hu, X.-C.; Huang, H. Compositional shift in lipid fractions during lipid accumulation and turnover in *Schizochytrium* sp. *Bioresour. Technol.* **2014**, *157*, 107–113. [\[CrossRef\]](#)
128. Du, H.; Liao, X.; Gao, Z.; Li, Y.; Lei, Y.; Chen, W.; Chen, L.; Fan, X.; Zhang, K.; Chen, S.; et al. Effects of Methanol on Carotenoids as Well as Biomass and Fatty Acid Biosynthesis in *Schizochytrium limacinum* B4D1. *Appl. Environ. Microbiol.* **2019**, *85*, e01243-19. [\[CrossRef\]](#) [\[PubMed\]](#)
129. Bi, Z.-Q.; Ren, L.-J.; Hu, X.-C.; Sun, X.-M.; Zhu, S.-Y.; Ji, X.-J.; Huang, H. Transcriptome and gene expression analysis of docosahexaenoic acid producer *Schizochytrium* sp. under different oxygen supply conditions. *Biotechnol. Biofuels* **2018**, *11*, 249. [\[CrossRef\]](#) [\[PubMed\]](#)
130. Yue, C.-J.; Jiang, Y. Impact of methyl jasmonate on squalene biosynthesis in microalga *Schizochytrium mangrovei*. *Process Biochem.* **2009**, *44*, 923–927. [\[CrossRef\]](#)
131. Hur, B.-K.; Cho, D.-W.; Kim, H.-J.; Park, C.-I.; Suh, H.-J. Effect of culture conditions on growth and production of docosahexaenoic acid (DHA) using *Thraustochytrium aureum* ATCC 34304. *Biotechnol. Bioprocess Eng.* **2002**, *7*, 10–15. [\[CrossRef\]](#)
132. Kendrick, A.; Ratledge, C. Lipids of selected molds grown for production of n-3 and n-6 polyunsaturated fatty acids. *Lipids* **1992**, *27*, 15–20. [\[CrossRef\]](#)
133. Bajpai, P.K.; Bajpai, P.; Ward, O.P. Optimization of production of docosahexaenoic acid (DHA) by *Thraustochytrium aureum* ATCC 34304. *J. Am. Oil Chem. Soc.* **1991**, *68*, 509–514. [\[CrossRef\]](#)
134. Chandrasekaran, K.; Roy, R.K.; Chadha, A. Docosahexaenoic acid production by a novel high yielding strain of *Thraustochytrium* sp. of Indian origin: Isolation and bioprocess optimization studies. *Algal Res.* **2018**, *32*, 93–100. [\[CrossRef\]](#)
135. Manikan, V.; Kalil, M.S.; Hamid, A.A. Response surface optimization of culture medium for enhanced docosahexaenoic acid production by a Malaysian thraustochytrid. *Sci. Rep.* **2015**, *5*, 8611. [\[CrossRef\]](#)
136. Ugalde, V.; Armenta, R.E.; Kermanshahi-pour, A.; Sun, Z.; Berryman, K.T.; Brooks, M.S. Improvement of culture conditions for cell biomass and fatty acid production by marine thraustochytrid F24-2. *J. Appl. Phycol.* **2018**, *30*, 329–339. [\[CrossRef\]](#)
137. Nakazawa, A.; Matsuura, H.; Kose, R.; Ito, K.; Ueda, M.; Honda, D.; Inouye, I.; Kaya, K.; Watanabe, M.M. Optimization of Biomass and Fatty Acid Production by *Aurantiochytrium* sp. Strain 4W-1b. *Procedia Environ. Sci.* **2012**, *15*, 27–33. [\[CrossRef\]](#)
138. Raghukumar, S.; Sathe-Pathak, V.; Sharma, S.; Raghukumar, C. Thraustochytrid and fungal component of marine detritus. III. Field studies on decomposition of leaves of the mangrove *Rhizophora apiculata*. *Aquat. Microb. Ecol.* **1995**, *9*, 117–125. [\[CrossRef\]](#)
139. Sathe-Pathak, V.; Raghukumar, S.; Raghukumar, C.; Sharma, S. Thraustochytrid and fungal component of marine detritus. I—Field studies on decomposition of the brown alga *Sargassum cinereum* J. Ag. *Indian J. Mar. Species* **1993**, *22*, 159–167.
140. Raghukumar, S.; Anil, A.C.; Khandeparker, L.; Patil, J.S. Thraustochytrid protists as a component of marine microbial films. *Mar. Biol.* **2000**, *136*, 603–609. [\[CrossRef\]](#)
141. Dalirian, N.; Abedini Najafabadi, H.; Movahedirad, S. Surface attached cultivation and filtration of microalgal biofilm in a ceramic substrate photobioreactor. *Algal Res.* **2021**, *55*, 102239. [\[CrossRef\]](#)
142. Rincon, S.M.; Romero, H.M.; Aframehr, W.M.; Beyenal, H. Biomass production in *Chlorella vulgaris* biofilm cultivated under mixotrophic growth conditions. *Algal Res.* **2017**, *26*, 153–160. [\[CrossRef\]](#)
143. Mantzourou, A.; Ververidis, F. Microalgal biofilms: A further step over current microalgal cultivation techniques. *Sci. Total Environ.* **2019**, *651*, 3187–3201. [\[CrossRef\]](#) [\[PubMed\]](#)
144. Li, T.; Strous, M.; Melkonian, M. Biofilm-based photobioreactors: Their design and improving productivity through efficient supply of dissolved inorganic carbon. *FEMS Microbiol. Lett.* **2017**, *364*, fnx218. [\[CrossRef\]](#) [\[PubMed\]](#)
145. Jeh, E.-J.; Kumaran, R.S.; Hur, B.-K. Lipid body formation by *Thraustochytrium aureum* (ATCC 34304) in response to cell age. *Korean J. Chem. Eng.* **2008**, *25*, 1103–1109. [\[CrossRef\]](#)
146. Egeland, E.S.; Liaaen-Jensen, S. Ten minor carotenoids from prasinophyceae (chlorophyta). *Phytochemistry* **1995**, *40*, 515–520. [\[CrossRef\]](#)
147. Latasa, M.; Scharek, R.; Le Gall, F.; Guillou, L. Pigment Suites and Taxonomic Groups in Prasinophyceae. *J. Phycol.* **2004**, *40*, 1149–1155. [\[CrossRef\]](#)
148. Makino, T.; Harada, H.; Ikenaga, H.; Matsuda, S.; Takaichi, S.; Shindo, K.; Sandmann, G.; Ogata, T.; Misawa, N. Characterization of cyanobacterial carotenoid ketolase CrtW and hydroxylase CrtR by complementation analysis in *Escherichia coli*. *Plant Cell Physiol.* **2008**, *49*, 1867–1878. [\[CrossRef\]](#)
149. Fraser, P.D.; Shimada, H.; Misawa, N. Enzymic confirmation of reactions involved in routes to astaxanthin formation, elucidated using a direct substrate in vitro assay. *Eur. J. Biochem.* **1998**, *252*, 229–236. [\[CrossRef\]](#)
150. Hornero-Méndez, D.; Limón, M.C.; Avalos, J. HPLC Analysis of Carotenoids in Neurospora xanthin-Producing Fungi. *Methods Mol. Biol.* **2018**, *1852*, 269–281. [\[CrossRef\]](#)
151. Verdoes, J.C.; Krubasik, K.P.; Sandmann, G.; van Ooyen, A.J. Isolation and functional characterisation of a novel type of carotenoid biosynthetic gene from *Xanthophyllomyces dendrorhous*. *Mol. Gen. Genet.* **1999**, *262*, 453–461. [\[CrossRef\]](#)
152. Barredo, J.L.; García-Estrada, C.; Kosalkova, K.; Barreiro, C. Biosynthesis of Astaxanthin as a Main Carotenoid in the Heterobasidiomycetous Yeast *Xanthophyllomyces dendrorhous*. *J. Fungi* **2017**, *3*, 44. [\[CrossRef\]](#) [\[PubMed\]](#)
153. Zvezdanović, J.; Petrović, S.; Marković, D. Hematoporphyrin derivatives: The ultrahigh performance liquid chromatography: Diode array: Electrospray ionization: Mass spectrometry analysis. *Adv. Technol.* **2017**, *6*, 26–30. [\[CrossRef\]](#)
154. Sernicola, A.; Cama, E.; Pelizzo, M.G.; Tessarolo, E.; Nicolli, A.; Viero, G.; Alaibac, M. In vitro Assessment of Solar Filters for Erythropoietic Protoporphyrin in the Action Spectrum of Protoporphyrin IX. *Front. Med.* **2021**, *8*, 796884. [\[CrossRef\]](#)



155. Lim, C.K.; Razzaque, M.A.; Luo, J.; Farmer, P.B. Isolation and characterization of protoporphyrin glycoconjugates from rat Harderian gland by HPLC, capillary electrophoresis and HPLC/electrospray ionization MS. *Biochem. J.* **2000**, *347*, 757–761. [\[CrossRef\]](#) [\[PubMed\]](#)
156. Lan, M.; Zhao, H.; Yuan, H.; Jiang, C.; Zuo, S.; Jiang, Y. Absorption and EPR spectra of some porphyrins and metalloporphyrins. *Dyes Pigment.* **2007**, *74*, 357–362. [\[CrossRef\]](#)
157. Giovannetti, R. The Use of Spectrophotometry UV-Vis for the Study of Porphyrins. In *Macro To Nano Spectroscopy*; Uddin, J., Ed.; InTech: London, UK, 2012; ISBN 978-953-51-0664-7.
158. Kim, B.F.; Bohandy, J. Spectroscopy of Porphyrins. *Johns Hopkins APL Tech. Dig.* **1981**, *2*, 153–163.
159. Chamberlain, A.H.; Moss, S.T. The thraustochytrids: A protist group with mixed affinities. *BioSystems* **1988**, *21*, 341–349. [\[CrossRef\]](#)
160. Ulken, A. Zwei neue Thraustochytrien aus der Außenweser. *Veröff. Inst. Meeresforsch. Bremerh.* **1965**, *9*, 289–296.
161. Konstantinov, D.K.; Menzorov, A.; Krivenko, O.; Doroshkov, A.V. Isolation and transcriptome analysis of a biotechnologically promising Black Sea protist, *Thraustochytrium aureum* ssp. *strugatskii*. *PeerJ* **2022**, *10*, e12737. [\[CrossRef\]](#)
162. Goldstein, S.; Belsky, M. Axenic culture studies of a new marine phycomycete possessing an unusual type of asexual reproduction. *Am. J. Bot.* **1964**, *51*, 72–78. [\[CrossRef\]](#)
163. Chi, G.; Xu, Y.; Cao, X.; Li, Z.; Cao, M.; Chisti, Y.; He, N. Production of polyunsaturated fatty acids by *Schizochytrium* (*Aurantiochytrium*) spp. *Biotechnol. Adv.* **2022**, *55*, 107897. [\[CrossRef\]](#)
164. Lv, J.; Yang, X.; Ma, H.; Hu, X.; Wei, Y.; Zhou, W.; Li, L. The oxidative stability of microalgae oil (*Schizochytrium aggregatum*) and its antioxidant activity after simulated gastrointestinal digestion: Relationship with constituents. *Eur. J. Lipid Sci. Technol.* **2015**, *117*, 1928–1939. [\[CrossRef\]](#)
165. Ulken, A. Über einige Thraustochytrien des polyhalinen Brackwassers. *Veröff. Inst. Meeresforsch. Bremerh.* **1964**, *9*, 31–41.
166. Goldstein, S. Zoospore marine fungi (Thraustochytriaceae and Dermocystidiaceae). *Annu. Rev. Microbiol.* **1973**, *27*, 13–26. [\[CrossRef\]](#) [\[PubMed\]](#)
167. Raghukumar, S. Bacterivory: A novel dual role for thraustochytrids in the sea. *Mar. Biol.* **1992**, *113*, 165–169. [\[CrossRef\]](#)
168. Gaertner, A. Revision of the Thraustochytriaceae (Lower Marine Fungi) I. *Ulkenia* nov. gen., with Description of Three New Species. *Veröff. Inst. Meeresforsch. Bremerh.* **1977**, *16*, 139–157.
169. Sparrow, F.K. Zoospore marine fungi from the Pacific Northwest (U.S.A.). *Arch. Mikrobiol.* **1969**, *66*, 129–146. [\[CrossRef\]](#)
170. Schneider, J. Ein neuer mariner Phycomycet aus der Kieler Bucht (*Thraustochytrium striatum* spec. nov.). *Kieler Meeresforsch.* **1967**, *27*, 16–20.
171. Harrison, J.L.; Gareth Jones, E.B. Zoospore discharge in *Thraustochytrium striatum*. *Trans. Br. Mycol. Soc.* **1974**, *62*, 283–288. [\[CrossRef\]](#)
172. Gaertner, A. Ökologische Untersuchungen an einem marinen Pilz aus der Umgebung von Helgoland. *Helgol. Mar. Res.* **1967**, *15*, 181–192. [\[CrossRef\]](#)
173. Gaertner, A. Beobachtungen über die Sporulation der dickwandigen Sporangien von *Thraustochytrium kinnei* GAERTNER. *Veröff. Inst. Meeresforsch. Bremerh.* **1970**, *12*, 321–327.
174. Moss, S.T. Ultrastructure of the Endomembrane—Sagenogenetosome—Ectoplasmic Net Complex in *Ulkenia visurgensis* (Thraustochytriales). *Bot. Mar.* **1980**, *23*, 73–94. [\[CrossRef\]](#)
175. Iwata, I.; Honda, D. Nutritional Intake by Ectoplasmic Nets of *Schizochytrium aggregatum* (Labyrinthulomycetes, Stramenopiles). *Protist* **2018**, *169*, 727–743. [\[CrossRef\]](#)
176. Hamamoto, Y.; Honda, D. Nutritional intake of *Aplanochytrium* (Labyrinthulea, Stramenopiles) from living diatoms revealed by culture experiments suggesting the new prey-predator interactions in the grazing food web of the marine ecosystem. *PLoS ONE* **2019**, *14*, e0208941. [\[CrossRef\]](#)
177. Perkins, F.O. Observations of thraustochytriaceous (Phycomycetes) and labyrinthulid (Rhizopodea) ectoplasmic nets on natural and artificial substrates—An electron microscope study. *Can. J. Bot.* **1973**, *51*, 485–491. [\[CrossRef\]](#)
178. Coleman, N.K.; Vestal, J.R. An epifluorescent microscopy study of enzymatic hydrolysis of fluorescein diacetate associated with the ectoplasmic net elements of the protist *Thraustochytrium striatum*. *Can. J. Microbiol.* **1987**, *33*, 841–843. [\[CrossRef\]](#)
179. Weete, J.D.; Kim, H.; Gandhi, S.R.; Wang, Y.; Dute, R. Lipids and ultrastructure of *Thraustochytrium* sp. ATCC 26185. *Lipids* **1997**, *32*, 839–845. [\[CrossRef\]](#)
180. Ganuza, E.; Yang, S.; Amezcua, M.; Giraldo-Silva, A.; Andersen, R.A. Genomics, Biology and Phylogeny *Aurantiochytrium acetophilum* sp. nov. (Thraustochytriaceae), Including First Evidence of Sexual Reproduction. *Protist* **2019**, *170*, 209–232. [\[CrossRef\]](#)
181. Geraci-Yee, S.; Brianik, C.J.; Rubin, E.; Collier, J.L.; Allam, B. Erection of a New Genus and Species for the Pathogen of Hard Clams ‘Quahog Parasite Unknown’ (QPX): *Mucochytrium quahogii* gen. nov., sp. nov. *Protist* **2021**, *172*, 125793. [\[CrossRef\]](#)
182. Leipe, D.D.; Tong, S.M.; Goggin, C.L.; Slemenda, S.B.; Pieniazek, N.J.; Sogin, M.L. 16S-like rDNA sequences from *Developayella elegans*, *Labyrinthuloides haliotis*, and *Proteromonas lacertae* confirm that the stramenopiles are a primarily heterotrophic group. *Eur. J. Protistol.* **1996**, *32*, 449–458. [\[CrossRef\]](#)
183. Gaertner, A. Einiges zur Kultur mariner niederer Pilze. *Helgol. Mar. Res.* **1970**, *20*, 29–38. [\[CrossRef\]](#)
184. Raghu Kumar, S. A New Species of the Genus *Ulkenia* GAERTNER (Lower Marine Fungi) from the North Sea. *Veröff. Inst. Meeresforsch. Bremerh.* **1977**, *16*, 159–165.



185. Raghu Kumar, S. *Thraustochytrium benthicola* sp. nov.: A new marine fungus from the North Sea. *Trans. Br. Mycol. Soc.* **1980**, *74*, 607–614. [\[CrossRef\]](#)
186. Raghu Kumar, S. Fine structure of the thraustochytrid *Ulkenia amoeboides*. I. Vegetative thallus and formation of the amoeboid stage. *Can. J. Bot.* **1982**, *60*, 1092–1102. [\[CrossRef\]](#)
187. Burmeister, A. *Ein Vergleich von Identifikationsmethoden zur Bestimmung von Thraustochytriaceae*. Bachelorthesis; Hochschule für Angewandte Wissenschaften Hamburg: Hamburg, Germany, 2014.
188. Seehusen, L. Molekularbiologische Analyse der Taxonomie von Thraustochytriaceae. Bachelor's Thesis, University of Applied Sciences Flensburg, Flensburg, Germany, 2020.
189. Gupta, A.; Wilkens, S.; Adcock, J.L.; Puri, M.; Barrow, C.J. Pollen baiting facilitates the isolation of marine thraustochytrids with potential in omega-3 and biodiesel production. *J. Ind. Microbiol. Biotechnol.* **2013**, *40*, 1231–1240. [\[CrossRef\]](#)
190. Lee Chang, K.J.; Dumsday, G.; Nichols, P.D.; Dunstan, G.A.; Blackburn, S.I.; Koutoulis, A. High cell density cultivation of a novel *Aurantiochytrium* sp. strain TC 20 in a fed-batch system using glycerol to produce feedstock for biodiesel and omega-3 oils. *Appl. Microbiol. Biotechnol.* **2013**, *97*, 6907–6918. [\[CrossRef\]](#) [\[PubMed\]](#)
191. Mo, C.; Douek, J.; Rinkevich, B. Development of a PCR strategy for thraustochytrid identification based on 18S rDNA sequence. *Mar. Biol.* **2002**, *140*, 883–889. [\[CrossRef\]](#)
192. Nakayama, T.; Watanabe, S.; Mitsui, K.; Uchida, H.; Inouye, I. The phylogenetic relationship between the Chlamydomonadales and Chlorococcales inferred from 18SrDNA sequence data. *Phycol. Res.* **1996**, *44*, 47–55. [\[CrossRef\]](#)
193. Tamura, K.; Nei, M. Estimation of the number of nucleotide substitutions in the control region of mitochondrial DNA in humans and chimpanzees. *Mol. Biol. Evol.* **1993**, *10*, 512–526. [\[CrossRef\]](#)
194. Tamura, K.; Stecher, G.; Kumar, S. MEGA11: Molecular Evolutionary Genetics Analysis Version 11. *Mol. Biol. Evol.* **2021**, *38*, 3022–3027. [\[CrossRef\]](#) [\[PubMed\]](#)
195. Holtin, K.; Kuehnle, M.; Rehbein, J.; Schuler, P.; Nicholson, G.; Albert, K. Determination of astaxanthin and astaxanthin esters in the microalgae *Haematococcus pluvialis* by LC-(APCI)MS and characterization of predominant carotenoid isomers by NMR spectroscopy. *Anal. Bioanal. Chem.* **2009**, *395*, 1613–1622. [\[CrossRef\]](#) [\[PubMed\]](#)
196. Euglert, G.; Vecchi, M. *trans/cis* Isomerization of Astaxanthin Diacetate/Isolation by HPLC. and Identification by <sup>1</sup>H-NMR. Spectroscopy of Three Mono-*cis*- and Six Di-*cis*-Isomers. *Helv. Chim. Acta* **1980**, *63*, 1711–1718. [\[CrossRef\]](#)
197. Casella, P.; Iovine, A.; Mehariya, S.; Marino, T.; Musmarra, D.; Molino, A. Smart Method for Carotenoids Characterization in *Haematococcus pluvialis* red phase and Evaluation of Astaxanthin Thermal Stability. *Antioxidants* **2020**, *9*, 422. [\[CrossRef\]](#) [\[PubMed\]](#)
198. Subramanian, B.; Tchoukanova, N.; Djaoued, Y.; Pelletier, C.; Ferron, M.; Robichaud, J. Investigations on the geometrical isomers of astaxanthin: Raman spectroscopy of conjugated polyene chain with electronic and mechanical confinement. *J. Raman Spectrosc.* **2014**, *45*, 299–304. [\[CrossRef\]](#)
199. Kulikov, E.A.; Kulikova, I.S.; Vasilov, R.G.; Selishcheva, A.A. The Effect of the Solvent Nature and Lighting on Isomerization and Oxidative Degradation of Astaxanthin. *Biophysics* **2020**, *65*, 433–442. [\[CrossRef\]](#)
200. de Bruijn, W.J.C.; Weesepoel, Y.; Vincken, J.-P.; Gruppen, H. Fatty acids attached to all-*trans*-astaxanthin alter its *cis-trans* equilibrium, and consequently its stability, upon light-accelerated autoxidation. *Food Chem.* **2016**, *194*, 1108–1115. [\[CrossRef\]](#)
201. Bjerkeng, B.; Følling, M.; Lagocki, S.; Storebakken, T.; Olli, J.J.; Alsted, N. Bioavailability of all-*E*-astaxanthin and *Z*-isomers of astaxanthin in rainbow trout (*Oncorhynchus mykiss*). *Aquaculture* **1997**, *157*, 63–82. [\[CrossRef\]](#)
202. Doi, K.; Honda, D. Proposal of *Monorhizochytrium globosum* gen. nov., comb. nov. (Stramenopiles, Labyrinthulomycetes) for former *Thraustochytrium globosum* based on morphological features and phylogenetic relationships. *Phycol. Res.* **2017**, *65*, 188–201. [\[CrossRef\]](#)
203. Schärer, L.; Knoflach, D.; Vizoso, D.B.; Rieger, G.; Peintner, U. Thraustochytrids as novel parasitic protists of marine free-living flatworms: *Thraustochytrium caudivorum* sp. nov. parasitizes *Macrostomum lignano*. *Mar. Biol.* **2007**, *152*, 1095–1104. [\[CrossRef\]](#)
204. Fossier Marchan, L.; Lee Chang, K.J.; Nichols, P.D.; Polglase, J.L.; Mitchell, W.J.; Gutierrez, T. Screening of new British thraustochytrids isolates for docosahexaenoic acid (DHA) production. *J. Appl. Phycol.* **2017**, *29*, 2831–2843. [\[CrossRef\]](#) [\[PubMed\]](#)

**Disclaimer/Publisher's Note:** The statements, opinions and data contained in all publications are solely those of the individual author(s) and contributor(s) and not of MDPI and/or the editor(s). MDPI and/or the editor(s) disclaim responsibility for any injury to people or property resulting from any ideas, methods, instructions or products referred to in the content.







### Synthesis and General Discussion

The steady and fast growth of society and the associated technological developments have led to various conveniences but also challenges. Global life expectancy increased tremendously over the last century, from an estimate of around 30 years in the middle of the 19<sup>th</sup> century [358] to 66.8 years in 2000 and 73.3 years in 2019 [359]. Associated with this is the desire to lead a healthy and active lifestyle, preferably into old age. Therein lies one of many challenges. Health depends on a variety of factors, but nutrition is very important. A healthy and balanced diet can help the body maintain vital functions, resist harmful environmental influences, and avoid the intake of detrimental substances. Carotenoids have been shown to be non-toxic colorants and are applied in various foods, such as sweets, meat, beverages, and dairy products. Likewise, they are also used in animal feed, e.g., to enhance the color of eggs and fish. These products appeal to consumers without the drawbacks of potentially problematic chemicals. Such dyes are especially important when consumers have become accustomed to particular product colors and are willing to pay higher prices if these colors meet their expectations. A prominent example is the striking red color of salmon [360], which is lost in fish from aquaculture if it is not added to the fish's diet. Therefore, as the population grows, so does the demand for harmless colorants such as carotenoids.

Some carotenoids, especially  $\beta$ -carotene, are known for their provitamin A activity. Although vitamin A deficiency has generally declined and largely disappeared in Western society, it is still a problem in some poorer African and Asian regions [361]. Higher carotenoid consumption might be a step toward overcoming related diseases [158,161]. In addition, many carotenoids have gained a reputation for having a positive effect on human health, based on recent optimistic scientific studies but without clinical proof. For many people, self-responsible and healthy behavior includes dietary supplements. As a result, the demand for dietary supplements, foods, and cosmetics enriched with carotenoids has increased.

This demand for carotenoids can be met in different ways, either by chemical synthesis or biotechnological production. Both ways are valid and have advantages and disadvantages, but three major aspects need to be considered. First, in the context of bulk colorants, synthetic chemistry is currently indispensable for providing the large quantities of carotenoids needed for all already established applications. In addition, synthetic carotenoids might become a possible alternative for other dyes that are still under discussion because of possible negative effects on humans [362,363], e.g., azo dyes like tartrazine [364] and Allura Red [365]. The white dye titan dioxide, formerly widely regarded as harmless, has recently been withdrawn from the market due to safety concerns [366]. These issues underscore the need for non-toxic and non-controversial dyes. Second, consumers increasingly demand sustainable, natural, environmentally friendly, and fossil-free products in the context of nutraceuticals, food supplements, cosmetics, or products in general, where the carotenoid moiety contributes considerably to the sales argument. For direct human consumption, often only naturally produced carotenoids are approved by law. In this context, biotechnological production is an important part of the



supply, especially for certain carotenoids. Third, given the ongoing climatic change and in order to reduce carbon dioxide emissions and achieve sustainability goals, processes must be evaluated along these lines. Biotechnological production is a fairly young discipline and needs to develop rapidly to use resources as efficiently as possible. It offers new solution possibilities, such as the direct use of solar energy, carbon dioxide, and waste streams, for the production of microorganisms and carotenoids in circular economy approaches, as side streams might be used along the value chain.

There are different possibilities to fuel these developments, and this work aims to contribute by filling gaps and providing new insights at different stages of the biotechnological production of carotenoids. Typically, this can be done by approaching the production at the strain or process level, where the process level itself is a very broad term for a variety of possible steps, which need to be coordinated and are often interdependent. The strain level is also quite complex. Only a fraction of the microbial diversity is used for biotechnological processes. Recent projections suggest that up to a trillion different species of microorganisms live on earth [367]. The estimate of the proportion of bacteria and archaea that can be cultivated is the subject of ongoing discussion [368,369], but most likely, it is very small. Numbers for unicellular eukaryotes are probably similar. The discovery of new production organisms and knowledge of their metabolic potential can be crucial to making great leaps toward high yields.

The present work aims to address both of these issues. First, already established downstream processes should be improved to achieve higher carotenoid yield and lower energy consumption. Second, the focus should be extended to use new production organisms whose specific properties could favor production. It should also shed light on the conditions that induce carotenoid synthesis in these organisms. Both approaches required accurate and robust determination of carotenoids to draw clear and confident conclusions about the optimal process and cultivation parameters. Therefore, the development of such analytic methods was the first step to improve biotechnological carotenoid production.

### **Quantification of Astaxanthin from Natural Sources**

In chapter 1, a method for measuring biotechnologically produced carotenoids was developed and adapted, using astaxanthin from *H. pluvialis* as an example. As described, natural astaxanthin differs from its chemical counterpart by the spatial isomers and their linkage with fatty acids. It was shown that enzymatic deesterification is a valuable tool to obtain free astaxanthin from its esters. Attention must be paid to the source material and the amount used in the process since the yield is limited by the enzymatic capacity and depends on the quality of the starting material in the subsequent extraction. This may need to be considered when adapting this method to measure carotenoids produced by other microorganisms or plants. The enzymatic cleavage process was very robust, allowing direct treatment of ethanolic extracts such as those obtained from supercritical CO<sub>2</sub> (SC-CO<sub>2</sub>) extraction. The observation of remarkable changes in the distribution of diastereomers in different samples and sample types showed that isomer proportions cannot be generalized. Still, difficulties remain to estimate how the method and



its many steps affected the original isomer composition of the sample. Studies have shown that isomerization of astaxanthin and other carotenoids is common in different solvents and with temperature or light treatment [42,370–373]. The measurements performed in this study with different solvents gave similar results. This problem is not inherent to this particular developed process but is a general obstacle in invasive measurements. Developments towards non-invasive methods, such as Raman microscopy and spectroscopy, which are already capable of measuring some carotenoids in living cells [9] and distinguishing between diastereomers [45], may in the future be able to detect the composition of more carotenoids and their isomers in living cells. In particular, in the context of the different bioavailability and antioxidant activity of *Z*-isomers [243,244,353–355], a precise knowledge of their distribution might be useful.

Nevertheless, the question remains as to the applicability and usefulness of sophisticated methods in production processes. The developed method was compared with photometric astaxanthin determination in order to answer how accurate very simple but inexpensive photometric approaches are and whether they are sufficient to determine the astaxanthin content, e.g., to find an optimal harvest time. It was found that photometric astaxanthin determination can show differences depending on the astaxanthin proportion or culture age. Such an approach may be sufficient for stressed cells (astaxanthin >2% w/w) and monitoring processes. More sophisticated and accurate methods like the one developed here should be applied for process developments or optimizations. Astaxanthin is the most abundant carotenoid in highly stressed *H. pluvialis* cells. In organisms containing diverse and evenly distributed carotenoids, a simple photometric measurement might be even more biased. Here, it may be helpful to use methods such as Gauss Peak Spectra [374,375] to support the evaluation of photometric measurements. In this context, it is also important to consider that processes might be adapted not only to a maximum carotenoid content but also to a specific diastereomer composition. Here, simple photometric approaches are unlikely to achieve sufficient accuracy.

Another aspect is the proportion of different enantiomers, which cannot be evaluated by the developed method. However, it is possible to measure enantiomers using (U)HPLC approaches with chiral columns [376]. The enantiomeric mixture of carotenoids derived from natural sources is generally regarded to be safer for consumption than the mixture obtained by chemical synthesis. It is questionable what the relative importance of this will be for application, but there is still a knowledge gap about possible different effects, efficacy levels, and bioavailability of different enantiomers. This gap needs to be addressed for several reasons: Currently, many synthetic carotenoids are not approved for direct human consumption, partly because of their different enantiomer ratios. If there were no differences in the effects, this could open up the market for direct consumption and reduce the need for the hitherto energy-intensive biotechnological production processes. If there was a difference, especially if some carotenoid structures should be clinically proven to have health-promoting effects, the choice of the best process, whether chemical or biotechnological synthesis, and the selection of the right production strain would become even more relevant, as these may have tremendous differences in their enantiomer profile of



otherwise similar carotenoids. The associated second question is about the possibility and necessity of the biological host systems of the consumer to transform carotenoids [146]. Clarifying these questions is important regarding ongoing and future (clinical) trials in terms of study design and future feasibility of producing the carotenoids of interest. It might be even more important considering that some carotenoids offer a greater diversity of enantiomers than astaxanthin due to a higher number of stereogenic carbon atoms. This problem also applies to diastereomers.

The developed method was also applied to measure the shelf life of differently pretreated and stored astaxanthin-containing samples. Not surprisingly, the reduction of light, temperature, and oxygen atmosphere generally had a positive effect on astaxanthin stability, as also reported in other studies [333,334,377]. Interestingly, the ‘natural packaging’ of intact *H. pluvialis* cells also provided some protection against degradation. This information might be useful to producers who can store harvested algal material for some time but should carry out rapid processing once the biomass has been disrupted.

### Optimization of Downstream Processing for Astaxanthin Production

The method developed in chapter 1 was applied in chapter 2 to evaluate astaxanthin recovery throughout different process steps of the downstream processing of *H. pluvialis*. The objective was to find optimal processes and process combinations to maximize astaxanthin yield and to find the most economical process considering further monetary parameters like energy costs and labor. Different processes were applied and compared, i.e., bead milling, high-pressure-homogenization, and no disruption were performed to analyze the influence of cell disruption on astaxanthin content. Spray-drying, freeze-drying, and vacuum-drying were used to compare drying approaches. All possible combinations of these processes were tested. The samples obtained were extracted with SC-CO<sub>2</sub> to investigate the influence of the pretreatment on extractability. The best result was achieved by coupling high-pressure-homogenization with freeze-drying. Though, high-pressure-homogenization-spray-drying, bead milling-freeze-drying, and bead milling-spray-drying yielded only slightly less astaxanthin and did not differ significantly among themselves. Only the absence of disruption and including vacuum-drying in the processing had stronger negative effects on the astaxanthin yield. Considering the economic aspects, bead milling in combination with spray-drying proved to be the optimal combination.

Another important finding was that temperature and oxygen had only little adverse effects on astaxanthin content. Spray-drying of broken cells especially provides a large surface area for oxidation. However, it appears that cooling by evaporation and the short exposure prevent degradation. This was demonstrated at laboratory and pilot scale. This finding opens further possibilities for drying. Oven-drying [378] or belt-drying [379] might also be alternatives if carried out using thin layers and short drying times. Sun-drying, as performed for the production of *Arthrospira platensis*, should be used with caution because solar radiation has a detrimental influence on pigments. The use of heat generated by solar radiation, as with solar-drying [380], might overcome this problem. However, it is still inferior to methods such as freeze-drying to recover certain carotenoids [381]. Further developments of the known techniques, such



as refractive window drying [382], or the application of new technologies, such as Concentrating Solar Power (CSP) [383], might open new possibilities for fast and energy-extensive drying. Conventional drying is very energy demanding. Direct use of solar energy or heat could minimize carbon footprints [380] but increases weather dependence. Changing the order of processing steps, i.e., drying before disruption, is possible but may not be necessary to protect astaxanthin, as shown. It was demonstrated that disruption itself was necessary for good extractability using SC-CO<sub>2</sub>. There are several techniques for cell disruption. Mechanical disruption such as grinding has become widely used on a larger scale [317,384]. SC-CO<sub>2</sub> extraction also required a specific sample texture to function efficiently. The dense and rigid biomass obtained from vacuum-drying could not be extracted very well. At larger scale and higher throughput, powders like those obtained from spray-drying tend to clog filters and impair extraction as well. Finding an optimal sample texture and pre-processing must also be evaluated in the context of SC-CO<sub>2</sub> extraction, increasing the challenge for the downstream process.

SC-CO<sub>2</sub> extraction was a process step that influenced the isomeric composition of astaxanthin. The exact reason for this was not evaluated, so it cannot be said whether the isomerization was caused by some part of the process, the CO<sub>2</sub> or the co-solvent ethanol. The isomerization resulted in higher proportions of most *Z*-isomers, which might be favorable in terms of the possible higher bioavailability and antioxidant activity [243,244,353–355]. However, in the course of further clarification of the mechanisms of action of astaxanthin isomers, this influence should be kept in mind and the reasons should be elucidated.

SC-CO<sub>2</sub> has been described as an environmentally friendly, nontoxic, and ‘green’ solvent, which can be applied in many processes [385]. Nevertheless, SC-CO<sub>2</sub> extraction requires sophisticated equipment and much energy [386]. Therefore, the question arises whether there is a possibility to rigorously shorten the downstream processing, e.g., by extracting astaxanthin directly from *H. pluvialis* using natural, sustainable oils [387]. This might have other disadvantages, like low concentrations and the need for axenic microalgal cultures to ensure product safety. Regardless, it would simplify the downstream process immensely, and the oil could be applied directly to certain food and feed products. An even simpler approach is to eliminate the extraction part of the downstream processing. However, this would be only possible under certain conditions. The most important aspect is product safety, which had to be determined and which is accompanied by regulatory approval. As far as astaxanthin is concerned, so far only extracts from *H. pluvialis* have been approved for human consumption [201], and matrix effects of cell biomass had to be considered. Some other green microalgae like *Arthrospira platensis* and *Chlorella* spp. are approved for human consumption as whole cells in the EU because they are not considered novel foods [388,389] and in the USA (GRN No. 986, 519, 417). Another aspect is applicability. If the final product is intended to be incorporated into certain formulations such as creams, an oily extract might still be required. Finally, the whole downstream process could also be extended. Thinking of integrated multiple uses in the context of a biorefinery approach [21,315,390], other valuable metabolites might be co-extracted, and the remaining proteins, carbohydrates, or the leftover cell



biomass could be used to produce other products or to fortify food and feed. This would probably prolong downstream processing but might increase its efficiency and economic feasibility.

### **Production of Carotenoids Using Novel Groups of Microorganisms**

To date, of the more than 500 known carotenoids, only a handful are produced for large-scale applications. Due to safety concerns and the inability to chemically and biotechnologically synthesize some of the more complicated chemical structures, no more carotenoids have been applied. Other problematic aspects that particularly affect the biotechnological production are the low efficiency and yield of the production strains and the disadvantages of phototrophic production. The possibility of overcoming these and finding ways to produce different carotenoids might be provided by the discovery of new production organisms.

In chapter 3, an attempt was made to find such organisms by screening a strain collection of Thraustochytriaceae and analyzing their molecular identity and phylogenetic relationship. The collection was evaluated for its potential to produce already established but also novel or unusual carotenoids. The ability to synthesize certain carotenoids was matched with molecular phylogeny to identify species and genera with high carotenoid production potential. It was tested whether the production of the triterpene squalene correlated with the production of carotenoids and could increase the value of a putative extract or product. It was evaluated if the yield of these substances could be improved by creating models for growth behavior and terpene production as a function of medium composition.

Most of the strains studied were capable of producing carotenoids, and all synthesized squalene. Cluster analysis of the carotenoid composition showed that certain species had high similarities in their carotenoid profiles but that the composition of other species also varied greatly. This was only partially reflected in the molecular phylogeny. Astaxanthin,  $\beta$ -carotene, and canthaxanthin had the highest proportions. Simply stated, the composition and amount of carotenoids depended on species and strain and were influenced by medium composition and solidity. Higher carotenoid concentrations were obtained on agar-containing solid media rather than in liquid cultures, while the opposite was true for squalene. The different genera responded differently to the variation of media components, but most strains analyzed grew best on a medium with high glucose and yeast extract concentration. The highest carotenoid concentration was generally obtained with a comparably higher carbon-to-nitrogen (C/N) ratio and squalene with a lower C/N ratio. In terms of yields, some species and strains produced higher total biomass and higher carotenoid concentration compared to others, resulting in overall high carotenoid yields.

The results are difficult to compare with those of already established production strains because yield calculations for upscaling the cultivation on agar are difficult to estimate. Nevertheless, further development is certainly needed to establish competitiveness. This might be achieved in several ways. One of them could be further screening of the Thraustochytriaceae. This and other research have shown



that production capacity can vary widely among genera, species and strains. In particular, the genus *Aurantiochytrium* has a high potential for carotenoid production [279,391]. Another approach for higher carotenoid productivity is the optimization of medium and growth parameters. The concentrations of carbon and nitrogen sources were shown to have a major impact on growth and metabolite formation. As observed in other strains, further optimization could be achieved by elevating the nutrient concentrations or changing other potentially influencing parameters, such as light, oxygen, and temperature [276,392–395]. The complex life cycle of the Thraustochytriaceae might have an impact on carotenoid synthesis but is not well studied. Altering the composition of the medium or other external parameters is a quick approach to change metabolite profiles and promote gene expression. However, a deeper understanding of metabolic pathways might enable tailored process adaptation and genetic engineering to improve strains beyond their natural capacity to synthesize carotenoids and other valuable metabolites. Genome and transcriptome evaluation is a valuable tool that has been scarce but is increasingly used in thraustochytrids. Analysis was performed with emphasis on fatty acid production [396–403], carotenoids [401,403,404], and other characteristics [323]. Studies revealed a few peculiar features. The formation of isopentenyl diphosphate (IPP) was dependent solely on the mevalonate pathway [401,403]. Fusion of three enzymes was responsible for the formation of  $\beta$ -carotene from geranylgeranyl diphosphate (GGPP), which in most other carotenoid-producing organisms is regulated by individual enzymes [403–405]. A genetic engineering approach to enhance GGPP production increased the synthesis of carotenoids (mainly  $\beta$ -carotene) and fatty acids but decreased squalene levels [403]. Another study increased carotenoid but decreased fatty acid production [406]. Further research on the formation of xanthophylls may allow control of the synthesis of certain carotenoids such as astaxanthin. However, not only understanding the carotenoid biosynthetic pathways but also the interaction with the synthesis of other metabolites, such as squalene and fatty acids, is important because they share common precursors. The modification of individual genes likely influences the regulation of others as well [406], and also external parameters change gene expression [407]. The regulatory mechanisms of gene expression must be understood to enable different optimization strategies at the metabolic and process levels. This comprehension is essential to maximize yield and modify carotenoid composition. Again, it is particularly important when considering biorefinery approaches [408] and balancing the co-production of valuable metabolites. Finally, it is also necessary to take into account the approval process for potential products synthesized by genetically modified organisms, as they are subject to strict regulations in numerous countries worldwide.

Thraustochytrids, along with microalgae and other production strains, might become a part of a diversified strategy for carotenoid production. The choice of the production systems and organisms will likely depend on a variety of factors including target carotenoids, location, and availability of space and resources. The influencing factors need to be carefully weighed and process flows further optimized to enable an efficient biotechnological production of carotenoids.



## Perspectives

Given climate change, population growth, and the accompanying increase in demand for energy and a plethora of goods and services, we need to completely rethink processes, methods, and strategies for meeting people's needs. For the synthesis of certain molecules, biotechnological production processes currently represent an important alternative to chemical production processes. They may be operated largely fossil-free and offer the advantage of harnessing the potential of microorganisms to synthesize sophisticated molecules, which may not be producible by chemical means. For some applications, biotechnological processes are already used for the bulk production of chemicals. Prominent examples are citric acid and enzymes from *Aspergillus niger* [409] or vitamin B and enzymes from *B. subtilis* [410]. Nevertheless, biotechnology is a comparatively young discipline and cannot compete with chemical processes in all areas. The production of carotenoids may be one of them where a strong development is necessary to catch up with well-established chemical processes. So far, biotechnological production has been economical mainly for carotenoids applied in special, high-priced products. However, there is a broad spectrum of possible progress in biotechnological processes. One approach is to develop new and more efficient production organisms, both by discovering new strains and by improving the potential of already established ones. Increased productivity can be achieved through metabolic engineering and a better understanding of carotenoid production pathways, their induction and regulation by adjusting external parameters. Additionally, the optimization of upstream and downstream processes and the development of new techniques offer much scope for maximizing yields and minimizing process energy and costs.

Another aspect is the question of the superiority of biotechnological or chemical production of carotenoids with regard to their subsequent application. Paradoxically, this question covers a wide spectrum, ranging from clarification of the general harmlessness of some carotenoids to their positive effects on health. Specifically, it needs to be clarified whether there are indeed adverse health effects as reported for  $\beta$ -carotene [179–181] and if such effects are different when carotenoids are chemically or naturally produced as assumed for astaxanthin. Another aspect is the lack of comparability of the health effects of different carotenoids. Comparative studies for a broad spectrum of carotenoids, especially those already in use, might help to enable coherent legislation and application of the various substances. A positive side effect might be a better understanding of the mechanism of action based on structural differences. Structural differences are particularly important in carotenoids with chiral centers such as astaxanthin. There is a need to investigate the differences in the effects of enantiomers on human and animal health. A similar elucidation might be useful for zeaxanthin and lutein with its even higher number of possible enantiomers, provided that the chemical synthesis is further developed. Additionally, the role of matrix effects in the bioaccessibility of carotenoids needs to be examined. It must be known whether the matrix has inherent effects on human health and, if so, which components contribute. Clinical efficacy is at the other end of the spectrum. It has yet to be proven, but it would dramatically change the entire market if it occurred. All this would help to clarify whether synthetic carotenoids are



truly inferior to their naturally produced counterparts and which carotenoids are best suited for specific applications in terms of their production organism, biotechnological or chemical production, and downstream processing.

The improvement of production processes and the speed at which relationships and mechanisms are understood are likely to be fueled by the development of artificial intelligence (AI). There are still some hurdles to overcome and issues to be addressed, such as the quality of input data, underlying analytical approaches for data assessment, and ethical implications [411]. However, AI and Big Data were already expected to have the strongest influence on the biopharmaceutical industry among the newly emerging technologies in 2023 [412]. The potential of AI to compute and analyze large datasets, perform predictive modeling, metabolite screening, and data visualization are just a few examples of where it is likely to contribute to developments in biotechnology [413] and many other research areas. It has already been shown to drive innovation and support in diagnosis of genetic disease [414] and virus identification [415] through genome interpretation. Applications for drug discovery, evaluation, synthesis, and process development are at least conceivable or have already been tested [416,417]. This potential could further assist in finding the most suitable producer strains, refining process conditions, and determining the optimal composition of carotenoids for a range of applications. With the rapid advancement of AI, many more implementations are sure to follow and constantly improve.

The final question to be addressed concerns the necessity and boundaries of the system. With the increase in world population and the demand for wealth and growth, we have created an economy that does not calculate the social and environmental costs. A recent strategy is to strive for green growth. The endeavors to produce many molecules, carotenoids included, in a sustainable and environmentally friendly manner should also be seen in this light. Current developments are a step toward achieving climate and environmental goals. Nevertheless, given the urgency of the situation, the question remains whether these advancements go far enough. We need a fast clarification of the suspected health effects of carotenoids, both positive and negative. As knowledge of carotenoids increases, more effective advice could be given on a balanced diet rich in products that naturally contain carotenoids, which might largely eliminate the need for supplements. Such a varied diet, reduced and responsible consumption of processed foods, a knowledgeable and targeted application of supplemental carotenoids, and the development of sustainable processes for their production will then support a healthy lifestyle for humankind.







## References

1. Martínez-Cámara, S.; Ibañez, A.; Rubio, S.; Barreiro, C.; Barredo, J.-L. Main carotenoids produced by microorganisms. *Encycl.* **2021**, *1*, 1223–1245, doi:10.3390/encyclopedia1040093.
2. Lafarga, T.; Clemente, I.; Garcia-Vaquero, M. Carotenoids from microalgae. In *Carotenoids: Properties, Processing and Applications*; Galanakis, C.M., Ed.; Elsevier: London, 2020; pp 149–187, ISBN 9780128170670.
3. Ram, S.; Mitra, M.; Shah, F.; Tirkey, S.R.; Mishra, S. Bacteria as an alternate biofactory for carotenoid production: A review of its applications, opportunities and challenges. *J. Funct. Foods* **2020**, *67*, 103867, doi:10.1016/j.jff.2020.103867.
4. Sun, T.; Rao, S.; Zhou, X.; Li, L. Plant carotenoids: recent advances and future perspectives. *Mol. Horticulture* **2022**, *2*, doi:10.1186/s43897-022-00023-2.
5. Xu, Y.; Harvey, P.J. Carotenoid production by *Dunaliella salina* under red light. *Antioxidants* **2019**, *8*, 123, doi:10.3390/antiox8050123.
6. Liu, J.; Sun, Z.; Gerken, H.; Liu, Z.; Jiang, Y.; Chen, F. *Chlorella zofingiensis* as an alternative microalgal producer of astaxanthin: biology and industrial potential. *Mar. Drugs* **2014**, *12*, 3487–3515, doi:10.3390/md12063487.
7. Yuan, J.-P.; Chen, F.; Liu, X.; Li, X.-Z. Carotenoid composition in the green microalga *Chlorococcum*. *Food Chem.* **2002**, *76*, 319–325, doi:10.1016/S0308-8146(01)00279-5.
8. Yi, Z.; Su, Y.; Cherek, P.; Nelson, D.R.; Lin, J.; Rolfsson, O.; Wu, H.; Salehi-Ashtiani, K.; Brynjolfsson, S.; Fu, W. Combined artificial high-silicate medium and LED illumination promote carotenoid accumulation in the marine diatom *Phaeodactylum tricornutum*. *Microb. Cell Fact.* **2019**, *18*, 209, doi:10.1186/s12934-019-1263-1.
9. Collins, A.M.; Jones, H.D.T.; Han, D.; Hu, Q.; Beechem, T.E.; Timlin, J.A. Carotenoid distribution in living cells of *Haematococcus pluvialis* (Chlorophyceae). *PLoS One* **2011**, *6*, e24302, doi:10.1371/journal.pone.0024302.
10. Park, W.S.; Kim, H.-J.; Li, M.; Lim, D.H.; Kim, J.; Kwak, S.-S.; Kang, C.-M.; Ferruzzi, M.G.; Ahn, M.-J. Two classes of pigments, carotenoids and C-phycocyanin, in *Spirulina* powder and their antioxidant activities. *Molecules* **2018**, *23*, 2065, doi:10.3390/molecules23082065.
11. Vila, E.; Hornero-Méndez, D.; Azziz, G.; Lareo, C.; Saravia, V. Carotenoids from heterotrophic bacteria isolated from Fildes Peninsula, King George Island, Antarctica. *Biotechnol. Rep.* **2019**, *21*, e00306, doi:10.1016/j.btre.2019.e00306.
12. Reis-Mansur, M.C.P.P.; Cardoso-Rurr, J.S.; Silva, J.V.M.A.; Souza, G.R. de; Da Cardoso, V.S.; Mansoldo, F.R.P.; Pinheiro, Y.; Schultz, J.; Lopez Balottin, L.B.; da Silva, A.J.R.; et al. Carotenoids from UV-resistant Antarctic *Microbacterium* sp. LEMMJ01. *Sci. Rep.* **2019**, *9*, 9554, doi:10.1038/s41598-019-45840-6.
13. Yokoyama, A.; Miki, W.; Izumida, H.; Shizuri, Y. New trihydroxy-keto-carotenoids isolated from an astaxanthin-producing marine bacterium. *Biosci. Biotechnol. Biochem.* **1996**, *60*, 200–203, doi:10.1271/bbb.60.200.
14. Calo, P.; Miguel, T. de; Sieiro, C.; Velazquez, J.B.; Villa, T.G. Ketocarotenoids in halobacteria: 3-hydroxy-echinenone and *trans*-astaxanthin. *J. Appl. Bacteriol.* **1995**, *79*, 282–285, doi:10.1111/j.1365-2672.1995.tb03138.x.
15. Fang, C.-J.; Ku, K.-L.; Lee, M.-H.; Su, N.-W. Influence of nutritive factors on C<sub>50</sub> carotenoids production by *Haloferax mediterranei* ATCC 33500 with two-stage cultivation. *Bioresour. Technol.* **2010**, *101*, 6487–6493, doi:10.1016/j.biortech.2010.03.044.
16. Tran, T.N.; Tran, Q.-V.; Huynh, H.T.; Hoang, N.-S.; Nguyen, H.C.; Ngo, D.-N. Astaxanthin production by newly isolated *Rhodospiridium toruloides*: Optimization of medium compositions by response surface methodology. *Not. Bot. Horti Agrob.* **2018**, *47*, 320–327, doi:10.15835/nbha47111361.
17. Andrewes, A.G.; Phaff, H.J.; Starr, M.P. Carotenoids of *Phaffia rhodozyma*, a red-pigmented fermenting yeast. *Phytochemistry* **1976**, *15*, 1003–1007, doi:10.1016/S0031-9422(00)84390-3.
18. Yokoyama, R.; Honda, D. Taxonomic rearrangement of the genus *Schizochytrium* sensu lato based on morphology, chemotaxonomic characteristics, and 18S rRNA gene phylogeny (Thraustochytriaceae, Labyrinthulomycetes): emendation for *Schizochytrium* and erection of *Aurantiochytrium* and *Oblongichytrium* gen. nov. *Mycoscience* **2007**, *48*, 199–211, doi:10.1007/s10267-006-0362-0.
19. Yokoyama, R.; Salleh, B.; Honda, D. Taxonomic rearrangement of the genus *Ulkenia* sensu lato based on morphology, chemotaxonomical characteristics, and 18S rRNA gene phylogeny (Thraustochytriaceae, Labyrinthulomycetes): emendation for *Ulkenia* and erection of *Botryochytrium*, *Parietichytrium*, and *Sicyoidochytrium* gen. nov. *Mycoscience* **2007**, *48*, 329–341, doi:10.1007/s10267-007-0377-1.
20. Aki, T.; Hachida, K.; Yoshinaga, M.; Katai, Y.; Yamasaki, T.; Kawamoto, S.; Kakizono, T.; Maoka, T.; Shigeta, S.; Suzuki, O.; et al. Thraustochytrid as a potential source of carotenoids. *J. Amer. Oil Chem. Soc.* **2003**, *80*, 789–794, doi:10.1007/s11746-003-0773-2.
21. Gupta, A.; Barrow, C.J.; Puri, M. Multiproduct biorefinery from marine thraustochytrids towards a circular bioeconomy. *Trends Biotechnol.* **2022**, *40*, 448–462, doi:10.1016/j.tibtech.2021.09.003.



22. Gupta, A.; Singh, D.; Barrow, C.J.; Puri, M. Exploring potential use of Australian thraustochytrids for the bioconversion of glycerol to omega-3 and carotenoids production. *Biochem. Eng. J.* **2013**, *78*, 11–17, doi:10.1016/j.bej.2013.04.028.
23. Maoka, T.; Kawase, N.; Hironaka, M.; Nishida, R. Carotenoids of hemipteran insects, from the perspective of chemosystematic and chemical ecological studies. *Biochem. Syst. Ecol.* **2021**, *95*, 104241, doi:10.1016/j.bse.2021.104241.
24. Latscha, T. The role of astaxanthin in shrimp pigmentation. *Advances in Tropical Aquaculture* **1989**, 319–325.
25. Maoka, T.; Kawase, N.; Ueda, T.; Nishida, R. Carotenoids of dragonflies, from the perspective of comparative biochemical and chemical ecological studies. *Biochem. Syst. Ecol.* **2020**, *89*, 104001, doi:10.1016/j.bse.2020.104001.
26. Friedman, N.R.; McGraw, K.J.; Omland, K.E. Evolution of carotenoid pigmentation in caticques and meadowlarks (Icteridae): repeated gains of red plumage coloration by carotenoid C4-oxygenation. *Evolution* **2014**, *68*, 791–801, doi:10.1111/evo.12304.
27. Czezug, B. Carotenoids in some parts of certain species of lizards. *Comp. Biochem. Physiol.* **1980**, *65*, 755–757, doi:10.1016/0305-0491(80)90194-7.
28. Kwiatkowski, M.A.; Sullivan, B.K. Geographic variation in sexual selection among populations of an iguanid lizard, *Sauromalus obesus* (=ater). *Evolution* **2002**, *56*, 2039–2051, doi:10.1111/j.0014-3820.2002.tb00130.x.
29. Newton-Youens, J.; Michaels, C.J.; Preziosi, R. Keeping the golden mantella golden: The effect of dietary carotenoid supplementation and UV provision on the colouration and growth of *Mantella aurantiaca*. *J. Zoo Aquarium Res.* **2022**, *2022*, 74–81, doi:10.19227/jzar.v10i2.598.
30. Ogilvy, V.; Preziosi, R.F.; Fidgett, A.L. A brighter future for frogs? The influence of carotenoids on the health, development and reproductive success of the red-eye tree frog. *Anim. Conserv.* **2012**, *15*, 480–488, doi:10.1111/j.1469-1795.2012.00536.x.
31. Maoka, T. Carotenoids in marine animals. *Mar. Drugs* **2011**, *9*, 278–293, doi:10.3390/md9020278.
32. Gaillard, M.; Juillet, C.; Cézilly, F.; Perrot-Minnot, M.-J. Carotenoids of two freshwater amphipod species (*Gammarus pulex* and *G. roeseli*) and their common acanthocephalan parasite *Polymorphus minutus*. *Comp. Biochem. Physiol. B* **2004**, *139*, 129–136, doi:10.1016/j.cbpc.2004.07.001.
33. Mariutti, L.R.B.; Pereira, D.M.; Mercadante, A.Z.; Valentão, P.; Teixeira, N.; Andrade, P.B. Further insights on the carotenoid profile of the echinoderm *Marthasterias glacialis* L. *Mar. Drugs* **2012**, *10*, 1498–1510, doi:10.3390/md10071498.
34. Kawakami, T.; Tsushima, M.; Katabami, Y.; Mine, M.; Ishida, A.; Matsuno, T. Effect of  $\beta$ , $\beta$ -carotene,  $\beta$ -echinenone, astaxanthin, fucoxanthin, vitamin A and vitamin E on the biological defense of the sea urchin *Pseudocentrotus depressus*. *J. Exp. Mar. Biol. Ecol.* **1998**, *226*, 165–174, doi:10.1016/S0022-0981(97)00236-0.
35. Maoka, T.; Akimoto, N.; Tsushima, M.; Komemushi, S.; Mezaki, T.; Iwase, F.; Takahashi, Y.; Sameshima, N.; Mori, M.; Sakagami, Y. Carotenoids in marine invertebrates living along the Kuroshio current coast. *Mar. Drugs* **2011**, *9*, 1419–1427, doi:10.3390/md9081419.
36. Moran, N.A.; Jarvik, T. Lateral transfer of genes from fungi underlies carotenoid production in aphids. *Science* **2010**, *328*, 624–627, doi:10.1126/science.1187113.
37. Altincicek, B.; Kovacs, J.L.; Gerardo, N.M. Horizontally transferred fungal carotenoid genes in the two-spotted spider mite *Tetranychus urticae*. *Biol. Lett.* **2012**, *8*, 253–257, doi:10.1098/rsbl.2011.0704.
38. Cobbs, C.; Heath, J.; Stireman, J.O.; Abbot, P. Carotenoids in unexpected places: gall midges, lateral gene transfer, and carotenoid biosynthesis in animals. *Mol. Phylogenet. Evol.* **2013**, *68*, 221–228, doi:10.1016/j.ympev.2013.03.012.
39. Galván, I.; Garrido-Fernández, J.; Ríos, J.; Pérez-Gálvez, A.; Rodríguez-Herrera, B.; Negro, J.J. Tropical bat as mammalian model for skin carotenoid metabolism. *Proc. Natl. Acad. Sci. USA* **2016**, *113*, 10932–10937, doi:10.1073/pnas.1609724113.
40. *Carotenoids: Handbook*; Britton, G.; Liaaen-Jensen, S.; Pfander, H., Eds.; Springer Basel AG, 2004, ISBN 9783034878364.
41. Maoka, T. Recent progress in structural studies of carotenoids in animals and plants. *Arch. Biochem. Biophys.* **2009**, *483*, 191–195, doi:10.1016/j.abb.2008.10.019.
42. Zechmeister, L. *Cis-trans* isomerization and stereochemistry of carotenoids and diphenyl-polyenes. *Chem. Rev.* **1944**, *34*, 267–344, doi:10.1021/cr60108a004.
43. Zechmeister, L. *Cis-trans isomeric carotenoids vitamins A and arylpolyenes*; Springer: Vienna, 1962, ISBN 978-3-7091-5550-9.
44. Euglert, G.; Vecchi, M. *trans/cis* isomerization of astaxanthin diacetate/isolation by HPLC. and Identification by  $^1\text{H}$ -NMR. spectroscopy of three mono-*cis*- and six di-*cis*-isomers. *Helv. Chim. Acta* **1980**, *63*, 1711–1718, doi:10.1002/hlca.19800630640.
45. Subramanian, B.; Tchoukanova, N.; Djaoued, Y.; Pelletier, C.; Ferron, M.; Robichaud, J. Investigations on the geometrical isomers of astaxanthin: Raman spectroscopy of conjugated polyene chain with electronic and mechanical confinement. *J. Raman Spectrosc.* **2014**, *45*, 299–304, doi:10.1002/jrs.4459.



## References

46. Murakami, K.; Honda, M.; Wahyudiono; Kanda, H.; Goto, M. Thermal isomerization of (all-*E*)-lycopene and separation of the *Z*-isomers by using a low boiling solvent: Dimethyl ether. *Sep. Sci. Technol.* **2017**, *52*, 2573–2582, doi:10.1080/01496395.2017.1374412.
47. Rodríguez-Concepción, M. Supply of precursors for carotenoid biosynthesis in plants. *Arch. Biochem. Biophys.* **2010**, *504*, 118–122, doi:10.1016/j.abb.2010.06.016.
48. Ruiz-Sola, M.Á.; Rodríguez-Concepción, M. Carotenoid biosynthesis in Arabidopsis: a colorful pathway. *Arabidopsis Book* **2012**, *10*, e0158, doi:10.1199/tab.0158.
49. Giuliano, G.; Tavazza, R.; Diretto, G.; Beyer, P.; Taylor, M.A. Metabolic engineering of carotenoid biosynthesis in plants. *Trends Biotechnol.* **2008**, *26*, 139–145, doi:10.1016/j.tibtech.2007.12.003.
50. Tamaki, S.; Mochida, K.; Suzuki, K. Diverse biosynthetic pathways and protective functions against environmental stress of antioxidants in microalgae. *Plants* **2021**, *10*, 1250, doi:10.3390/plants10061250.
51. Lao, Y.M.; Jin, H.; Zhou, J.; Zhang, H.J.; Cai, Z.H. Functional characterization of a missing branch component in *Haematococcus pluvialis* for control of algal carotenoid biosynthesis. *Front. Plant. Sci.* **2017**, *8*, 1341, doi:10.3389/fpls.2017.01341.
52. Barredo, J.L.; García-Estrada, C.; Kosalkova, K.; Barreiro, C. Biosynthesis of astaxanthin as a main carotenoid in the heterobasidiomycetous yeast *Xanthophyllomyces dendrorhous*. *J. Fungi* **2017**, *3*, 44, doi:10.3390/jof3030044.
53. Misawa, N. Carotenoid  $\beta$ -ring hydroxylase and ketolase from marine bacteria-promiscuous enzymes for synthesizing functional xanthophylls. *Mar. Drugs* **2011**, *9*, 757–771, doi:10.3390/md9050757.
54. Lokstein, H.; Renger, G.; Götze, J.P. Photosynthetic light-harvesting (antenna) complexes-structures and functions. *Molecules* **2021**, *26*, 3378, doi:10.3390/molecules26113378.
55. Hashimoto, H.; Sugai, Y.; Uragami, C.; Gardiner, A.T.; Cogdell, R.J. Natural and artificial light-harvesting systems utilizing the functions of carotenoids. *J. Photochem. Photobiol. C Photochem. Rev.* **2015**, *25*, 46–70, doi:10.1016/j.jphotochemrev.2015.07.004.
56. Demmig-Adams, B.; Adams, W.W. Photoprotection in an ecological context: the remarkable complexity of thermal energy dissipation. *New Phytol.* **2006**, *172*, 11–21, doi:10.1111/j.1469-8137.2006.01835.x.
57. Ruban, A.V.; Johnson, M.P.; Duffy, C.D.P. The photoprotective molecular switch in the photosystem II antenna. *Biochim. Biophys. Acta* **2012**, *1817*, 167–181, doi:10.1016/j.bbabi.2011.04.007.
58. Niedzwiedzki, D.M.; Tronina, T.; Liu, H.; Staleva, H.; Komenda, J.; Sobotka, R.; Blankenship, R.E.; Polívka, T. Carotenoid-induced non-photochemical quenching in the cyanobacterial chlorophyll synthase-HliC/D complex. *Biochim. Biophys. Acta* **2016**, *1857*, 1430–1439, doi:10.1016/j.bbabi.2016.04.280.
59. Mozzo, M.; Dall'Osto, L.; Hienerwadel, R.; Bassi, R.; Croce, R. Photoprotection in the antenna complexes of photosystem II: role of individual xanthophylls in chlorophyll triplet quenching. *J. Biol. Chem.* **2008**, *283*, 6184–6192, doi:10.1074/jbc.M708961200.
60. Pospíšil, P. Production of reactive oxygen species by photosystem II as a response to light and temperature stress. *Front. Plant. Sci.* **2016**, *7*, 1950, doi:10.3389/fpls.2016.01950.
61. Viljanen, K.; Sundberg, S.; Ohshima, T.; Heinonen, M. Carotenoids as antioxidants to prevent photooxidation. *Eur. J. Lipid Sci. Technol.* **2002**, *104*, 353–359, doi:10.1002/1438-9312(200206)104:6<353:AID-EJLT353>3.0.CO;2-5.
62. Di Mascio, P.; Kaiser, S.; Sies, H. Lycopene as the most efficient biological carotenoid singlet oxygen quencher. *Arch. Biochem. Biophys.* **1989**, *274*, 532–538, doi:10.1016/0003-9861(89)90467-0.
63. Conn, P.F.; Schalch, W.; Truscott, T. The singlet oxygen and carotenoid interaction. *J. Photochem. Photobiol. B Biol.* **1991**, *11*, 41–47, doi:10.1016/1011-1344(91)80266-k.
64. Miki, W. Biological functions and activities of animal carotenoids. *Pure Appl. Chem.* **1991**, *63*, 141–146, doi:10.1351/pac199163010141.
65. Shimidzu, N.; Goto, M.; Miki, W. Carotenoids as singlet oxygen quenchers in marine organisms. *Fish. Sci.* **1996**, *62*, 134–137, doi:10.2331/fishsci.62.134.
66. Rodrigues, E.; Mariutti, L.R.B.; Mercadante, A.Z. Scavenging capacity of marine carotenoids against reactive oxygen and nitrogen species in a membrane-mimicking system. *Mar. Drugs* **2012**, *10*, 1784–1798, doi:10.3390/md10081784.
67. Ramel, F.; Birtic, S.; Cuiné, S.; Triantaphylidès, C.; Ravanat, J.-L.; Havaux, M. Chemical quenching of singlet oxygen by carotenoids in plants. *Plant Physiol.* **2012**, *158*, 1267–1278, doi:10.1104/pp.111.182394.
68. Nishino, A.; Maoka, T.; Yasui, H. Analysis of reaction products of astaxanthin and its acetate with reactive oxygen species using LC/PDA ESI-MS and ESR spectrometry. *Tetrahedron Lett.* **2016**, *57*, 1967–1970, doi:10.1016/j.tetlet.2016.03.078.
69. Yamauchi, R.; Tsuchihashi, K.; Kato, K. Oxidation products of  $\beta$ -carotene during the peroxidation of methyl linoleate in the bulk phase. *Biosci. Biotechnol. Biochem.* **1998**, *62*, 1301–1306, doi:10.1271/bbb.62.1301.
70. Ramel, F.; Birtic, S.; Ginies, C.; Soubigou-Taconnat, L.; Triantaphylidès, C.; Havaux, M. Carotenoid oxidation products are stress signals that mediate gene responses to singlet oxygen in plants. *Proc. Natl. Acad. Sci. USA* **2012**, *109*, 5535–5540, doi:10.1073/pnas.1115982109.



71. Felemban, A.; Braguy, J.; Zurbriggen, M.D.; Al-Babili, S. Apocarotenoids involved in plant development and stress response. *Front. Plant. Sci.* **2019**, *10*, 1168, doi:10.3389/fpls.2019.01168.
72. Jia, K.-P.; Baz, L.; Al-Babili, S. From carotenoids to strigolactones. *J. Exp. Bot.* **2018**, *69*, 2189–2204, doi:10.1093/jxb/erx476.
73. Moreno, J.C.; Mi, J.; Alagoz, Y.; Al-Babili, S. Plant apocarotenoids: from retrograde signaling to interspecific communication. *Plant J.* **2021**, *105*, 351–375, doi:10.1111/tj.15102.
74. Zheng, X.; Yang, Y.; Al-Babili, S. Exploring the diversity and regulation of apocarotenoid metabolic pathways in plants. *Front. Plant. Sci.* **2021**, *12*, 787049, doi:10.3389/fpls.2021.787049.
75. Wang, J.Y.; Haider, I.; Jamil, M.; Fiorilli, V.; Saito, Y.; Mi, J.; Baz, L.; Kountche, B.A.; Jia, K.-P.; Guo, X.; et al. The apocarotenoid metabolite zaxinone regulates growth and strigolactone biosynthesis in rice. *Nat. Commun.* **2019**, *10*, 810, doi:10.1038/s41467-019-08461-1.
76. Ablazov, A.; Mi, J.; Jamil, M.; Jia, K.-P.; Wang, J.Y.; Feng, Q.; Al-Babili, S. The apocarotenoid zaxinone is a positive regulator of strigolactone and abscisic acid biosynthesis in Arabidopsis roots. *Front. Plant. Sci.* **2020**, *11*, 578, doi:10.3389/fpls.2020.00578.
77. Jia, K.-P.; Dickinson, A.J.; Mi, J.; Cui, G.; Xiao, T.T.; Kharbatia, N.M.; Guo, X.; Sugiono, E.; Aranda, M.; Blilou, I.; et al. Anchorene is a carotenoid-derived regulatory metabolite required for anchor root formation in Arabidopsis. *Sci. Adv.* **2019**, *5*, eaaw6787, doi:10.1126/sciadv.aaw6787.
78. Jia, K.-P.; Mi, J.; Ablazov, A.; Ali, S.; Yang, Y.; Balakrishna, A.; Berqdar, L.; Feng, Q.; Blilou, I.; Al-Babili, S. Iso-anchorene is an endogenous metabolite that inhibits primary root growth in Arabidopsis. *Plant J.* **2021**, *107*, 54–66, doi:10.1111/tj.15271.
79. Murata, M.; Kobayashi, T.; Seo, S.  $\alpha$ -Ionone, an apocarotenoid, induces plant resistance to western flower thrips, *Frankliniella occidentalis*, independently of jasmonic acid. *Molecules* **2019**, *25*, 17, doi:10.3390/molecules25010017.
80. Cáceres, L.A.; Lakshminarayan, S.; Yeung, K.K.-C.; McGarvey, B.D.; Hannoufa, A.; Sumarah, M.W.; Benitez, X.; Scott, I.M. Repellent and attractive effects of  $\alpha$ -,  $\beta$ -, and dihydro- $\beta$ -ionone to generalist and specialist herbivores. *J. Chem. Ecol.* **2016**, *42*, 107–117, doi:10.1007/s10886-016-0669-z.
81. Murata, M.; Nakai, Y.; Kawazu, K.; Ishizaka, M.; Kajiwar, H.; Abe, H.; Takeuchi, K.; Ichinose, Y.; Mitsuhashi, I.; Mochizuki, A.; et al. Loliolide, a carotenoid metabolite, is a potential endogenous inducer of herbivore resistance. *Plant Physiol.* **2019**, *179*, 1822–1833, doi:10.1104/pp.18.00837.
82. Ohmiya, A. Diversity of carotenoid composition in flower petals. *Jpn. Agric. Res. Q.* **2011**, *45*, 163–171, doi:10.6090/jarq.45.163.
83. Ohmiya, A. Qualitative and quantitative control of carotenoid accumulation in flower petals. *Sci. Hortic.* **2013**, *163*, 10–19, doi:10.1016/j.scienta.2013.06.018.
84. Wan, H.; Yu, C.; Han, Y.; Guo, X.; Le Luo, Pan, H.; Zheng, T.; Wang, J.; Cheng, T.; Zhang, Q. Determination of flavonoids and carotenoids and their contributions to various colors of rose cultivars (*Rosa* spp.). *Front. Plant. Sci.* **2019**, *10*, 123, doi:10.3389/fpls.2019.00123.
85. Wang, Y.; Zhang, C.; Dong, B.; Fu, J.; Hu, S.; Zhao, H. Carotenoid accumulation and its contribution to flower coloration of *Osmanthus fragrans*. *Front. Plant. Sci.* **2018**, *9*, 1499, doi:10.3389/fpls.2018.01499.
86. Saini, R.K.; Nile, S.H.; Park, S.W. Carotenoids from fruits and vegetables: Chemistry, analysis, occurrence, bioavailability and biological activities. *Food Res. Int.* **2015**, *76*, 735–750, doi:10.1016/j.foodres.2015.07.047.
87. Mangels, A.R.; Holden, J.M.; Beecher, G.R.; Forman, M.R.; Lanza, E. Carotenoid content of fruits and vegetables: an evaluation of analytic data. *J. Am. Diet. Assoc.* **1993**, *93*, 284–296, doi:10.1016/0002-8223(93)91553-3.
88. Bradshaw, H.D.; Schemske, D.W. Allele substitution at a flower colour locus produces a pollinator shift in monkeyflowers. *Nature* **2003**, *426*, 176–178, doi:10.1038/nature02106.
89. Nawade, B.; Shaltiel-Harpaz, L.; Yahyaa, M.; Bosamia, T.C.; Kabaha, A.; Kedoshim, R.; Zohar, M.; Isaacson, T.; Ibdah, M. Analysis of apocarotenoid volatiles during the development of *Ficus carica* fruits and characterization of carotenoid cleavage dioxygenase genes. *Plant Sci.* **2020**, *290*, 110292, doi:10.1016/j.plantsci.2019.110292.
90. Narbona, E.; Del Valle, J.C.; Arista, M.; Buide, M.L.; Ortiz, P.L. Major flower pigments originate different colour signals to pollinators. *Front. Ecol. Evol.* **2021**, *9*, 743850, doi:10.3389/fevo.2021.743850.
91. Cipollini, M.L. Secondary metabolites of vertebrate-dispersed fruits: evidence for adaptive functions. *Rev. chil. hist. nat.* **2000**, *73*, 421–440, doi:10.4067/S0716-078X2000000300006.
92. Zheng, X.; Mi, J.; Deng, X.; Al-Babili, S. LC-MS-based profiling provides new insights into apocarotenoid biosynthesis and modifications in citrus fruits. *J. Agric. Food Chem.* **2021**, *69*, 1842–1851, doi:10.1021/acs.jafc.0c06893.
93. Mahattanatawee, K.; Rouseff, R.; Valim, M.F.; Naim, M. Identification and aroma impact of norisoprenoids in orange juice. *J. Agric. Food Chem.* **2005**, *53*, 393–397, doi:10.1021/jf049012k.
94. Baldwin, E.A.; Scott, J.W.; Shewmaker, C.K.; Schuch, W. Flavor trivia and tomato aroma: Biochemistry and possible mechanisms for control of important aroma components. *HortScience* **2000**, *35*, 1013–1022, doi:10.21273/HORTSCI.35.6.1013.



## References

95. Dieser, M.; Greenwood, M.; Foreman, C.M. Carotenoid pigmentation in Antarctic heterotrophic bacteria as a strategy to withstand environmental stresses. *Arct. Antarct. Alp. Res.* **2010**, *42*, 396–405, doi:10.1657/1938-4246-42.4.396.
96. Giani, M.; Martínez-Espinosa, R.M. Carotenoids as a protection mechanism against oxidative stress in *Haloferox mediterranei*. *Antioxidants* **2020**, *9*, 1060, doi:10.3390/antiox9111060.
97. Zhao, W.; Han, Y.; Zhao, B.; Hirota, S.; Hou, J.; Xin, W. Effect of carotenoids on the respiratory burst of rat peritoneal macrophages. *Biochim. Biophys. Acta* **1998**, *1381*, 77–88, doi:10.1016/s0304-4165(98)00013-0.
98. McNulty, H.P.; Byun, J.; Lockwood, S.F.; Jacob, R.F.; Mason, R.P. Differential effects of carotenoids on lipid peroxidation due to membrane interactions: X-ray diffraction analysis. *Biochim. Biophys. Acta* **2007**, *1768*, 167–174, doi:10.1016/j.bbamem.2006.09.010.
99. Woodall, A.A.; Britton, G.; Jackson, M.J. Carotenoids and protection of phospholipids in solution or in liposomes against oxidation by peroxy radicals: relationship between carotenoid structure and protective ability. *Biochim. Biophys. Acta* **1997**, *1336*, 575–586, doi:10.1016/S0304-4165(97)00007-X.
100. Gruszecki, W.I.; Strzałka, K. Carotenoids as modulators of lipid membrane physical properties. *Biochim. Biophys. Acta* **2005**, *1740*, 108–115, doi:10.1016/j.bbadis.2004.11.015.
101. Mishra, N.N.; Liu, G.Y.; Yeaman, M.R.; Nast, C.C.; Proctor, R.A.; McKinnell, J.; Bayer, A.S. Carotenoid-related alteration of cell membrane fluidity impacts *Staphylococcus aureus* susceptibility to host defense peptides. *Antimicrob. Agents Chemother.* **2011**, *55*, 526–531, doi:10.1128/AAC.00680-10.
102. Bykowski, M.; Mazur, R.; Wójtowicz, J.; Suski, S.; Garstka, M.; Mostowska, A.; Kowalewska, Ł. Too rigid to fold: Carotenoid-dependent decrease in thylakoid fluidity hampers the formation of chloroplast grana. *Plant Physiol.* **2021**, *185*, 210–227, doi:10.1093/plphys/kiaa009.
103. Subczynski, W.K.; Markowska, E.; Siewiewsiuk, J. Effect of polar carotenoids on the oxygen diffusion-concentration product in lipid bilayers. An EPR spin label study. *Biochim. Biophys. Acta* **1991**, *1068*, 68–72, doi:10.1016/0005-2736(91)90061-c.
104. Wisniewska, A.; Subczynski, W.K. Effects of polar carotenoids on the shape of the hydrophobic barrier of phospholipid bilayers. *Biochim. Biophys. Acta* **1998**, *1368*, 235–246, doi:10.1016/s0005-2736(97)00182-x.
105. Seel, W.; Baust, D.; Sons, D.; Albers, M.; Etzbach, L.; Fuss, J.; Lipski, A. Carotenoids are used as regulators for membrane fluidity by *Staphylococcus xylosus*. *Sci. Rep.* **2020**, *10*, 330, doi:10.1038/s41598-019-57006-5.
106. Yokoyama, A.; Sandmann, G.; Hoshino, T.; Adachi, K.; Sakai, M.; Shizuri, Y. Thermozeaxanthins, new carotenoid-glycoside-esters from thermophilic eubacterium *Thermus thermophilus*. *Tetrahedron Lett.* **1995**, *36*, 4901–4904, doi:10.1016/0040-4039(95)00881-C.
107. Blount, J.D.; Metcalfe, N.B.; Birkhead, T.R.; Surai, P.F. Carotenoid modulation of immune function and sexual attractiveness in zebra finches. *Science* **2003**, *300*, 125–127, doi:10.1126/science.1082142.
108. Badyaev, A.V.; Hill, G.E. Evolution of sexual dichromatism: contribution of carotenoid- versus melanin-based coloration. *Biol. J. Linn. Soc.* **2000**, *69*, 153–172, doi:10.1006/bjil.1999.0350.
109. Pryke, S.R.; Andersson, S.; Lawes, M.J. Sexual selection of multiple handicaps in the red-collared widowbird: female choice of tail length but not carotenoid display. *Evolution* **2001**, *55*, 1452–1463, doi:10.1111/j.0014-3820.2001.tb00665.x.
110. Pryke, S.R.; Lawes, M.J.; Andersson, S. Agonistic carotenoid signalling in male red-collared widowbirds: aggression related to the colour signal of both the territory owner and model intruder. *Anim. Behav.* **2001**, *62*, 695–704, doi:10.1006/anbe.2001.1804.
111. Amundsen, T.; Forsgren, E. Male mate choice selects for female coloration in a fish. *Proc. Natl. Acad. Sci. USA* **2001**, *98*, 13155–13160, doi:10.1073/pnas.211439298.
112. Houde, A.E.; Torio, A.J. Effect of parasitic infection on male color pattern and female choice in guppies. *Behav. Ecol.* **1992**, *3*, 346–351, doi:10.1093/beheco/3.4.346.
113. Evans, M.R.; Norris, K. The importance of carotenoids in signaling during aggressive interactions between male firemouth cichlids (*Cichlasoma meeki*). *Behav. Ecol.* **1996**, *7*, 1–6, doi:10.1093/beheco/7.1.1.
114. Foote, C.J.; Brown, G.S.; Hawryshyn, C.W. Female colour and male choice in sockeye salmon: implications for the phenotypic convergence of anadromous and nonanadromous morphs. *Anim. Behav.* **2004**, *67*, 69–83, doi:10.1016/j.anbehav.2003.02.004.
115. Thorogood, R.; Kilner, R.M.; Karadaş, F.; Ewen, J.G. Spectral mouth colour of nestlings changes with carotenoid availability. *Funct. Ecol.* **2008**, *22*, 1044–1051, doi:10.1111/j.1365-2435.2008.01455.x.
116. Kilner, R. Mouth colour is a reliable signal of need in begging canary nestlings. *Proc. R. Soc. Lond. B* **1997**, *264*, 963–968, doi:10.1098/rspb.1997.0133.
117. Blount, J.D.; McGraw, K.J. Signal functions of carotenoid colouration. In *Carotenoids*; Britton, G., Liaaen-Jensen, S., Pfander, H., Eds.; Birkhäuser Basel: Basel, 2008; pp 213–236, ISBN 978-3-7643-7498-3.
118. Matsuno, T.; Maoka, T.; Toriiminami, Y. Carotenoids in the Japanese stick insect *Neophirasea japonica*. *Comp. Biochem. Physiol.* **1990**, 583–587.



119. Kayser, H. Carotenoids in the stick insect, *Ectatosoma tiaratum* isolation of  $\beta,\epsilon$ -caroten-2-ol and  $\beta,\epsilon$ -caroten-2-one. *Z. Naturforsch.* **1981**, 755–764.
120. Britton, G.; Lockley, W.J.; Harriman, G.A.; Godwin, T.W. Pigmentation of the ladybird beetle *Coccinella septempunctata* by carotenoids not of plant origin. *Nature* **1977**, 266, 49–50, doi:10.1038/266049a0.
121. Arenas, L.M.; Walter, D.; Stevens, M. Signal honesty and predation risk among a closely related group of aposematic species. *Sci. Rep.* **2015**, 5, 11021, doi:10.1038/srep11021.
122. Sacchi, R.; Cancian, S.; Ghia, D.; Fea, G.; Coladonato, A. Color variation in signal crayfish *Pacifastacus leniusculus*. *Curr. Zool.* **2021**, 67, 35–43, doi:10.1093/cz/zoaa031.
123. Cianci, M.; Rizkallah, P.J.; Olczak, A.; Raftery, J.; Chayen, N.E.; Zagalsky, P.F.; Helliwell, J.R. The molecular basis of the coloration mechanism in lobster shell:  $\beta$ -crustacyanin at 3.2-Å resolution. *Proc. Natl. Acad. Sci. USA* **2002**, 99, 9795–9800, doi:10.1073/pnas.152088999.
124. Cianci, M.; Rizkallah, P.J.; Olczak, A.; Raftery, J.; Chayen, N.E.; Zagalsky, P.F.; Helliwell, J.R. Structure of lobster apocrustacyanin A1 using softer X-rays. *Acta Crystallogr. D Biol. Crystallogr.* **2001**, 57, 1219–1229, doi:10.1107/s0907444901009350.
125. Tan, K.; Zhang, H.; Lim, L.-S.; Ma, H.; Li, S.; Zheng, H. Roles of carotenoids in invertebrate immunology. *Front. Immunol.* **2019**, 10, 3041, doi:10.3389/fimmu.2019.03041.
126. McGraw, K.J.; Ardia, D.R. Carotenoids, immunocompetence, and the information content of sexual colors: an experimental test. *Am. Nat.* **2003**, 162, 704–712, doi:10.1086/378904.
127. Nakano, T.; Wiegertjes, G. Properties of carotenoids in fish fitness: a review. *Mar. Drugs* **2020**, 18, 568, doi:10.3390/md18110568.
128. Liu, F.; Qu, Y.-K.; Wang, A.-M.; Yu, Y.-B.; Yang, W.-P.; Lv, F.; Nie, Q. Effects of carotenoids on the growth performance, biochemical parameters, immune responses and disease resistance of yellow catfish (*Pelteobagrus fulvidraco*) under high-temperature stress. *Aquaculture* **2019**, 503, 293–303, doi:10.1016/j.aquaculture.2019.01.008.
129. Lim, K.C.; Yusoff, F.M.; Shariff, M.; Kamarudin, M.S.; Nagao, N. Dietary supplementation of astaxanthin enhances hemato-biochemistry and innate immunity of Asian seabass, *Lates calcarifer* (Bloch, 1790). *Aquaculture* **2019**, 512, 734339, doi:10.1016/j.aquaculture.2019.734339.
130. Cheng, C.-H.; Guo, Z.-X.; Ye, C.-X.; Wang, A.-L. Effect of dietary astaxanthin on the growth performance, non-specific immunity, and antioxidant capacity of pufferfish (*Takifugu obscurus*) under high temperature stress. *Fish Physiol. Biochem.* **2018**, 44, 209–218, doi:10.1007/s10695-017-0425-5.
131. Blount, J.D.; Houston, D.C.; Surai, P.F.; Møller, A.P. Egg-laying capacity is limited by carotenoid pigment availability in wild gulls *Larus fuscus*. *Proc. R. Soc. Lond. B* **2004**, 271, 79–81, doi:10.1098/rsbl.2003.0104.
132. García-Campa, J.; Müller, W.; González-Braojos, S.; García-Juárez, E.; Morales, J. Dietary carotenoid supplementation facilitates egg laying in a wild passerine. *Ecol. Evol.* **2020**, 10, 4968–4978, doi:10.1002/ece3.6250.
133. Surai, P.F.; Speake, B.K. Distribution of carotenoids from the yolk to the tissues of the chick embryo. *J. Nutr. Biochem.* **1998**, 9, 645–651, doi:10.1016/S0955-2863(98)00068-0.
134. Speake, B.K.; Surai, P.F.; Noble, R.C.; Beer, J.V.; Wood, N.A. Differences in egg lipid and antioxidant composition between wild and captive pheasants and geese. *Comp. Biochem. Physiol. B* **1999**, 124, 101–107, doi:10.1016/S0305-0491(99)00108-X.
135. Surai, P.F.; Speake, B.K.; Wood, N.A.; Blount, J.D.; Bortolotti, G.R.; Sparks, N.H. Carotenoid discrimination by the avian embryo: a lesson from wild birds. *Comp. Biochem. Physiol. B* **2001**, 128, 743–750, doi:10.1016/S1096-4959(00)00369-9.
136. Li, H.; Tyndale, S.T.; Heath, D.D.; Letcher, R.J. Determination of carotenoids and all-*trans*-retinol in fish eggs by liquid chromatography-electrospray ionization-tandem mass spectrometry. *J. Chromatogr. B Analyt. Technol. Biomed. Life Sci.* **2005**, 816, 49–56, doi:10.1016/j.jchromb.2004.11.005.
137. Winston, G.W.; Lemaire, D.G.E.; Lee, R.F. Antioxidants and total oxyradical scavenging capacity during grass shrimp, *Palaemonetes pugio*, embryogenesis. *Comp. Biochem. Physiol. C* **2004**, 139, 281–288, doi:10.1016/j.cca.2004.12.006.
138. Karadas, F.; Pappas, A.C.; Surai, P.F.; Speake, B.K. Embryonic development within carotenoid-enriched eggs influences the post-hatch carotenoid status of the chicken. *Comp. Biochem. Physiol. B* **2005**, 141, 244–251, doi:10.1016/j.cbpc.2005.04.001.
139. Christiansen, R.; Lie, Ø.; Torrissen, O.J. Effect of astaxanthin and vitamin A on growth and survival during first feeding of Atlantic salmon, *Salmo salar* L. *Aquac. Res.* **1994**, 25, 903–914, doi:10.1111/j.1365-2109.1994.tb01352.x.
140. Koch, R.E.; Kavazis, A.N.; Hasselquist, D.; Hood, W.R.; Zhang, Y.; Toomey, M.B.; Hill, G.E. No evidence that carotenoid pigments boost either immune or antioxidant defenses in a songbird. *Nat. Commun.* **2018**, 9, 491, doi:10.1038/s41467-018-02974-x.
141. Navara, K.J.; Hill, G.E. Dietary carotenoid pigments and immune function in a songbird with extensive carotenoid-based plumage coloration. *Behav. Ecol.* **2003**, 14, 909–916, doi:10.1093/beheco/arg085.



## References

142. Christiansen, R.; Torrissen, O.J. Effects of dietary astaxanthin supplementation on fertilization and egg survival in Atlantic salmon (*Salmo salar* L.). *Aquaculture* **1997**, *153*, 51–62, doi:10.1016/S0044-8486(97)00016-1.
143. Green, A.S.; Fascetti, A.J. Meeting the vitamin A requirement: The efficacy and importance of  $\beta$ -carotene in animal species. *Sci. World J.* **2016**, *2016*, 7393620, doi:10.1155/2016/7393620.
144. Zhong, M.; Kawaguchi, R.; Kassai, M.; Sun, H. Retina, retinol, retinal and the natural history of vitamin A as a light sensor. *Nutrients* **2012**, *4*, 2069–2096, doi:10.3390/nu4122069.
145. Bernstein, P.S.; Khachik, F.; Carvalho, L.S.; Muir, G.J.; Zhao, D.Y.; Katz, N.B. Identification and quantitation of carotenoids and their metabolites in the tissues of the human eye. *Exp. Eye Res.* **2001**, *72*, 215–223, doi:10.1006/exer.2000.0954.
146. Bone, R.A.; Landrum, J.T.; Hime, G.W.; Cains, A.; Zamor, J. Stereochemistry of the human macular carotenoids. *Invest. Ophthalmol. Vis. Sci.* **1993**, *34*, 2033–2040.
147. Krinsky, N.I.; Landrum, J.T.; Bone, R.A. Biologic mechanisms of the protective role of lutein and zeaxanthin in the eye. *Annu. Rev. Nutr.* **2003**, *23*, 171–201, doi:10.1146/annurev.nutr.23.011702.073307.
148. Toomey, M.B.; Collins, A.M.; Frederiksen, R.; Cornwall, M.C.; Timlin, J.A.; Corbo, J.C. A complex carotenoid palette tunes avian colour vision. *J. R. Soc. Interface* **2015**, *12*, 20150563, doi:10.1098/rsif.2015.0563.
149. Khachik, F.; Beecher, G.R.; Goli, M.B.; Lusby, W.R. Separation, identification, and quantification of carotenoids in fruits, vegetables and human plasma by high performance liquid chromatography. *Pure Appl. Chem.* **1991**, *63*, 71–80, doi:10.1351/pac199163010071.
150. Al-Delaimy, W.K.; van Kappel, A.L.; Ferrari, P.; Slimani, N.; Steghens, J.-P.; Bingham, S.; Johansson, I.; Wallström, P.; Overvad, K.; Tjønneland, A.; et al. Plasma levels of six carotenoids in nine European countries: report from the European Prospective Investigation into Cancer and Nutrition (EPIC). *Public Health Nutr.* **2004**, *7*, 713–722, doi:10.1079/PHN2004598.
151. Olmedilla, B.; Granado, F.; Southon, S.; Wright, A.J.; Blanco, I.; Gil-Martinez, E.; Berg, H.; Corridan, B.; Roussel, A.M.; Chopra, M.; et al. Serum concentrations of carotenoids and vitamins A, E, and C in control subjects from five European countries. *Br. J. Nutr.* **2001**, *85*, 227–238, doi:10.1079/BJN2000248.
152. von Lintig, J.; Vogt, K. Filling the gap in vitamin A research. Molecular identification of an enzyme cleaving  $\beta$ -carotene to retinal. *J. Biol. Chem.* **2000**, *275*, 11915–11920, doi:10.1074/jbc.275.16.11915.
153. Lindqvist, A.; Andersson, S. Biochemical properties of purified recombinant human  $\beta$ -carotene 15,15'-monooxygenase. *J. Biol. Chem.* **2002**, *277*, 23942–23948, doi:10.1074/jbc.M202756200.
154. von Lintig, J. von; Hessel, S.; Isken, A.; Kiefer, C.; Lampert, J.M.; Voolstra, O.; Vogt, K. Towards a better understanding of carotenoid metabolism in animals. *Biochim. Biophys. Acta* **2005**, *1740*, 122–131, doi:10.1016/j.bbadis.2004.11.010.
155. Biesalski, H.K.; Chichili, G.R.; Frank, J.; Lintig, J. von; Nohr, D. Conversion of  $\beta$ -carotene to retinal pigment. *Vitam. Horm.* **2007**, *75*, 117–130, doi:10.1016/S0083-6729(06)75005-1.
156. Bauernfeind, J.C. Carotenoid vitamin A precursors and analogs in foods and feeds. *J. Agric. Food Chem.* **1972**, *20*, 456–473, doi:10.1021/jf60181a003.
157. West, K.P.; LeClerq, S.C.; Shrestha, S.R.; Wu, L.S.; Pradhan, E.K.; Khatry, S.K.; Katz, J.; Adhikari, R.; Sommer, A. Effects of vitamin A on growth of vitamin A-deficient children: field studies in Nepal. *J. Nutr.* **1997**, *127*, 1957–1965, doi:10.1093/jn/127.10.1957.
158. Christian, P.; West, K.P.; Khatry, S.K.; Katz, J.; LeClerq, S.; Pradhan, E.K.; Shrestha, S.R. Vitamin A or  $\beta$ -carotene supplementation reduces but does not eliminate maternal night blindness in Nepal. *J. Nutr.* **1998**, *128*, 1458–1463, doi:10.1093/jn/128.9.1458.
159. Sommer, A. Vitamin A deficiency, child health, and survival. *Nutrition* **1997**, *13*, 484–485, doi:10.1016/S0899-9007(97)00013-0.
160. Manorama, R.; Brahmam, G.N.; Rukmini, C. Red palm oil as a source of  $\beta$ -carotene for combating vitamin A deficiency. *Plant Foods Hum. Nutr.* **1996**, *49*, 75–82, doi:10.1007/BF01092524.
161. Carlier, C.; Coste, J.; Etchepare, M.; Périquet, B.; Amédée-Manesme, O. A randomised controlled trial to test equivalence between retinyl palmitate and  $\beta$  carotene for vitamin A deficiency. *BMJ* **1993**, *307*, 1106–1110, doi:10.1136/bmj.307.6912.1106.
162. Grune, T.; Lietz, G.; Palou, A.; Ross, A.C.; Stahl, W.; Tang, G.; Thurnham, D.; Yin, S.; Biesalski, H.K.  $\beta$ -Carotene is an important vitamin A source for humans. *J. Nutr.* **2010**, *140*, 2268S–2285S, doi:10.3945/jn.109.119024.
163. Combs, G.F.; McClung, J.P. Vitamin A. *The Vitamins*; Elsevier, 2017; pp 109–159, ISBN 9780128029657.
164. van Loo-Bouwman, C.A.; Naber, T.H.J.; Schaafsma, G. A review of vitamin A equivalency of  $\beta$ -carotene in various food matrices for human consumption. *Br. J. Nutr.* **2014**, *111*, 2153–2166, doi:10.1017/S0007114514000166.
165. Burri, B.J. Beta-cryptoxanthin as a source of vitamin A. *J. Sci. Food Agric.* **2015**, *95*, 1786–1794, doi:10.1002/jsfa.6942.



166. Burri, B.J.; Chang, J.S.T.; Neidlinger, T.R.  $\beta$ -Cryptoxanthin- and  $\alpha$ -carotene-rich foods have greater apparent bioavailability than  $\beta$ -carotene-rich foods in Western diets. *Br. J. Nutr.* **2011**, *105*, 212–219, doi:10.1017/S0007114510003260.
167. Olmedilla-Alonso, B.; Rodríguez-Rodríguez, E.; Beltrán-de-Miguel, B.; Estévez-Santiago, R. Dietary  $\beta$ -cryptoxanthin and  $\alpha$ -carotene have greater apparent bioavailability than  $\beta$ -carotene in subjects from countries with different dietary patterns. *Nutrients* **2020**, *12*, 2639, doi:10.3390/nu12092639.
168. Jiang, H.; Yin, Y.; Wu, C.-R.; Liu, Y.; Guo, F.; Li, M.; Le Ma. Dietary vitamin and carotenoid intake and risk of age-related cataract. *Am. J. Clin. Nutr.* **2019**, *109*, 43–54, doi:10.1093/ajcn/nqy270.
169. Wilson, L.M.; Tharmarajah, S.; Jia, Y.; Semba, R.D.; Schaumberg, D.A.; Robinson, K.A. The effect of lutein/zeaxanthin intake on human macular pigment optical density: a systematic review and meta-analysis. *Adv. Nutr.* **2021**, *12*, 2244–2254, doi:10.1093/advances/nmab071.
170. Lutein + zeaxanthin and omega-3 fatty acids for age-related macular degeneration: the Age-Related Eye Disease Study 2 (AREDS2) randomized clinical trial. *JAMA* **2013**, *309*, 2005–2015, doi:10.1001/jama.2013.4997.
171. Berson, E.L.; Rosner, B.; Sandberg, M.A.; Weigel-DiFranco, C.; Brockhurst, R.J.; Hayes, K.C.; Johnson, E.J.; Anderson, E.J.; Johnson, C.A.; Gaudio, A.R.; et al. Clinical trial of lutein in patients with retinitis pigmentosa receiving vitamin A. *Arch. Ophthalmol.* **2010**, *128*, 403–411, doi:10.1001/archophthalmol.2010.32.
172. Ishikawa, S.; Hashizume, K.; Nishigori, H.; Tezuka, Y.; Sanbe, A.; Kurosaka, D. Effect of astaxanthin on cataract formation induced by glucocorticoids in the chick embryo. *Curr. Eye Res.* **2015**, *40*, 535–540, doi:10.3109/02713683.2014.935445.
173. Yang, M.; Chen, Y.; Zhao, T.; Wang, Z. Effect of astaxanthin on metabolic cataract in rats with type 1 diabetes mellitus. *Exp. Mol. Pathol.* **2020**, *113*, 104372, doi:10.1016/j.yexmp.2020.104372.
174. Kim, J.A.; Jang, J.-H.; Lee, S.-Y. An updated comprehensive review on vitamin A and carotenoids in breast cancer: mechanisms, genetics, assessment, current evidence, and future clinical implications. *Nutrients* **2021**, *13*, 3162, doi:10.3390/nu13093162.
175. Chang, S.; Erdman, J.W.; Clinton, S.K.; Vadiveloo, M.; Strom, S.S.; Yamamura, Y.; Duphorne, C.M.; Spitz, M.R.; Amos, C.I.; Contois, J.H.; et al. Relationship between plasma carotenoids and prostate cancer. *Nutr. Cancer* **2005**, *53*, 127–134, doi:10.1207/s15327914nc5302\_1.
176. van Hoang, D.; Pham, N.M.; Lee, A.H.; Tran, D.N.; Binns, C.W. Dietary carotenoid intakes and prostate cancer risk: a case-control study from vietnam. *Nutrients* **2018**, *10*, 70, doi:10.3390/nu10010070.
177. Michaud, D.S.; Feskanich, D.; Rimm, E.B.; Colditz, G.A.; Speizer, F.E.; Willett, W.C.; Giovannucci, E. Intake of specific carotenoids and risk of lung cancer in 2 prospective US cohorts. *Am. J. Clin. Nutr.* **2000**, *72*, 990–997, doi:10.1093/ajcn/72.4.990.
178. Rohan, T.E.; Jain, M.; Howe, G.R.; Miller, A.B. A cohort study of dietary carotenoids and lung cancer risk in women (Canada). *Cancer Causes Control* **2002**, *13*, 231–237, doi:10.1023/A:1015048619413.
179. Goralczyk, R.  $\beta$ -Carotene and lung cancer in smokers: review of hypotheses and status of research. *Nutr. Cancer* **2009**, *61*, 767–774, doi:10.1080/01635580903285155.
180. Middha, P.; Weinstein, S.J.; Männistö, S.; Albanes, D.; Mondul, A.M.  $\beta$ -Carotene supplementation and lung cancer incidence in the alpha-tocopherol, beta-carotene cancer prevention study: the role of tar and nicotine. *Nicotine Tob. Res* **2019**, *21*, 1045–1050, doi:10.1093/ntr/nty115.
181. Blumberg, J.; Block, G. The alpha-tocopherol, beta-carotene cancer prevention study in Finland. *Nutr. Rev.* **1994**, *52*, 242–245, doi:10.1111/j.1753-4887.1994.tb01430.x.
182. Abidov, M.; Ramazanov, Z.; Seifulla, R.; Grachev, S. The effects of Xanthigen in the weight management of obese premenopausal women with non-alcoholic fatty liver disease and normal liver fat. *Diabetes Obes. Metab.* **2010**, *12*, 72–81, doi:10.1111/j.1463-1326.2009.01132.x.
183. Zhang, Y.; Xu, W.; Huang, X.; Zhao, Y.; Ren, Q.; Hong, Z.; Huang, M.; Xing, X. Fucoxanthin ameliorates hyperglycemia, hyperlipidemia and insulin resistance in diabetic mice partially through IRS-1/PI3K/Akt and AMPK pathways. *J. Funct. Foods* **2018**, *48*, 515–524, doi:10.1016/j.jff.2018.07.048.
184. Gille, A.; Stojnic, B.; Derwenskus, F.; Trautmann, A.; Schmid-Staiger, U.; Posten, C.; Briviba, K.; Palou, A.; Bonet, M.L.; Ribot, J. A lipophilic fucoxanthin-rich *Phaeodactylum tricornutum* extract ameliorates effects of diet-induced obesity in C57BL/6J mice. *Nutrients* **2019**, *11*, 796, doi:10.3390/nu11040796.
185. Maeda, H.; Hosokawa, M.; Sashima, T.; Funayama, K.; Miyashita, K. Fucoxanthin from edible seaweed, *Undaria pinnatifida*, shows antiobesity effect through UCP1 expression in white adipose tissues. *Biochem. Biophys. Res. Commun.* **2005**, *332*, 392–397, doi:10.1016/j.bbrc.2005.05.002.
186. Kim, M.-B.; Bae, M.; Lee, Y.; Kang, H.; Hu, S.; Pham, T.X.; Park, Y.-K.; Lee, J.-Y. Consumption of low dose fucoxanthin does not prevent hepatic and adipose inflammation and fibrosis in mouse models of diet-induced obesity. *Nutrients* **2022**, *14*, 2280, doi:10.3390/nu14112280.



## References

187. Rebello, C.J.; Greenway, F.L.; Johnson, W.D.; Ribnick, D.; Poulev, A.; Stadler, K.; Coulter, A.A. Fucoxanthin and its metabolite fucoxanthinol do not induce browning in human adipocytes. *J. Agric. Food Chem.* **2017**, *65*, 10915–10924, doi:10.1021/acs.jafc.7b03931.
188. Kaulmann, A.; Bohn, T. Carotenoids, inflammation, and oxidative stress-implications of cellular signaling pathways and relation to chronic disease prevention. *Nutr. Res.* **2014**, *34*, 907–929, doi:10.1016/j.nutres.2014.07.010.
189. Park, J.S.; Chyun, J.H.; Kim, Y.K.; Line, L.L.; Chew, B.P. Astaxanthin decreased oxidative stress and inflammation and enhanced immune response in humans. *Nutr. Metab.* **2010**, *7*, 18, doi:10.1186/1743-7075-7-18.
190. Zhang, M.; Cui, Z.; Cui, H.; Cao, Y.; Zhong, C.; Wang, Y. Astaxanthin alleviates cerebral edema by modulating NKCC1 and AQP4 expression after traumatic brain injury in mice. *BMC Neurosci.* **2016**, *17*, 60, doi:10.1186/s12868-016-0295-2.
191. Ji, X.; Peng, D.; Zhang, Y.; Zhang, J.; Wang, Y.; Gao, Y.; Lu, N.; Tang, P. Astaxanthin improves cognitive performance in mice following mild traumatic brain injury. *Brain Res.* **2017**, *1659*, 88–95, doi:10.1016/j.brainres.2016.12.031.
192. Masoudi, A.; Dargahi, L.; Abbaszadeh, F.; Pourgholami, M.H.; Asgari, A.; Manoochehri, M.; Jorjani, M. Neuroprotective effects of astaxanthin in a rat model of spinal cord injury. *Behav. Brain Res.* **2017**, *329*, 104–110, doi:10.1016/j.bbr.2017.04.026.
193. Hussein, G.; Nakamura, M.; Zhao, Q.; Iguchi, T.; Goto, H.; Sankawa, U.; Watanabe, H. Antihypertensive and neuroprotective effects of astaxanthin in experimental animals. *Biol. Pharm. Bull.* **2005**, *28*, 47–52, doi:10.1248/bpb.28.47.
194. Jiang, X.; Chen, L.; Shen, L.; Chen, Z.; Xu, L.; Zhang, J.; Yu, X. Trans-astaxanthin attenuates lipopolysaccharide-induced neuroinflammation and depressive-like behavior in mice. *Brain Res.* **2016**, *1649*, 30–37, doi:10.1016/j.brainres.2016.08.029.
195. Ke, Y.; Bu, S.; Ma, H.; Gao, L.; Cai, Y.; Zhang, Y.; Zhou, W. Preventive and therapeutic effects of astaxanthin on depressive-like behaviors in high-fat diet and streptozotocin-treated rats. *Front. Pharmacol.* **2019**, *10*, 1621, doi:10.3389/fphar.2019.01621.
196. Grand View Research. Carotenoids market size, share & trends analysis report by source (natural, synthetic), by product ( $\beta$ -carotene, lutein, lycopene, astaxanthin, zeaxanthin, canthaxanthin), by application, and segment forecasts, 2018 - 2025 *GVR-I-68038-321-8*, **2016**. Available online: <https://www.grandviewresearch.com/industry-analysis/carotenoids-market> (accessed on 13 March 2023).
197. European Parliament. Regulation (EC) No 1333/2008 on food additives. *Official Journal of the European Union* **2008**.
198. U.S. Food & Drug Administration. Color additive status list. Available online: <https://www.fda.gov/industry/color-additive-inventories/color-additive-status-list> (accessed on 13 March 2023).
199. González-Peña, M.A.; Ortega-Regules, A.E.; Anaya de Parrodi, C.; Lozada-Ramírez, J.D. Chemistry, occurrence, properties, applications, and encapsulation of carotenoids-a review. *Plants* **2023**, *12*, 313, doi:10.3390/plants12020313.
200. Lehto, S.; Buchweitz, M.; Klimm, A.; Straßburger, R.; Bechtold, C.; Ulberth, F. Comparison of food colour regulations in the EU and the US: a review of current provisions. *Food Addit. Contam. Part A Chem. Anal. Control Expo. Risk Assess.* **2017**, *34*, 335–355, doi:10.1080/19440049.2016.1274431.
201. European Commission. Commission Implementing Regulation (EU) 2017/2470 of 20 December 2017 establishing the Union list of novel foods in accordance with Regulation (EU) 2015/2283 of the European Parliament and of the Council on novel foods. *Official Journal of the European Union* **2017**, *L 351/72*.
202. U.S. Food & Drug Administration. GRAS Notices. Available online: <https://www.cfsanappsexternal.fda.gov/scripts/fdcc/index.cfm?set=GRASNotices> (accessed on 13 March 2023).
203. Turck, D.; Castenmiller, J.; Henauw, S. de; Hirsch-Ernst, K.I.; Kearney, J.; Maciuk, A.; Mangelsdorf, I.; McArdle, H.J.; Naska, A.; Pelaez, C.; et al. Safety of astaxanthin for its use as a novel food in food supplements. *EFSA Journal* **2020**, *18*, e05993, doi:10.2903/j.efsa.2020.5993.
204. European Food Safety Authority. Scientific Opinion on the safety of astaxanthin-rich ingredients (AstaREAL A1010 and AstaREAL L10) as novel food ingredients. *EFSA Journal* **2014**, *12*, 3757, doi:10.2903/j.efsa.2014.3757.
205. EFSA Panel on Additives and Products or Substances used in Animal Feed. Scientific Opinion on the safety and efficacy of astaxanthin (CAROPHYLL® Pink 10% CWS) for salmonids and ornamental fish. *EFSA Journal* **2014**, *12*, doi:10.2903/j.efsa.2014.3725.
206. European Food Safety Authority. Statement on the safety of synthetic zeaxanthin as an ingredient in food supplements. *EFSA Journal* **2012**, *10*, 2891, doi:10.2903/j.efsa.2012.2891.
207. Bampidis, V.; Azimonti, G.; Lourdes Bastos, M. de; Christensen, H.; Dusemund, B.; Kouba, M.; Kos Durjava, M.; López-Alonso, M.; López Puente, S.; Marcon, F.; et al. Safety and efficacy of lutein and lutein/zeaxanthin extracts from *Tagetes erecta* for poultry for fattening and laying (except turkeys). *EFSA Journal* **2019**, *17*, e05698, doi:10.2903/j.efsa.2019.5698.



208. Liu, X.; Shibata, T.; Hisaka, S.; Osawa, T. Astaxanthin inhibits reactive oxygen species-mediated cellular toxicity in dopaminergic SH-SY5Y cells via mitochondria-targeted protective mechanism. *Brain Res.* **2009**, *1254*, 18–27, doi:10.1016/j.brainres.2008.11.076.
209. Chen, Y.-Y.; Lee, P.-C.; Wu, Y.-L.; Liu, L.-Y. *In Vivo* Effects of free form astaxanthin powder on anti-oxidation and lipid metabolism with high-cholesterol diet. *PLoS One* **2015**, *10*, e0134733, doi:10.1371/journal.pone.0134733.
210. Farruggia, C.; Kim, M.-B.; Bae, M.; Lee, Y.; Pham, T.X.; Yang, Y.; Han, M.J.; Park, Y.-K.; Lee, J.-Y. Astaxanthin exerts anti-inflammatory and antioxidant effects in macrophages in NRF2-dependent and independent manners. *J. Nutr. Biochem.* **2018**, *62*, 202–209, doi:10.1016/j.jnutbio.2018.09.005.
211. Sindhu, E.R.; Preethi, K.C.; Kuttan, R. Antioxidant activity of carotenoid lutein *in vitro* and *in vivo*. *Indian J. Exp. Biol.* **2010**, *48*, 843–848.
212. Chidambara Murthy, K.N.; Vanitha, A.; Rajesha, J.; Mahadeva Swamy, M.; Sowmya, P.R.; Ravishankar, G.A. *In vivo* antioxidant activity of carotenoids from *Dunaliella salina* - a green microalga. *Life Sci.* **2005**, *76*, 1381–1390, doi:10.1016/j.lfs.2004.10.015.
213. Martini, D.; Negri, L.; Marino, M.; Riso, P.; Del Bo, C.; Porrini, M. What Is the current direction of the research on carotenoids and human health? An overview of registered clinical trials // What Is the Current Direction of the Research on Carotenoids and Human Health? An Overview of Registered Clinical Trials. *Nutrients* **2022**, *14*, 1191, doi:10.3390/nu14061191.
214. Nishida, Y.; Yamashita, E.; Wataru Miki. Quenching activities of common hydrophilic and lipophilic antioxidants against singlet oxygen using chemiluminescence detection system. *Carotenoid Sci.* **2007**, *11*, 16–20.
215. Brendler, T.; Williamson, E.M. Astaxanthin: How much is too much? A safety review. *Phytother. Res.* **2019**, *33*, 3090–3111, doi:10.1002/ptr.6514.
216. Capelli, B.; Bagchi, D.; Cysewski, G.R. Synthetic astaxanthin is significantly inferior to algal-based astaxanthin as an antioxidant and may not be suitable as a human nutraceutical supplement. *Nutrafoods* **2013**, *12*, 145–152, doi:10.1007/s13749-013-0051-5.
217. European Commission. Commission Implementing Regulation (EU) 2015/1415 of 20 August 2015 concerning the authorisation of astaxanthin as a feed additive for fish, crustaceans and ornamental fish. *Official Journal of the European Union* **2015**, L 220/7.
218. Zhou, X.; Cao, Q.; Orfila, C.; Zhao, J.; Zhang, L. Systematic review and meta-analysis on the effects of astaxanthin on human skin ageing. *Nutrients* **2021**, *13*, 2917, doi:10.3390/nu13092917.
219. Marchena, A.M.; Franco, L.; Romero, A.M.; Barriga, C.; Rodríguez, A.B. Lycopene and melatonin: antioxidant compounds in cosmetic formulations. *Skin Pharmacol. Physiol.* **2020**, *33*, 237–243, doi:10.1159/000508673.
220. Darvin, M.E.; Fluhr, J.W.; Meinke, M.C.; Zastrow, L.; Sterry, W.; Lademann, J. Topical beta-carotene protects against infra-red-light-induced free radicals. *Exp. Dermatol.* **2011**, *20*, 125–129, doi:10.1111/j.1600-0625.2010.01191.x.
221. Singh, A.; Mukherjee, T. Application of carotenoids in sustainable energy and green electronics. *Mater. Adv.* **2022**, *3*, 1341–1358, doi:10.1039/D1MA01070K.
222. Bazyar Lakeh, A.A.; Ahmadi, M.R.; Safi, S.; Ytrestøyl, T.; Bjerkeng, B. Growth performance, mortality and carotenoid pigmentation of fry offspring as affected by dietary supplementation of astaxanthin to female rainbow trout (*Oncorhynchus mykiss*) broodstock. *J. Appl. Ichthyol.* **2010**, *26*, 35–39, doi:10.1111/j.1439-0426.2009.01349.x.
223. Tuan Harith, Z.; Mohd Sukri, S.; Remlee, N.F.S.; Mohd Sabir, F.N.; Zakaria, N.N.A. Effects of dietary astaxanthin enrichment on enhancing the colour and growth of red tilapia, *Oreochromis* sp. *Aquac. Fish.* **2022**, doi:10.1016/j.aaf.2022.06.001.
224. Cheng, Y.; Wu, S. Effect of dietary astaxanthin on the growth performance and nonspecific immunity of red swamp crayfish *Procambarus clarkii*. *Aquaculture* **2019**, *512*, 734341, doi:10.1016/j.aquaculture.2019.734341.
225. Li, F.; Huang, S.; Lu, X.; Wang, J.; Lin, M.; An, Y.; Wu, S.; Cai, M. Effects of dietary supplementation with algal astaxanthin on growth, pigmentation, and antioxidant capacity of the blood parrot (*Cichlasoma citrinellum* × *Cichlasoma synspilum*). *J. Ocean. Limnol.* **2018**, *36*, 1851–1859, doi:10.1007/s00343-019-7172-7.
226. Christiansen, R.; Lie, O.; Torrissen, O.J. Growth and survival of Atlantic salmon, *Salmo salar* L., fed different dietary levels of astaxanthin. First-feeding fry. *Aquac. Nutr.* **1995**, *1*, 189–198, doi:10.1111/j.1365-2095.1995.tb00043.x.
227. Han, T.; Li, X.-Y.; Yang, Y.-X.; Yang, M.; Wang, C.-L.; Wang, J.-T. Effects of different dietary vitamin E and astaxanthin levels on growth, fatty acid composition and coloration of the juvenile swimming crab, *Portunus trituberculatus*. *Aquac. Nutr.* **2018**, *24*, 1244–1254, doi:10.1111/anu.12662.
228. Wang, W.; Ishikawa, M.; Koshio, S.; Yokoyama, S.; Dawood, M.A.O.; Zhang, Y. Effects of dietary astaxanthin supplementation on survival, growth and stress resistance in larval and post-larval kuruma shrimp, *Marsupenaeus japonicus*. *Aquac. Res.* **2018**, *49*, 2225–2232, doi:10.1111/are.13679.
229. Palma, J.; Andrade, J.P.; Bureau, D.P. The impact of dietary supplementation with astaxanthin on egg quality and growth of long snout seahorse (*Hippocampus guttulatus*) juveniles. *Aquac. Nutr.* **2017**, *23*, 304–312, doi:10.1111/anu.12394.



## References

230. Wade, N.M.; Cheers, S.; Bourne, N.; Irvin, S.; Blyth, D.; Glencross, B.D. Dietary astaxanthin levels affect colour, growth, carotenoid digestibility and the accumulation of specific carotenoid esters in the Giant Tiger Shrimp, *Penaeus monodon*. *Aquac. Res.* **2015**, *48*, 395–406, doi:10.1111/are.12888.
231. Surai, A.P.; Surai, P.F.; Steinberg, W.; Wakeman, W.G.; Speake, B.K.; Sparks, N.H.C. Effect of canthaxanthin content of the maternal diet on the antioxidant system of the developing chick. *Br. Poult. Sci.* **2003**, *44*, 612–619, doi:10.1080/00071660310001616200.
232. Liu, Y.-Q.; Davis, C.R.; Schmaelzle, S.T.; Rocheford, T.; Cook, M.E.; Tanumihardjo, S.A.  $\beta$ -Cryptoxanthin biofortified maize (*Zea mays*) increases  $\beta$ -cryptoxanthin concentration and enhances the color of chicken egg yolk. *Poult. Sci.* **2012**, *91*, 432–438, doi:10.3382/ps.2011-01719.
233. Pérez-Vendrell, A.M.; Hernández, J.M.; Llauradó, L.; Schierle, J.; Brufau, J. Influence of source and ratio of xanthophyll pigments on broiler chicken pigmentation and performance. *Poult. Sci.* **2001**, *80*, 320–326, doi:10.1093/ps/80.3.320.
234. Umar Faruk, M.; Roos, F.F.; Cisneros-Gonzalez, F. A meta-analysis on the effect of canthaxanthin on egg production in brown egg layers. *Poult. Sci.* **2018**, *97*, 84–87, doi:10.3382/ps/pex236.
235. Rosa, A.P.; Bonilla, C.E.V.; Londero, A.; Giacomini, C.B.S.; Orso, C.; Fernandes, M.O.; Moura, J.S.; Hermes, R. Effect of broiler breeders fed with corn or sorghum and canthaxanthin on lipid peroxidation, fatty acid profile of hatching eggs, and offspring performance. *Poult. Sci.* **2017**, *96*, 647–658, doi:10.3382/ps/pew294.
236. Nabi, F.; Arain, M.A.; Rajput, N.; Alagawany, M.; Soomro, J.; Umer, M.; Soomro, F.; Wang, Z.; Ye, R.; Liu, J. Health benefits of carotenoids and potential application in poultry industry: A review. *J. Anim. Physiol. Anim. Nutr.* **2020**, *104*, 1809–1818, doi:10.1111/jpn.13375.
237. Takahashi, K.; Takimoto, T.; Sato, K.; Akiba, Y. Effect of dietary supplementation of astaxanthin from *Phaffia rhodozyma* on lipopolysaccharide-induced early inflammatory responses in male broiler chickens (*Gallus gallus*) fed a corn-enriched diet. *Anim. Sci. J.* **2011**, *82*, 753–758, doi:10.1111/j.1740-0929.2011.00898.x.
238. Jeong, J.S.; Kim, I.H. Effect of astaxanthin produced by *Phaffia rhodozyma* on growth performance, meat quality, and fecal noxious gas emission in broilers. *Poult. Sci.* **2014**, *93*, 3138–3144, doi:10.3382/ps.2013-03847.
239. Weber, G.M.; Machander, V.; Schierle, J.; Aureli, R.; Roos, F.; Pérez-Vendrell, A.M. Tolerance of poultry against an overdose of canthaxanthin as measured by performance, different blood variables and post-mortem evaluation. *Anim. Feed Sci. Technol.* **2013**, *186*, 91–100, doi:10.1016/j.anifeedsci.2013.09.005.
240. Nakada, T.; Ota, S. What is the correct name for the type of *Haematococcus* Flot. (Volvocales, Chlorophyceae)? *Taxon* **2016**, *65*, 343–348, doi:10.12705/652.11.
241. Moretti, V.M.; Mentasti, T.; Bellagamba, F.; Luzzana, U.; Caprino, F.; Turchini, G.M.; Giani, I.; Valfrè, F. Determination of astaxanthin stereoisomers and colour attributes in flesh of rainbow trout (*Oncorhynchus mykiss*) as a tool to distinguish the dietary pigmentation source. *Food Addit. Contam.* **2006**, *23*, 1056–1063, doi:10.1080/02652030600838399.
242. Renström, B.; Borch, G.; Skulberg, O.M.; Liaaen-Jensen, S. Optical purity of (3S,3'S)-astaxanthin from *Haematococcus pluvialis*. *Phytochemistry* **1981**, *20*, 2561–2564, doi:10.1016/0031-9422(81)83094-4.
243. Liu, X.; Osawa, T. *Cis* astaxanthin and especially 9-*cis* astaxanthin exhibits a higher antioxidant activity *in vitro* compared to the all-*trans* isomer. *Biochem. Biophys. Res. Commun.* **2007**, *357*, 187–193, doi:10.1016/j.bbrc.2007.03.120.
244. Bjerkeng, B.; Følling, M.; Lagocki, S.; Storebakken, T.; Olli, J.J.; Alsted, N. Bioavailability of all-*E*-astaxanthin and *Z*-isomers of astaxanthin in rainbow trout (*Oncorhynchus mykiss*). *Aquaculture* **1997**, *157*, 63–82, doi:10.1016/S0044-8486(97)00146-4.
245. Victoria-Campos, C.I.; Ornelas-Paz, J.d.J.; Yahia, E.M.; Jiménez-Castro, J.A.; Cervantes-Paz, B.; Ibarra-Junquera, V.; Pérez-Martínez, J.D.; Zamudio-Flores, P.B.; Escalante-Minakata, P. Effect of ripening, heat processing, and fat type on the micellarization of pigments from jalapeño peppers. *J. Agric. Food Chem.* **2013**, *61*, 9938–9949, doi:10.1021/jf4032124.
246. Chitchumroonchokchai, C.; Failla, M.L. Hydrolysis of zeaxanthin esters by carboxyl ester lipase during digestion facilitates micellarization and uptake of the xanthophyll by Caco-2 human intestinal cells. *J. Nutr.* **2006**, *136*, 588–594, doi:10.1093/jn/136.3.588.
247. Dhuique-Mayer, C.; Borel, P.; Reboul, E.; Caporiccio, B.; Besancon, P.; Amiot, M.-J.  $\beta$ -cryptoxanthin from *Citrus* juices: assessment of bioaccessibility using an *in vitro* digestion/Caco-2 cell culture model. *Br. J. Nutr.* **2007**, *97*, 883–890, doi:10.1017/S0007114507670822.
248. Breithaupt, D.E.; Weller, P.; Wolters, M.; Hahn, A. Plasma response to a single dose of dietary  $\beta$ -cryptoxanthin esters from papaya (*Carica papaya* L.) or non-esterified  $\beta$ -cryptoxanthin in adult human subjects: a comparative study. *Br. J. Nutr.* **2003**, *90*, 795–801, doi:10.1079/BJN2003962.
249. Isler, O.; Zeller, P. Total syntheses of carotenoids. *Vitam. Horm.* **1957**, *15*, 31–71, doi:10.1016/S0083-6729(08)60507-5.



250. Widmer, E.; Zell, R.; Broger, E.A.; Cramer, Y.; Wagner, H.P.; Dinkel, J.; Schlageter, M.; Lukáč, T. Technische Verfahren zur Synthese von Carotinoiden und verwandten Verbindungen aus 6-Oxo-isophoron. II. Ein neues Konzept für die Synthese von (3R,3'R)-Astaxanthin. *Helv. Chim. Acta* **1981**, *64*, 2436–2446, doi:10.1002/hlca.19810640751.
251. Paust, J. Recent progress in commercial retinoids and carotenoids. *Pure Appl. Chem.* **1991**, *63*, 45–58, doi:10.1351/pac199163010045.
252. Paust, J. Herstellung und Anwendung von Carotinoiden. *Chimia* **1994**, *48*, 494–498, doi:10.2533/chimia.1994.494.
253. Ernst, H. Recent advances in industrial carotenoid synthesis. *Pure Appl. Chem.* **2002**, *74*, 2213–2226, doi:10.1351/pac200274112213.
254. Stachowiak, B.; Szulc, P. Astaxanthin for the food industry. *Molecules* **2021**, *26*, 2666, doi:10.3390/molecules26092666.
255. Khachik, F.; Chang, A.-N. Total synthesis of (3R,3'R,6'R)-lutein and its stereoisomers. *J. Org. Chem.* **2009**, *74*, 3875–3885, doi:10.1021/jo900432r.
256. Riaz, N.; Yousaf, Z.; Yasmin, Z.; Munawar, M.; Younas, A.; Rashid, M.; Aftab, A.; Shamsheer, B.; Yasin, H.; Najeebullah, M.; et al. Development of carrot nutraceutical products as an alternative supplement for the prevention of nutritional diseases. *Front. Nutr.* **2021**, *8*, 787351, doi:10.3389/fnut.2021.787351.
257. Šivel, M.; Kráčmar, S.; Fišera, M.; Klejdus, B.; Kubán, V. Lutein content in marigold flower (*Tagetes erecta* L.) concentrates used for production of food supplements. *Czech J. Food Sci.* **2014**, *32*, 521–525, doi:10.17221/104/2014-CJFS.
258. Reif, C.; Arrigoni, E.; Berger, F.; Baumgartner, D.; Nyström, L. Lutein and  $\beta$ -carotene content of green leafy *Brassica* species grown under different conditions. *LWT Food Sci. Technol.* **2013**, *53*, 378–381, doi:10.1016/j.lwt.2013.02.026.
259. Zuurro, A. Enhanced lycopene extraction from tomato peels by optimized mixed-polarity solvent mixtures. *Molecules* **2020**, *25*, 2038, doi:10.3390/molecules25092038.
260. Papaioannou, E.H.; Liakopoulou-Kyriakides, M.; Karabelas, A.J. Natural origin lycopene and its "green" downstream processing. *Crit. Rev. Food. Sci. Nutr.* **2016**, *56*, 686–709, doi:10.1080/10408398.2013.817381.
261. Fung, A.; Hamid, N.; Lu, J. Fucoxanthin content and antioxidant properties of *Undaria pinnatifida*. *Food Chem.* **2013**, *136*, 1055–1062, doi:10.1016/j.foodchem.2012.09.024.
262. García-González, M.; Moreno, J.; Manzano, J.C.; Florencio, F.J.; Guerrero, M.G. Production of *Dunaliella salina* biomass rich in 9-*cis*- $\beta$ -carotene and lutein in a closed tubular photobioreactor. *J. Biotechnol.* **2005**, *115*, 81–90, doi:10.1016/j.jbiotec.2004.07.010.
263. Olaizola, M. Commercial production of astaxanthin from *Haematococcus pluvialis* using 25,000-liter outdoor photobioreactors. *J. Appl. Phycol.* **2000**, *12*, 499–506, doi:10.1023/A:1008159127672.
264. Torzillo, G.; Goksan, T.; Faraloni, C.; Kopecky, J.; Masojídek, J. Interplay between photochemical activities and pigment composition in an outdoor culture of *Haematococcus pluvialis* during the shift from the green to red stage. *J. Appl. Phycol.* **2003**, *15*, 127–136, doi:10.1023/A:1023854904163.
265. Aflalo, C.; Meshulam, Y.; Zarka, A.; Boussiba, S. On the relative efficiency of two- vs. one-stage production of astaxanthin by the green alga *Haematococcus pluvialis*. *Biotechnol. Bioeng.* **2007**, *98*, 300–305, doi:10.1002/bit.21391.
266. Wang, J.; Han, D.; Sommerfeld, M.R.; Lu, C.; Hu, Q. Effect of initial biomass density on growth and astaxanthin production of *Haematococcus pluvialis* in an outdoor photobioreactor. *J. Appl. Phycol.* **2013**, *25*, 253–260, doi:10.1007/s10811-012-9859-4.
267. Liyanaarachchi, V.C.; Nishshanka, G.K.S.H.; Premaratne, R.G.M.M.; Ariyadasa, T.U.; Nimarshana, P.H.V.; Malik, A. Astaxanthin accumulation in the green microalga *Haematococcus pluvialis*: Effect of initial phosphate concentration and stepwise/continuous light stress. *Biotechnol. Rep.* **2020**, *28*, e00538, doi:10.1016/j.btre.2020.e00538.
268. Chekanov, K. Diversity and distribution of carotenogenic algae in Europe: a review. *Mar. Drugs* **2023**, *21*, 108, doi:10.3390/md21020108.
269. Yang, R.; Wei, D. Improving fucoxanthin production in mixotrophic culture of marine diatom *Phaeodactylum tricorutum* by LED light shift and nitrogen supplementation. *Front. Bioeng. Biotechnol.* **2020**, *8*, 820, doi:10.3389/fbioe.2020.00820.
270. Del Campo, J.A.; Rodríguez, H.; Moreno, J.; Vargas, M.A.; Rivas, J.; Guerrero, M.G. Accumulation of astaxanthin and lutein in *Chlorella zofingiensis* (Chlorophyta). *Appl. Microbiol. Biotechnol.* **2004**, *64*, 848–854, doi:10.1007/s00253-003-1510-5.
271. Mantzouridou, F. Biotechnological production of carotenoids – Case *Blakeslea trispora*. *COST Action EUROCAROTEN (CA15136) Scientific Newsletter* **2020**, *12*, 1–8.
272. Papadaki, E.; Mantzouridou, F.T. Natural  $\beta$ -carotene production by *Blakeslea trispora* cultivated in Spanish-style green olive processing wastewaters. *Foods* **2021**, *10*, 327, doi:10.3390/foods10020327.
273. Schmidt, I.; Schewe, H.; Gassel, S.; Jin, C.; Buckingham, J.; Hümbelin, M.; Sandmann, G.; Schrader, J. Biotechnological production of astaxanthin with *Phaffia rhodozyma*/*Xanthophyllomyces dendrorhous*. *Appl. Microbiol. Biotechnol.* **2011**, *89*, 555–571, doi:10.1007/s00253-010-2976-6.



## References

274. Bampidis, V.; Azimonti, G.; Bastos, M.d.L.; Christensen, H.; Dusemund, B.; Fašmon Durjava, M.; Kouba, M.; López-Alonso, M.; López Puente, S.; Marcon, F.; et al. Safety and efficacy of a feed additive consisting of astaxanthin-rich *Phaffia rhodozyma* for salmon and trout (Igene Biotechnology, Inc.). *EFSA Journal* **2022**, *20*, e07161, doi:10.2903/j.efsa.2022.7161.
275. Pawar, P.R.; Velani, S.; Kumari, S.; Lali, A.M.; Prakash, G. Isolation and optimization of a novel thraustochytrid strain for DHA rich and astaxanthin comprising biomass as aquafeed supplement. *3 Biotech* **2021**, *11*, 71, doi:10.1007/s13205-020-02616-4.
276. Park, H.; Kwak, M.; Seo, J.; Ju, J.; Heo, S.; Park, S.; Hong, W. Enhanced production of carotenoids using a Thraustochytrid microalgal strain containing high levels of docosahexaenoic acid-rich oil. *Bioprocess Biosyst. Eng.* **2018**, *41*, 1355–1370, doi:10.1007/s00449-018-1963-7.
277. Aasen, I.M.; Ertesvåg, H.; Heggeset, T.M.B.; Liu, B.; Brautaset, T.; Vadstein, O.; Ellingsen, T.E. Thraustochytrids as production organisms for docosahexaenoic acid (DHA), squalene, and carotenoids. *Appl. Microbiol. Biotechnol.* **2016**, *100*, 4309–4321, doi:10.1007/s00253-016-7498-4.
278. Singh, D.; Gupta, A.; Wilkens, S.L.; Mathur, A.S.; Tuli, D.K.; Barrow, C.J.; Puri, M. Understanding response surface optimisation to the modeling of astaxanthin extraction from a novel strain *Thraustochytrium* sp. S7. *Algal Res.* **2015**, *11*, 113–120, doi:10.1016/j.algal.2015.06.005.
279. Carmona, M.L.; Naganuma, T.; Yamaoka, Y. Identification by HPLC-MS of carotenoids of the *Thraustochytrium* CHN-1 strain isolated from the Seto Inland Sea. *Biosci. Biotechnol. Biochem.* **2003**, *67*, 884–888, doi:10.1271/bbb.67.884.
280. Armenta, R.E.; Burja, A.; Radianingtyas, H.; Barrow, C.J. Critical assessment of various techniques for the extraction of carotenoids and co-enzyme Q10 from the Thraustochytrid strain ONC-T18. *J. Agric. Food Chem.* **2006**, *54*, 9752–9758, doi:10.1021/jf061260o.
281. Raghukumar, S. Ecology of the marine protists, the Labyrinthulomycetes (Thraustochytrids and Labyrinthulids). *Eur. J. Protistol.* **2002**, *38*, 127–145, doi:10.1078/0932-4739-00832.
282. Raghukumar, S.; Damare, V.S. Increasing evidence for the important role of Labyrinthulomycetes in marine ecosystems. *Bot. Mar.* **2011**, *54*, 3–11, doi:10.1515/bot.2011.008.
283. Patel, A.; Rova, U.; Christakopoulos, P.; Matsakas, L. Mining of squalene as a value-added byproduct from DHA producing marine thraustochytrid cultivated on food waste hydrolysate. *Sci. Total Environ.* **2020**, *736*, 139691, doi:10.1016/j.scitotenv.2020.139691.
284. Patel, A.; Rova, U.; Christakopoulos, P.; Matsakas, L. Simultaneous production of DHA and squalene from *Aurantiochytrium* sp. grown on forest biomass hydrolysates. *Biotechnol. Biofuels* **2019**, *12*, 255, doi:10.1186/s13068-019-1593-6.
285. Patel, A.; Liefeldt, S.; Rova, U.; Christakopoulos, P.; Matsakas, L. Co-production of DHA and squalene by thraustochytrid from forest biomass. *Sci. Rep.* **2020**, *10*, 1992, doi:10.1038/s41598-020-58728-7.
286. Humhal, T.; Kastanek, P.; Jezkova, Z.; Cadkova, A.; Kohoutkova, J.; Branyik, T. Use of saline waste water from demineralization of cheese whey for cultivation of *Schizochytrium limacinum* PA-968 and *Japonochytrium marinum* AN-4. *Bioprocess Biosyst. Eng.* **2017**, *40*, 395–402, doi:10.1007/s00449-016-1707-5.
287. Janthanomsuk, P.; Verduyn, C.; Chauvatcharin, S. Improved docosahexaenoic acid production in *Aurantiochytrium* by glucose limited pH-auxostat fed-batch cultivation. *Bioresour. Technol.* **2015**, *196*, 592–599, doi:10.1016/j.biortech.2015.08.023.
288. Chen, C.-Y.; Yang, Y.-T. Combining engineering strategies and fermentation technology to enhance docosahexaenoic acid (DHA) production from an indigenous *Thraustochytrium* sp. BM2 strain. *Biochem. Eng. J.* **2018**, *133*, 179–185, doi:10.1016/j.bej.2018.02.010.
289. Gupta, A.; Barrow, C.J.; Puri, M. Omega-3 biotechnology: Thraustochytrids as a novel source of omega-3 oils. *Biotechnol. Adv.* **2012**, *30*, 1733–1745, doi:10.1016/j.biotechadv.2012.02.014.
290. European Commission. Commission implementing regulation (EU) 2022/1365 of 4 August 2022 amending Implementing Regulation (EU) 2017/2470 as regards the conditions of use of the novel food *Schizochytrium* sp. oil rich in DHA and EPA. *Official Journal of the European Union* **2022**, *L 205/230*.
291. Turck, D.; Castenmiller, J.; Henauw, S. de; Hirsch-Ernst, K.I.; Kearney, J.; Maciuk, A.; Mangelsdorf, I.; McArdle, H.J.; Naska, A.; Pelaez, C.; et al. Safety of *Schizochytrium* sp. oil as a novel food pursuant to Regulation (EU) 2015/2283. *EFSA Journal* **2020**, *18*, e06242, doi:10.2903/j.efsa.2020.6242.
292. Verwaal, R.; Wang, J.; Meijnen, J.-P.; Visser, H.; Sandmann, G.; van den Berg, J.A.; van Ooyen, A.J.J. High-level production of beta-carotene in *Saccharomyces cerevisiae* by successive transformation with carotenogenic genes from *Xanthophyllomyces dendrorhous*. *Appl. Environ. Microbiol.* **2007**, *73*, 4342–4350, doi:10.1128/AEM.02759-06.
293. Scaife, M.A.; Prince, C.A.; Norman, A.; Armenta, R.E. Progress toward an *Escherichia coli* canthaxanthin bioprocess. *Process Biochem.* **2012**, *47*, 2500–2509, doi:10.1016/j.procbio.2012.10.012.



294. Zhang, C.; Chen, X.; Too, H.-P. Microbial astaxanthin biosynthesis: recent achievements, challenges, and commercialization outlook. *Appl. Microbiol. Biotechnol.* **2020**, *104*, 5725–5737, doi:10.1007/s00253-020-10648-2.
295. van Rooyen, I.L.; Nicol, W. Optimal hydroponic growth of *Brassica oleracea* at low nitrogen concentrations using a novel pH-based control strategy. *Sci. Total Environ.* **2021**, *775*, 145875, doi:10.1016/j.scitotenv.2021.145875.
296. Vree, J.H. de; Bosma, R.; Janssen, M.; Barbosa, M.J.; Wijffels, R.H. Comparison of four outdoor pilot-scale photobioreactors. *Biotechnol. Biofuels* **2015**, *8*, 215, doi:10.1186/s13068-015-0400-2.
297. Sirohi, R.; Kumar Pandey, A.; Ranganathan, P.; Singh, S.; Udayan, A.; Kumar Awasthi, M.; Hoang, A.T.; Chilakamarthy, C.R.; Kim, S.H.; Sim, S.J. Design and applications of photobioreactors- a review. *Bioresour. Technol.* **2022**, *349*, 126858, doi:10.1016/j.biortech.2022.126858.
298. Chanquia, S.N.; Vernet, G.; Kara, S. Photobioreactors for cultivation and synthesis: specifications, challenges, and perspectives. *Eng. Life Sci.* **2022**, *22*, 712–724, doi:10.1002/elsc.202100070.
299. Carvalho, A.P.; Meireles, L.A.; Malcata, F.X. Microalgal reactors: a review of enclosed system designs and performances. *Biotechnol. Prog.* **2006**, *22*, 1490–1506, doi:10.1021/bp060065r.
300. Molina Grima, E.; Fernández, F.; García Camacho, F.; Chisti, Y. Photobioreactors: light regime, mass transfer, and scaleup. *J. Biotechnol.* **1999**, *70*, 231–247, doi:10.1016/s0168-1656(99)00078-4.
301. Goetz, V.; Le Borgne, F.; Pruvost, J.; Plantard, G.; Legrand, J. A generic temperature model for solar photobioreactors. *Chem. Eng. J.* **2011**, *175*, 443–449, doi:10.1016/j.cej.2011.09.052.
302. Béchet, Q.; Shilton, A.; Fringer, O.B.; Muñoz, R.; Guieysse, B. Mechanistic modeling of broth temperature in outdoor photobioreactors. *Environ. Sci. Technol.* **2010**, *44*, 2197–2203, doi:10.1021/es903214u.
303. Molina Grima, E.; Belarbi, E.-H.; Acién Fernández, F.G.; Robles Medina, A.; Chisti, Y. Recovery of microalgal biomass and metabolites: process options and economics. *Biotechnol. Adv.* **2003**, *20*, 491–515, doi:10.1016/S0734-9750(02)00050-2.
304. Nawar, A.; Khoja, A.H.; Akbar, N.; Ansari, A.A.; Qayyum, M.; Ali, E. Physical abrasion method using submerged spike balls to remove algal biofilm from photobioreactors. *BMC Res. Notes.* **2017**, *10*, 666, doi:10.1186/s13104-017-2995-9.
305. Huang, Q.; Jiang, F.; Wang, L.; Yang, C. Design of photobioreactors for mass cultivation of photosynthetic organisms. *Engineering* **2017**, *3*, 318–329, doi:10.1016/J.ENG.2017.03.020.
306. Zhang, W.-W.; Zhou, X.-F.; Zhang, Y.-L.; Cheng, P.-F.; Ma, R.; Cheng, W.-L.; Chu, H.-Q. Enhancing astaxanthin accumulation in *Haematococcus pluvialis* by coupled light intensity and nitrogen starvation in column photobioreactors. *J. Microbiol. Biotechnol.* **2018**, *28*, 2019–2028, doi:10.4014/jmb.1807.07008.
307. Boussiba, S.; Vonshak, A. Astaxanthin accumulation in the green alga *Haematococcus pluvialis*. *Plant Cell Physiol.* **1991**, *32*, 1077–1082, doi:10.1093/oxfordjournals.pcp.a078171.
308. Kobayashi, M.; Kurimura, Y.; Kakizono, T.; Nishio, N.; Tsuji, Y. Morphological changes in the life cycle of the green alga *Haematococcus pluvialis*. *J. Ferment. Bioeng.* **1997**, *84*, 94–97, doi:10.1016/S0922-338X(97)82794-8.
309. Loeblich, L.A. Photosynthesis and pigments influenced by light intensity and salinity in the halophile *Dunaliella salina* (Chlorophyta). *J. Mar. Biol. Ass.* **1982**, *62*, 493–508, doi:10.1017/S0025315400019706.
310. Chowdhary, A.K.; Kishi, M.; Toda, T. Enhanced growth of *Chromochloris zofingiensis* through the transition of nutritional modes. *Algal Res.* **2022**, *65*, 102723, doi:10.1016/j.algal.2022.102723.
311. Chen, Q.; Chen, Y.; Xu, Q.; Jin, H.; Hu, Q.; Han, D. Effective two-stage heterotrophic cultivation of the unicellular green microalga *Chromochloris zofingiensis* enabled ultrahigh biomass and astaxanthin production. *Front. Bioeng. Biotechnol.* **2022**, *10*, 834230, doi:10.3389/fbioe.2022.834230.
312. Pawar, P.R.; Lali, A.M.; Prakash, G. Integration of continuous-high cell density-fed-batch fermentation for *Aurantiochytrium limacinum* for simultaneous high biomass, lipids and docosahexaenoic acid production. *Bioresour. Technol.* **2021**, *325*, 124636, doi:10.1016/j.biortech.2020.124636.
313. Liu, Y.-S.; Wu, J.-Y. Modeling of *Xanthophyllomyces dendrorhous* growth on glucose and overflow metabolism in batch and fed-batch cultures for astaxanthin production. *Biotechnol. Bioeng.* **2008**, *101*, 996–1004, doi:10.1002/bit.21978.
314. Rodríguez-Sifuentes, L.; Marszałek, J.E.; Hernández-Carbajal, G.; Chuck-Hernández, C. Importance of downstream processing of natural astaxanthin for pharmaceutical application. *Front. Chem. Eng.* **2021**, *2*, 601483, doi:10.3389/fceng.2020.601483.
315. Lam, G.P. 't; Vermuë, M.H.; Eppink, M.H.M.; Wijffels, R.H.; van den Berg, C. Multi-product microalgae biorefineries: from concept towards reality. *Trends Biotechnol.* **2018**, *36*, 216–227, doi:10.1016/j.tibtech.2017.10.011.
316. Li, J.; Zhu, D.; Niu, J.; Shen, S.; Wang, G. An economic assessment of astaxanthin production by large scale cultivation of *Haematococcus pluvialis*. *Biotechnol. Adv.* **2011**, *29*, 568–574, doi:10.1016/j.biotechadv.2011.04.001.
317. Panis, G.; Carreon, J.R. Commercial astaxanthin production derived by green alga *Haematococcus pluvialis*: a microalgae process model and a techno-economic assessment all through production line. *Algal Res.* **2016**, *18*, 175–190, doi:10.1016/j.algal.2016.06.007.



## References

318. Damiani, M.C.; Leonardi, P.I.; Pieroni, O.I.; Cáceres, E.J. Ultrastructure of the cyst wall of *Haematococcus pluvialis* (Chlorophyceae): wall development and behaviour during cyst germination. *Phycologia* **2006**, *45*, 616–623, doi:10.2216/05-27.1.
319. Hagen, C.; Siegmund, S.; Braune, W. Ultrastructural and chemical changes in the cell wall of *Haematococcus pluvialis* (Volvocales, Chlorophyta) during aplanospore formation. *Eur. J. Phycol.* **2002**, *37*, 217–226, doi:10.1017/S0967026202003669.
320. Sarada, R.; Vidhyavathi, R.; Usha, D.; Ravishankar, G.A. An efficient method for extraction of astaxanthin from green alga *Haematococcus pluvialis*. *J. Agric. Food Chem.* **2006**, *54*, 7585–7588, doi:10.1021/jf060737t.
321. Polle, J.E.; Roth, R.; Ben-Amotz, A.; Goodenough, U. Ultrastructure of the green alga *Dunaliella salina* strain CCAP19/18 (Chlorophyta) as investigated by quick-freeze deep-etch electron microscopy. *Algal Res.* **2020**, *49*, 101953, doi:10.1016/j.algal.2020.101953.
322. Alderman, D.J.; Harrison, J.L.; Bremer, G.B.; Jones, E.B.G. Taxonomic revisions in the marine biflagellate fungi: The ultrastructural evidence. *Mar. Biol.* **1974**, *25*, 345–357, doi:10.1007/BF00404978.
323. Ganuza, E.; Yang, S.; Amezquita, M.; Giraldo-Silva, A.; Andersen, R.A. Genomics, biology and phylogeny *Aurantiochytrium acetophilum* sp. nov. (Thraustochytriaceae), including first evidence of sexual reproduction. *Protist* **2019**, *170*, 209–232, doi:10.1016/j.protis.2019.02.004.
324. Lorenz, R.T.; Cysewski, G.R. Commercial potential for *Haematococcus* microalgae as a natural source of astaxanthin. *Trends Biotechnol.* **2000**, *18*, 160–167, doi:10.1016/S0167-7799(00)01433-5.
325. Praveenkumar, R.; Lee, J.; Vijayan, D.; Lee, S.Y.; Lee, K.; Sim, S.J.; Hong, M.E.; Kim, Y.-E.; Oh, Y.-K. Morphological change and cell disruption of *Haematococcus pluvialis* cyst during high-pressure homogenization for astaxanthin recovery. *Appl. Sci.* **2020**, *10*, 513, doi:10.3390/app10020513.
326. Chen, L.; Liu, X.; Li, D.; Chen, W.; Zhang, K.; Chen, S. Preparation of stable microcapsules from disrupted cell of *Haematococcus pluvialis* by spray drying. *Int. J. Food Sci. Technol.* **2016**, *51*, 1834–1843, doi:10.1111/ijfs.13155.
327. Ruen-ngam, D.; Shotipruk, A.; Pavasant, P. Comparison of extraction methods for recovery of astaxanthin from *Haematococcus pluvialis*. *Sep. Sci. Technol.* **2010**, *46*, 64–70, doi:10.1080/01496395.2010.493546.
328. Dong, S.; Huang, Y.; Zhang, R.; Wang, S.; Liu, Y. Four different methods comparison for extraction of astaxanthin from green alga *Haematococcus pluvialis*. *Sci. World J.* **2014**, *2014*, 694305, doi:10.1155/2014/694305.
329. Jaime, L.; Rodríguez-Meizoso, I.; Cifuentes, A.; Santoyo, S.; Suarez, S.; Ibáñez, E.; Señorans, F.J. Pressurized liquids as an alternative process to antioxidant carotenoids' extraction from *Haematococcus pluvialis* microalgae. *LWT Food Sci. Technol.* **2010**, *43*, 105–112, doi:10.1016/j.lwt.2009.06.023.
330. Mendes-Pinto, M.M.; Raposo, M.; Bowen, J.; Young, A.J.; Morais, R. Evaluation of different cell disruption processes on encysted cells of *Haematococcus pluvialis*: effects on astaxanthin recovery and implications for bio-availability. *J. Appl. Phycol.* **2001**, *13*, 19–24, doi:10.1023/A:1008183429747.
331. Zou, T.-B.; Jia, Q.; Li, H.-W.; Wang, C.-X.; Wu, H.-F. Response surface methodology for ultrasound-assisted extraction of astaxanthin from *Haematococcus pluvialis*. *Mar. Drugs* **2013**, *11*, 1644–1655, doi:10.3390/md11051644.
332. Zhao, L.; Chen, G.; Zhao, G.; Hu, X. Optimization of microwave-assisted extraction of astaxanthin from *Haematococcus pluvialis* by response surface methodology and antioxidant activities of the extracts. *Sep. Sci. Technol.* **2009**, *44*, 243–262, doi:10.1080/01496390802282321.
333. Ahmed, F.; Li, Y.; Fanning, K.; Netzel, M.; Schenk, P.M. Effect of drying, storage temperature and air exposure on astaxanthin stability from *Haematococcus pluvialis*. *Food Res. Int.* **2015**, *74*, 231–236, doi:10.1016/j.foodres.2015.05.021.
334. Raposo, M.F.J.; Morais, A.M.M.B.; Morais, R.M.S.C. Effects of spray-drying and storage on astaxanthin content of *Haematococcus pluvialis* biomass. *World J. Microbiol. Biotechnol.* **2012**, *28*, 1253–1257, doi:10.1007/s11274-011-0929-6.
335. Li, X.; Wang, X.; Duan, C.; Yi, S.; Gao, Z.; Xiao, C.; Agathos, S.N.; Wang, G.; Li, J. Biotechnological production of astaxanthin from the microalga *Haematococcus pluvialis*. *Biotechnol. Adv.* **2020**, *43*, 107602, doi:10.1016/j.biotechadv.2020.107602.
336. Nobre, B.; Marcelo, F.; Passos, R.; Beirão, L.; Palavra, A.; Gouveia, L.; Mendes, R. Supercritical carbon dioxide extraction of astaxanthin and other carotenoids from the microalga *Haematococcus pluvialis*. *Eur. Food Res. Technol.* **2006**, *223*, 787–790, doi:10.1007/s00217-006-0270-8.
337. Díaz-Reinoso, B.; Moure, A.; Domínguez, H.; Parajó, J.C. Supercritical CO<sub>2</sub> extraction and purification of compounds with antioxidant activity. *J. Agric. Food Chem.* **2006**, *54*, 2441–2469, doi:10.1021/jf052858j.
338. Espinosa Álvarez, C.; Vardanega, R.; Salinas-Fuentes, F.; Palma Ramírez, J.; Bugueño Muñoz, W.; Jiménez-Rondón, D.; Meireles, M.A.A.; Cereza Mezquita, P.; Ruiz-Domínguez, M.C. Effect of CO<sub>2</sub> flow rate on the extraction of astaxanthin and fatty acids from *Haematococcus pluvialis* using supercritical fluid technology. *Molecules* **2020**, *25*, 6044, doi:10.3390/molecules25246044.



339. Molino, A.; Mehariya, S.; Iovine, A.; Larocca, V.; Di Sanzo, G.; Martino, M.; Casella, P.; Chianese, S.; Musmarra, D. Extraction of astaxanthin and lutein from microalga *Haematococcus pluvialis* in the red phase using CO<sub>2</sub> supercritical fluid extraction technology with ethanol as co-solvent. *Mar. Drugs* **2018**, *16*, 432, doi:10.3390/md16110432.
340. Saks, L.; McGraw, K.; Hörak, P. How feather colour reflects its carotenoid content. *Funct. Ecol.* **2003**, *17*, 555–561, doi:10.1046/j.1365-2435.2003.00765.x.
341. Inouye, C.Y.; Hill, G.E.; Stradi, R.D.; Montgomerie, R.; Bosque, C. Carotenoid pigments in male house finch plumage in relation to age, subspecies, and ornamental coloration. *The Auk* **2001**, *118*, 900–915, doi:10.1093/auk/118.4.900.
342. Zhao, X.; Liu, H.; Zhang, X.; Zhang, G.; Zhu, H. Astaxanthin from *Haematococcus pluvialis* microencapsulated by spray drying: characterization and antioxidant activity. *J. Amer. Oil Chem. Soc.* **2019**, *96*, 93–102, doi:10.1002/aocs.12170.
343. Holtin, K.; Kuehnle, M.; Rehbein, J.; Schuler, P.; Nicholson, G.; Albert, K. Determination of astaxanthin and astaxanthin esters in the microalgae *Haematococcus pluvialis* by LC-(APCI)MS and characterization of predominant carotenoid isomers by NMR spectroscopy. *Anal. Bioanal. Chem.* **2009**, *395*, 1613–1622, doi:10.1007/s00216-009-2837-2.
344. Yuan, J.-P.; Chen, F. Purification of *trans*-astaxanthin from a high-yielding astaxanthin ester-producing strain of the microalga *Haematococcus pluvialis*. *Food Chem.* **2000**, *68*, 443–448, doi:10.1016/S0308-8146(99)00219-8.
345. Yuan, J.P.; Chen, F. Hydrolysis kinetics of astaxanthin esters and stability of astaxanthin of *Haematococcus pluvialis* during saponification. *J. Agric. Food Chem.* **1999**, *47*, 31–35, doi:10.1021/jf980465x.
346. Yuan, J.-P.; Chen, F. Chromatographic separation and purification of *trans*-astaxanthin from the extracts of *Haematococcus pluvialis*. *J. Agric. Food Chem.* **1998**, *46*, 3371–3375, doi:10.1021/jf980039b.
347. Casella, P.; Iovine, A.; Mehariya, S.; Marino, T.; Musmarra, D.; Molino, A. Smart method for carotenoids characterization in *Haematococcus pluvialis* red phase and evaluation of astaxanthin thermal stability. *Antioxidants* **2020**, *9*, 422, doi:10.3390/antiox9050422.
348. Viazau, Y.V.; Goncharik, R.G.; Kulikova, I.S.; Kulikov, E.A.; Vasilov, R.G.; Selishcheva, A.A. *E/Z* isomerization of astaxanthin and its monoesters *in vitro* under the exposure to light or heat and in overilluminated *Haematococcus pluvialis* cells. *Bioresour. Bioprocess.* **2021**, *8*, 55, doi:10.1186/s40643-021-00410-5.
349. Miao, F.; Lu, D.; Li, Y.; Zeng, M. Characterization of astaxanthin esters in *Haematococcus pluvialis* by liquid chromatography-atmospheric pressure chemical ionization mass spectrometry. *Anal. Biochem.* **2006**, *352*, 176–181, doi:10.1016/j.ab.2006.03.006.
350. Grewe, C.; Griehl, C. Time- and media-dependent secondary carotenoid accumulation in *Haematococcus pluvialis*. *Biotechnol. J.* **2008**, *3*, 1232–1244, doi:10.1002/biot.200800067.
351. Miao, F.; Da Lu, Y.; Zhang, C.; Zuo, J.; Geng, Y.; Hu, H.; Li, Y. The synthesis of astaxanthin esters, independent of the formation of cysts, highly correlates with the synthesis of fatty acids in *Haematococcus pluvialis*. *Sci. China C Life Sci.* **2008**, *51*, 1094–1100, doi:10.1007/s11427-008-0141-6.
352. Piccaglia, R.; Marotti, M.; Grandi, S. Lutein and lutein ester content in different types of *Tagetes patula* and *T. erecta*. *Ind. Crops Prod.* **1998**, *8*, 45–51, doi:10.1016/S0926-6690(97)10005-X.
353. Unlu, N.Z.; Bohn, T.; Francis, D.M.; Nagaraja, H.N.; Clinton, S.K.; Schwartz, S.J. Lycopene from heat-induced *cis*-isomer-rich tomato sauce is more bioavailable than from all-*trans*-rich tomato sauce in human subjects. *Br. J. Nutr.* **2007**, *98*, 140–146, doi:10.1017/S0007114507685201.
354. Müller, L.; Goupy, P.; Fröhlich, K.; Dangles, O.; Caris-Veyrat, C.; Böhm, V. Comparative study on antioxidant activity of lycopene (*Z*)-isomers in different assays. *J. Agric. Food Chem.* **2011**, *59*, 4504–4511, doi:10.1021/jf1045969.
355. Honda, M.; Nakayama, Y.; Nishikawa, S.; Tsuda, T. *Z*-Isomers of lycopene exhibit greater liver accumulation than the all-*E*-isomer in mice. *Biosci. Biotechnol. Biochem.* **2020**, *84*, 428–431, doi:10.1080/09168451.2019.1677144.
356. Etoh, H.; Suhara, M.; Tokuyama, S.; Kato, H.; Nakahigashi, R.; Maejima, Y.; Ishikura, M.; Terada, Y.; Maoka, T. Auto-oxidation products of astaxanthin. *J. Oleo Sci.* **2012**, *61*, 17–21, doi:10.5650/jos.61.17.
357. Henry, L.K.; Puspitasari-Nienaber, N.L.; Jarén-Galán, M.; van Breemen, R.B.; Catignani, G.L.; Schwartz, S.J. Effects of ozone and oxygen on the degradation of carotenoids in an aqueous model system. *J. Agric. Food Chem.* **2000**, *48*, 5008–5013, doi:10.1021/jf000503o.
358. Riley, J.C. Estimates of regional and global life expectancy, 1800–2001. *Popul. Dev. Rev.* **2005**, *31*, 537–543, doi:10.1111/j.1728-4457.2005.00083.x.
359. World Health Organization. *World Health Statistics 2022: monitoring health for the SDGs, sustainable development goals*, Geneva, 2022.
360. Steine, G.; Alfnes, F.; Rørå, M.B. The effect of color on consumer WTP for farmed salmon. *Mar. Resour. Econ.* **2005**, *20*, 211–219, doi:10.1086/mre.20.2.42629470.
361. Stevens, G.A.; Bennett, J.E.; Hennocq, Q.; Lu, Y.; De-Regil, L.M.; Rogers, L.; Danaei, G.; Li, G.; White, R.A.; Flaxman, S.R.; et al. Trends and mortality effects of vitamin A deficiency in children in 138 low-income and middle-



## References

- income countries between 1991 and 2013: a pooled analysis of population-based surveys. *Lancet Glob. Health* **2015**, *3*, e528–36, doi:10.1016/S2214-109X(15)00039-X.
362. McCann, D.; Barrett, A.; Cooper, A.; Crumpler, D.; Dalen, L.; Grimshaw, K.; Kitchin, E.; Lok, K.; Porteous, L.; Prince, E.; et al. Food additives and hyperactive behaviour in 3-year-old and 8/9-year-old children in the community: a randomised, double-blinded, placebo-controlled trial. *Lancet* **2007**, *370*, 1560–1567, doi:10.1016/S0140-6736(07)61306-3.
363. Park, M.; Park, H.R.; Kim, S.J.; Kim, M.-S.; Kong, K.H.; Kim, H.S.; Gong, E.J.; Kim, M.E.; Kim, H.S.; Lee, B.M.; et al. Risk assessment for the combinational effects of food color additives: neural progenitor cells and hippocampal neurogenesis. *J. Toxicol. Environ. Health A* **2009**, *72*, 1412–1423, doi:10.1080/15287390903212816.
364. Elhkim, M.O.; Héraud, F.; Bemrah, N.; Gauchard, F.; Lorino, T.; Lambré, C.; Frémy, J.M.; Poul, J.-M. New considerations regarding the risk assessment on Tartrazine An update toxicological assessment, intolerance reactions and maximum theoretical daily intake in France. *Regul. Toxicol. Pharmacol.* **2007**, *47*, 308–316, doi:10.1016/j.yrtph.2006.11.004.
365. Kwon, Y.H.; Banskota, S.; Wang, H.; Rossi, L.; Grondin, J.A.; Syed, S.A.; Yousefi, Y.; Schertzer, J.D.; Morrison, K.M.; Wade, M.G.; et al. Chronic exposure to synthetic food colorant Allura Red AC promotes susceptibility to experimental colitis via intestinal serotonin in mice. *Nat. Commun.* **2022**, *13*, 7617, doi:10.1038/s41467-022-35309-y.
366. European Commission. Commission Regulation (EU) 2022/63 of 14 Januar 2022 amending Annexes II and III to Regulation (EC) No 1333/2008 of the European Parliament and of the Council as regards the food additive titanium dioxide (E 171). *Official Journal of the European Union* **2022**, *L 11/1*.
367. Locey, K.J.; Lennon, J.T. Scaling laws predict global microbial diversity. *Proc. Natl. Acad. Sci. USA* **2016**, *113*, 5970–5975, doi:10.1073/pnas.1521291113.
368. Martiny, A.C. High proportions of bacteria are culturable across major biomes. *ISME J* **2019**, *13*, 2125–2128, doi:10.1038/s41396-019-0410-3.
369. Steen, A.D.; Crits-Christoph, A.; Carini, P.; DeAngelis, K.M.; Fierer, N.; Lloyd, K.G.; Cameron Thrash, J. High proportions of bacteria and archaea across most biomes remain uncultured. *ISME J* **2019**, *13*, 3126–3130, doi:10.1038/s41396-019-0484-y.
370. Kulikov, E.A.; Kulikova, I.S.; Vasilov, R.G.; Selishcheva, A.A. The effect of the solvent nature and lighting on isomerization and oxidative degradation of astaxanthin. *BIOPHYSICS* **2020**, *65*, 433–442, doi:10.1134/S0006350920030112.
371. Honda, M.; Sowa, T.; Kawashima, Y. Thermal- and photo-induced isomerization of all-*E*- and *Z*-isomer-rich xanthophylls: astaxanthin and its structurally-related xanthophylls, adonirubin, and adonixanthin. *Eur. J. Lipid Sci. Technol.* **2020**, *122*, 1900462, doi:10.1002/ejlt.201900462.
372. Honda, M.; Takahashi, N.; Kuwa, T.; Takehara, M.; Inoue, Y.; Kumagai, T. Spectral characterisation of *Z*-isomers of lycopene formed during heat treatment and solvent effects on the *E/Z* isomerisation process. *Food Chem.* **2015**, *171*, 323–329, doi:10.1016/j.foodchem.2014.09.004.
373. Aman, R.; Schieber, A.; Carle, R. Effects of heating and illumination on *trans-cis* isomerization and degradation of  $\beta$ -carotene and lutein in isolated spinach chloroplasts. *J. Agric. Food Chem.* **2005**, *53*, 9512–9518, doi:10.1021/jf050926w.
374. Küpper, H.; Seibert, S.; Parameswaran, A. Fast, sensitive, and inexpensive alternative to analytical pigment HPLC: quantification of chlorophylls and carotenoids in crude extracts by fitting with Gauss peak spectra. *Anal. Chem.* **2007**, *79*, 7611–7627, doi:10.1021/ac070236m.
375. Thrane, J.-E.; Kyle, M.; Striebel, M.; Haande, S.; Grung, M.; Rohrlack, T.; Andersen, T. Spectrophotometric analysis of pigments: a critical assessment of a high-throughput method for analysis of algal pigment mixtures by spectral deconvolution. *PLoS One* **2015**, *10*, e0137645, doi:10.1371/journal.pone.0137645.
376. Wang, C.; Armstrong, D.W.; Chang, C.-D. Rapid baseline separation of enantiomers and a mesoform of all-*trans*-astaxanthin, 13-*cis*-astaxanthin, adonirubin, and adonixanthin in standards and commercial supplements. *J. Chromatogr. A* **2008**, *1194*, 172–177, doi:10.1016/j.chroma.2008.04.063.
377. Miao, F.; Geng, Y.; Lu, D.; Zuo, J.; Li, Y. Stability and changes in astaxanthin ester composition from *Haematococcus pluvialis* during storage. *Chin. J. Ocean. Limnol.* **2013**, *31*, 1181–1189, doi:10.1007/s00343-013-2105-3.
378. Silva, A.F.R.; Abreu, H.; Silva, A.M.S.; Cardoso, S.M. Effect of oven-drying on the recovery of valuable compounds from *Ulva rigida*, *Gracilaria* sp. and *Fucus vesiculosus*. *Mar. Drugs* **2019**, *17*, 90, doi:10.3390/md17020090.
379. Hosseinizand, H.; Lim, C.J.; Webb, E.; Sokhansanj, S. Economic analysis of drying microalgae *Chlorella* in a conveyor belt dryer with recycled heat from a power plant. *Appl. Therm. Eng.* **2017**, *124*, 525–532, doi:10.1016/j.applthermaleng.2017.06.047.
380. Silva, J.P.S.; Veloso, C.R.R.; Souza Barrozo, M.A. de; Vieira, L.G.M. Indirect solar drying of *Spirulina platensis* and the effect of operating conditions on product quality. *Algal Res.* **2021**, *60*, 102521, doi:10.1016/j.algal.2021.102521.



381. Schmid, B.; Navalho, S.; Schulze, P.S.C.; van de Walle, S.; van Royen, G.; Schüler, L.M.; Maia, I.B.; Bastos, C.R.V.; Baune, M.-C.; Januschewski, E.; et al. Drying microalgae using an industrial solar dryer: a biomass quality assessment. *Foods* **2022**, *11*, 1873, doi:10.3390/foods11131873.
382. Rezvani, Z.; Mortezaipoor, H.; Ameri, M.; Akhavan, H.-R.; Arslan, S. Drying of *Spirulina* with a continuous infrared-assisted refractance window™ dryer equipped with a photovoltaic-thermal solar collector. *Heat Mass Transfer* **2022**, *58*, 1739–1755, doi:10.1007/s00231-022-03210-5.
383. Toygar, E.M.; Bayram, T.; Daş, O.; Demir, A. The design and development of solar flat mirror (Solarux) system. *Renewable Sustainable Energy Rev.* **2016**, *54*, 1278–1284, doi:10.1016/j.rser.2015.10.085.
384. Greenwell, H.C.; Laurens, L.M.L.; Shields, R.J.; Lovitt, R.W.; Flynn, K.J. Placing microalgae on the biofuels priority list: a review of the technological challenges. *J. R. Soc. Interface* **2010**, *7*, 703–726, doi:10.1098/rsif.2009.0322.
385. Ramsey, E.; Sun, Q.; Zhang, Z.; Zhang, C.; Gou, W. Mini-review: green sustainable processes using supercritical fluid carbon dioxide. *J. Environ. Sci.* **2009**, *21*, 720–726, doi:10.1016/S1001-0742(08)62330-X.
386. Hämäläinen, H.; Ruusunen, M. Identification of a supercritical fluid extraction process for modelling the energy consumption. *Energy* **2022**, *252*, 124033, doi:10.1016/j.energy.2022.124033.
387. Kang, C.D.; Sim, S.J. Direct extraction of astaxanthin from *Haematococcus* culture using vegetable oils. *Biotechnol. Lett.* **2008**, *30*, 441–444, doi:10.1007/s10529-007-9578-0.
388. European Commission. Consultation request for the determination of the novel food status ARTICLE 4 of Regulation (EU) 2015/2283 **2022**.
389. European Commission. EU Novel food catalogue. Available online: [https://webgate.ec.europa.eu/fip/novel\\_food\\_catalogue/](https://webgate.ec.europa.eu/fip/novel_food_catalogue/) (accessed on 28 April 2023).
390. Ruiz, J.; Olivieri, G.; Vree, J. de; Bosma, R.; Willems, P.; Reith, J.H.; Eppink, M.H.M.; Kleinegris, D.M.M.; Wijffels, R.H.; Barbosa, M.J. Towards industrial products from microalgae. *Energy Environ. Sci.* **2016**, *9*, 3036–3043, doi:10.1039/c6ee01493c.
391. Furlan, V.J.M.; Batista, I.; Bandarra, N.; Mendes, R.; Cardoso, C. Conditions for the production of carotenoids by *Thraustochytrium* sp. ATCC 26185 and *Aurantiochytrium* sp. ATCC PRA-276. *J. Aquat. Food Prod. Technol.* **2019**, *28*, 465–477, doi:10.1080/10498850.2019.1603175.
392. Bahnweg, G. Studies on the physiology of Thraustochytriales I. Growth requirements and nitrogen nutrition of *Thraustochytrium* sp., *Japonochytrium* sp., *Ulkenia* spp., and *Labyrinthuloides* spp. *Veröff. Inst. Meeresforsch. Bremerh.* **1979**, 245–268.
393. Kalidasan, K.; Vinithkumar, N.V.; Peter, D.M.; Dharani, G.; Dufossé, L. Thraustochytrids of mangrove habitats from Andaman Islands: species diversity, PUFA profiles and biotechnological potential. *Mar. Drugs* **2021**, *19*, 571, doi:10.3390/md19100571.
394. Goldstein, S. Studies of a new species of *Thraustochytrium* that displays light stimulated growth. *Mycologia* **1963**, *55*, 799–811, doi:10.1080/00275514.1963.12018072.
395. Xiao, R.; Li, X.; Leonard, E.; Tharayil, N.; Zheng, Y. Investigation on the effects of cultivation conditions, fed-batch operation, and enzymatic hydrolysate of corn stover on the astaxanthin production by *Thraustochytrium striatum*. *Algal Res.* **2019**, *39*, 101475, doi:10.1016/j.algal.2019.101475.
396. Liang, L.; Zheng, X.; Fan, W.; Chen, D.; Huang, Z.; Peng, J.; Zhu, J.; Tang, W.; Chen, Y.; Xue, T. Genome and transcriptome analyses provide insight into the omega-3 long-chain polyunsaturated fatty acids biosynthesis of *Schizochytrium limacinum* SR21. *Front. Microbiol.* **2020**, *11*, 687, doi:10.3389/fmicb.2020.00687.
397. Bi, Z.-Q.; Ren, L.-J.; Hu, X.-C.; Sun, X.-M.; Zhu, S.-Y.; Ji, X.-J.; Huang, H. Transcriptome and gene expression analysis of docosahexaenoic acid producer *Schizochytrium* sp. under different oxygen supply conditions. *Biotechnol. Biofuels* **2018**, *11*, 249, doi:10.1186/s13068-018-1250-5.
398. Konstantinov, D.K.; Menzorov, A.; Krivenko, O.; Doroshkov, A.V. Isolation and transcriptome analysis of a biotechnologically promising Black Sea protist, *Thraustochytrium aureum* ssp. *strugatskii*. *PeerJ* **2022**, *10*, e12737, doi:10.7717/peerj.12737.
399. Zhu, X.; Li, S.; Liu, L.; Li, S.; Luo, Y.; Lv, C.; Wang, B.; Cheng, C.H.K.; Chen, H.; Yang, X. Genome sequencing and analysis of *Thraustochytriidae* sp. SZU445 provides novel insights into the polyunsaturated fatty acid biosynthesis pathway. *Mar. Drugs* **2020**, *18*, 118, doi:10.3390/md18020118.
400. Song, Z.; Stajich, J.E.; Xie, Y.; Liu, X.; He, Y.; Chen, J.; Hicks, G.R.; Wang, G. Comparative analysis reveals unexpected genome features of newly isolated Thraustochytrids strains: on ecological function and PUFAs biosynthesis. *BMC Genomics* **2018**, *19*, 541, doi:10.1186/s12864-018-4904-6.
401. Leyton, A.; Flores, L.; Shene, C.; Chisti, Y.; Larama, G.; Asenjo, J.A.; Armenta, R.E. Antarctic thraustochytrids as sources of carotenoids and high-value fatty acids. *Mar. Drugs* **2021**, *19*, 386, doi:10.3390/md19070386.
402. Chang, M.; Zhang, T.; Li, L.; Lou, F.; Ma, M.; Liu, R.; Jin, Q.; Wang, X. Choreography of multiple omics reveals the mechanism of lipid turnover in *Schizochytrium* sp. S31. *Algal Res.* **2021**, *54*, 102182, doi:10.1016/j.algal.2021.102182.



## References

403. Ye, J.; Liu, M.; He, M.; Ye, Y.; Huang, J. Illustrating and enhancing the biosynthesis of astaxanthin and docosahexaenoic acid in *Aurantiochytrium* sp. SK4. *Mar. Drugs* **2019**, *17*, 45, doi:10.3390/md17010045.
404. Iwasaka, H.; Koyanagi, R.; Satoh, R.; Nagano, A.; Watanabe, K.; Hisata, K.; Satoh, N.; Aki, T. A possible trifunctional  $\beta$ -carotene synthase gene identified in the draft genome of *Aurantiochytrium* sp. strain KH105. *Genes* **2018**, *9*, 200, doi:10.3390/genes9040200.
405. Rius, M.; Rest, J.S.; Filloramo, G.V.; Novák Vanclová, A.M.G.; Archibald, J.M.; Collier, J.L. Horizontal gene transfer and fusion spread carotenogenesis among diverse heterotrophic protists. *Genome Biol. Evol.* **2023**, *15*, 1–15, doi:10.1093/gbe/evad029.
406. Song, Y.; Zhu, X.; Wang, B.; Ibrar, M.; Hu, Z.; Li, S.; Yang, X. Overexpression of the KAS III-like gene YxwZ3 increases carotenoids production in *Aurantiochytrium* sp. SZU445. *Ind. Crops Prod.* **2022**, *187*, 115435, doi:10.1016/j.indcrop.2022.115435.
407. Paredes, P.; Larama, G.; Flores, L.; Leyton, A.; Ili, C.G.; Asenjo, J.A.; Chisti, Y.; Shene, C. Temperature differentially affects gene expression in Antarctic thaustochytrid *Oblongichytrium* sp. RT2316-13. *Mar. Drugs* **2020**, *18*, 563, doi:10.3390/md18110563.
408. Chauhan, A.S.; Chen, C.-W.; Yadav, H.; Parameswaran, B.; Singhanian, R.R.; Dong, C.-D.; Patel, A.K. Assessment of thaustochytrids potential for carotenoids, terpenoids and polyunsaturated fatty acids biorefinery. *J. Food Sci. Technol.* **2023**, doi:10.1007/s13197-023-05740-0.
409. Cairns, T.C.; Nai, C.; Meyer, V. How a fungus shapes biotechnology: 100 years of *Aspergillus niger* research. *Fungal Biol. Biotechnol.* **2018**, *5*, 13, doi:10.1186/s40694-018-0054-5.
410. Su, Y.; Liu, C.; Fang, H.; Zhang, D. *Bacillus subtilis*: a universal cell factory for industry, agriculture, biomaterials and medicine. *Microb. Cell Fact.* **2020**, *19*, 173, doi:10.1186/s12934-020-01436-8.
411. Williams, A.M.; Liu, Y.; Regner, K.R.; Jotterand, F.; Liu, P.; Liang, M. Artificial intelligence, physiological genomics, and precision medicine. *Physiol. Genomics* **2018**, *50*, 237–243, doi:10.1152/physiolgenomics.00119.2017.
412. GlobalData. *State of the Biopharmaceutical Industry 2023* GDHCHT367, 2022. Available online: <https://www.globaldata.com/store/report/state-of-biopharmaceutical-industry-analysis/> (accessed on 30 April 2023).
413. Holzinger, A.; Keiblinger, K.; Holub, P.; Zatloukal, K.; Müller, H. AI for life: trends in artificial intelligence for biotechnology. *New Biotechnol.* **2023**, *74*, 16–24, doi:10.1016/j.nbt.2023.02.001.
414. La Vega, F.M. de; Chowdhury, S.; Moore, B.; Frise, E.; McCarthy, J.; Hernandez, E.J.; Wong, T.; James, K.; Guidugli, L.; Agrawal, P.B.; et al. Artificial intelligence enables comprehensive genome interpretation and nomination of candidate diagnoses for rare genetic diseases. *Genome Med.* **2021**, *13*, 153, doi:10.1186/s13073-021-00965-0.
415. Ahmed, I.; Jeon, G. Enabling artificial intelligence for genome sequence analysis of COVID-19 and alike viruses. *Interdiscip. Sci. Comput. Life Sci.* **2022**, *14*, 504–519, doi:10.1007/s12539-021-00465-0.
416. Stosch, M. von; Portela, R.M.C.; Varsakelis, C. A roadmap to AI-driven *in silico* process development: bioprocessing 4.0 in practice. *Curr. Opin. Chem. Eng.* **2021**, *33*, 100692, doi:10.1016/j.coche.2021.100692.
417. Chan, H.C.S.; Shan, H.; Dahoun, T.; Vogel, H.; Yuan, S. Advancing drug discovery via artificial intelligence. *Trends Pharmacol. Sci.* **2019**, *40*, 592–604, doi:10.1016/j.tips.2019.06.004.







## Appendix

## Chapter 1: Development and Validation of Reliable Astaxanthin Quantification from Natural Sources

S1 Table. Overview of the astaxanthin content in the various experiments.

	num- ber of trials	all- <i>E</i> -astaxanthin proportion			9 <i>Z</i> -astaxanthin proportion			13 <i>Z</i> -astaxanthin proportion			di- <i>Z</i> -astaxanthin proportion			Total astaxanthin			
		of biomass % w/w	SD <sup>b</sup>	of total Ax <sup>a</sup> %	of biomass % w/w	SD	%	of total Ax %	of biomass % w/w	SD	%	of total Ax %	of biomass % w/w	SD	% of biomass % w/w	SD	
Detection limits and linearity of astaxanthin standards																	
Ax standard in acetone	29	-	-	98.0	0.2	-	2.4	0.2	-	-	0.4	0.09	-	-	0.2	-	
Ax standard in extraction phase	9	-	-	92.8	0.3	-	5.9	0.5	-	-	1.3	0.5	-	-	-	-	
Ax-Mp <sup>c</sup> in extraction phase	8	-	-	93.0	0.7	-	4.9	0.3	-	-	2.1	0.9	-	-	-	-	
Enzymolysis with cholesterol esterase																	
2.0 U	3	3.6	0.05	86.4	0.7	0.2	0.01	4.9	0.2	0.19	0.02	4.5	0.5	0.2	0.01	4.2	0.03
1.5 U	3	3.5	0.06	86.3	0.6	0.2	0.00	5.0	0.1	0.18	0.02	4.4	0.5	0.2	0.01	4.4	0.06
1.0 U	2	3.5	0.01	86.3	0.3	0.2	0.04	5.0	0.3	0.18	0.01	4.4	0.4	0.2	0.01	4.3	0.01
0.5 U	3	3.2	0.1	87.3	0.1	0.2	0.01	4.8	0.2	0.14	0.01	3.9	0.1	0.2	0.01	4.1	0.1
0.1 U	3	1.5	0.5	87.4	0.3	0.08	0.03	4.5	0.2	0.06	0.02	3.6	0.2	0.08	0.02	4.6	0.6
0.05 U	3	0.8	0.3	87.8	0.3	0.04	0.01	4.4	0.1	0.03	0.01	3.6	0.2	0.04	0.01	4.3	0.3
0.5 U and 1.5 h incubation	3	3.4	0.1	88.3	0.2	0.2	0.01	4.3	0.2	0.15	0.01	3.8	0.3	0.1	0.01	3.6	0.1
2.0 U and 1.5 h incubation	3	3.6	0.1	88.3	0.9	0.2	0.01	4.1	0.07	0.17	0.02	4.2	0.5	0.1	0.02	3.5	0.2
Processing of liquid-liquid extracts																	
AX standard in extraction phase	4	-	-	94.9	0.8	-	-	4.5	0.8	-	-	0.7	0.1	-	-	-	-
AX standard, aliquot in acetone	4	-	-	97.1	0.4	-	-	1.5	0.02	-	-	1.1	0.3	-	-	0.3	0.07
AX standard, all in acetone	3	-	-	96.9	0.3	-	-	1.5	0.01	-	-	1.3	0.2	-	-	0.3	0.05
Detection limits and linearity of astaxanthin determination																	
0.04 mg <i>H. pluvialis</i>	3	3.3	0.05	88.2	0.8	0.1	0.002	2.9	0.07	0.2	0.01	5.1	0.2	0.2	0.03	3.8	0.06
0.2 mg <i>H. pluvialis</i>	3	3.7	0.06	89.0	0.6	0.1	0.004	3.0	0.1	0.2	0.02	4.6	0.4	0.1	0.03	3.4	0.7
0.4 mg <i>H. pluvialis</i>	3	3.7	0.01	88.9	0.7	0.1	0.01	2.9	0.3	0.2	0.02	4.4	0.5	0.2	0.01	3.8	0.3
0.8 mg <i>H. pluvialis</i>	3	3.7	0.01	87.9	0.4	0.1	0.002	3.0	0.06	0.2	0.01	5.2	0.3	0.2	0.01	4.9	0.2
1.2 mg <i>H. pluvialis</i>	3	3.7	0.07	86.8	1.9	0.2	0.008	3.5	0.2	0.2	0.05	4.9	1.1	0.2	0.03	4.8	0.6
1.6 mg <i>H. pluvialis</i>	3	3.6	0.03	85.4	1.3	0.1	0.005	3.3	0.05	0.3	0.03	6.3	0.5	0.2	0.04	5.1	0.8
2.0 mg <i>H. pluvialis</i>	3	3.6	0.02	85.7	1.2	0.1	0.002	3.4	0.07	0.3	0.03	6.1	0.6	0.2	0.03	4.8	0.7
3.3 mg <i>H. pluvialis</i>	1	3.2	-	75.7	-	0.3	-	7.1	-	0.3	-	7.7	-	0.4	-	9.4	-
4.0 mg <i>H. pluvialis</i>	1	2.9	-	74.9	-	0.3	-	6.6	-	0.3	-	8.1	-	0.4	-	10.4	-



Precision of astaxanthin determination																				
		5	3.5	0.04	80.4	0.8	0.2	0.01	5.0	0.3	0.3	0.03	6.9	0.6	0.3	0.01	7.7	0.3	4.3	0.04
		4	4.0	0.04	81.3	0.6	0.3	0.02	5.0	0.3	0.4	0.02	7.8	0.4	0.3	0.01	5.9	0.1	4.9	0.06
<i>H. pluvialis</i> liquid cultures																				
	M1	3	3.8	0.2	91.0	0.7	0.1	0.004	3.0	0.05	0.1	0.01	3.4	0.3	0.1	0.01	2.7	0.3	4.2	0.1
	M2	5	2.4	0.1	84.1	2.1	0.1	0.02	4.3	0.7	0.1	0.02	3.9	0.4	0.2	0.03	7.7	0.9	2.8	0.1
	M3	3	2.3	0.04	83.6	0.08	0.1	0.03	5.0	0.2	0.1	0.02	3.8	0.09	0.2	0.03	7.6	0.2	2.8	0.5
	M4	3	0.7	0.04	77.7	1.9	0.03	0.002	3.6	0.3	0.04	0.004	4.2	0.5	0.1	0.008	14.5	1.2	0.9	0.02
Oleoresins																				
	O1	3	5.4	0.4	78.8	1.2	0.4	0.02	5.6	0.04	0.3	0.04	4.9	0.4	0.7	0.05	10.8	1.0	6.9	0.4
	O2	7	1.3	0.03	82.7	1.2	0.08	0.003	5.1	0.2	0.06	0.001	3.7	0.2	0.1	0.02	8.5	1.4	1.6	0.04
	O3	3	3.4	0.3	60.1	1.8	0.7	0.1	13.0	0.4	0.4	0.08	7.2	0.6	1.1	0.2	19.7	0.8	5.7	0.7
Method comparison to photometric astaxanthin extraction																				
	Batch A, day 22	1	1.0	-	88.2	-	0.04	-	3.5	-	0.04	-	3.5	-	0.05	-	4.8	-	1.1	-
	Batch A, day 23	1	1.3	-	88.3	-	0.05	-	3.7	-	0.04	-	3.7	-	0.06	-	4.3	-	1.4	-
	Batch A, day 24	1	1.9	-	87.7	-	0.09	-	4.2	-	0.08	-	3.8	-	0.09	-	4.3	-	2.1	-
	Batch A, day 27	1	2.3	-	88.3	-	0.1	-	4.2	-	0.1	-	3.9	-	0.09	-	3.6	-	2.6	-
	Batch A, day 28	1	2.5	-	88.8	-	0.1	-	3.9	-	0.1	-	3.9	-	0.09	-	3.6	-	2.8	-
	Batch B, day 22	1	1.3	-	87.6	-	0.05	-	3.5	-	0.05	-	3.5	-	0.08	-	5.4	-	1.5	-
	Batch B, day 23	1	1.8	-	87.8	-	0.08	-	3.8	-	0.07	-	3.7	-	0.09	-	4.7	-	2.0	-
	Batch B, day 24	1	1.9	-	87.7	-	0.09	-	4.1	-	0.08	-	3.8	-	0.09	-	4.4	-	2.1	-
	Batch B, day 27	1	2.5	-	88.3	-	0.1	-	3.9	-	0.1	-	3.9	-	0.1	-	4.0	-	2.9	-
	Batch B, day 28	1	2.7	-	88.0	-	0.1	-	4.0	-	0.1	-	3.9	-	0.1	-	4.2	-	3.1	-
Shelf life of lyophilized and undisturbed <i>H. pluvialis</i> biomass partially exposed to ambient atmosphere																				
	0 days at ambient atmosphere	2	0.8	0.2	80.8	0.003	0.04	0.004	3.8	0.4	0.03	0	3.2	0.08	0.1	0	12.3	0.5	1.0	0.01
	7 days at ambient atmosphere	1	0.7	-	80.3	-	0.03	-	4.1	-	0.02	-	2.8	-	0.1	-	12.8	-	0.8	-
	104 days at ambient atmosphere	1	0.4	-	78.9	-	0.02	-	3.9	-	0.01	-	2.5	-	0.08	-	14.8	-	0.5	-
	489 days at ambient atmosphere	1	0.3	-	80.8	-	0.02	-	3.9	-	0.01	-	2.5	-	0.05	-	12.7	-	0.4	-



Dried and disrupted <i>H. pluvialis</i> biomass vacuumed and exposed to ambient atmosphere															
Opened	5	3.5	0.04	80.4	0.8	0.2	0.01	5.0	0.3	0.3	0.03	6.9	0.6	0.3	0.01
Closed	4	4.0	0.04	81.3	0.6	0.3	0.02	5.0	0.3	0.4	0.02	7.8	0.4	0.3	0.01

<sup>a</sup>Ax = Astaxanthin  
<sup>b</sup>SD = Standard deviation  
<sup>c</sup>Ax-Mp = Astaxanthin monopalmitate



## Chapter 2: Optimization of Astaxanthin Recovery in the Downstream Process of *Haematococcus pluvialis*

**Table S1:** Overview of process parameters and results of the conducted experiments for model regression and evaluation in spray-drying.

Run	Input						Output				
	Inlet temperature	Spray flow	Feed rate	Cooling	Biomass conc.	<i>H. pluvialis</i> biomass recovery	Astaxanthin content			Outlet temperature	
							per biomass	recovery			
	(°C)	(NL/h)	(%)	-	(g/L)	(g)	(%)	(% w/w)	SD <sup>a)</sup>	(%)	°C
Before					99.4			1.32	0.03	-	
1	140	500	5	no	99.4	1.2	6.04	1.17	0.04	88.6	99
2	160	500	10	no	99.4	0.56	2.82	1.08	0.07	81.8	98
3	160	600	15	no	99.4	1.03	5.18	1.06	0.05	80.3	80
4	180	400	10	no	99.4	4.6	23.01	1.14	0.07	86.4	112
4.2	180	400	10	no	99.4	4.93	25.1	-			134
5	140	400	5	no	99.4	3.78	19.54	1.21	0.003	91.7	95
6	160	400	5	no	99.4	3.92	19.51	1.1	0.04	83.3	124
7	120	500	5	no	99.4	0.43	2.09	1.1	0.03	83.3	85
8	180	600	10	no	99.4	0.18	0.9	0.91	0.03	68.9	111
9	180	500	10	no	99.4	2.31	12.02	1.15	0.15	87.1	122
10	180	400	5	no	99.4	2.81	14.12	1.16	0.04	87.9	134
11	180	400	15	no	99.4	3.68	18.5	1.22	0.09	92.4	115
12	160	400	10	no	99.4	2.36	11.84	1.22	0.1	92.4	107
13	180	500	15	no	99.4	1.82	9.83	1.15	0.08	87.1	114
14	180	400	10	yes	99.4	4.74	23.41	-		-	123
15	180	400	10	yes	49.7	2.58	24.62	-		-	121
16	180	400	10	yes	198.7	6.13	15.2	-		-	122

<sup>a)</sup>SD = Standard deviation



**Table S2:** Content and proportion of astaxanthin and its diastereomers after various processing steps. Colors indicate comparison of samples.

Process Step	n <sup>b)</sup>	Total astaxanthin			all-E-astaxanthin			9Z-astaxanthin			13Z-astaxanthin			di-Z-astaxanthin		
		Ax/H.p. <sup>b)</sup>	SD <sup>c)</sup>	Sig <sup>d)</sup>	Ax/H.p.	SD	Sig	Ax/H.p.	SD	Sig	Ax/H.p.	SD	Sig	Ax/H.p.	SD	Sig
<b>Analytical scale</b>																
Non-disrupted	6	2.73	0.15	-	2.31	0.09	-	0.12	0.03	-	0.12	0.02	-	0.20	0.04	-
BM <sup>g)</sup> (1x)	10	2.68	0.15	a	2.20	0.14	e	0.13	0.02	e	0.13	0.02	*	0.23	0.03	e
BM (2x)	9	2.62	0.11	-	2.14	0.11	*	0.13	0.01	e	0.13	0.01	*	0.23	0.02	e
BM (3x)	8	2.59	0.11	e	2.13	0.12	a	0.13	0.01	e	0.12	0.01	*	0.22	0.02	e
BM - SD <sup>h)</sup>	9	2.68	0.09	a	2.24	0.08	*	0.12	0.01	*	0.10	0.00	*	0.23	0.01	e
BM - FD <sup>h)</sup>	9	2.52	0.05	e	2.11	0.05	e	0.11	0.01	*	0.12	0.01	e	0.19	0.01	*
BM - SD - SC-CO <sub>2</sub> <sup>h)</sup>	9	2.25	0.11	c	1.87	0.09	*	0.10	0.01	*	0.09	0.00	*	0.20	0.01	*
BM - FD - SC-CO <sub>2</sub>	3	8.33	0.20	*	7.18	0.18	*	0.28	0.02	*	0.28	0.01	*	0.58	0.02	*
BM - VD - SC-CO <sub>2</sub>	3	8.78	0.11	-	7.58	0.08	*	0.29	0.02	*	0.29	0.01	*	0.63	0.04	*
BM - VD - SC-CO <sub>2</sub>	3	6.90	0.16	*	5.91	0.14	*	0.22	0.00	*	0.22	0.01	*	0.54	0.01	*
Non-disrupted	6	2.73	0.15	-	2.31	0.09	-	0.12	0.03	-	0.10	0.02	-	0.20	0.04	-
HPH <sup>k)</sup> (1x)	12	2.76	0.06	e	2.34	0.05	e	0.12	0.01	e	0.09	0.01	e	0.21	0.02	e
HPH (2x)	12	2.67	0.14	e	2.26	0.12	e	0.11	0.01	e	0.09	0.01	e	0.21	0.02	e
HPH - SD	9	2.45	0.14	b	2.05	0.12	*	0.11	0.01	e	0.09	0.00	e	0.20	0.01	e
HPH - FD	9	2.64	0.19	a	2.21	0.15	e	0.11	0.02	e	0.13	0.02	*	0.19	0.02	e
HPH - VD	9	2.27	0.25	b	1.90	0.20	*	0.10	0.01	*	0.09	0.01	e	0.18	0.03	*
HPH - SD - SC-CO <sub>2</sub>	4	10.15	0.14	*	8.68	0.17	*	0.38	0.06	*	0.35	0.01	*	0.74	0.03	*
HPH - FD - SC-CO <sub>2</sub>	3	8.83	0.09	*	7.50	0.10	*	0.36	0.04	*	0.30	0.03	*	0.66	0.06	*
HPH - VD - SC-CO <sub>2</sub>	3	7.17	0.08	*	6.11	0.07	*	0.26	0.02	*	0.24	0.01	*	0.56	0.04	*
Non-disrupted	6	2.73	0.15	-	2.31	0.09	-	0.12	0.03	-	0.10	0.02	-	0.20	0.04	-
ND <sup>l)</sup> - SD	9	2.50	0.12	b	2.09	0.08	*	0.12	0.03	e	0.09	0.02	e	0.20	0.05	e
ND - FD	9	2.58	0.18	ab	2.16	0.13	*	0.11	0.02	e	0.12	0.02	e	0.20	0.03	e
ND - VD	9	2.70	0.05	e	2.25	0.05	e	0.11	0.01	e	0.11	0.01	e	0.23	0.01	*
ND - SD - SC-CO <sub>2</sub>	3	3.38	0.07	*	2.96	0.03	*	0.10	0.01	e	0.11	0.01	e	0.21	0.02	e
ND - FD - SC-CO <sub>2</sub>	3	6.73	0.17	*	5.89	0.13	*	0.21	0.03	*	0.21	0.02	*	0.42	0.04	*
ND - VD - SC-CO <sub>2</sub>	3	8.98	0.18	*	7.83	0.07	*	0.28	0.04	*	0.30	0.02	*	0.57	0.05	*
<b>Pilot scale</b>																
Non-disrupted	4	2.15	0.07	a	1.92	0.06	-	0.06	0.00	-	0.06	0.00	-	0.11	0.00	-
BM (1x)	3	2.01	0.04	a	1.78	0.04	*	0.06	0.01	e	0.06	0.00	*	0.11	0.01	e
BM (2x)	3	2.00	0.08	a	1.78	0.08	*	0.06	0.01	e	0.06	0.01	e	0.10	0.01	e
BM (3x)	3	1.88	0.34	e	1.66	0.32	e	0.06	0.00	e	0.05	0.01	*	0.10	0.01	e
BM - SD	3	1.85	0.11	e	1.64	0.09	e	0.05	0.01	e	0.05	0.01	e	0.11	0.02	e



- a) n = Number of measurements  
 b) Ax/H.p. = Proportion of astaxanthin in relation to total *H. pluvialis* biomass (% w/w)  
 c) SD = Standard deviation  
 d) Sig = Indicates significant differences ( $\sigma=0.05$ ) between the sample and its predececcor. All milled and high-pressure homogenized samples are compared to the undisrupted samples. \* means significant difference and e indicates no significant difference. Samples highlighted in the same color were compared. Equal letter indicate no significant difference and unequal letters indicate significant differences.  
 e) Prop. = Proportion of astaxanthin isomers in relation to total astaxanthin (% w/w)  
 f) BM = Bead-milling  
 g) SD = Spray-drying  
 h) FD = Freeze-drying  
 i) VD = Vacuum-drying  
 j) SC-CO<sub>2</sub> = Supercritical CO<sub>2</sub> extraction  
 k) HPH = High-pressure homogenization  
 l) ND = No disruption

**Table S3:** Estimated model coefficients, p-values and optimized parameters regarding maximal astaxanthin yield in spray-drying. Significant p-values ( $\sigma=0.05$ ) are highlighted bold.

	Linear model		Quadratic model		Quadratic model + interactions	
	coefficient	p-value	coefficient	p-value	coefficient	p-value
a (Intercept)	1.8038		-0.1508		0.9095	
b <sub>1</sub> (Spray <sup>a</sup> )	-0.001	<b>0.0011</b>	0.0046	0.2196	0.004	0.5303
b <sub>2</sub> (Feed <sup>b</sup> )	0.0096	0.0848	-0.0123	0.6699	0.0797	0.749
b <sub>3</sub> (Temp <sup>c</sup> )	-0.0017	0.1054	0.0065	0.6521	-0.0094	0.8376
b <sub>11</sub> (Spray <sup>2</sup> )			0	0.1453	0	0.3004
b <sub>22</sub> (Feed <sup>2</sup> )			0.0011	0.4536	0.0021	0.5842
b <sub>33</sub> (Temp <sup>2</sup> )			0	0.6002	0	0.8778
b <sub>12</sub> (Spray*Feed)					0	0.8265
b <sub>13</sub> (Spray*Temp)					0	0.747
b <sub>23</sub> (Feed*Temp)					-0.0005	0.6942
R <sup>2</sup>	0.7151		0.8122		0.8244	
R <sup>2</sup> adjusted	0.6201		0.6244		0.2975	
<b>Optimized parameters</b>						
Feed	15		15		15	
Spray	400		400		400	
Temp	120		136.88		120	

<sup>a</sup>Spray = Spray gas flow (NL/h)

<sup>b</sup>Feed = Product feed rate (%)

<sup>c</sup>Temp = Inlet Temperature (°C)



**Chapter 3: Screening of a Thraustochytrid Strain Collection for Carotenoid and Squalene Production**  
 Characterized by Cluster Analysis, Comparison of 18S rRNA Gene Sequences, Growth Behavior, and Morphology

**Table S1.** Assignment of the investigated strains based on sequence similarity to strains in the NCBI database on the basis of their 18S rRNA gene data. The corresponding strains with the highest score are shown.

strain information			BLAST parameters						
strain	strain assignment	GenBank accession	next relative in BLAST	max score	total score	query cover	E value	per. ident	acc. len
154f	<i>Thraustochytrium aggregatum</i>	OQ514291	<i>Thraustochytrium aggregatum</i>	1716	2751	92%	0	98.15%	1681
N557a	<i>Schizochytrium aggregatum</i>	OQ514292	<i>Schizochytrium</i> sp. BAFCCult 3502	2693	2693	99%	0	98.55%	1715
N561b	<i>Schizochytrium aggregatum</i>	OQ514293	<i>Schizochytrium</i> sp. BAFCCult 3502	2643	2643	100%	0	98.85%	1715
561bx	<i>Schizochytrium aggregatum</i>	OQ514294	<i>Schizochytrium</i> sp. BAFCCult 3502	2745	2745	99%	0	99.27%	1715
N1001	<i>Ulkenia visurgensis</i>	OQ514295	<i>Thraustochytrium</i> aff. <i>aureum</i> BAFCCult 3543	3201	3201	96%	0	99.66%	1750
N1438e	<i>Thraustochytrium kinnei</i>	OQ514296	<i>Thraustochytrium kinnei</i>	3251	3251	100%	0	99.66%	1796
1450d	<i>Thraustochytrium kinnei</i>	OQ514297	<i>Thraustochytrium kinnei</i>	3068	3068	100%	0	99.52%	1796
1462d	<i>Thraustochytrium kinnei</i>	OQ514298	<i>Thraustochytrium kinnei</i>	3099	3099	99%	0	98.23%	1796
1465d	<i>Thraustochytrium kinnei</i>	OQ514299	<i>Thraustochytrium kinnei</i>	3136	3136	99%	0	98.80%	1796
1471d	<i>Thraustochytrium kinnei</i>	OQ514300	<i>Thraustochytrium kinnei</i>	3127	3127	99%	0	98.69%	1796
1471f	<i>Thraustochytrium kinnei</i>	OQ514301	<i>Thraustochytrium kinnei</i>	3169	3169	99%	0	98.87%	1796
1472e	<i>Thraustochytrium kinnei</i>	OQ514302	<i>Thraustochytrium kinnei</i>	3116	3116	99%	0	98.57%	1796
1473e	<i>Thraustochytrium kinnei</i>	OQ514303	<i>Thraustochytrium kinnei</i>	3140	3140	99%	0	98.91%	1796
1476b	<i>Thraustochytrium kinnei</i>	OQ514304	<i>Thraustochytrium kinnei</i>	3153	3153	99%	0	98.75%	1796
N1476c	<i>Thraustochytrium kinnei</i>	OQ514305	<i>Thraustochytrium kinnei</i>	2820	2820	99%	0	98.54%	1796
1485a	<i>Thraustochytrium kinnei</i>	OQ514306	<i>Thraustochytrium kinnei</i>	3304	3304	99%	0	99.67%	1821
1518e	<i>Thraustochytrium kinnei</i>	OQ514307	<i>Thraustochytrium kinnei</i>	3299	3299	99%	0	99.61%	1821
1526d	<i>Thraustochytrium kinnei</i>	OQ514308	<i>Thraustochytrium kinnei</i>	3265	3265	99%	0	99.66%	1796
1527a	<i>Thraustochytrium kinnei</i>	OQ514309	<i>Thraustochytrium kinnei</i>	3225	3225	99%	0	99.66%	1796
1527c	<i>Thraustochytrium kinnei</i>	OQ514310	<i>Thraustochytrium kinnei</i>	3282	3282	99%	0	99.67%	1796
1531c	<i>Thraustochytrium kinnei</i>	OQ514311	<i>Thraustochytrium kinnei</i>	3236	3236	99%	0	99.66%	1796
N1694d	<i>Thraustochytrium kinnei</i>	L34668.1	<i>Thraustochytrium kinnei</i>	3169	3169	99%	0	99.83%	1796
N1709d	<i>Thraustochytrium kinnei</i>	OQ514312	<i>Thraustochytrium kinnei</i>	3297	3297	99%	0	99.56%	1821
N2820a	<i>Schizochytrium aggregatum</i>	OQ514313	<i>Schizochytrium</i> sp. BAFCCult 3502	2789	2789	99%	0	98.97%	1715
N2845c	<i>Thraustochytrium kinnei</i>	OQ514314	<i>Thraustochytrium kinnei</i>	3079	3079	99%	0	98.06%	1796
3041c	<i>Thraustochytrium kinnei</i>	OQ514315	<i>Thraustochytrium kinnei</i>	3005	3005	100%	0	98.58%	1796
N4930a	<i>Thraustochytrium aggregatum</i>	OQ514316	<i>Thraustochytrium aggregatum</i>	1709	2572	94%	0	97.94%	1681
N4930b	<i>Thraustochytrium aggregatum</i>	OQ514317	<i>Thraustochytrium aggregatum</i>	1679	2525	85%	0	97.12%	1681
4992b	<i>Thraustochytrium aggregatum</i>	OQ514318	<i>Thraustochytrium aggregatum</i>	1742	2687	92%	0	98.97%	1681
N4994b	<i>Thraustochytriidae</i> sp.	OQ514319	<i>Thraustochytriidae</i> sp. SEK 690	3234	3234	98%	0	99.94%	1754
N4994d	<i>Thraustochytriidae</i> sp.	OQ514320	<i>Thraustochytriidae</i> sp. SEK 690	3216	3216	99%	0	99.89%	1754



N495d	<i>Thraustochytriidae</i> sp.	QQ514321	<i>Thraustochytriidae</i> sp. SEK 690	3107	3107	100%	0	99.88%	1754	AB973545.1
N5589c	<i>Ulkenia visurgensis</i>	QQ514322	<i>Ulkenia visurgensis</i>	3299	3299	99%	0	99.61%	1812	AB022116.1
N5594d	<i>Ulkenia visurgensis</i>	QQ514323	<i>Ulkenia visurgensis</i>	3301	3301	99%	0	99.67%	1812	AB022116.1
N5629e	<i>Ulkenia profunda</i>	QQ514324	<i>Ulkenia profunda</i>	3003	3003	99%	0	97.61%	1762	DQ023615.1
N5658a	<i>Ulkenia profunda</i>	QQ514325	<i>Ulkenia profunda</i>	2811	2811	100%	0	96.65%	1762	DQ023615.1
N5661	<i>Ulkenia profunda</i>	QQ514326	<i>Ulkenia profunda</i>	3249	3249	99%	0	99.11%	1815	L34054.1
N5670c	<i>Thraustochytriidae</i> sp.	QQ514327	<i>Thraustochytriidae</i> sp. SEK 690	3234	3234	98%	0	99.94%	1754	AB973545.1
N5676f	<i>Ulkenia profunda</i>	QQ514328	<i>Ulkenia profunda</i>	3127	3127	100%	0	99.02%	1762	DQ023615.1
N5905	<i>Ulkenia profunda</i>	QQ514329	<i>Ulkenia profunda</i>	3184	3184	99%	0	99.21%	1762	DQ023615.1
N5976	<i>Ulkenia profunda</i>	QQ514330	<i>Ulkenia profunda</i>	3158	3158	99%	0	99.09%	1762	DQ023615.1
5985	<i>Thraustochytrium aureum</i>	QQ514331	<i>Thraustochytrium aureum</i>	1620	1620	99%	0	99.33%	1630	KT598546.1
N5995	<i>Oblongichytrium minutum</i>	QQ514332	<i>Schizochytrium minutum</i>	3195	3195	99%	0	99.77%	1794	AB022108.1
5996	<i>Oblongichytrium minutum</i>	QQ514333	<i>Schizochytrium minutum</i>	3105	3105	100%	0	99.76%	1794	AB022108.1
N5997	<i>Thraustochytrium striatum</i>	QQ514334	<i>Thraustochytrium</i> sp. Yonez6-8	3051	3051	99%	0	99.23%	1767	AB810969.1
N5998	<i>Thraustochytrium aureum</i>	QQ514335	<i>Thraustochytrium aureum</i>	3166	3166	100%	0	99.65%	1807	AB022110.1
5999	<i>Schizochytrium aggregatum</i>	QQ514336	<i>Schizochytrium</i> sp. BAFCCult 3502	2612	2612	100%	0	98.63%	1715	HQ228969.1
N6000b	<i>Ulkenia visurgensis</i>	QQ514337	<i>Thraustochytrium</i> aff. <i>aureum</i> BAFCCult 3543	3193	3193	98%	0	99.66%	1750	HQ228981.1
N6001b	<i>Thraustochytrium aureum</i>	QQ514338	<i>Thraustochytrium roseum</i>	3105	3105	100%	0	99.94%	1749	AB973566.1
N6002a	<i>Thraustochytrium aureum</i>	QQ514339	<i>Thraustochytrium aureum</i>	3290	3290	99%	0	99.56%	1807	AB022110.1
N6005a	<i>Thraustochytrium aureum</i>	QQ514340	<i>Thraustochytrium aureum</i>	3291	3291	99%	0	99.56%	1807	AB022110.1
N6006d	<i>Thraustochytrium aureum</i>	QQ514341	<i>Thraustochytrium aureum</i>	3265	3265	100%	0	99.66%	1807	AB022110.1
N6006e	<i>Thraustochytrium aureum</i>	QQ514342	<i>Thraustochytrium aureum</i>	3038	3038	99%	0	98.60%	1807	AB022110.1
N6007e	<i>Thraustochytrium aureum</i>	QQ514343	<i>Thraustochytrium aureum</i>	3265	3265	100%	0	99.78%	1807	AB022110.1
N6421	<i>Paranamyces uniporus</i>	QQ514345	uncultured <i>Rhizophydiales</i>	2730	2730	99%	0	96.18%	4481	OL869115.1
N6422	<i>Paranamyces uniporus</i>	QQ514346	<i>Paranamyces uniporus</i>	2870	2870	98%	0	96.04%	4569	MT731025.1
N6423	<i>Paranamyces uniporus</i>	QQ514347	<i>Paranamyces uniporus</i>	2789	2789	97%	0	96.45%	4569	MT731025.1
N6424	<i>Paranamyces uniporus</i>	QQ514348	<i>Paranamyces uniporus</i>	2870	2870	98%	0	96.04%	4569	MT731025.1
N6523	<i>Paranamyces uniporus</i>	QQ514349	<i>Paranamyces uniporus</i>	2870	2870	98%	0	96.04%	4569	MT731025.1
Sakar7	<i>Ulkenia visurgensis</i>	QQ514344	<i>Thraustochytrium</i> aff. <i>aureum</i> BAFCCult 3543	3201	3201	96%	0	99.66%	1750	HQ228981.1



**Table S2.** Coefficients of determination and p-values of model 1-3 for the regression of growth data.

	Strain											
	<i>Ulkenia visurgensis</i>			<i>U. profunda</i>		<i>Thraustochytriidae</i> sp.			<i>T. striatum</i>	<i>Thraustochytrium aureum</i>		
	Sakar7	N6000b	N5589c	N5594d	N5658a	N4994d	N4995d	N5670c	N5997	N6007e	N6006d	N5998
Model 1	R <sup>2</sup>	0.9611	0.9471	0.8515	0.9719	0.7791	0.9091	0.9126	0.7475	0.7535	0.8045	0.4640
	R <sup>2</sup> adjusted	0.9092	0.8765	0.6533	0.9344	0.3371	0.7635	0.7961	0.4107	0.3592	0.5438	-0.2506
	p-value	0.0011	0.0026	0.0462	0.0004	0.3061	0.0295	0.0002	0.0109	0.1735	0.2465	0.0935
Model 2	R <sup>2</sup>	0.9444	0.9171	0.9093	0.9322	0.8231	0.9761	0.9626	0.6942	0.9051	0.9140	0.5546
	R <sup>2</sup> adjusted	0.8888	0.8341	0.8199	0.8643	0.5754	0.9482	0.9253	0.3885	0.7944	0.8281	0.1093
	p-value	0.0007	0.0026	0.0034	0.0013	0.1024	0.0002	0.0002	0.0011	0.1508	0.0103	0.3898
Model 3	R <sup>2</sup>	0.9536	0.9627	0.9497	0.9841	0.9571	0.9981	0.9800	0.9252	0.9324	0.9348	0.9637
	R <sup>2</sup> adjusted	0.7834	0.8257	0.7651	0.9256	0.4846	0.9879	0.9065	0.6511	0.5604	0.6959	0.8251
	p-value	0.0913	0.0675	0.1019	0.0199	0.5031	0.0102	0.0005	0.0278	0.1726	0.3196	0.1442

	Strain											
	<i>Schizochytrium aggregatum</i>			<i>Thraustochytrium kinnei</i>			<i>T. aggregatum</i>			<i>O. minutum</i>		
	5999	N2820a	561bx	N1709d	N1694d	N1476c	1465d	1462d	3041c	4992b	154f	N5995
Model 1	R <sup>2</sup>	0.6964	0.8407	0.8247	0.9263	0.8848	0.9532	0.8851	0.6529	0.8885	0.9080	0.7846
	R <sup>2</sup> adjusted	0.2916	0.6282	0.5441	0.7788	0.7312	0.8595	0.7319	0.1900	0.7399	0.7241	-0.2044
	p-value	0.2624	0.0554	0.1251	0.0468	0.0234	0.0211	0.0200	0.0232	0.3472	0.0213	0.0701
Model 2	R <sup>2</sup>	0.7117	0.7652	0.6763	0.9201	0.9833	0.8790	0.8881	0.7125	0.8867	0.9237	0.8023
	R <sup>2</sup> adjusted	0.4234	0.5303	0.2986	0.8081	0.9667	0.7580	-0.4227	0.4250	0.7734	0.8170	0.6046
	p-value	0.1280	0.0709	0.2475	0.017	<0.0001	0.0090	0.8103	0.0070	0.1271	0.0072	0.0423
Model 3	R <sup>2</sup>	0.9810	0.8727	0.9997	0.9936	0.9986	0.9791	0.9972	0.9925	0.9698	0.9970	0.8946
	R <sup>2</sup> adjusted	0.9113	0.4059	0.9983	0.9228	0.9933	0.9023	0.9669	0.9652	0.8689	0.9644	0.5084
	p-value	0.0257	0.3322	0.0015	0.2055	0.0006	0.0296	0.1354	0.0168	0.0065	0.0501	0.2655



**Table S3.** Estimated model coefficients, p-values, and optimized parameters of model 2 for all analyzed strains regarding maximal biomass yield. Significant p-values are indicated with \*\* ( $\sigma = 0.01$ ) and \* ( $\sigma = 0.05$ ). The variance of the yield is given for a 0.95 confidence interval. Discussed strains are highlighted bold. Dry weight was approximated using data from the other trials.

	<b>Sakar7</b>			<i>Ulkaria visurgensis</i>			<i>Ulkaria profunda</i>			<i>Thraustochytridae</i> sp.			<i>T. striatum</i>		
	coefficient	p-value		N6000b	N5589c	N5594d	N5655a	N4994d	N4995d	N5570c			coefficient	p-value	
a (intercept)	21.27			60.29	169.61	66.79	116.00	188.4	93.6	203.85			976.49		
b1 (Glucose)	1.13	0.0720		2.07	0.3353	-0.01	1.99	0.5893	3.2	0.2093	0.24	0.0757	25.93	0.0620	
b2 (Yeast extract)	-1.39	0.0001**		14.51	0.009**	-4.39	6.52	0.1112	32.9	0.0005**	8.73	0.0003**	12.08	0.2435	
b3 (pH)	-0.80	0.9426		-7.02	0.6240	-17.41	0.1173	0.0044**	-12.7	0.1512	-26.31	0.1512	-160.97	0.5680	
b4 (Phosphate)	27.40	0.2651		-38.66	0.2238	-13.43	56.52	0.4316	-80.0	0.1011	-37.74	0.3106	1041.81	0.1093	
c1 (Glucose <sup>2</sup> )	-0.02	0.2029		-0.03	0.1151	0.01	0.2817	0.01	0.1807	0.0558	-0.01	0.6775	-0.26	0.3974	
c2 (Yeast extract <sup>2</sup> )	0.39	0.0660		-0.66	0.0244*	0.46	-0.33	0.2772	-0.2	0.0025**	-0.29	0.3289	-1.81	0.6994	
d12 (Glucose*Yeast)	0.02	0.4857		-0.04	0.3523	0.03	-0.11	0.0542	0.0	0.9998	0.09	0.0789	-0.21	0.7891	
R <sup>2</sup>	0.9444			0.9171	0.9093	0.9322	0.8231	0.9761	0.9626	0.9353			0.6942		
adj. R <sup>2</sup>	0.8888			0.8341	0.8199	0.8643	0.5754	0.9482	0.9253	0.8706			0.3885		
Pvalue	0.0007			0.0026	0.0034	0.0013	0.1024	0.0002	0.0002	0.0011			0.1508		
<b>Optimized parameters</b>															
Glucose (g/L)	45.6			32.3	60.0	60.0	38.1	60.0	34.3	60.0			50.3		
Yeast extract (g/L)	15.0			10.1	15.0	15.0	3.5	15.0	10.1	15.0			0.5		
pH	6.5			6.5	6.5	6.5	6.5	6.5	6.5	6.5			6.5		
Phosphate addition (g/L)	0.5			0.0	0.5	0.0	0.5	0.0	0.0	0.0			0.0		
Expected growth (g/L)	2.3			2.1	2.8	2.2	1.7	2.8	4.0	3.0			19.2		
Confidence interval (g/L)	0.7			0.5	0.9	0.6	1.0	0.7	0.7	1.1			14.9		

	<b>Schizochytrium aggregatum</b>			<i>Thraustochytrium kinei</i>			<i>Thraustochytrium kinei</i>			<i>Thraustochytrium kinei</i>			<i>Thraustochytrium kinei</i>		
	coefficient	p-value		N2820a	N561bx	N1709d	N1694d	N1476c	N1465d	N1462d			coefficient	p-value	
a (intercept)	166.78			175.10	933.45	49.94	236.51	91.77	-91.763	174.33			74.35		
b1 (Glucose)	-4.18	0.0202*		2.23	-0.33	0.68	0.09	0.95	-0.063	1.79	0.0229*		1.53	0.4096	
b2 (Yeast extract)	19.14	0.3138		5.60	-31.96	5.17	2.91	9.19	11.460	3.58	0.0075**		9.57	0.2983	
b3 (pH)	-22.66	0.8097		-20.66	0.5088	-7.88	-28.88	-13.76	13.293	-24.22	0.2024		-10.55	0.5640	
b4 (Phosphate)	110.48	0.5823		3.64	0.968	7.50	-66.23	4.16	-19.513	22.53	0.5556		-6.62	0.8625	
c1 (Glucose <sup>2</sup> )	0.09	0.3611		-0.01	0.7645	-0.01	-0.01	-0.01	0.8933	-0.03	0.2079		-0.02	0.3201	
c2 (Yeast extract <sup>2</sup> )	-1.47	0.3653		-0.35	0.6476	-0.25	-0.10	-0.46	0.0912	-0.08	0.7864		-0.39	0.2211	
d12 (Glucose*Yeast)	0.34	0.2238		0.07	0.5682	0.01	0.16	0.03	-0.080	0.06	0.2384		-0.07	0.1720	
R <sup>2</sup>	0.7117			0.7652	0.6763	0.9201	0.9833	0.8790	0.4072	0.8881			0.7125		
adj. R <sup>2</sup>	0.4234			0.5303	0.2986	0.8081	0.9667	0.7580	-0.4227	0.7763			0.4250		
Pvalue	0.1280			0.0709	0.2475	0.017	<0.0001	0.0090	0.8103	0.0070			0.1271		
<b>Optimized parameters</b>															
Glucose (g/L)	60.0			60.0	60.0	55.5	60.0	60.0	0.0	53.6			19.3		
Yeast extract (g/L)	13.3			14.1	15.0	11.7	15.0	11.9	9.9	15.0			10.4		
pH	6.5			6.5	6.5	6.5	6.5	6.5	8.5	6.5			6.5		
Phosphate addition (g/L)	0.5			0.5	0.5	0.5	0.0	0.5	0.0	0.5			0.0		
Expected growth (g/L)	7.4			3.5	10.5	0.9	3.4	1.5	1.4	2.4			1.2		
Confidence interval (g/L)	7.1			3.3	11.4	0.6	0.6	1.0	3.2	1.4			0.6		



	<i>Thraustochytrium aureum</i>				<i>Thraustochytrium aggregatum</i>				<i>Oblongichytrium minutum</i>			
	<b>N6007e</b>		<b>N6006d</b>		<b>5985</b>		<b>4992b</b>		<b>154f</b>		<b>N5995</b>	
	coefficient	p-value	coefficient	p-value	coefficient	p-value	coefficient	p-value	coefficient	p-value	coefficient	p-value
a (intercept)	1028.19		-39.23		1256.05		568.27		-482.96		-336.71	
b1 (Glucose)	-25.19	0.0018**	-0.39	0.0009**	16.95	0.0962	20.41	0.0032**	17.80	0.0478*	3.15	0.0467*
b2 (Yeast extract)	40.91	0.0187*	68.98	0.0137*	12.98	0.9569	38.27	0.1135	50.03	0.0125*	5.84	0.0427*
b3 (pH)	-140.59	0.5951	-6.46	0.9614	28.00	0.7600	-88.41	0.5711	65.23	0.4109	55.33	0.0181*
b4 (Phosphate)	347.70	0.5814	246.66	0.5375	80.12	0.6802	274.29	0.4121	-134.01	0.5617	-161.00	0.0192*
c1 (Glucose <sup>2</sup> )	0.45	0.1053	0.05	0.7913	-0.02	0.8559	-0.27	0.1366	-0.29	0.0542	-0.06	0.0574
c2 (Yeast extract <sup>2</sup> )	-3.66	0.3964	-4.95	0.1615	-1.34	0.8087	-2.65	0.3231	-2.53	0.2163	-0.49	0.3039
d12 (Glucose*Yeast)	2.09	0.0191*	1.52	0.02*	0.30	0.7455	0.68	0.1444	0.46	0.1630	-0.08	0.3255
R <sup>2</sup>	0.9051		0.9140		0.5309		0.8867		0.9237		0.8023	
adj. R <sup>2</sup>	0.7944		0.8281		0.1093		0.7734		0.8170		0.6046	
Pvalue	0.0103		0.0029		0.4373		0.0072		0.0152		0.0423	
<b>Optimized parameters</b>												
Glucose (g/L)	60.0		60.0		60.0		57.0		41.3		24.8	
Yeast extract (g/L)	15.0		15.0		11.5		14.5		13.6		4.1	
pH	6.5		6.5		6.5		6.5		8.5		8.5	
Phosphate addition (g/L)	0.5		0.5		0.5		0.5		0.0		0.0	
Expected growth (g/L)	36.2		25.9		15.5		17.2		13.6		3.2	
Confidence interval (g/L)	23.9		15.9		21.9		12.0		5.8		1.7	

**Table S4.** Biomass yield of the analyzed strains on the DoE media. Dry weight was approximated using data from the other trials.

	<i>Ulkenia visurgensis</i>		<i>U. profunda</i>		<i>Thraustochytridae</i> sp.		<i>T. striatum</i>		<i>Thraustochytrium aureum</i>	
	Sakar7	N6000b	N5594d	N5658a	N4994d	N4995d	N5670c	N5997	N6007e	N6006d
Mean biomass yield (g/L)	0.9	1.1	1.0	0.8	0.9	1.9	1.0	5.4	6.7	6.7
Median of biomass yield (g/L)	0.8	1.4	1.0	0.8	0.8	2.0	0.7	2.2	3.0	4.0
Maximum biomass yield (g/L)	1.8	1.9	1.9	1.7	2.1	3.4	2.2	21.0	27.3	21.7
DoE medium for highest yield	10	10	8	8	8	7	8	9	8	8

	<i>Schizochytrium aggregatum</i>		<i>Thraustochytrium kinnei</i>		<i>T. aggregatum</i>		<i>O. minutum</i>	
	5999	N2820a	N1709d	N1694d	N1476c	1465d	4992b	154f
Mean biomass yield (g/L)	1.9	1.5	0.3	0.8	0.6	0.3	6.5	4.9
Median of biomass yield (g/L)	1.0	1.4	0.4	0.7	0.5	0.1	4.8	3.1
Maximum biomass yield (g/L)	7.7	3.2	0.8	2.5	1.4	1.3	16.8	11.6
DoE medium for highest yield	9	9	9	8	12	11	9	8



**Table S5.** Carotenoid content and proportion in the analyzed strains used for cluster analysis. Values display the mean of the carotenoids obtained from all DoE experiments with a low salt concentration (15g/L).

[illegible]

**Table S6-1.** Cluster means of carotenoid composition obtained from k-means clustering of all strains grown on DoE experiments with a low salt concentration (15g/L).

[illegible]

**Table S6-2.** Cluster means of carotenoid composition obtained from k-means clustering of all strains grown on DoE experiments with a low salt concentration (15g/L) including strains that only grew on a high salt concentration (30g/L). The latter are marked with an asterisk.

[illegible]



**Table S7.** Carotenoid content and proportion in the analyzed strains in the DoE with a high salt concentration (30 g/L). Values display the mean of the carotenoids obtained from all DoE experiments with a high salt concentration (30g/L). Dry weight was approximated using data from the other trials.

carotenoid content (µg/g)		proportion of individual carotenoids in the total amount (%)													
species	strain	astaxanthin	9Z-astaxanthin	Di-Z-astaxanthin	13Z-astaxanthin	phoenico-xanthin	cantha-xanthin	9Z-cantha-xanthin	echine-none	lycopene	β-carotene	unknown 1	unknown 2	unknown 4	unknown 5
Thraustochytridae sp.	N4995d	15.5	0.6	0.3	1.1	12.5	33.4	9.7	1.2	3.5	5.3	0	6.8	10.1	0
	N4994d	71.3	36.5	0.6	1.1	3.7	16.5	25.6	6.8	0.5	0.7	1.5	0	4.1	2.6
	N6006d	85.8	0	0	0	0	35.5	7.7	8.9	1.8	34.6	3.9	4.2	1.6	1.7
T. aureum	N6007e	84.8	0	0	0	0	27.2	9.7	8.2	1.3	42.6	3.5	4.1	1.2	2.3
	N5905	16.5	64.8	0.3	0.9	4.8	14.7	2.1	0	3.4	2.0	4.2	0	2.7	0
U. profunda	N5658a	27.0	67.9	0.3	4.9	15.5	7.1	0	0	0.6	0	1.0	0	2.8	0
	N5629e	2.9	64.4	0	1.9	8.5	23.0	2.3	0	0	0	0	0	0	0
U. visurgensis	Sakar7	19.0	67.4	1.2	3.7	12.4	3.8	0	0	1.5	0	7.1	0	2.9	0
	N6000b	16.1	61.5	1.4	3.6	10.7	3.7	0	0	1.2	1.7	10.0	0	6.4	0
	N5589c	34.6	41.5	0.6	0.8	3.9	6.3	0.4	0	7.7	0.1	37.3	0	1.4	0
S. aggregatum	5999	16.9	0.4	0.1	0.0	0.1	0.02	0	0	2.9	87.5	0	0	8.3	0.8
	561bx	27.5	0.2	0.1	0	0	0	0	0	1.5	91.1	0	0	6.7	0.4
	N2820a	3.5	0	0	0	0	0	0	0	0	98.4	0	0	0	1.6

**Table S8.** Carotenoid and squalene content and carotenoid proportion in *T. striatum* N5997 depending on the medium composition. Dry weight was approximated using data from the other trials.

medium number	carotenoid content (µg/g)	proportion of individual carotenoids in the total amount (%)												astaxanthin mono-palmitate	squalene content (µg/g)
		astaxanthin	9Z-astaxanthin	Di-Z-astaxanthin	13Z-astaxanthin	phoenico-xanthin	cantha-xanthin	9Z-cantha-xanthin	unknown 3	unknown 6	lycopene	β-carotene	unknown 4		
1	46.1	67.2	8.8	1.1	5.5	4.6	1.1	0.1	0.5	1.0	2.9	6.7	0.3	0.3	0.6
2	32.1	74.6	7.7	1.9	6.1	4.7	0.8	0	0.9	1.6	0.5	1.2	0	0.6	0.6
3	11.8	64.0	5.4	2.9	8.2	10.0	2.2	0	0	3.1	0	4.0	0	9.3	0.3
4	32.0	70.7	3.9	2.5	7.1	5.1	1.3	0.3	1.8	3.0	1.5	1.5	0.4	9.5	0.1
5	55.6	68.3	2.5	0.9	5.6	4.5	1.0	0.1	0.4	0.3	0.9	14.9	0.5	0.1	0.1
6	28.4	69.6	6.1	2.1	6.5	5.9	1.0	0	1.3	2.1	2.2	2.7	0.4	4.1	0.1
7	17.5	67.3	0.9	0.6	3.6	3.3	1.2	0	2.7	0.9	1.2	10.2	2.1	2.8	0.1
9	61.1	49.3	1.5	0.7	13.2	5.4	0.9	0.1	2.5	0.5	1.9	20.7	2.3	0.9	0.9
10	33.8	63.9	7.0	0.9	3.9	5.1	0.8	0	1.8	3.0	6.2	5.4	1.0	2.7	0.1
11	37.0	62.1	4.4	2.1	6.3	7.5	1.2	0.3	2.6	4.0	5.5	2.6	1.4	13.3	0.1
12	23.9	66.0	1.8	0.6	3.2	5.1	0.8	0	1.8	0.9	2.9	13.7	3.3	0.8	0.1
13	24.9	68.5	10.8	1.1	5.5	5.2	1.2	0	0.5	0.3	1.2	5.6	0	0.2	0.1
14	43.4	56.7	2.3	2.5	8.4	3.0	1.9	0.5	5.1	6.0	4.5	1.8	1.5	9.9	0.1
15	69.1	62.7	1.0	0.6	5.3	3.4	1.7	0.2	1.3	0.2	1.0	14.7	1.9	0.6	0.1



**Table S9.** Extract content in dependency of strain, medium composition and medium solidity.

species	strain	DoE number	medium	biomass amount (mg)	extract amount (mg)	extract content (%)
<i>U. visurgensis</i>	N1001	6	solid	9.3	0.4	4.1
		9	solid	16.3	0.7	4.3
		15	solid	34.2	3.2	9.3
		7	solid	60.8	3.3	5.4
		7	liquid	27.9	1.4	5.2
	N6000b	6	solid	9.1	0.3	3.2
		9	solid	22.3	0.6	2.8
		15	solid	37.4	5.6	14.9
	N5594d	6	solid	8.2	0.2	2.4
		9	solid	24.6	0.6	2.6
		15	solid	31.9	3.2	10.1
	N5589c	6	solid	5.5	0.4	6.9
		9	solid	29.4	1.0	3.5
		15	solid	26.7	4.2	15.5
<i>U. profunda</i>	N5658a	6	solid	8.3	0.4	4.9
		9	solid	24.5	0.8	3.5
		15	solid	30.5	5.7	18.7
		7	solid	43.0	2.3	5.4
		7	liquid	9.8	0.4	3.6
<i>T. aureum</i>	N6006d	6	solid	81.3	6.0	7.3
		9	solid	94.3	48.2	51.1
		15	solid	92.7	39.0	42.0
		7	solid	93.9	11.4	12.2
		7	liquid	40.4	1.8	4.5
	5985	6	solid	25.8	1.2	4.6
		9	solid	98.9	39.9	40.3
		15	solid	78.4	23.9	30.5
<i>S. aggregatum</i>	5999	6	solid	8.4	0.8	9.7
		9	solid	73.0	23.3	31.9
		15	solid	73.9	25.8	34.9
	N2820a	6	solid	7.1	0.7	10.4
		9	solid	74.7	15.9	21.2
		15	solid	62.3	20.6	33.0
<i>O. minutum</i>	5996	6	solid	67.1	3.1	4.5
		9	solid	97.8	14.2	14.6
		15	solid	32.0	3.2	10.0
<i>Thraustochytriidae</i> sp.	N4994d	6	solid	13.7	0.9	6.7
		9	solid	45.4	2.7	6.0
		15	solid	1.0	-	-
		7	solid	85.2	4.6	5.4
		7	solid	41.5	1.4	3.5
	N5670c	6	solid	13.2	0.7	5.1
		9	solid	72.3	3.2	4.5
		15	solid	7.8	0.2	2.4



Table S10. Carotenoid content and proportion in strains cultivated on different solid media.

carotenoid content (µg/g)			proportion of individual carotenoids in the total amount (%)															
species	strain	medium	asta-xanthin	9Z-asta-xanthin	di-Z-asta-xanthin	13Z-asta-xanthin	phoenico-xanthin	cantha-xanthin	9Z-cantha-xanthin	echine-none	lycopene	β-carotene	unknown 1	unknown 2	unknown 3	unknown 4	unknown 5	
Thraustochytridae sp.	N4994d	6	300.3	23.5	0.6	0.6	2.5	15.4	36.3	8.6	0.4	1.1	2.0	0	5.1	0	3.9	0
		9	130.2	13.0	0.5	0.3	1.1	17.1	46.2	10.9	0.3	0.3	1.6	0	7.3	0	1.3	0
		15	99.2	14.9	0.6	0.3	1.3	21.3	43.1	7.7	0	0	0	7.7	0	10.8	0	0
	N5670c	6	138.6	19.4	1.4	0.7	2.1	9.3	27.2	26.9	0.5	1.4	3.0	0	3.0	0	5.0	0
		9	122.8	31.1	1.2	0.9	3.8	19.8	27.6	7.0	0.1	0.1	1.1	0	6.4	0.07	0.8	0
T. aureum	N6006d	15	106.7	14.9	0.7	0.4	1.5	21.5	40.6	6.7	0	0	0.6	0	7.5	5.5	0	0
		6	48.4	0	0	0	0	0	34.8	6.6	7.5	10.8	26.1	0.1	2.1	0	10.9	1.0
		9	243.8	0	0	0	0	0	25.8	2.9	6.7	0.3	53.3	4.2	4.6	0	0.9	1.3
	5985	15	342.6	0	0	0	0	0	35.7	4.6	8.7	0.1	43.3	1.1	4.8	0	0.2	1.5
		6	169.0	0	0	0	0	0	45.8	8.7	8.3	0	23.0	0.2	2.4	0	11.1	0.4
U. profunda	N5658a	9	241.0	0	0	0	0	0	40.4	3.3	6.3	0.3	36.3	5.5	6.4	0	0.5	1.1
		15	346.0	0	0	0	0	0	44.7	4.5	5.5	0.1	29.2	5.4	9.1	0	0	1.6
		6	43.7	58.7	0.6	1.8	7.6	5.1	0.8	0	0	10.4	3.4	0	0.6	1.6	9.4	0
	N5658a	9	76.7	71.5	0.4	2.4	9.5	5.1	0.6	0	0.2	2.4	2.3	0	0.7	1.7	3.3	0
		15	112.1	82.2	0.6	0.8	5.5	5.3	0.4	0	0.3	0	1.8	0	0.5	0.8	1.8	0
U. visurgensis	N6000b	6	16.4	37.7	0	1.8	7.5	3.3	0	0	0.9	10.3	21.3	0	0	1.4	15.8	0
		9	41.8	62.3	0.9	2.3	10.5	4.7	0	0	0.3	3.6	4.8	0	0.6	1.1	8.9	0
		15	81.0	70.8	1.3	0.9	4.3	2.9	0	0	0.3	0	15.2	0	0.2	1.1	2.9	0
	N1001	6	42.3	58.7	2.0	2.3	7.6	9.3	0.8	0	0.6	1.7	10.4	0	0.9	1.7	4.1	0
		9	101.7	63.2	1.4	3.3	9.6	10.7	0.8	0	0.5	0.2	4.6	0	1.7	2.4	1.4	0
S. aggregatum	N5589c	15	305.0	77.0	0.8	1.0	6.8	6.8	0.2	0	0.4	0	2.6	0	0.8	0.9	2.7	0
		6	50.8	18.9	0.2	0.5	3.6	4.1	0	0	0.7	7.2	45.6	0	1.0	4.5	13.6	0
		9	72.0	40.6	0.4	0.4	3.1	8.2	0.2	0	0.4	2.0	32.2	0	0.5	7.0	5.0	0
	N5594d	15	101.2	36.1	0.3	0.4	2.6	3.3	0.2	0	0.4	0	49.0	0	0.3	3.7	3.7	0
		6	47.1	17.5	0.2	0.3	2.2	2.8	0	0	0.4	1.9	59.7	0	0.5	7.3	7.2	0
O. minutum	5999	9	69.1	44.6	0.6	0.9	4.9	5.8	0	0	0.3	0.8	26.9	0	0.6	10.6	4.0	0
		15	131.8	53.8	0.7	0.5	3.0	6.7	0	0	0.6	0.2	29.2	0	0.4	4.3	0.5	0
		6	27.8	0	0	0	0	0	0	0	0	0	89.5	0	0	0.0	10.5	0
	N2820a	9	39.6	0	0	0	0	0	0	0	0	3.0	93.6	0	0	0	3.3	0.1
		15	49.0	0	0	0	0	0	0	0	0	0	98.5	0	0	0	0.8	0.6
O. minutum	5996	6	17.1	0	0	0	0	0	0	0	0	0	88.5	0	0	0	11.5	0
		9	27.2	0	0	0	0	0	0	0	0	2.6	93.4	0	0	0	3.8	0.1
		15	34.4	0	0	0	0	0	0	0	0	0	98.6	0	0	0	0.9	0.5



**Table S11.** Carotenoid content and proportion in strains cultivated on medium 7 in either liquid medium (liquid) or in form of agar (solid).

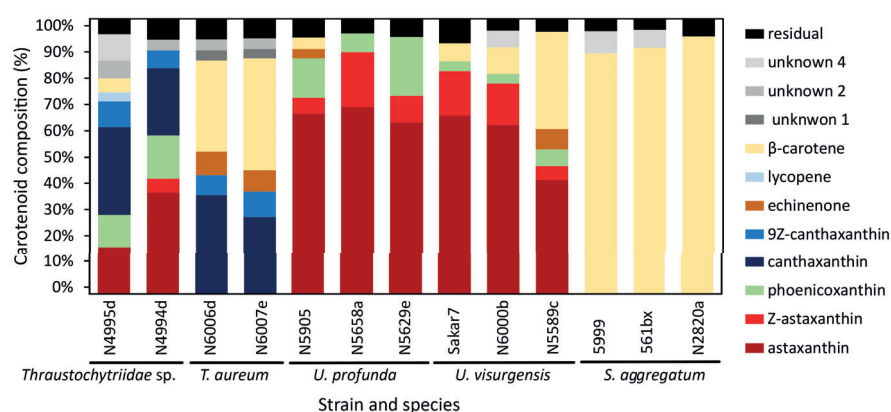
			carotenoid content (µg/g)	proportion of individual carotenoids in the total amount (%)														
species	strain	medium		asta- xanthin	9Z-asta- xanthin	Di-Z-asta- xanthin	13Z-asta- xanthin	phoenico- xanthin	cantha- xanthin	9Z-cantha- xanthin	echine- none	lycopene	β- carotene	unknown 1	unknown 2	unknown 3	unknown 4	unknown 5
<i>Thraustochy- triidae</i> sp.	N4994d	solid	217.6	21.7	1.0	0.4	1.8	15.7	28.8	6.2	0.8	2.5	5.0	0	7.1	0	9.0	0
	N4994d	liquid	87.0	3.6	0.3	0.2	0.5	3.8	18.6	7.7	4.4	3.2	44.8	0	4.8	0	8.1	0
<i>U. profunda</i>	N5658a	solid	91.1	69.5	0.4	1.2	6.6	6.9	0.7	0	0.3	3.8	3.1	0	0.7	2.8	4.1	0
	N5658a	liquid	69.9	52.0	1.0	2.4	8.4	6.6	0.5	0	0.8	1.0	15.3	0	1.0	10.1	0.9	0
<i>U. visurgensis</i>	N1001	solid	134.1	58.9	1.2	2.3	8.9	8.8	0.8	0	0.5	1.4	8.9	0	1.7	1.8	4.8	0
	N1001	liquid	85.3	29.9	0.8	1.0	4.0	4.4	0.3	0	0.5	1.8	45.7	0	0.6	4.9	6.1	0
<i>T. aureum</i>	N6006d	solid	60.0	0	0	0	0	0	32.7	5.9	9.6	5.5	30.7	0.1	1.3	0	13.5	0.6
	N6006d	liquid	15.6	0	0	0	0	0	29.6	8.5	8.9	5.1	36.9	0.3	2.4	0	7.5	0.9



Table S12. Review of strains reported in the literature by comparison with the phylogenetic analysis of our study. "(Re)classification" refers primarily to the GenBank entries and, if none were available, to the information in the literature.

strain / isolate	designation	reference	GenBank - 18s rRNA sequence - organism	GenBank accession number	ATCC denomination	ATCC number	(Re)classification	Added to molecular phylogeny for comparison	Added to figure 1
S15	<i>T. kinnei</i>	87	-	-	-	-	-	-	Isolate S14
<i>T. aureum</i> ATCC 34304	<i>T. aureum</i>	93, 100, 131-133	-	-	<i>T. aureum</i> Goldstein	34304	-	-	-
<i>Aurantiochytrium</i> sp. UMACC-T023	<i>Aurantiochytrium</i> sp.	94	<i>Aurantiochytrium</i> sp.	KP015193.1	-	-	-	-	-
<i>Thraustochytrium</i> sp. ONC-T18	<i>Thraustochytrium</i> sp. / <i>T. striatum</i>	95	<i>Thraustochytrium</i> sp.	DQ374149	-	-	<i>Aurantiochytrium</i> sp.	yes	yes
<i>Schizochytrium</i> sp. G13/25	<i>Schizochytrium</i> sp.	96	-	-	-	-	-	-	-
<i>Thraustochytrium</i> sp. AMCCQ5-5	<i>Thraustochytrium</i>	74	<i>Thraustochytrium</i> sp.	JX993841	-	-	<i>T. aureum</i>	yes	yes
<i>Thraustochytrium</i> sp. AMCCQ5-3	<i>Thraustochytrium</i>	74	<i>Thraustochytrium</i> sp.	JX993839	-	-	<i>T. aureum</i>	yes	yes
<i>Thraustochytrium</i> sp. AMCCQ5-1-9	<i>Schizochytrium</i>	74	<i>Schizochytrium</i> sp.	JX993843	-	-	<i>Aurantiochytrium</i> sp.	yes	-
<i>A. limacinum</i> ICTSG-17	<i>A. limacinum</i>	19	-	-	-	-	-	-	-
<i>Thraustochytrium</i> sp. ATCC 26185	<i>Thraustochytrium</i> sp.	97, 126, 179	<i>Thraustochytrium</i> sp.	FJ821482.1	<i>Thraustochytrium</i> sp.	26185	<i>Aurantiochytrium</i> sp.	yes	yes
<i>Aurantiochytrium</i> sp. ATCC PRA-276	<i>Aurantiochytrium</i> sp.	69, 70, 97	-	-	<i>Aurantiochytrium</i> sp.	PRA-276	-	-	-
<i>A. limacinum</i>	<i>A. limacinum</i>	84	-	-	-	-	-	-	-
<i>Thraustochytrium</i> sp. T01	<i>Thraustochytrium</i> sp.	134	-	-	-	-	-	-	-
<i>Aurantiochytrium</i> sp. SW1	<i>Aurantiochytrium</i> sp.	135	<i>Schizochytrium</i> sp.	KF500513	-	-	<i>Aurantiochytrium</i> sp.	-	-
<i>thraustochytrid</i> F24-2	<i>Thraustochytrium</i> sp.	136	-	-	-	-	<i>Aurantiochytrium</i> sp.	yes	yes
<i>Aurantiochytrium</i> sp. 4W-1b	<i>Aurantiochytrium</i> sp.	137	-	-	-	-	-	-	-
<i>Aurantiochytrium</i> B072	<i>Aurantiochytrium</i> sp.	72	<i>Aurantiochytrium</i> sp.	JF266572	-	-	-	-	-
<i>Ulkenia</i> sp. SEK 214	<i>Ulkenia</i> sp.	64	<i>Ulkenia</i> sp.	AB290355.1	-	-	-	yes	yes
<i>Ulkenia</i> sp. ATCC 28207	<i>Ulkenia</i> sp. ( <i>Jupanochytrium</i> sp.)	64	<i>Jupanochytrium</i> sp.	AB022104.1	<i>Jupanochytrium</i> sp.	28207	<i>Ulkenia</i> sp.	yes	yes
<i>S. aggregatum</i> ATCC 28209	<i>S. aggregatum</i>	63, 175	<i>S. aggregatum</i>	AB022106.1	<i>S. aggregatum</i> Goldstein et Belsky	28209	-	yes	yes
<i>Schizochytrium</i> sp. SEK 210	<i>Schizochytrium</i> sp.	63	<i>Schizochytrium</i> sp.	AB290576.1	-	-	-	yes	yes
<i>Schizochytrium</i> sp. SEK 345	<i>Schizochytrium</i> sp.	63	<i>Schizochytrium</i> sp.	AB290577.1	-	-	-	yes	yes
<i>Schizochytrium</i> sp. S31	<i>Schizochytrium</i> sp.	74, 104	<i>Schizochytrium</i> sp.	DQ367050.1	<i>Schizochytrium</i> sp.	20888	<i>Aurantiochytrium</i> sp.	yes	yes
<i>T. aureum</i> BT6	<i>T. aureum</i>	109	-	-	-	-	-	-	-
<i>Thraustochytrium</i> sp. RT2316-16	<i>Thraustochytrium</i> sp.	106, 112, 113	<i>Thraustochytrium</i> sp.	MT648462	-	-	<i>Phycopatorium</i> sp.	-	-
<i>T. striatum</i> ATCC 24473	<i>T. striatum</i>	63, 114, 117	<i>T. striatum</i>	AB022112.1	<i>T. striatum</i> Schneider	24473	-	yes	yes
<i>Thraustochytrium</i> sp. S7.	<i>Thraustochytrium</i> sp.	81	<i>Thraustochytrium</i> sp.	KF683340.1	-	-	<i>T. striatum</i>	yes	-
<i>Oblongichytrium</i> sp. SEK347	<i>Oblongichytrium</i> sp.	63	<i>Oblongichytrium</i> sp.	AB290575.1	-	-	-	yes	-
<i>Thraustochytrid</i> CHN-1	<i>Thraustochytrium</i>	82	<i>Thraustochytrium</i> sp.	AB126669.1	-	-	<i>Aurantiochytrium</i> sp.	yes	yes
<i>T. striatum</i> AL16	<i>T. striatum</i>	115	<i>T. striatum</i>	KT598545.1	-	-	-	yes	yes
<i>Aurantiochytrium</i> sp. 18W-13a	<i>Aurantiochytrium</i> sp.	119	<i>Aurantiochytrium</i> sp.	AB636147	-	-	-	yes	yes
<i>Aurantiochytrium</i> sp. BR-MP4-A1	<i>Aurantiochytrium</i> sp.	121	<i>Aurantiochytrium</i> sp.	FJ004948.1	-	-	-	yes	yes
<i>S. limacinum</i> SR21	<i>S. limacinum</i>	71	<i>A. limacinum</i>	AB973564.1	<i>A. limacinum</i> (Honda et Yokochi) Yokoyama et Honda	MVA-1381	-	yes	yes
<i>S. mangrovei</i> PQ6	<i>S. mangrovei</i>	122	<i>A. mangrovei</i>	EU728656.1	-	-	-	yes	-
<i>S. mangrovei</i> FB1	<i>S. mangrovei</i>	123	-	-	-	-	<i>A. mangrovei</i>	-	-
<i>S. mangrovei</i> FB3 / <i>A. mangrovei</i> FB3	<i>S. mangrovei</i> / <i>A. mangrovei</i>	79, 123	-	-	-	-	<i>A. mangrovei</i>	-	-
<i>S. mangrovei</i> FB5	<i>S. mangrovei</i>	123	-	-	-	-	-	-	-
<i>Thraustochytridae</i> sp. M4-103	<i>Thraustochytridae</i> sp.	88	<i>Thraustochytridae</i> sp.	AB073307.1	-	-	-	yes	-
<i>Schizochytrium</i> ACEM 6063	<i>Schizochytrium</i> sp.	124	-	-	-	-	-	-	-
<i>S. limacinum</i> B4D1	<i>S. limacinum</i>	108	-	-	-	-	<i>A. limacinum</i>	-	-
<i>Labyrinthuloides</i> haliotidis	<i>Labyrinthuloides</i> haliotidis	182	<i>Labyrinthulachytrium</i> haliotidis	U21338.1	-	-	-	-	-
<i>S. minutum</i> KPMB N-BA-77	<i>S. minutum</i>	62	<i>S. minutum</i>	AB022108.1	-	-	<i>O. minutum</i>	yes	yes
<i>T. multirudimentale</i> KMPB N-BA-113	<i>T. multirudimentale</i>	62	<i>T. multirudimentale</i>	AB022111.1	-	-	<i>O. multirudimentale</i>	yes	yes
<i>Schizochytrium</i> sp. SH104	-	-	<i>Schizochytrium</i> sp.	KX379459.1	-	-	<i>Aurantiochytrium</i> sp.	yes	yes





**Figure S1.** Carotenoid composition of the analyzed strains grown on media with a high salinity (30 g/L). Mean values of the individual experiments from each strain whose contribution to the total carotenoids exceeded 3% are displayed individually (Table S7). Diastereomers of astaxanthin are summarized as “Z-astaxanthin”.

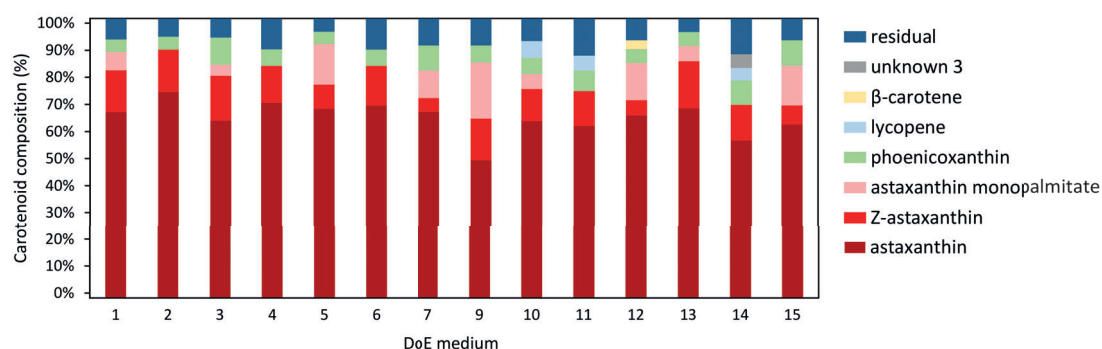


**Figure S2.** Carotenoid composition of *Thraustochytrium striatum* N5997 on various DoE media. Only carotenoids whose contribution to the total carotenoids exceeded 3% are displayed individually (Table S8). Diastereomers of astaxanthin are summarized as “Z-astaxanthin”.



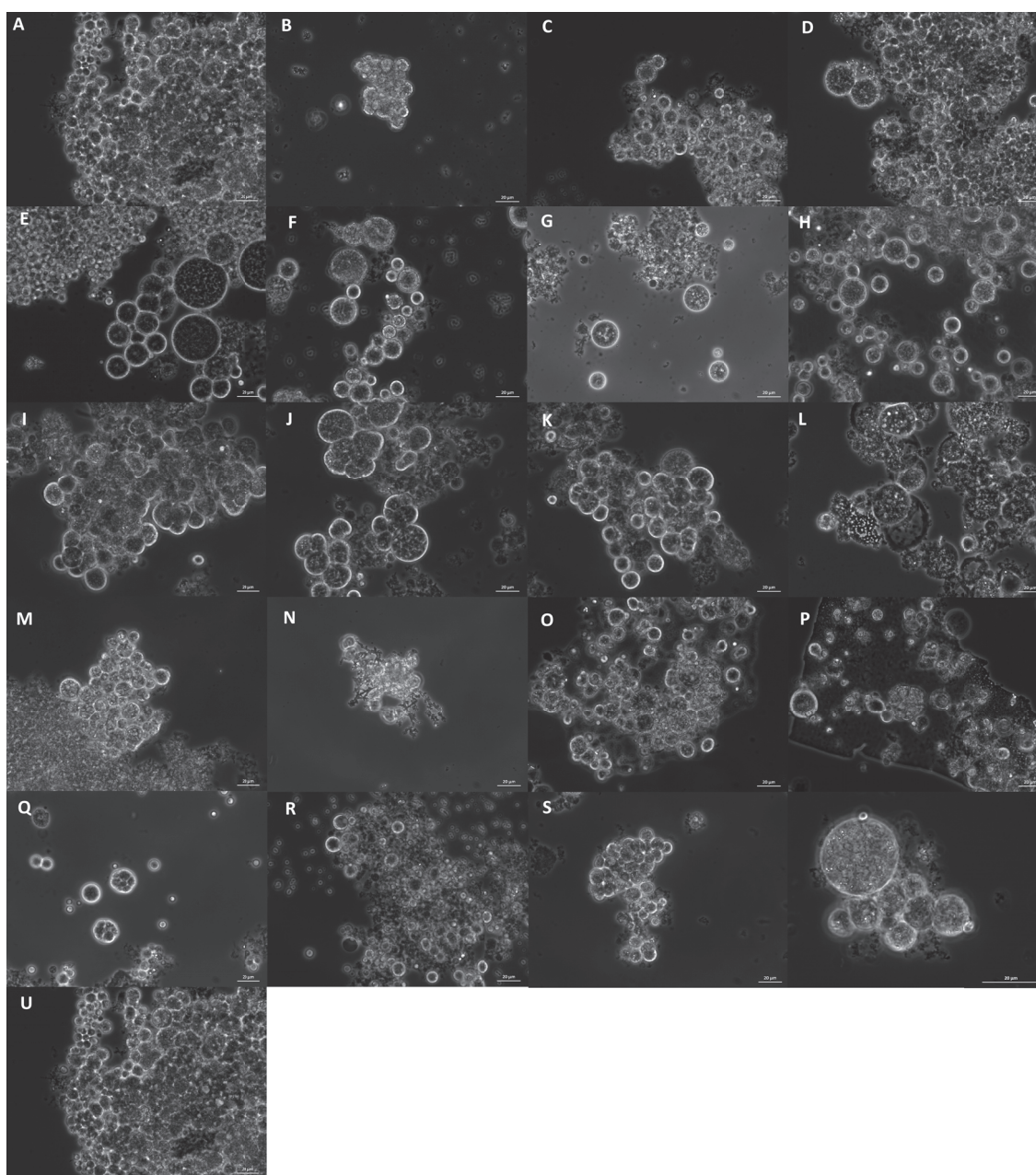


**Figure S3.** Morphology of various strains observed in medium 3 after cultivation in microtiter plates. *U. profunda* N5905 (A), N5658a (B), *U. visurgensis* 6000b (C), Sakar7 (D), N5594d (E), N5589c (F), *T. aggregatum* 4992b (G), N4930a (H), *S. aggregatum* 561bx (I), N2820a (J), 5999 (K), *T. striatum* 5997 (L), *O. minutum* N5995 (M), 5996 (N), *T. kinnei* N1694d (O), 1476c (P), *Thraustochytriidae* sp. N5670c (Q), N4994d (R), *T. aureum* N6006d (S), N6007e (T), and 5985 (U). Scale bars show 20  $\mu$ m.



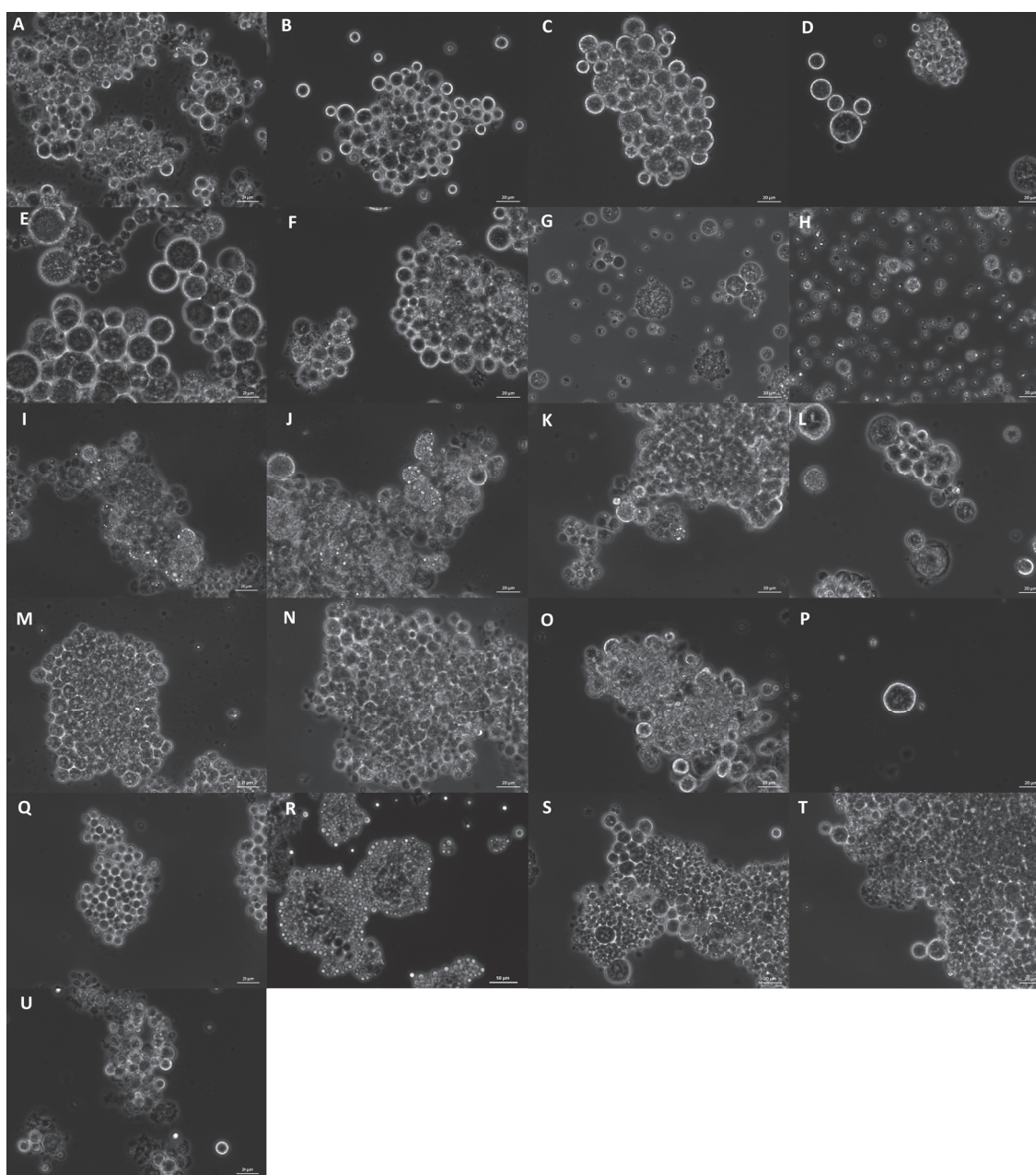


**Figure S4.** Morphology of various strains observed in medium 6 after cultivation in microtiter plates. *U. profunda* N5905 (A), N5658a (B), *U. visurgensis* 6000b (C), Sakar7 (D), N5594d (E), N5589c (F), *T. aggregatum* 4992b (G), N4930a (H), *S. aggregatum* 561bx (I), N2820a (J), 5999 (K), *T. striatum* 5997 (L), *O. minutum* N5995 (M), 5996 (N), *T. kinnei* N1694d (O), 1476c (P), *Thraustochytriidae* sp. N5670c (Q), N4994d (R), *T. aureum* N6006d (S), N6007e (T), and 5985 (U).



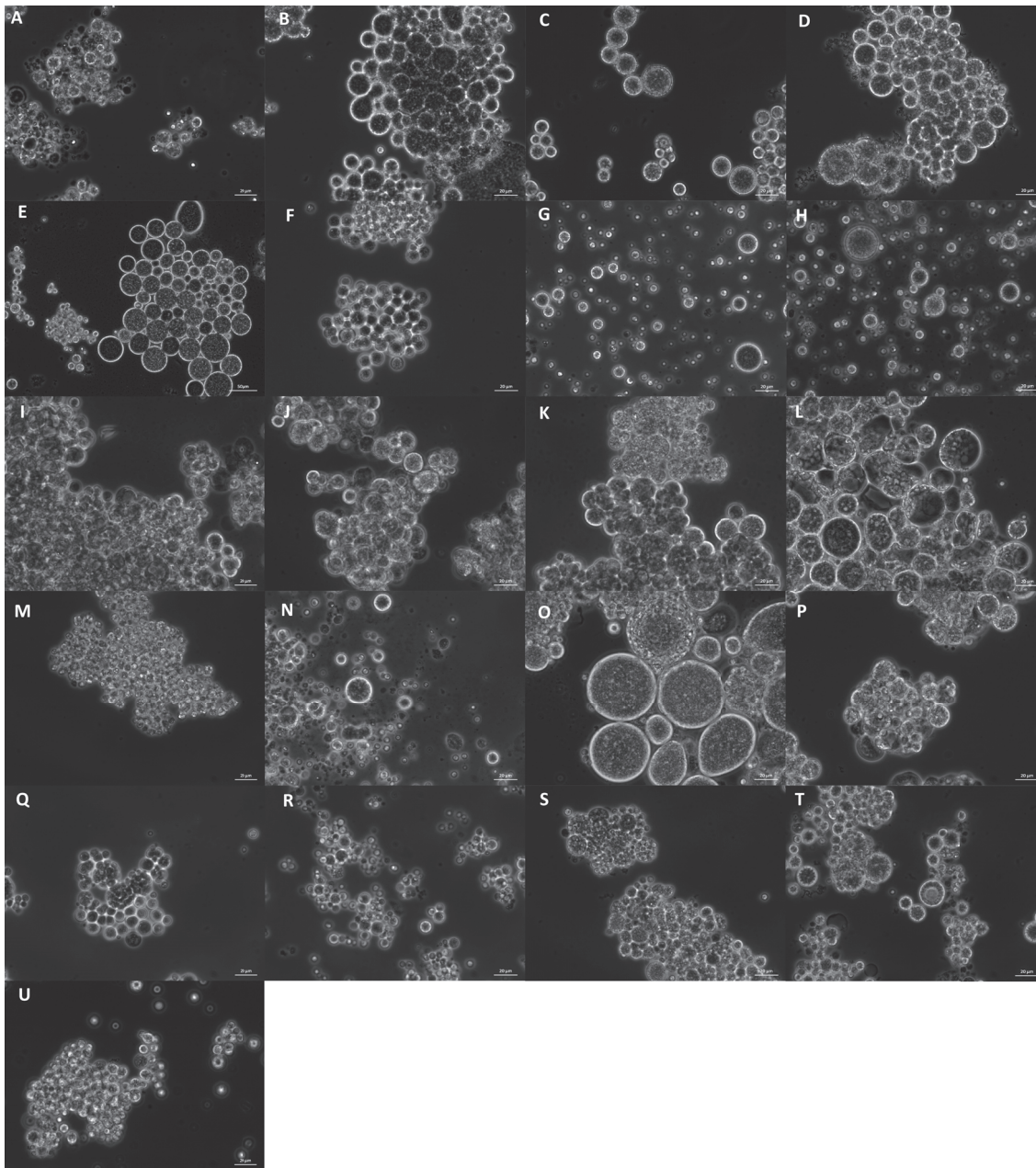


**Figure S5.** Morphology of various strains observed in medium 12 after cultivation in microtiter plates. *U. profunda* N5905 (A), N5658a (B), *U. visurgensis* 6000b (C), Sakar7 (D), N5594d (E), N5589c (F), *T. aggregatum* 4992b (G), N4930a (H), *S. aggregatum* 561bx (I), N2820a (J), 5999 (K), *T. striatum* 5997 (L), *O. minutum* N5995 (M), 5996 (N), *T. kinnei* N1694d (O), 1476c (P), *Thraustochytriidae* sp. N5670c (Q), N4994d (R), *T. aureum* N6006d (S), N6007e (T), and 5985 (U).



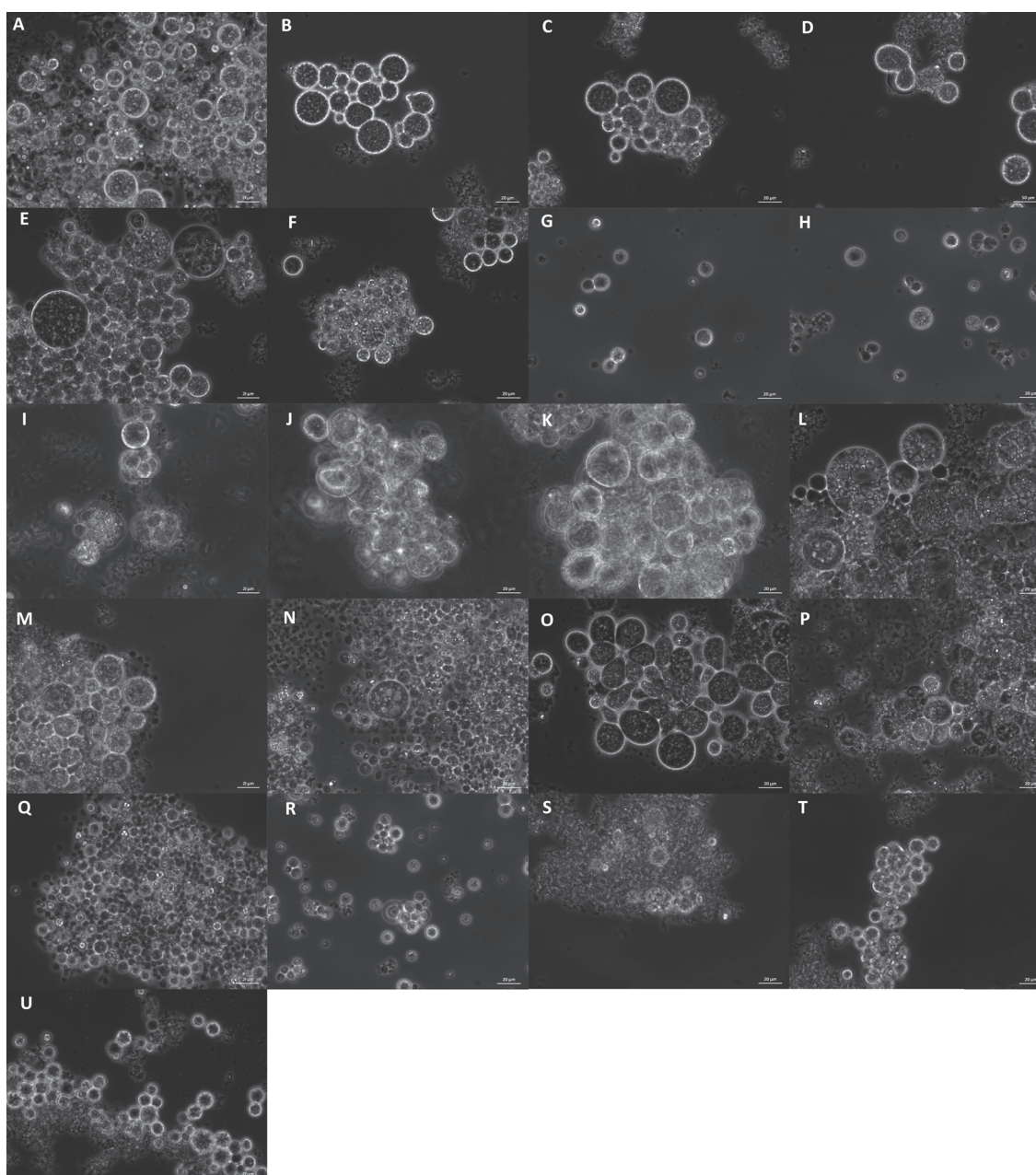


**Figure S6.** Morphology of various strains observed in medium 14 after cultivation in microtiter plates. *U. profunda* N5905 (A), N5658a (B), *U. visurgensis* 6000b (C), Sakar7 (D), N5594d (E), N5589c (F), *T. aggregatum* 4992b (G), N4930a (H), *S. aggregatum* 561bx (I), N2820a (J), 5999 (K), *T. striatum* 5997 (L), *O. minutum* N5995 (M), 5996 (N), *T. kinnei* N1694d (O), 1476c (P), *Thraustochytriidae* sp. N5670c (Q), N4994d (R), *T. aureum* N6006d (S), N6007e (T), and 5985 (U).







## Danksagung

Zuallererst möchte ich Frau Prof. Dr. Labes und Herrn Prof. Dr. Schulz für ihre Unterstützung und Betreuung bei dieser Arbeit danken.

Antje, Dir gilt meine besondere Dankbarkeit und Anerkennung. Durch Deine herausragende Betreuung, Deine fachliche Kompetenz, Deine Geduld und Deine Wertschätzung hast du mich persönlich wie fachlich sehr gefördert. Der Dialog mit Dir hat meine wissenschaftliche Denkweise geschärft und Arbeitsmethoden verbessert und letztendlich dazu geführt, meine Forschung auf ein höheres Niveau zu heben. Trotz Deiner ohnehin schon hohen Arbeitsbelastung hattest Du immer ein offenes Ohr für mich. Herr Prof. Schulz, vielen Dank für das Vertrauen, das Sie in mich gesetzt haben und besonders für die Unterstützung beim Abschluss meiner Promotion.

Vielen Dank dem Team vom ZAiT. Birte, auch an Dich konnte ich mich immer wenden. Du hast mir bei Fragen geholfen und mich sehr unterstützt. Annemarie, Dein fachlicher und Dein emotionaler Beistand haben dazu beigetragen, dass ich auch die Schwierigkeiten der Promotion gut meistern konnte. Deniz, Deine muntere und kreative Art haben meinen Arbeitsalltag erhellt, und Deine Laborexpertise hat mir den Rücken freigehalten, meine Arbeit zügig fertigzustellen. Lena, Deine pragmatische Natur hat alles so viel unkomplizierter erscheinen lassen und Deine Unterstützung hat mir viel bedeutet.

Ebenso gilt mein Dank meinen Mitpromovierenden Akira und Rebekka. Durch Euch haben sich mir spannende neue Blickwinkel eröffnet und die Problemanalysen unserer Hardware waren deutlich angenehmer. Nicht zuletzt haben mir auch die fachfremden Debatten mit Euch immer sehr viel Freude gebracht.

Ich danke allen Mitgliedern der Arbeitsgruppe Bio- und Lebensmitteltechnologie im weitesten Sinne. Ohne Euch, wäre vieles nicht möglich und sicher alles nicht so schön gewesen. Andreas, Anja, Holger, Jörg, Larissa, Leif, Lisa, Marlies, Meike, Michael, Simone, Udo, Eure konstruktive Unterstützung hat mir viel bedeutet. Vielen Dank insbesondere Dir, Holger, für Deine Anleitung und die Ermöglichung, neue Methoden kennenzulernen, und Deine allzeit kompetente und bereichernde Hilfe. Vielen Dank Lisa, Leif und Marlies für Eure Expertise und Hilfe bei der Nutzung der Geräte. Vielen Dank Euch allen für all die netten Gespräche, die mir sowohl geholfen haben meinen Horizont zu erweitern als auch mein Weltbild zu stabilisieren.

Dem Team der Firma Sea & Sun Technology, insbesondere Heinz, Stefan und Clemens möchte ich für die Unterstützung meiner Arbeit, die Versorgung mit Probenmaterial und die angenehme Zusammenarbeit danken.

Auch meinen (anderen) Coautoren gilt ein besonderer Dank. Simone und Bettina, ohne Eure Mitarbeit, Eure Ideen und Euer Engagement wären große Teile der Publikationen nicht die, die sie heute sind. Die Zusammenarbeit mit Euch war mir eine große Freude.

Thank you Jane, for sharing your knowledge about our little friends, the thraustochytrids, for inviting me to Scotland, for the wonderful week, I was allowed to spend with you, and for all our discussions.

Danke Dr. Matthias Kellermann für die Untersuchung und Beurteilung der ersten Carotinoidproben am Institute for Chemistry and Biology of the Marine Environment der Carl-von-Ossietzky University Oldenburg. Deine Einschätzung hat mir bei der Planung meiner Versuche sehr geholfen.

Vielen Dank den Studierenden der Wahlpflichtkurse Marine Biotechnology und den HiWis, die mir geholfen haben, erste Eindrücke in die Thematik der Thraustochytriden zu erlangen.

Und schließlich möchte ich auch meinen Eltern danke sagen, Ihr habt stets an mich geglaubt, mir emotional beigestanden und mich unterstützt, wo Ihr nur konntet.

Jasper, danke dafür, dass Du Dein Fachwissen mit mir geteilt hast und vor allem, dass Du an meiner Seite bist.







### **Eidesstattliche Erklärung**

Hiermit erkläre ich eidesstattlich, dass die vorliegende Abhandlung, abgesehen von der Beratung durch meine Betreuer und den angegebenen Hilfsmitteln, nach Inhalt und Form meine eigene Arbeit ist. Weiterhin versichere ich, dass die Arbeit weder im Ganzen noch zum Teil schon einer anderen Stelle im Rahmen eines Prüfungsverfahrens vorgelegen hat, noch veröffentlicht oder zur Veröffentlichung eingereicht wurde. Die Arbeit ist unter Einhaltung der Regeln guter wissenschaftlicher Praxis der Deutschen Forschungsgemeinschaft entstanden. Bisher wurde mir kein akademischer Grad entzogen.

Flensburg, d. 10.08.2023

Inga Klara Koopmann